ANALYTICA CHIMICA ACTA

International monthly devoted to all branches of analytical chemistry
Revue mensuelle internationale consacrée à tous les domaines de la chimie analytique
Internationale Monatsschrift für alle Gebiete der analytischen Chemie

ELSEVIER PUBLISHING COMPANY
AMSTERDAM

Anal. Chim. Acta, Vol. 60, No. 1, 1–260, June 1972
Published monthly

Publication Schedule for 1972

Vol. 58, No. 1	January 1972	
Vol. 58, No. 2	February 1972	**(completing Vol. 58)**
Vol. 59, No. 1	March 1972	
Vol. 59, No. 2	April 1972	
Vol. 59, No. 3	May 1972	**(completing Vol. 59)**
Vol. 60, No. 1	June 1972	
Vol. 60, No. 2	July 1972	**(completing Vol. 60)**
Vol. 61, No. 1	August 1972	
Vol. 61, No. 2	September 1972	
Vol. 61, No. 3	October 1972	**(completing Vol. 61)**
Vol. 62, No. 1	November 1972	
Vol. 62, No. 2	December 1972	**(completing Vol. 62)**

Subscription price: Dfl. 364.00 plus Dfl. 21.00 postage (US $ 120.30 including postage). Additional cost for copies by airmail available on request. For subscribers in the U.S.A. and Canada, 2nd class postage paid at Long Island City, N.Y. and at additional mailing offices. For advertising rates apply to the publishers.

GENERAL INFORMATION

Languages

Papers will be published in English, French or German.

Submission of papers

Papers should be sent to:

PROF. PHILIP W. WEST,
Coates Chemical Laboratories,
College of Chemistry and Physics,
Louisiana State University,
Baton Rouge 3,
La. 70803 (U.S.A.)

or to:

DR. A. M. G. MACDONALD,
Department of Chemistry,
The University,
P.O. Box 363
Birmingham B15 2TT (Great Britain)

Reprints

Fifty reprints will be supplied free of charge. Additional reprints (minimum 100) can be ordered at quoted prices. They must be ordered on order forms which are sent together with the proofs.

MERCK

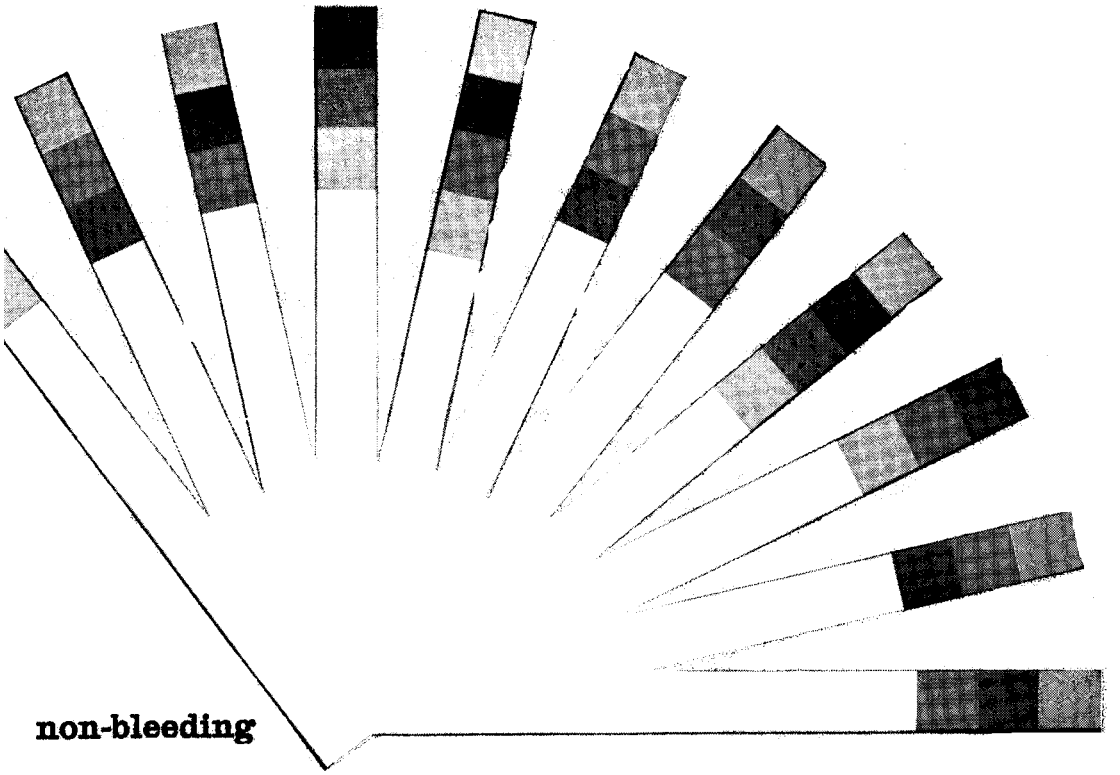

non-bleeding

Universal Indicator Strips: pH 0–14
Special Indicator Strips: pH 0–2.5
pH 2.5–4.5 pH 4.0–7.0 pH 6.5–10.0 pH 11.0–13.0
Neutralit® pH 5–10 Acilit® pH 0–6
Alkalit® pH 7.5–14

Special advantages:

Reactive zones sealed onto plastic strips

Non-bleeding

Prolonged immersion possible

Weakly buffered and even coloured solutions may be measured

Distinctive colour differences

Highly stable to light

Please request our special brochure

E. Merck, Darmstadt Germany

317/I-EO

Volume 1:
Carcinogens, Mutagens and Teratogens
of the 4 volume work

CHROMATOGRAPHY OF ENVIRONMENTAL HAZARDS

By **L. FISHBEIN**, National Institute of Environmental Health Sciences Research, Triangle Park.

1972, 506 pages, 210 tables, 239 illus. Dfl. 135.00 (ca. $42.25) ISBN 0-444-40948-3

Contents: **1. Introduction. 2. Tabular Summaries of Environmental Hazards. 3. Alkylating Agents:** Nitrosamines. Aziridine, aziridine phosphine oxides, sulfide, and melamine. Epoxides (ethylene and propylene oxides and their degradation products). Glycidol. Epichlorohydrin. Di(2,3-epoxypropyl) ether. 1,2:3,4-diepoxybutane. Aldehydes. Lactones. Trimethylphosphate. Pyrrolizidine alkaloids. **4. Pesticides:** Maleic hydrazide. Captan. Hemel and hempa. Aramite. DDVP. Trichlorfon. 2,4,5-T and dioxins. 3,4-dichloropropionanilide, 3,4-dichloroaniline and chloroazobenzenes. 3-amino-1H-1,2,4-triazole. Chlorobenzilate. Pentachloronitrobenzene. Mirex. β-hydroxyethylhydrazine. **5. Drugs:** Chlora hydrate. Antineoplastic drugs. Monoalkyl methanesulfonates. Antibiotics. N-hydroxyurea. Isonicotinylhydrazide. Thalidomide. Vinca alkaloids. D-lysergic acid diethylamide. **6. Food and Feed Additives and Contaminants:** Cyclamate and cyclohexylamine. Dulcin. Allyl isothiocyanate. Safrole. EDTA. Caffeine. Nitrofurazone. Cycasin. Mycotoxins. **7. Miscellaneous Toxicants:** Hydrazine and its derivatives. Naphthylamines and their metabolites. Urethan and N-hydroxyurethan. Organic peroxides. Hydrogen peroxide.

Elsevier
Book Division, P.O. Box 3489
Amsterdam, The Netherlands

479E

ANALYTICA CHIMICA ACTA
Vol. 60 (1972)

ANALYTICA CHIMICA ACTA

International monthly devoted to all branches of analytical chemistry
Revue mensuelle internationale consacrée à tous les domaines de la chimie analytique
Internationale Monatsschrift für alle Gebiete der analytischen Chemie

ELSEVIER PUBLISHING COMPANY
AMSTERDAM

Anal. Chim. Acta, Vol. 60 (1972)

Analytica Chimica Acta
Elsevier Publishing Company, Amsterdam
Printed in The Netherlands

N.M.R. STUDIES OF CHLORINATED POLYCYCLODIENE PESTICIDES

LAWRENCE H. KEITH and ANN L. ALFORD

Environmental Protection Agency, Federal Water Quality Administration, Southeast Water Laboratory, Athens, Ga. 30601 (*U.S.A.*)

and JAMES D. McKINNEY

National Institute of Environmental Health Sciences, National Institute of Health, Public Health Service and Department of Health, Education, and Welfare, Research Triangle Park, N. C. 27709 (*U.S.A.*)

(Received 18th December 1971)

Widespread usage of pesticides has raised the question of their influence on the environment, and n.m.r. spectroscopy is useful in the structural elucidation of their degradation or metabolic products[1]. This study is concerned with the n.m.r. spectra of the chlorinated polycyclodiene pesticides aldrin (I), dieldrin (II), isodrin (III), endrin (IV) and the important photolytic product of IV, photodieldrin (V). The

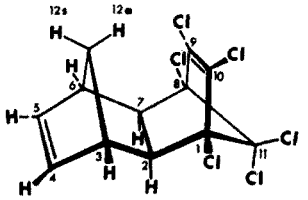

I

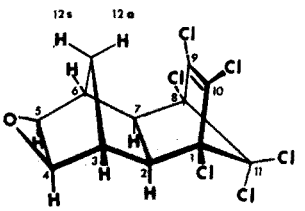

II

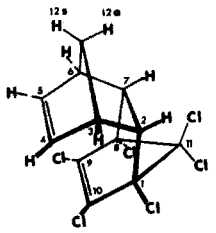

III

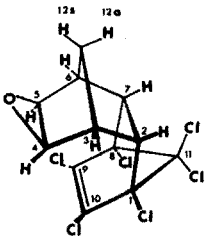

IV

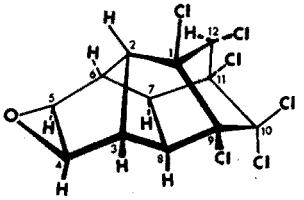

V

spectra of I–IV are similar in many respects and the various proton signals of these four compounds are discussed as a group. The spectra of photodieldrin are considered separately. The numbering system used herein for these compounds complies with that suggested by Benson[2].

THE N.M.R. SPECTRA OF COMPOUNDS I–IV

The methylene protons

Assignments of the relative chemical shifts for the methylene bridge proton resonances[3-6] are inconsistent—especially those of aldrin. The present assignments (Table I) are based on decoupling experiments involving long-range coupling of $H_{4,5}$ with H_{12a} (*anti* to the epoxide or CH=CH) and of $H_{2,7}$ with H_{12s} (*syn* to the epoxide or CH=CH). H_{12a} is upfield, relative to H_{12s}, in dieldrin, isodrin, and endrin, but downfield in aldrin. This anomaly in the spectrum of aldrin is caused by a unique combination of the diamagnetic anisotropy of the carbon–carbon double bond at C_4–C_5 shielding H_{12s} and steric compression of H_{12a} against the π-cloud of the

TABLE I

CHEMICAL SHIFTS (τ) OF COMPOUNDS I–V IN VARIOUS SOLVENTS

Compound	*Solvents*			
	H	*$CDCl_3$*	*C_6D_6*	*CD_3CN*
Aldrin (I)	2=7	7.26	7.42	7.24
	3=6	7.10	7.44	7.11
	4=5	3.72	4.22	3.66
	12a	8.42	8.46	8.44
	12s	8.68	8.91	8.70
Dieldrin (II)	2=7	7.30	7.68	7.14
	3=6	7.34	7.80	7.35
	4=5	6.89	7.65	6.76
	12a	9.00	9.14	9.03
	12s	8.73	8.84	8.77
Isodrin (III)	2=7	6.65	7.01	6.58
	3=6	7.01	7.50	7.00
	4=5	4.01	4.19	3.98
	12a	8.46	9.12	8.39
	12s	8.22	8.66	8.27
Endrin (IV)	2=7	6.78	7.25	6.74
	3=6	7.11	7.69	7.16
	4=5	6.70	6.89	6.78
	12a	9.07	9.78	9.01
	12s	8.21	8.48	8.34
Photodieldrin (V)	2	7.47	7.97	7.57
	3	6.81	8.09	6.79
	4	6.51	7.44	6.51
	5	6.71	7.74	6.70
	6	6.91	7.43	6.88
	7	7.33	8.09	7.24
	8	6.94	7.64	6.90
	12	5.14	5.69	4.74

ethano bridge. Protons situated above the plane of an olefinic double bond are shielded[7], and this would seem to be the case in both I and III; Dreiding models show no difference in the location of H_{12s} in these molecules. However, the H_{12s} signal of aldrin appears 0.25–0.46 p.p.m. upfield (depending on the solvent) from the corresponding proton signal of isodrin. McCulloch *et al.*[6] have provided evidence that the *anti* methylene proton in *exo–endo* fused ring systems such as I and II is sterically compressed against the π-cloud of the ethano bridge. This should change the dihedral angles of the bridge methylene protons in these systems from what they are in the *endo–endo* ring fusions where such compression is not possible. H_{12a} should be pushed up relative to the plane described by the *exo–endo* fused rings and in turn push H_{12s} closer to the π-cloud above the C_4–C_5 carbon–carbon double bond.

Irradiation of $H_{4,5}$ collapses the downfield multiplet of aldrin to a pair of triplets and irradiation of $H_{2,7}$ produces the same effect on the upfield multiplet[8],

TABLE II

COUPLING CONSTANTS (J) OF ALDRIN, DIELDRIN, ISODRIN AND ENDRIN

	2	3	4	5	6	7	12*a*
Aldrin							
3	0						
4	0	2.1					
5	0	1.5	0				
6	0	0	1.5	2.1			
7	0	0	0	0	0		
12a	0	1.8	0.6	0.6	1.8	0	
12s	0.8	1.3	< 0.5	< 0.5	1.3	0.8	10.5
Dieldrin							
3	0						
4	0	2.1					
5	0	1.5	0				
6	0	0	1.5	2.1			
7	0	0	0	0	0		
12a	0	1.8	0.6	0.6	1.8	0	
12s	0.8	1.3	< 0.5	< 0.5	1.3	0.8	10.5
Isodrin							
3	2.3						
4	0	2.0					
5	0	2.0	0				
6	1.5	0	2.0	2.0			
7	0	1.5	0	0	2.3		
12a	0	1.4	0.6	0.6	1.4	0	
12s	0	1.8	< 0.5	< 0.5	1.8	0	8.5
Endrin							
3	2.5						
4	0	0.9					
5	0	0.9	0				
6	1.5	0	0.9	0.9			
7	0	1.5	0	0	2.5		
12a	0	1.3	0.5	0.5	1.3	0	
12s	0	2.0	< 0.5	< 0.5	2.0	0	10.3

allowing the unambiguous assignments of 12-*anti* and 12-*syn* to the downfield and the upfield AB pair of doublets, respectively (Meinwald's "W-letter rule"[9]). These decouplings allow the $H_{3,6}$–H_{12a} coupling constant and the $H_{3,6}$–H_{12s} coupling constant to be observed (Table II).

When this same decoupling technique was attempted with dieldrin, it was discovered that the signal of $H_{2,7}$ was too close to $H_{3,6}$ in $CDCl_3$ to permit a clean decoupling of only the former protons from H_{12s} (Table I). In C_6D_6, problems arose because of the similar chemical shifts of $H_{2,7}$ and $H_{4,5}$. However, addition of a drop of trifluoroacetic acid to the C_6D_6 solution, or dissolving compound II in CD_3CN, produced signals separated enough so that decoupling of $H_{4,5}$ and $H_{2,7}$ from H_{12a} and H_{12s} was accomplished. $J_{3,6-12s}$ and $J_{3,6-12a}$ were identical with these same couplings in aldrin (Table II).

$J_{3,6-12s}$ and $J_{3,6-12a}$ in isodrin and endrin are similar but not identical (Table II). These two compounds, with *endo–endo* ring fusion, have the reverse order of the larger and smaller coupling constants; $J_{3,6-12a}$ is the larger constant in compounds I and II while $J_{3,6-12s}$ is the larger in compounds III and IV. This observation corroborates the postulated change in the dihedral angles of the bridge methylene protons in compounds I and II caused by steric compression of H_{12a} against the ethano bridge π-cloud—it would lessen the angle between $H_{3,6}$ and H_{12a} (from about 60° in compound III, increasing $J_{3,6-12a}$) and increase the angle between $H_{3,6}$ and H_{12s} (from about 60° in compound III) as the latter proton is pushed closer to the C_4–C_5 double bond (decreasing $J_{3,6-12s}$).

The $H_{4,5}$ protons

Bukowski and Cisak[5] describe the olefinic proton signals of aldrin and isodrin as "triplets" ($J=2$ Hz) caused from coupling with the equivalent adjacent bridgehead protons. We find that these signals are really each composed of a pair of doublets with the inner legs superimposed so that an *apparent* "triplet" is produced. Theoretical considerations preclude true triplets from these couplings. Irradiation of the bridgehead protons does indeed collapse the "triplet" to a singlet[5] but the explanation is that H_4 is coupled directly with H_3 and, through long-range coupling, with H_6; likewise, the equivalent H_5 is coupled directly with H_6 and, through long-range coupling, with H_3 (Table II). The spectrum of aldrin (Fig. 1) exhibits a further fine splitting of this "triplet" at a smaller sweepwidth ($J=0.6$ Hz). Irradiation of H_{12a} removes this coupling, proving it is the normal "W" long-range coupling.

The $H_{4,5}$ signals of dieldrin and endrin appear as multiplets that give no stereochemical information about the configuration of the epoxide oxygens. Irradiation of the endrin $H_{3,6}$ signal produces a small splitting in the $H_{4,5}$ signal ($J=0.5$ Hz) attributed to "W" long-range coupling of $H_{4,5}$ with H_{12a} that had been masked by $H_{3,6}$–$H_{4,5}$ coupling (Fig. 2). Irradiation of either H_{12a} or H_{12s} sharpens the $H_{4,5}$ multiplet and indicated the presence of "non-W" long-range coupling of $H_{4,5}$ with H_{12s}. Double-decoupling H_{12a} and H_{12s} from $H_{4,5}$ produces a clear "triplet" and proves the existence of "non-W" long-range coupling between $H_{4,5}$ and H_{12s} and enables $J_{3-4}=J_{5-6}$ and $J_{4-6}=J_{5-3}$ to be measured (Table II). Marchand *et al.*[10] also recently reported a similar small, but finite, "non-W" type of coupling in a substituted norbornane. Observing the methylene proton signals of endrin while irradiating $H_{4,5}$ provides further evidence for the $H_{4,5}$–H_{12s} coupling—*both* of the

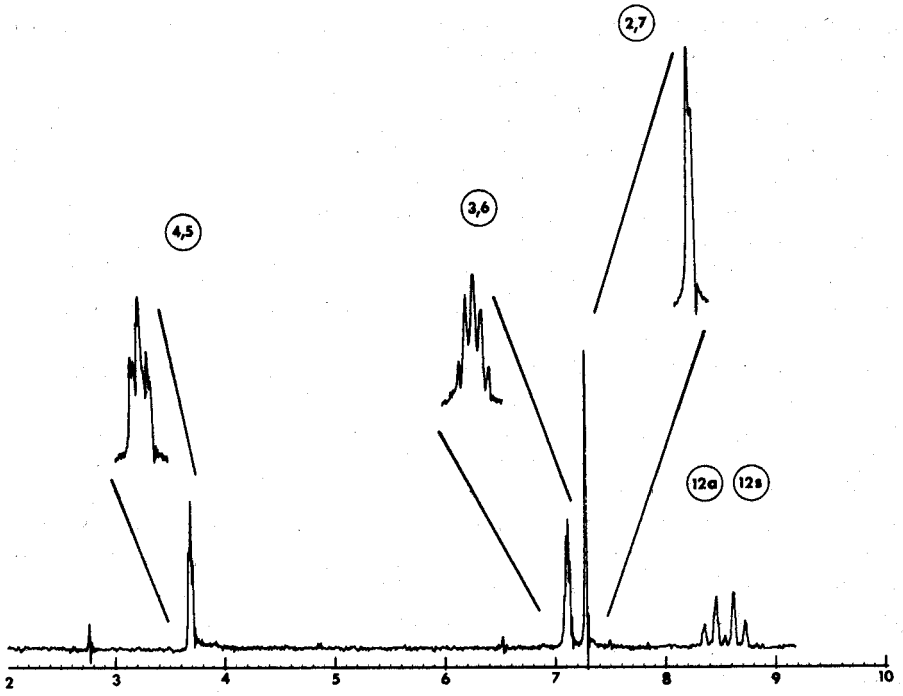

Fig. 1. The n.m.r. spectrum of aldrin with 250 Hz sweepwidth expansions.

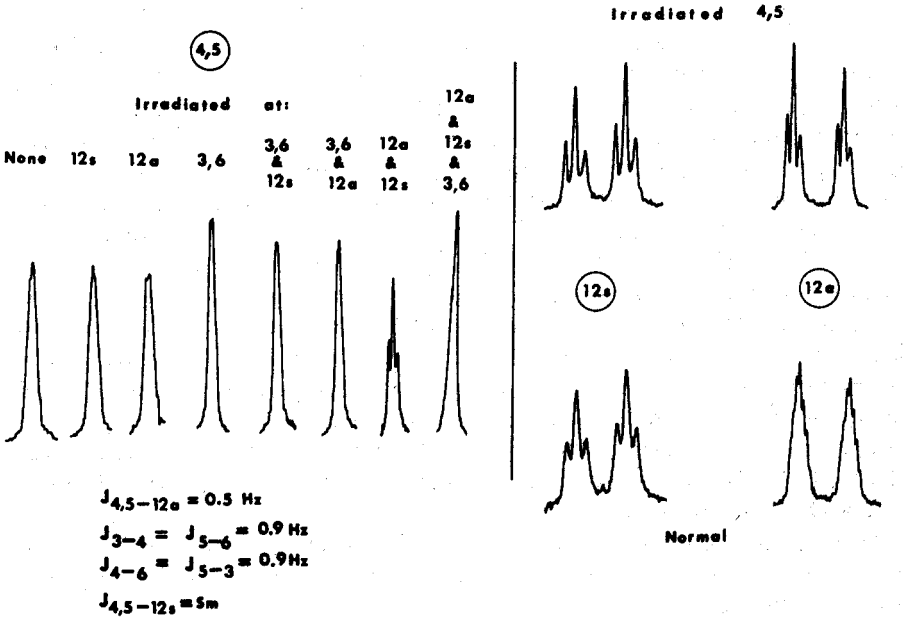

Fig. 2. The $H_{4,5}$ and methylene signals of endrin with the specified decoupling experiments.

signals are changed into an AB pair of *sharp* triplets. The downfield signal (H_{12s}) was already a pair of triplets, but irradiation of $H_{4,5}$ sharpened them.

Irradiation of dieldrin's $H_{4,5}$ perturbs the H_{12s} signal and irradiation of H_{12s} sharpens $H_{4,5}$ so that $J_{4,5-12a}$ can be observed (Table II). Double irradiation of H_{12s} and H_{12a} did not produce the pair of overlapping doublets in compound II as it did with compound IV. This same "non-W" coupling is also manifested in the spectra of isodrin and aldrin. The overlapping pair of doublets of isodrin is affected slightly by irradiation of H_{12s} but double decoupling produces a much greater sharpening of this signal than single decoupling of either H_{12a} or H_{12s}. Both methylene proton signals are affected when $H_{4,5}$ is irradiated; the AB pair of triplets from H_{12s} is sharpened as it was with endrin (Fig. 2).

If steric compression from the π-cloud of the ethano bridge could affect the dihedral angles of the methylene protons of dieldrin then it could possibly affect the dihedral angles of the $H_{4,5}$ protons in endrin also. Dreiding models show no difference in the $H_{3,6}$–$H_{4,5}$ dihedral angles of compounds II and IV, but the coupling constant between the bridgehead and the adjacent epoxy methine protons of compound IV is half that of the same constant in compound II (Table II). Based on molecular models, steric compression should cause a dihedral angle of lesser magnitude between these protons in compound IV than in compound II (about 45°). This usually results in a larger coupling constant, but the reverse effect was noted.

The fused-ring protons

P.m.r. spectroscopy is useful to differentiate between the *endo–exo* skeleton (I and II) and the *endo–endo* skeleton (III and IV) of the chlorinated polycyclodiene pesticides and their derivatives[8]. In the former, the $H_{2,7}$ signals appear as a singlet in the spectra, while in the latter these protons produce a pair of doublets because of vicinal coupling with the adjacent bridgehead proton and virtual coupling with the distant bridgehead proton. Double irradiation of the bridgehead protons collapses both doublets to a singlet in the spectra of the compounds possessing the *endo–endo* skeleton. The presence or absence of these couplings in the parent pesticides and their conversion products[11] (*cis*-aldrin-4,5-diol, *trans*-aldrin-4,5-diol, *cis*-isodrin-4,5-diol, 4-hydroxyaldrin, 4-ketoaldrin, photodieldrin, 4,5-dihydroaldrin, and 4,5-dihydroisodrin) distinguishes their skeletal systems and illustrates the applicability of this method for defining the ring fusion of unknown metabolites of these pesticides.

In addition to the expected "W" long-range coupling between H_{12s} and $H_{2,7}$ in aldrin, a "non-W" long-range coupling between H_{12a} and $H_{2,7}$ was observed. Figure 3 shows the $H_{2,7}$ singlet of aldrin in which a finer splitting is barely detectable. Irradiation of H_{12s} removes this splitting and irradiation of H_{12a} makes it more evident. For the latter phenomenon to occur there must be a small, but detectable coupling between H_{12a} and $H_{2,7}$. Double irradiation of H_{12a} and H_{12s} produces a sharp singlet for the $H_{2,7}$ signal. The line width of this signal at half height decreases from 2.8 Hz to 2.5 Hz with irradiation of either H_{12a} or H_{12s} and further decreases to 1.5 Hz with double irradiation.

These same decoupling experiments were applied to dieldrin with identical results, showing that both the normal "W" and also the unusual "non-W" long-range couplings were in effect.

Isodrin and endrin possess the *endo–endo* ring fusion, and this configuration

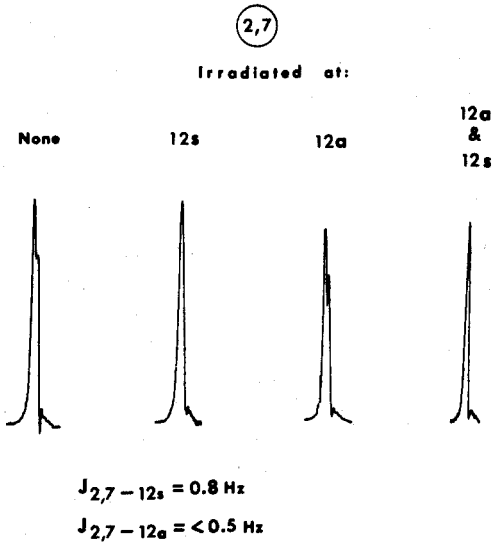

Fig. 3. The $H_{2,7}$ signal of aldrin with the specified decoupling experiments.

precludes the normal "W" long-range coupling between H_{12s} and $H_{2,7}$. The splitting of the $H_{2,7}$ signal into a pair of doublets tends to mask any small "non-W" coupling between $H_{2,7}$ and H_{12a} that may occur.

In view of the "non-W" long-range couplings between H_{12a} and $H_{2,7}$ in compounds I and II as well as others in compound V (discussed in the photodieldrin section), it seems likely that the H_{12s}–$H_{4,5}$ "non-W" long-range couplings are transmitted through the carbon–carbon *sigma* bonds rather than through space as first postulated[8].

The bridgehead protons

In all four pesticides the signals from the bridgehead protons were gross multiplets. The $H_{3,6}$ coupling constants were derived indirectly from decouplings involving irradiation of $H_{3,6}$ and by observing the effects on the other signals in the spectrum.

THE N.M.R. SPECTRA OF PHOTODIELDRIN AND PARAMAGNETIC CHEMICAL SHIFTS INDUCED BY $Eu(DPM)_3$

Robinson *et al.*[12] and Rosen *et al.*[13] independently and simultaneously proposed structure V for photodieldrin, and Parsons and Moore[14] presented data which corroborated this structure and reported chemical shift assignments and coupling constants after extensive study of the n.m.r. spectrum of compound V. However, there exists no evidence for the configuration of H_{12} and, depending on the mechanism of formation, it is possible for this proton to be either *syn* or *anti* to the epoxide.

Since H_{12} was reported to be uncoupled[14], there appeared to be no immediate method, other than by X-ray analysis, of confirming or revising the postulated

structure until the recent discovery of the chemical shift reagent, tris(dipivalomethanato)europium [Eu(DPM)$_3$][15,16]. This shift reagent behaves as a Lewis acid and associates with organic molecules (R-B) having a sterically unhindered basic coordinating site, such as O or N.

$$\text{Eu(DPM)}_3 + \text{R-B} \overset{k}{\rightleftarrows} \text{R-B} \cdot \text{Eu(DPM)}_3$$

The magnitude of the shift is thus dependent on the concentration of the shift reagent (assuming constant concentration of R-B) and the equilibrium constant. Since the affected n.m.r. signals show an "averaged" shift, the exchange between associated and unassociated organic molecules must be rapid relative to the n.m.r. time scale. Hinckley[15] recognized that the pseudocontact interaction is the major contributor to these paramagnetic shifts, with the possible exception of protons nearest the metal complex. Demarco *et al.*[17] confirmed that the pseudocontact interaction was the major contributor to the paramagnetic shifts in a series of alcohols studied, except for the protons geminal to the hydroxyl group and the OH proton itself; sizable contact contributions to the shifts of these protons were indicated. In addition, the extent of deshielding of protons vicinal to the hydroxyl appeared to be dependent on the dihedral angle between the OH and the vicinal proton.

Nevertheless, paramagnetic shifts for most protons in studies to date have been primarily influenced by the pseudocontact interaction in which the angular contribution to the shift is small or negligible. With the above exceptions in mind, most shifts are proportional to R^{-3} [at a given concentration of R-B and Eu(DPM)$_3$] where R is the distance of the proton in question from the europium atom. This dependence on R enables the relative distance of the various protons from the europium to be determined and, in the case of photodieldrin, to decide whether the migrated proton was *syn* or *anti* to the epoxide. Fraser and Wigfield[18] similarly used this reagent for assignments of configuration to rigid sulfoxides but the principal use of it has been to make signal assignments[19-22].

We found that Eu(DPM)$_3$ (prepared by the method of Eisentraut and Sievers[23]) associates with the epoxide oxygens of endrin (IV), dieldrin (II) and photodieldrin (V) and induces large paramagnetic shifts ($\Delta\delta$) of the signals of protons in adjacent and distant rings. Studies of the effects of varied concentrations of Eu(DPM)$_3$ on the n.m.r. spectra of these three compounds reflect the relationship between the distance of the protons from the europium atom and the magnitude of the chemical shift (Fig. 4). A family of curves is obtained from each compound. Endrin and dieldrin were run in carbon tetrachloride, but photodieldrin was run in deuterochloroform since it was only slightly soluble in CCl_4. The small amount of ethanol present in the $CDCl_3$ as a stabilizer apparently competes effectively with the epoxide oxygen for the europium complex; the curves for compound V do not extrapolate to zero. The deviations from linearity which endrin and dieldrin exhibit at low Eu(DPM)$_3$ concentrations are similar to those noted by Demarco *et al.*[17]; the deviations at high concentrations may be due to solubility problems.

Graphs of $\Delta\delta$ *versus* R^{-3} are straight lines for all three epoxides. The europium was moved in an arc around the oxygen in the Dreiding model and the distances to each were measured for several possible positions until the best fit on a curve was obtained. Figure 5 shows the plot obtained for photodieldrin by this method[24].

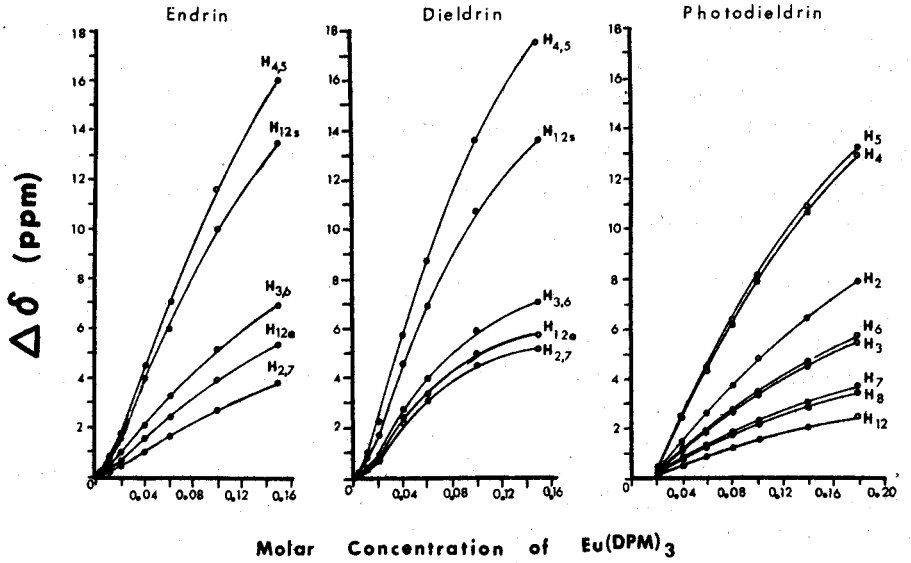

Fig. 4. Effect of varied concentrations of $Eu(DPM)_3$ on $\Delta\delta$ of 0.2 *M* endrin (in CCl_4), 0.2 *M* dieldrin (in CCl_4), and 0.2 *M* photodieldrin (in $CDCl_3$).

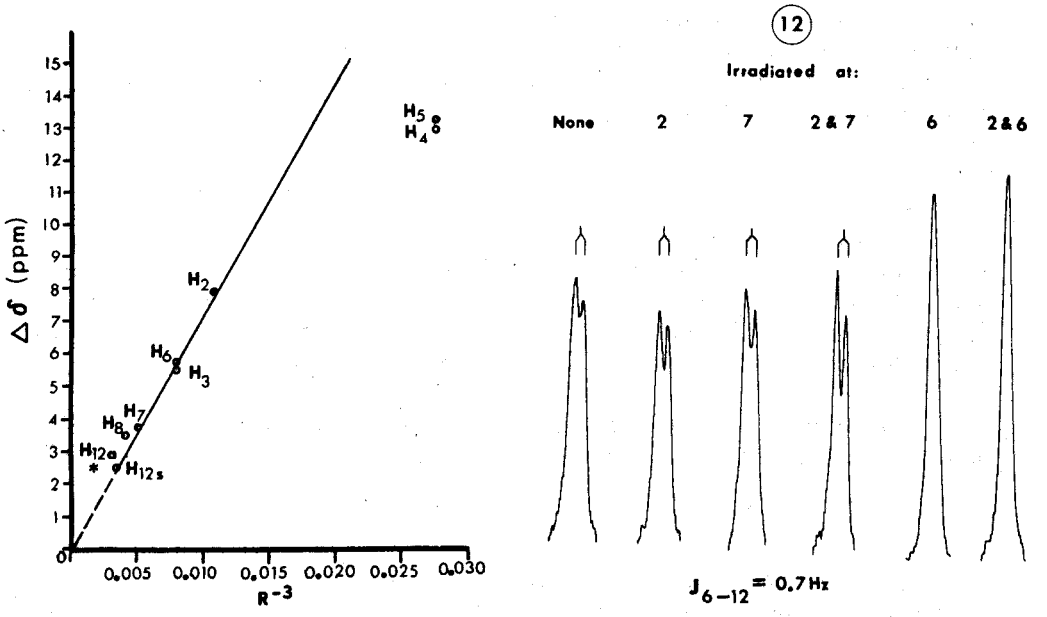

Fig. 5. Plot of the change in chemical shift ($\Delta\delta$) *vs.* the reciprocal of the cube of the distance of each proton from Eu of a 0.20 *M* solution of photodieldrin and 0.18 *M* solution of $Eu(DPM)_3$ in CCl_4.

Fig. 6. The H_{12} signal of photodieldrin with the specified decoupling experiments.

All except the two protons closest to the europium (H_4 and H_5) fit the curve; these are close enough to the europium so that other effects, such as contact interactions and/or angular dependence terms in the pseudocontact equation[15], may make significant contributions to the change in chemical shift and produce the resultant deviation from the curve. $\Delta\delta$ of H_{12} plotted for the configuration *syn* to the epoxide (H_{12s}) conforms well with the curve whereas the value for H_{12} in the *anti* configuration (H_{12a}, designated by the asterisk) does not. This indicates that the H_{12} is *syn* to the epoxide.

Close examination of the H_{12} "singlet" at a 100-Hz sweepwidth revealed that it is really a poorly resolved doublet with a small coupling constant ($J = 0.7$ Hz). Irradiation of either H_2 or H_7 sharpens the doublet perceptibly, and triple resonance at these frequencies doubles this effect (Fig. 6). Thus, both H_2 and H_7 have small long-range coupling (< 0.5 Hz) with H_{12}. Normally, such coupling is confined to protons separated by four bonds and in a "W" conformation with respect to one another—this would indicate that H_{12} is *anti* to the epoxide and would contradict the results obtained with Eu(DPM)$_3$. Irradiation of H_6 collapses H_{12} to a sharp singlet and double irradiation of H_2 and H_6 confirmed that H_6 was, indeed, coupled with H_{12}. It is unlikely that a coupling constant of this magnitude would be transferred through five *sigma* bonds; therefore, these two protons must be spatially close to one another. Examination of the model of photodieldrin reveals that H_6 and H_{12s} are the "bowsprit" and "flagpole" hydrogens on a six-membered ring rigidly held in a skewboat conformation. The distance between these two protons in a Dreiding model is only about 1.6 Å whereas the sum of the van der Waals radii of two hydrogens is 2.4 Å[25], so a transannular through-space coupling of these protons is the most likely cause of the H_{12} doublet. This observation confirms the H_{12s} assignment made on the basis of the $\Delta\delta$ *vs.* R^{-3} plot (Fig. 5). The $H_{12s-2,7}$ couplings are then two more examples of "non-W" long-range couplings, which seem to be prevalent in this family of pesticides and their derivatives.

EXPERIMENTAL

All spectra were recorded with a Varian* HA-100 nuclear magnetic resonance spectrometer, a 2–3% solution of tetramethylsilane (TMS) being used as internal standard. Homonuclear decoupling experiments were performed with three Hewlett Packard* Model 200-AB audiooscillators. All chemical shifts are expressed in terms of τ values and all coupling constants (J) are expressed in Hertz (Hz).

The authors wish to express their thanks to the suppliers of the pesticide standards used in this research and to Ronald G. Webb for the synthesis of Eu(DPM)$_3$.

SUMMARY

Complete n.m.r. coupling constants for aldrin, dieldrin, isodrin, endrin, and photodieldrin were derived by double, triple, and, where necessary, quadruple

* The trade names mentioned herein do not imply endorsement by the Water Quality Office or the Environmental Protection Agency.

resonance studies. Both the normal "W" long-range couplings as well as "non-W" long-range couplings were prevalent. Large paramagnetic shifts were induced by $Eu(DPM)_3$, and plots of the change in chemical shift *versus* the reciprocal of the cube of the distance from europium permitted tentative configurational assignment of the migrated proton in photodieldrin. Transannular, through-space coupling of the migrated proton with the nearby bridgehead proton confirmed this assignment.

RÉSUMÉ

Des études sont effectuées sur les constantes de r.m.n. de divers pesticides, soit par double, soit par triple, et même par quadruple résonance.

ZUSAMMENFASSUNG

Vollständige n.m.r.-Kopplungskonstanten für Aldrin, Dieldrin, Isodrin, Endrin und Photodieldrin wurden aus Doppel-, Dreifach- und, sofern notwendig, Vierfachresonanzuntersuchungen abgeleitet. Es traten sowohl die normalen "W"-förmigen "long range"-Kopplungen als auch nicht-"W"-förmige "long range"-Kopplungen auf. Grosse paramagnetische Verschiebungen wurden durch $Eu(DPM)_3$ hervorgerufen, und die Auftragungen der Änderung der chemischen Verschiebung gegen die reziproke dritte Potenz des Abstandes vom Europium erlaubten die versuchsweise konfigurationsmässige Zuordnung des gewanderten Protons in Photodieldrin. Transannulare "through space"-Kopplung des gewanderten Protons mit dem nahegelegenen Brückenproton bestätigte diese Zuordnung.

REFERENCES

1 For a summarizing reference, see: L. H. Keith and A. L. Alford, *J. Assoc. Off. Anal. Chem.*, 53 (1970) 1018.
2 W. R. Benson, *J. Assoc. Off. Anal. Chem.*, 52 (1969) 1109.
3 A. M. Parsons and D. J. Moore, *J. Chem. Soc., C*, (1966) 2026.
4 A. P. Marchand and J. E. Rose, *J. Amer. Chem. Soc.*, 90 (1968) 3724.
5 J. A. Bukowski and A. Cisak, *Ann. Soc. Chim. Polonorum*, 42 (1968) 1339.
6 R. McCulloch, A. R. Rye and D. Wege, *Tetrahedron Lett.*, (1969) 5163.
7 L. M. Jackman, *Applications of Nuclear Magnetic Resonance Spectroscopy in Organic Chemistry*, Pergamon Press, New York, 1959, p. 129.
8 L. H. Keith, A. L. Alford and J. D. McKinney, *Tetrahedron Lett.*, (1970) 2489.
9 J. Meinwald and A. Lewis, *J. Amer. Chem. Soc.*, 83 (1961) 2769.
10 A. P. Marchand, N. W. Marchand and A. L. Segre, *Tetrahedron Lett.*, (1969) 5207.
11 J. D. McKinney, L. H. Keith, A. L. Alford and C. E. Fletcher, *Can. J. Chem.*, 49 (1971) 1993.
12 J. Robinson, A. Richardson, B. Bush and K. E. Elgar, *Bull. Environ. Contam. Toxicol.*, 1 (1966) 127.
13 J. D. Rosen, D. J. Sutherland and G. R. Lipton, *Bull. Environ. Contam. Toxicol.*, 1 (1966) 133.
14 A. M. Parsons and D. J. Moore, *J. Chem. Soc.*, (1966) 2026.
15 C. C. Hinckley, *J. Amer. Chem. Soc.*, 91 (1969) 5160.
16 J. K. M. Sanders and D. H. Williams, *Chem. Commun.*, (1970) 422.
17 P. V. Demarco, T. K. Elzey, R. B. Lewis and E. Wenkert, *J. Amer. Chem. Soc.*, 92 (1969) 5734.
18 R. R. Fraser and Y. Y. Wigfield, *Chem. Commun.*, (1970) 1471.
19 C. C. Hinckley, *J. Org. Chem.*, 35 (1970) 2834.
20 P. V. Demarco, T. K. Elzey, R. B. Lewis and E. Wenkert, *J. Amer. Chem. Soc.*, 92 (1970) 5737.
21 G. H. Wahl, Jr. and M. R. Peterson, Jr., *Chem. Commun.*, (1970) 1167.
22 F. I. Carroll and J. T. Blackwell, *Tetrahedron Lett.*, (1970) 4173.
23 K. J. Eisentraut and R. E. Sievers, *J. Amer. Chem. Soc.*, 87 (1965) 5254.
24 L. H. Keith, *Tetrahedron Lett.*, (1) (1971) 3.
25 E. L. Eliel, *Stereochemistry of Carbon Compounds*, McGraw-Hill, New York, 1962, pp. 205–206.

Analytica Chimica Acta
Elsevier Publishing Company, Amsterdam
Printed in The Netherlands

METALLOFLUORESCENT INDICATORS AS SPRAY REAGENTS FOR THE *IN SITU* DETERMINATION OF ORGANOPHOSPHORUS PESTICIDES ON THIN-LAYER CHROMATOGRAMS*

T. F. BIDLEMAN, B. NOWLAN and R. W. FREI
Department of Chemistry, Dalhousie University, Halifax, Nova Scotia (Canada)
(Received 18th December 1971)

Although quantitation of thin-layer chromatograms by *in situ* fluorimetry has received much attention in recent years only a few procedures for the detection and determination of organophosphorus insecticides have been described[1-5]. Most of these methods depend on the reaction of bromine with easily oxidizable sulfur atoms in the pesticides to produce hydrobromic acid on the plate. The hydrobromic acid reacts with a pH-sensitive indicator[1] or liberates a fluorescent ligand from a non-fluorescent metal chelate[2-4]. Flavones have also been used as fluorigenic sprays after bromination[5], but are unselective.

Palladium chloride is a widely used detection reagent for sulfur-containing organophosphorus insecticides; although it is possible to distinguish these compounds from organophosphates which contain no sulfur[6], the sensitivity is poor and the chromogenic action is slow. The fluorescence of the so-called "metallofluorescent" indicators calcein (fluorescein-2,7-bis-methyliminodiacetic acid) and calcein blue (β-methylumbelliferonemethyleneiminodiacetic acid) is quenched by several transition metal ions, including palladium(II). When a quenched palladium(II)–indicator solution is sprayed on to a t.l.c. plate containing reactive sulfur-donating compounds, the fluorescent indicator is released. The method is highly sensitive and is suitable for quantitative *in situ* determination of organothiophosphorus insecticides.

EXPERIMENTAL

Reagents

Calcein and calcein blue were obtained from the G. Frederick Smith Chemical Co. (Columbus, Ohio, U.S.A.). Other calcein products were also tested (see Table I). The equivalent weights of the calcein products were determined by potentiometric titration with standard base[7,8]. Stock solutions (10^{-3} *M*) were prepared by dissolving the indicators in an equivalent amount of 0.1 *M* sodium hydroxide and diluting to volume. The solutions were stored at 4°. Fisher 5% palladium chloride in hydrochloric acid was used as a source of palladium. The concentration of the stock solution was checked spectrophotometrically by the iodide method[9] *versus* a standard solution prepared from 99.9% palladium wire (Alfa Inorganics Inc., Beverly, Mass.,

* Presented at the Pittsburgh Conference on Analytical Chemistry and Applied Spectroscopy, Cleveland, March, 1972.

TABLE I

COMPARISON OF CALCEIN PRODUCTS

Source	*Equiv. wt.*[a]	*Relative background fluor*[b]	*Fluor. ratio, spot : background*[c]
G. F. Smith	246	1.0	3.8
Fisher[d]	241	0.06	15
Koch-Light[e]	188	2.5	2.7

[a] Theoretical = 622.5/3 = 207.5[7,8].
[b] PdC I spray.
[c] 200 ng Guthion sprayed with PdC I.
[d] Fisher Scientific Co., Ltd., Montreal, Canada.
[e] Koch-Light Laboratories, Ltd., Colnbrook, England.

U.S.A.). Analytical standard pesticides were supplied by the manufacturers listed by Kenaga and Allison[10]. Stock solutions (1000 p.p.m.) were prepared in methylene chloride. All other chemicals and solvents were reagent-grade quality.

Apparatus

Fluorescence spectra were recorded with an Aminco-Bowman Spectrophotofluorimeter equipped with a t.l.c. scanning attachment. Quantitative measurements were carried out with a Zeiss Chromatogram Spectrophotometer with a mercury line excitation source. The instrument has been described in detail elsewhere[11]. An excitation wavelength of *ca.* 365 nm (Zeiss M365 filter) was used; fluorescence wavelengths were isolated with an emission monochromator. Peak areas of chromatograms were evaluated planimetrically.

Spray reagents

Solutions of the indicators, 0.005 *M* palladium chloride in 0.1 *M* hydrochloric acid, and buffer were mixed in the order given and diluted to volume to prepare stock spray reagents containing $2.0 \cdot 10^{-4}$ *M* palladium(II) and $1.6 \cdot 10^{-4}$ *M* calcein or $6.0 \cdot 10^{-4}$ *M* calcein blue. Phosphate buffer (0.05 *M*) was used to adjust the pH to 7.2. The sprays were allowed to stand for several hours or overnight to ensure maximum quenching, and were stable at room temperature for at least a month. The following working sprays were prepared immediately before use by dilution of the stock solutions.

PdC I $1.0 \cdot 10^{-4}$ *M* palladium(II), $8.0 \cdot 10^{-5}$ *M* calcein;
PdC II $5.0 \cdot 10^{-5}$ *M* palladium(II), $4.0 \cdot 10^{-5}$ *M* calcein;
PdCB $1.0 \cdot 10^{-4}$ *M* palladium(II), $3.0 \cdot 10^{-4}$ *M* calcein blue

(all sprays in 1:1 acetone–water).

Chromatography and spraying techniques

Glass t.l.c. plates (20 × 20 cm) were coated with a mixture of 30 g of silica gel N (Macherey, Nagel & Co., Düre, G.F.R. or Camag, Muttenz, Switzerland) and 80 ml of water with a Desaga t.l.c. applicator set at 0.25-mm layer thickness. Pesticides were spotted 2 cm from the bottom of the plate with 1-μl disposable "Microcaps"

(Drummond Scientific Co., Broomall, Pa., U.S.A.) or a Hamilton 10-μl syringe. The plates were developed by the ascending technique to a distance of 10 cm above the spotting line with the solvent systems in Table II and were sprayed until translucent with one of the above spray reagents. For qualitative detection the plates were dried with a hair dryer or placed in an oven at 60–70° for 15–30 min and then observed under long-wavelength u.v. light. For quantitative work the following drying techniques were employed. (1) The plates were allowed to stand for a few minutes after spraying

TABLE II

VISIBLE DETECTION LIMITS FOR ORGANOTHIOPHOSPHORUS INSECTICIDES

((−) indicates no visible reaction at the 100-ng level)

Pesticide	*Chemical name*	*Solvent system*[a]	R_F	*L.D. (ng)*[b]	
				PdC I	*PdCB*
Malathion	Diethyl mercaptosuccinate, S-ester with O,O-dimethyl phosphorodithioate	1	0.4	10–50	20
Cygon	O,O-Dimethyl-S-(methylcarbamoylmethyl) phosphorodithioate	2	0.2	10–20	20
Trithion	S-[(*p*-Chlorophenylthio)methyl] O,O-diethyl phosphorodithioate	1	0.8	10–50	10–50
Methyl trithion	S-[(*p*-Chlorophenylthio)methyl] O,O-dimethyl phosphorodithioate	4	0.5	10–20	10–50
Ethion	O,O,O′,O′-Tetraethyl-S,S′-methylene bisphosphorodithioate	1	0.7	10	10
Imidan	O,O-Dimethyl-S-phthalimidomethyl phosphorodithioate	1	0.3	10–20	10–20
Thimet	O,O-Diethyl-S-(ethylthio)methyl phosphorodithioate	4	0.6	10–50	20–50
Guthion	O,O-Dimethyl-S-4-oxo-1,2,3-benzotriazin-3-(4H)-ylmethyl phosphorodithioate	1	0.2	10–20	10–20
Di-Syston	O,O-Diethyl-S-2-(ethylthio)ethyl phosphorodithioate	4	0.6	10	10–50
Systox-thiol	O,O-Diethyl-S-2-(ethylthio)ethyl phosphorothioate	1	0.3	10–50	10–50
Ronnel	O,O-Dimethyl-O-2,4,5-trichlorophenyl phosphorothioate	4	0.6	50–100	100–(−)
Proban	O,O-Dimethyl-O-*p*-sulfamoylphenyl phosphorothioate	3	0.5	10–50	50–(−)
Fenthion	O,O-Dimethyl-O-[4-(methylthio)-*m*-tolyl] phosphorothioate	1	0.6	50–(−)	50–(−)
Parathion	O,O-Diethyl-O-*p*-nitrophenyl phosphorothioate	1	0.6	20–50	50–(−)
Folithion	O,O-Dimethyl-O-(3-methyl-4-nitrophenyl) phosphorothioate	1	0.5	50–100	100–(−)
Dursban	O,O-Diethyl-O-(3,5,6-trichloro-2-pyridyl) phosphorothioate	5	0.3	50–100	50–100

[a] Solvent systems: (1) 3:1 hexane–acetone, (2) 2:1 hexane–acetone, (3) 1:1 hexane–acetone, (4) 9:1 hexane–ethyl ether, (5) 99:1 hexane–ethyl ether.

[b] Visible within 1 h after drying the plate.

to ensure uniform distribution of the reagent and then oven-dried as above. After drying the plates were stored for 18–24 h in contact with the ambient air or in a closed chromatography tank containing a saturated solution of calcium nitrate to allow full fluorescence to develop. The saturated salt solution maintained the relative humidity of the tank at 51 %. The plates were protected from direct light during this storage time. (2) The plates were allowed to air-dry for 18–24 h at room temperature after spraying.

RESULTS AND DISCUSSION

Choice of spray compositions

The quenching ratios of palladium:calcein and palladium:calcein blue were found to be *ca.* 1:1 and 1:4, respectively. Definite confirmation of the stoichiometries was unobtainable because the purity of the indicators was unknown. Wallach and Steck[7] reported 1:1 metal:calcein quenching ratios for copper(II), nickel(II), and cobalt(II); Holzbecher[12] has found 1:4 metal:calcein blue quenching ratios for the same metals. It was found that an excess of palladium with respect to the quenching ratio resulted in a decrease in background fluorescence on the plate; however, a large excess reduced the sensitivity of the method. A 25–50 % excess of palladium was optimal. The fluorescence of the spots and background varied somewhat with the calcein product used to prepare the reagents. The background fluorescence is likely due in part to a fluorescein impurity in the calcein[13]. Calcein products from three sources are compared in Table I. Unless otherwise stated, the results in this work were obtained with the G. F. Smith calcein, which was found to contain 2.3 % residual fluorescein by the method of Diehl and Oulman[14].

Qualitative detection of pesticides

Detection studies were carried out with 100-, 50-, 20-, and 10-ng quantities of the pesticides in Table II. Each pesticide was tested on three or more plates with PdC I and PdCB reagents. For best results the plate should be sprayed until translucent, *i.e.* until the layer is saturated but not dripping. Over-spraying reduces the sensitivity. If there is a tendency to over-spray, the use of a more dilute reagent such as PdC II gives improved results. The fluorescence of the spots increases slowly after spraying and the detection limits given are for 1 h after drying the plate.

The organophosphorus insecticides tested may be classified as phosphates (A), phosphorothioates (B, C), and phosphorodithioates (D):

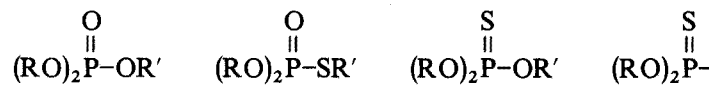

(A) (B) (C) (D)

Phosphate insecticides (A) do not react with the reagents. This is expected, since these compounds are not detectable with a palladium chloride spray[6]. The phosphorodithioate pesticides are the most reactive and gave more reproducible results than those of type (C). Only one pesticide of type (B) was tested. The thiol isomer of Systox appears to react similarly to the phosphorodithioate group, but general conclusions cannot be drawn from this single result.

The reactivities of some other classes of organic and inorganic compounds are listed in Table III. Since the mechanism of the fluorescence production involves the displacement of the indicator from the palladium by the pesticide, other compounds which complex palladium strongly would be expected to behave similarly. This is shown by the reaction of mercaptans and iodide ion, both of which are known to form stable complexes with palladium(II). The fact that organic sulfides are poorly detectable suggests that the thioether sulfur in pesticides such as Trithion and Thimet is not particularly reactive toward the reagents.

TABLE III

REACTIONS OF OTHER TYPES OF ORGANIC AND INORGANIC COMPOUNDS

(Reactivities: (+ + +) visible reaction at 0.1 μg; (+ +) visible reaction at 1 μg; (+) visible reaction at 10 μg; (−) no visible reaction at 10 μg)

Compound	*Reactivity*[a]	*Comments*
Phosphates, phosphoramidates:		
(no sulfur)		
O-4-*tert.*-Butyl-2-chlorophenyl O-methyl methylphosphoramidate (Ruelene insecticide)	(+)	Weak
O,O-Diethyl-O-(3,5,6-trichloro-2-pyridyl) phosphate (Dursban insecticide, oxygen analog)	(−)	
Phenols:		
Phenol	(−)	
Resorcinol	(−)	
Amines:		
n-Butylamine	(+ + +)–(+ +)	
Diethylamine	(+ +)	
Triethylamine	(+)	
Mercaptans:		
1-Mercaptohexadecane	(+ + +)	Fast reaction
1-Mercaptooctane	(+ + +)	Fast reaction
Organic sulfides:		
Ethyl sulfide (diethyl thioether)	(+)	
Phenyl sulfide (diphenyl thioether)	(−)	
Heterocyclic sulfur:		
3-Methylthiophene	(−)	
Tetrachlorothiophene (penphene insecticide)	(−)	
Sulfoxides, sulfones, sulfonic acids:		
Dimethyl sulfoxide	(+)–(−)	
p-Toluenesulfonic acid	(−)	
p-Chlorophenyl 2,4,5-trichlorophenyl sulfone (Tedion insecticide)	(−)	
Inorganic compounds:		
Sodium sulfate	(−)	
Sodium sulfite	(+ +)	
Sodium sulfide	(+ + +)	Fast reaction
Potassium bromide	(+)	
Potassium iodide	(+ + +)	

[a] PdC I spray.

Fluorescence spectra

The excitation and emission spectra (uncorrected) of calcein and calcein blue on dry silica gel N are shown in Fig. 1. The emission maxima of both indicators are independent of the excitation wavelength. Calcein in solution at pH 7.4 has an emission maximum at 511 nm[7,8] compared to 518±3 nm on the plate. The spectrum of a Cygon spot sprayed with palladium–calcein is the same as that of the free indicator (Fig. 2). The excitation maximum of calcein is too close to the emission peak to be useful for analytical work; however, excitation with the Zeiss M365 filter provided adequate sensitivity.

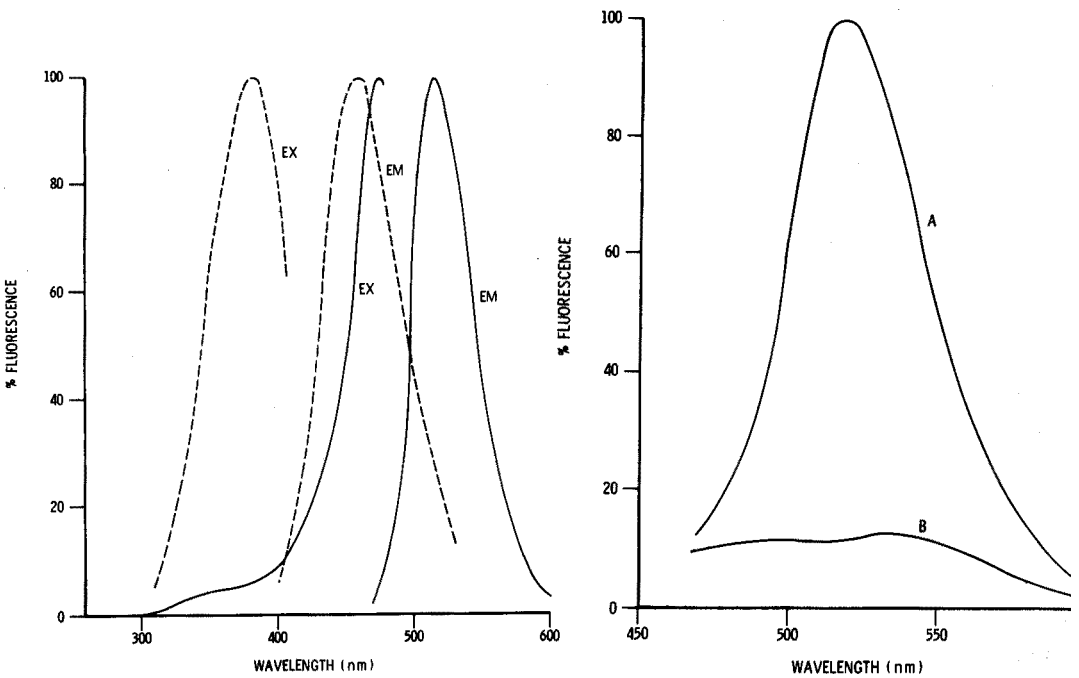

Fig. 1. Excitation (EX) and emission (EM) spectra (uncorrected) of calcein (——) and calcein blue (----) in pH 7.2 phosphate buffer spotted on Silica Gel N. Fluorescence is % of maximum value.

Fig. 2. Emission spectra of (A) 4 μg of Cygon sprayed with PdC I and (B) sprayed silica gel background. Excitation wavelength 350 nm.

Effect of time on the fluorescence

Several workers have commented on the slowness of palladium chloride detection methods for organophosphorus insecticides[6,15,16], although previous quantitative studies have not been made. The spots on a sprayed plate which is air-dried at room temperature become visible slowly and the fluorescence increases over several hours (Fig. 3). There did not appear to be a significant difference in the reaction rates of Guthion, Cygon, and Imidan (all phosphorodithioate pesticides); but the plate-to-plate variations were large, especially during the first few hours of drying. The reaction did not occur to an appreciable extent if the plate was kept wet, *e.g.* by covering with a glass sheet after spraying. The intensity of spots on plates

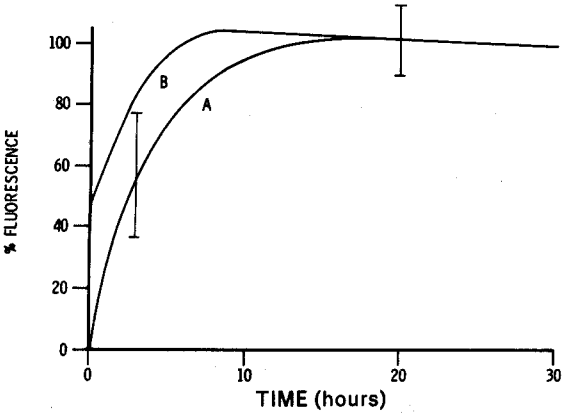

Fig. 3. Time dependence of the fluorescence of sprayed pesticide spots. Vertical lines represent the range of values obtained on 10 plates. Fluorescence is given as % of the 24-h value. (A) 200 ng Guthion, Cygon, or Imidan sprayed with PdC I. Plates allowed to air-dry at room temperature; time scale is from time of spraying; (B) 50–200 ng Guthion sprayed with PdC II. Plates dried for 20–30 min at 60° and allowed to stand in the ambient air; time scale is from end of oven-drying period.

which had been oven-dried (15–60 min) after spraying was about half of the maximum value (Fig. 3) and was independent of the drying time. The fluorescence increased after removing the plate from the oven if the plate was exposed to the ambient air or placed in a humidified atmosphere. The fluorescence did not increase if the oven-dried plate was stored in a desiccator over Drierite (anhydrous calcium sulfate).

According to these results, it appears that the reaction between palladium and the pesticide does not occur readily in solution but only in the adsorbed state. The plate must contain some moisture in order for the reaction to proceed, and that provided by the normal humidity of the laboratory (45–70%) is evidently sufficient.

Occasionally plates were found to have an abnormally high fluorescent background after the 18–24 h fluorescence development period. This did not occur if the plates were stored in the humidified chromatography tank after oven-drying rather than in the open air, and suggests that impure laboratory air was probably responsible.

Stability of the fluorescence to u.v. irradiation

The effects of continuous irradiation and replicate scanning of sprayed pesticide spots are shown in Figs. 4 and 5. Sprays containing calcein produced very stable spots which could be scanned repeatedly without a significant change in fluorescence. Calcein blue was much less stable to u.v. irradiation. For this reason palladium–calcein sprays were used in all quantitative work even though quantitative results could be obtained with the palladium–calcein blue reagent.

Quantitative study

An evaluation of the use of palladium–calcein spray reagents for the *in situ* determination of phosphorodithioate insecticides was carried out with Cygon and Guthion. Plots of peak area *versus* quantity of pesticide were linear over a 10–15 fold range; the linear region depended on the pesticide and the spray used. The approxi-

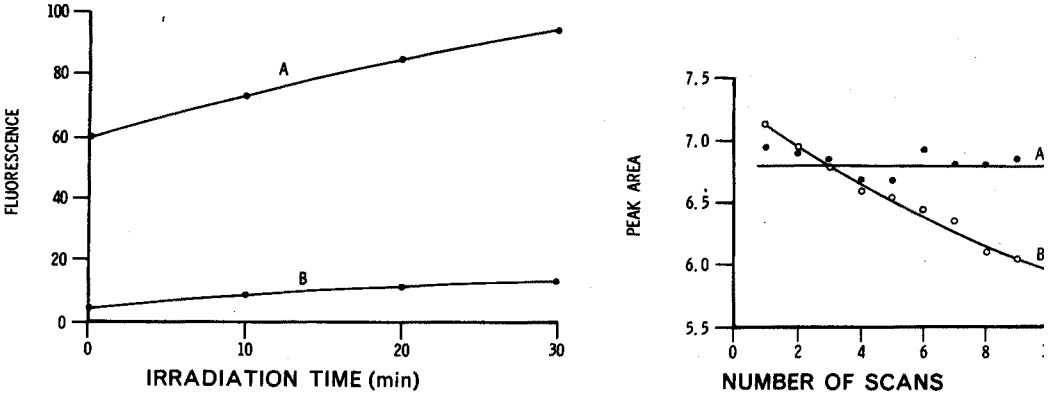

Fig. 4. 100 ng Guthion sprayed with PdC II and continuously irradiated (after fluorescence development) with u.v. light (Zeiss M365 filter). (A) Guthion spot; (B) sprayed background.

Fig. 5. Effect of repetitive scans on the fluorescence of 100-ng Cygon spots sprayed with (A) PdC I (518 nm emission); (B) PdCB (450 nm emission).

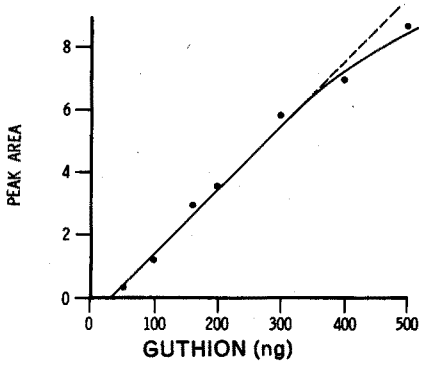

Fig. 6. Calibration curve for the determination of Guthion, PdC I spray.

mate linear ranges for the two pesticides studied were Guthion: 40–400 ng (PdC I), 10–150 ng (PdC II); Cygon: 10–150 ng (PdC I), 5–80 ng (PdC II). A typical calibration curve for Guthion is shown in Fig. 6. Such curves usually did not pass through the origin but intersected the abscissa at a positive value, probably because of the excess palladium in the spray reagents.

The relative standard deviations of replicate spots of Guthion or Cygon on a t.l.c. plate are given in Table IV. No attempt was made to compare spots on different plates. The reproducibility depended largely on the uniform distribution of the spray, and for this reason the plates were sprayed until translucent. Oven-drying was preferable to allowing the plates to dry at room temperature, as it minimized the spreading of the spots by diffusion.

APPLICATION OF THE METHOD

Samples of local lake water (500 ml) were spiked with 1–10 μg of Cygon. The

TABLE IV

REPRODUCIBILITY OF REPLICATE SPOTS OF GUTHION AND CYGON

Pesticide	*ng/spot*	*No. of plates*[a]	*% Rel. s.d., range and mean*[b]	*Spray*
Guthion	400	4	2.9– 5.5 (4.2)	PdC I
Guthion	200	5	3.3– 7.8 (5.5)	PdC I
Guthion	100	5	3.9– 7.7 (6.1)	PdC I
Guthion	200	6	3.4– 7.2 (5.8)	PdC II
Guthion	100	6	4.7– 8.2 (6.0)	PdC II
Guthion	50	7	2.5–11.7 (6.7)	PdC II
Guthion	20	6	4.7–23.6 (14.0)	PdC II
Cygon	100	5	2.4– 6.8 (5.4)	PdC II
Cygon	50	4	5.2–13.9 (8.9)	PdC II
Cygon	10	4	9.0–12.2 (10.0)	PdC II

[a] 7–9 spots per plate.

[b] $\text{s.d.} = \left(\frac{\Sigma(X-\bar{X})^2}{n-1}\right)^{\frac{1}{2}}$; $\%\,\text{Rel. s.d.} = \frac{\text{s.d.}}{\bar{X}} \cdot 100$.

samples were extracted with three portions of methylene chloride, shaking each portion for 1 min. The extracts were combined, dried with anhydrous sodium sulfate, and concentrated to a small volume with a rotary evaporator operated at 30°. The residue was transferred to a 1-ml volumetric flask and diluted with methylene chloride. Blanks were run in a similar manner on unspiked samples. Aliquots of the extract were spotted on t.l.c. plates along with suitable Cygon standards. The plates were developed in 2:1 hexane–acetone and sprayed and dried as previously described.

Recoveries of Cygon ranged from 87 to 113% with a mean of 102%. Interference from other compounds in the lake water was small. Spots of the extracts fluoresced on the plate even before spraying with the reagent. Most of this fluorescence remained at the origin however, and the interference with the Cygon spots at R_F = 0.2 corresponded to only 0.3 μg of the pesticide per liter. Two or three plates were run for every extracted sample, each containing two spots of the extract. The results in Table V are therefore the means of 4–6 replicate spots.

TABLE V

RECOVERY OF CYGON FROM LAKE WATER SAMPLES

Taken ($\mu g\ l^{-1}$)	*Found* ($\mu g\ l^{-1}$) $\pm$ *s.d.*[a]	*% Recovery*
20.0	20.7 $\pm$ 1.8	104
16.0	17.3 $\pm$ 1.0	109
8.00	8.00 $\pm$ 0.47	100
6.00	5.20 $\pm$ 0.43	87
4.00	3.94 $\pm$ 0.22	99
2.00	2.00 $\pm$ 0.05	100
2.00	2.25 $\pm$ 0.42	113

[a] Mean of 4–6 results.

CONCLUSIONS

The proposed method is the most sensitive yet developed for the *in situ* determination of phosphorodithioate insecticides on thin-layer chromatograms. Previously published methods[4,5] are applicable to quantities of pesticide up to several micrograms, but their reproducibility is poor below 100 ng. The slow reaction time is only a minor drawback, since it is convenient to spray the plates on one day and to measure the fluorescence on the next. Although gas chromatography is more sensitive for most organophosphorus pesticides, the fluorimetric t.l.c. procedure is useful as a check method and should prove especially valuable for certain pesticides (*e.g.* Guthion[17]) which are not easily analyzed by gas chromatography.

It is obvious that this ligand-displacement principle is not restricted to the analysis of pesticides. Mercaptans, for example, are very reactive and easily detected by this method. Palladium–calcein sprays have also been used to detect several metal–diethyldithiocarbamate chelates on thin-layer chromatograms[18]. Other metal–ligand combinations may be more suitable for the detection of different classes of organic compounds. The nature of the palladium–pesticide interaction is of considerable interest, and studies in this direction are in progress.

This work was supported by the Canada Department of Fisheries and Forestry.

SUMMARY

Fluorescence-quenched solutions of palladium(II)–calcein and palladium(II)–calcein blue are shown to be sensitive spray reagents for the detection and *in situ* determination of organothiophosphorus insecticides on thin-layer chromatograms. The palladium is displaced from its non-fluorescent indicator complex by the pesticide producing fluorescent spots on the plate. Visual detection limits for 16 insecticides are given. As little as 10–50 ng of phosphorodithioate pesticides can be detected within 1 h after spraying and drying the plate, while the detection limits for phosphorothioates are somewhat higher (*ca.* 50–100 ng). Quantitative measurements may be conveniently made 18–24 h after spraying and drying the plate. Plots of fluorescence (as peak area) *versus* quantity of pesticide are linear over a 10–15 fold range. The relative standard deviation of replicate spots of Guthion (50–400 ng) and Cygon (50–100 ng) is 4–9% and less than 15% for 10 ng of Cygon or 20 ng of Guthion. The method was applied to the analysis of lake water spiked with Cygon. The recovery of 2–20 $\mu g\ l^{-1}$ of the pesticide was 87–113% with no clean-up other than t.l.c. required.

RÉSUMÉ

Les solutions de palladium(II)–calcéine et de palladium(II)–bleu calcéine constituent des réactifs ("spray") sensibles pour la détection et le dosage d'insecticides organothiophosphorés sur chromatogrammes en couche mince. Le palladium est déplacé de son complexe non-fluorescent par le pesticide, produisant des taches fluorescentes sur la plaque. Les limites de détection visuelle sont données pour 16 produits. Des mesures quantitatives peuvent se faire 18 à 24 h après le spray et le séchage de la plaque. Cette méthode a été appliquée à l'analyse d'une eau de lac.

ZUSAMMENFASSUNG

Lösungen von Palladium(II)–Calcein und Palladium(II)–Calcein blau, deren Fluoreszenz gelöscht ist, sind empfindliche Sprühreagenzien für den Nachweis und die *in situ*-Bestimmung von Organothiophosphor-Insektiziden auf Dünnschicht-Chromatogrammen. Das Palladium wird aus seinem nichtfluoreszierenden Indikator-Komplex durch das Pestizid verdrängt, das auf der Platte fluoreszierende Flecken erzeugt. Die visuellen Nachweisgrenzen für 16 Insektizide werden angegeben. So geringe Mengen wie 10–50 ng Phosphordithioat-Pestizide können innerhalb 1 h nach dem Besprühen und Trocknen der Platte nachgewiesen werden, während die Nachweisgrenzen für Phosphorthioate etwas höher liegen (*ca.* 50–100 ng). Quantitative Messungen können günstig 18–24 h nach dem Besprühen und Trocknen der Platte durchgeführt werden. Die Auftragungen der Fluoreszenz (als Peakfläche) gegen die Menge des Pestizids sind über einen 10–15-fachen Bereich linear. Die relative Standardabweichung bei den von 50–400 ng Guthion und 50–100 ng Cygon erhaltenen Flecken ist 4–9 % und kleiner als 15 % bei 10 ng Cygon oder 20 ng Guthion. Die Methode wurde auf die Analyse von Seewasser, das mit bestimmten Mengen Cygon versetzt worden war, angewendet. Die Rückgewinnung von 2–20 $\mu g\ l^{-1}$ des Pestizids war 87–113 %, wobei ausser der Dünnschicht-Chromatographie keine Aufbereitung erforderlich war.

REFERENCES

1 P. E. Belliveau and R. W. Frei, *Chromatographia*, 4 (1971) 189.
2 M. T. H. Ragab, *J. Assoc. Off. Agric. Chem.*, 50 (1967) 1088.
3 P. E. Belliveau, V. Mallet and R. W. Frei, *J. Chromatogr.*, 48 (1970) 478.
4 R. W. Frei and V. Mallet, *Int. J. Environ. Anal. Chem.*, 1 (1971) 99, 141.
5 R. W. Frei, V. Mallet and C. Pothier, *J. Chromatogr.*, 59 (1971) 135.
6 O. Antoine and J. Mees, *J. Chromatogr.*, 58 (1971) 247.
7 D. Wallach and T. Steck, *Anal. Chem.*, 35 (1963) 1035.
8 D. Wallach, D. Surgenor, J. Soderberg and E. Delano, *Anal. Chem.*, 31 (1959) 456.
9 J. G. Fraser, F. E. Beamish and W. A. E. McBryde, *Anal. Chem.*, 26 (1954) 495.
10 E. E. Kenaga and W. E. Allison, *Bull. Entomol. Soc. Amer.*, 15 (1969) 85.
11 G. Pataki, *Chromatographia*, 1 (1968) 492.
12 J. Holzbecher, unpublished results, Dalhousie University, Halifax, Nova Scotia, Canada, 1971.
13 H. Diehl, *Calcein, Calmagite, and o,o'-Dihydroxyazobenzene. Titrimetric, Colorimetric and Fluorimetric Reagents for Calcium and Magnesium*, G. Frederick Smith Chemical Co., Columbus, Ohio, 1964.
14 H. Diehl and K. Oulman, in ref. 13 (otherwise unpublished work).
15 R. Blinn, *J. Assoc. Off. Agric. Chem.*, 46 (1963) 952; 47 (1964) 641.
16 M. Salamé, *J. Chromatogr.*, 16 (1964) 476.
17 J. Ruzicka, J. Thompson and B. B. Wheals, *J. Chromatogr.*, 30 (1967) 92.
18 R. M. Cassidy, V. Miketukova and R. W. Frei, *Anal. Lett.*, 5 (1971) 115.

Analytica Chimica Acta
Elsevier Publishing Company, Amsterdam
Printed in The Netherlands

A SIMPLE ATMOSPHERIC MICROWAVE-EXCITED EMISSIVE DETECTOR FOR GAS CHROMATOGRAPHY

R. M. DAGNALL, T. S. WEST and P. WHITEHEAD
Department of Chemistry, Imperial College of Science and Technology, London, SW7 2AY (England)
(Received 25th October 1971)

A survey of gas-chromatographic detectors emphasizes the fact that few detectors are selective and virtually none can be utilized for both quantitative and qualitative analytical purposes. At best, detectors such as the flame photometric detector offer high selectivity, but they can only be used for a very limited range of component vapors. At the other extreme the more common universal detectors offer few facilities for qualitative analysis. Indications are that future detector development should lie in the area of general spectroscopic detectors which are inherently selective in their mode of action, particularly in the atomic state, and which can be used for both quantitative and qualitative analyses. Probably the most promising new development in this area is the microwave-excited emissive detector[1-5]. However, those designs which have been used so far, have tended to be of the low-pressure type and have received in consequence a "high-complexity" rating[6]. The low-pressure system has been recommended because it provided greater sensitivity than an atmospheric system, but this obviously depends on the experimental system and wavelength of measurement.

In the work described here, atmospheric microwave-excited emissive detectors were examined. Unlike the original publications[1,2], special emphasis was placed on optimizing the microwave systems for highest sensitivity and linear working range in general routine analytical separations by gas chromatography. It has been established that the atmospheric-type detector is simpler than the low-pressure systems and is less limited in application and selectivity. The sensitivity, range of linearity and multi-channel aspects shown by this type of detector should encourage its use in gas-chromatographic analysis.

EXPERIMENTAL

The experimental arrangement is shown in Fig. 1. A Pye Model Series 104 Chromatograph was used and the microwave-excited detector was substituted for the more usual katharometer supplied with the instrument. The new detector consisted of a 2-mm i.d. quartz tube, some 20 cm in length, positioned directly above the oven through which the argon carrier gas and effluent from the column passed. The tube was surrounded by a three-quarter-wave microwave resonant cavity and power (2450 MHz$\pm$25 MHz) was supplied from a "Microtron 200" generator (Electro-Medical Supplies Ltd., Wantage) coupled to a reflected power meter. Emission from the argon plasma was monitored with a small grating monochromator (Rank

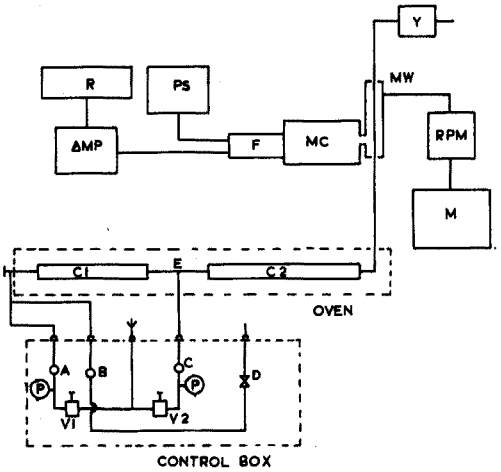

Fig. 1. Experimental arrangement. ○(A, B, C), On/off taps; P, pressure gauges (0.210 kN m^{-2}); V(1, 2), pressure controllers (Watts type 15-2, 0.175 kN m^{-2}); D, needle valve; C1 and C2, chromatographic columns; MW, microwave cavity; MC, monochromator; F, photomultiplier; PS, power supply; R, recorder; M, microtron; RPM, reflected power meter; Y, bubble meter; ΔMP, amplifier.

Precision Industries Ltd., London, U.K., Type D292) fitted with an EMI 9601B photomultiplier which was supplied at 1 kV from a Brandenburg PM2500R power supply. The read-out unit consisted of a microammeter and a 0–10 mV Honeywell recorder.

The analysis time was limited by use of the back-flushing system shown in Fig. 1. Columns 1 and 2 were Porapak S, 6-mm diameter columns of *ca.* 30 and 70 cm length, respectively. With taps B and C closed and tap A open, the system functioned normally and a sample injected travelled through both columns. A solvent with a long retention time was used generally and after the individual components to be resolved had passed through the T-piece (E) connecting the two columns, taps B and C were opened and tap A was closed. The pressure at E was adjusted by control valve V_2 and the needle valve D so that the gas flow through the second column and the plasma was unchanged. The solvent, still in column 1, was then back-flushed at *ca.* twice the previous flow rate and ejected. Hence, as soon as the sample peaks were recorded the flows could be reversed and a further sample injected.

Flow rates up to 9 l h^{-1} were measured with a bubble flow-meter, and flow rates up to 30 l min^{-1} with a MeTeRaTe D tube (Glass Precision Engineering Ltd., Hemel Hempstead).

The detector was arranged so that the quartz tube was held vertical and extended *ca.* 10 cm on each side of the cavity centre so that the argon plasma discharge was formed completely within the tube. The upper end of the tube was connected via polythene tubing to a 500-ml bottle and thence to the atmosphere. This arrangement was used to reduce the possibility of plasma noise caused by draughts and/or air diffusion at the top of the quartz tube.

Several microwave resonant cavities were examined, *viz.* quarter-wave and three-quarter-wave and variations of these; the three-quarter-wave cavity was preferred because it produced a long (*ca.* 8 cm) stable discharge with negligible local

overheating of the quartz tube. A long discharge is advantageous because only the emission from the more stable central section of the plasma enters the monochromator. This appears to be the first reported use of this type of cavity with an atmospheric detector system.

The narrower the quartz tubing used, the more intense was the emission from the plasma. However, with tubing of 1 mm i.d., local hot-spots developed with relatively high microwave powers (> 150 W). The 2-mm i.d. quartz tubing gave a decrease in emission of *ca.* 30% compared to the 1-mm tubing, but it gave a more stable plasma and negligible overheating.

Argon was used throughout as carrier gas. The addition of helium gave greater emission intensities, but the plasma was then more readily extinguished. For routine use, pure argon plasmas are quite suitable.

RESULTS

With the above experimental system it was possible to monitor a characteristic emission or emissions from all classes of compounds resolved in this study. Sulphur and phosphorus compounds were not evaluated because these compounds have been extensively studied previously, and it was not expected that significantly different emission characteristics would be obtained. The following summarizes the principal emission processes occurring and their probable analytical utility.

Carbon-containing compounds

From preliminary studies including spectral scanning with flowing systems, it was established that three main emission processes from carbon-containing compounds could be observed, *viz.* atomic carbon at 247.9 nm, C_2 emission at 516.5 nm, and C_2 and CN emission at 385–389 nm. No distinction between the C_2 band emission at 385 nm and the CN band emission (band head at 388 nm) was possible with the low-resolution monochromator used.

Only one previous study[5] has reported emission at 247.9 nm from atomic carbon. This is surprising because other workers have observed emission from C_2 and CN species which have been derived from recombination reactions involving atomic carbon. Also the use of the line emission at 247.9 nm should lead to better selectivity than a band emission.

Each emission region was evaluated for quantitative work with mixtures of ethyl iodide, benzene, acetone and ethanol.

The back-flushing system with Porapak S columns at 140° resolved, with base-line separation, a mixture of 790 p.p.m. ethanol and 790 p.p.m. acetone in toluene (retention times 3.15 min, 4.20 min and *ca.* 16 min, respectively, at a flow rate of 3.0 l h^{-1}). The system was switched to back-flush after 2.20 min and back to normal operation after 6 min. The monochromator wavelength control was optimized for maximum emission by repeated sample injection (1 μl) with a Hamilton syringe held in a Shandon multi-injector. The microwave power was also optimized for maximum emission intensity and the noise level at each setting was recorded. Further comparative and confirmatory results were obtained with 630 p.p.m. carbon disulphide in *n*-butanol at 150° (retention times 60 sec and *ca.* 4 min, respectively).

A similar series of measurements were made with a mixture of 1940 p.p.m.

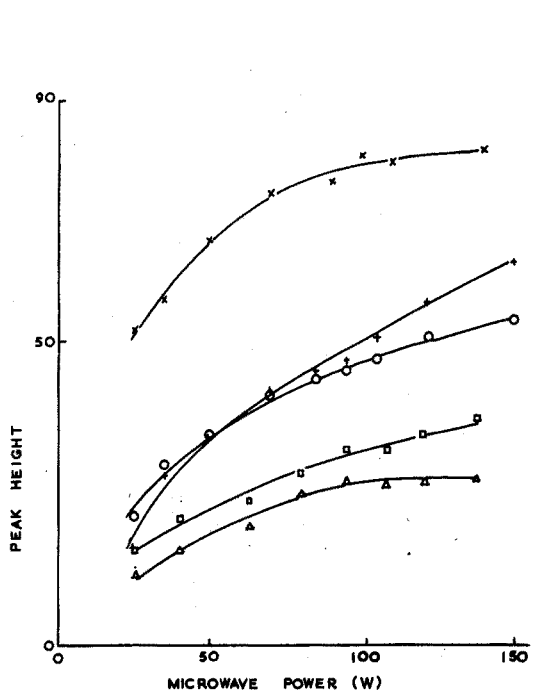

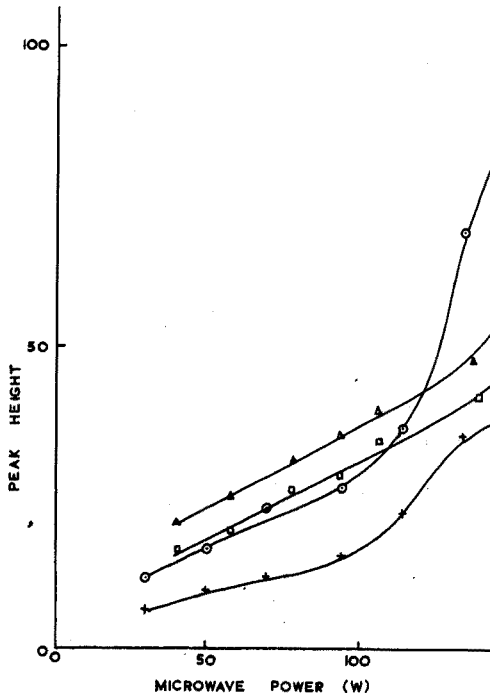

Fig. 2. Variation of peak height with microwave power for atomic carbon emission at 247.9 nm. (×) Carbon disulphide, (+) benzene, (○) ethyl iodide, (□) acetone, (△) ethanol.

Fig. 3. Variation of peak height with microwave power for C_2 emission at 516.5 nm. Symbols as for Fig. 2.

ethyl iodide and 440 p.p.m. benzene in ethanol; 1-μl injection volumes were used with a 3-mm diameter, 1-m column of Chromosorb 101 at 132°. The solvent was eluted first (retention time less than 90 sec) after which the plasma was initiated (the solvent invariably extinguishes the plasma, but unlike flame detectors this represents no safety hazard). The retention times for ethyl iodide and benzene were 3.30 min and 4.35 min, respectively. Spectroscopic measurements were also made at 206.2 nm which is characteristic of atomic iodine.

The results of these investigations are summarized in Figs. 2–4; even when measurements are made at unselective wavelengths (carbon would be present in most compounds separated by gas chromatography) some differential selectivity can be achieved by suitable choice of wavelength and microwave power setting. The maximum signal:noise ratios obtained are shown in Table I. The most sensitive emission region characteristic of carbon-containing compounds is that due to atomic carbon, which is recommended for analytical purposes. There was little variation in the emission intensity with microwave power at *ca.* 80 W (Fig. 5) and the plasma background emission was relatively low at this wavelength.

The effect of carrier gas flow rate variation was measured for the ethyl iodide–benzene mixture and the solution of carbon disulphide in *n*-butanol. The flow rate was measured immediately before and after recording each emission peak; the peak areas were approximated by triangulation. The linear increase of peak area with de-

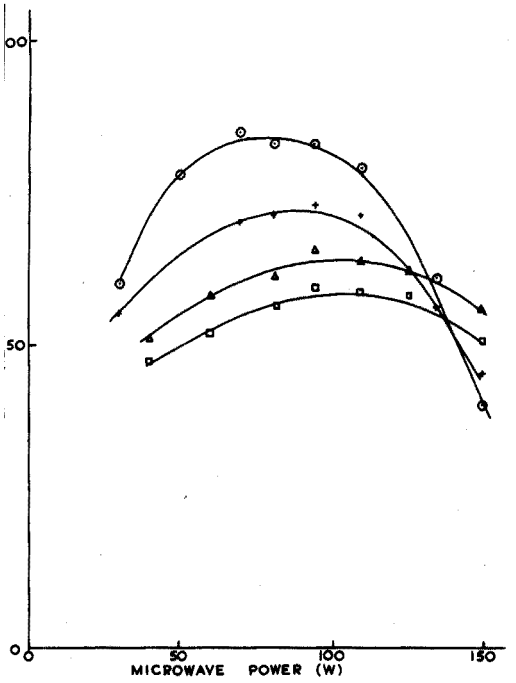

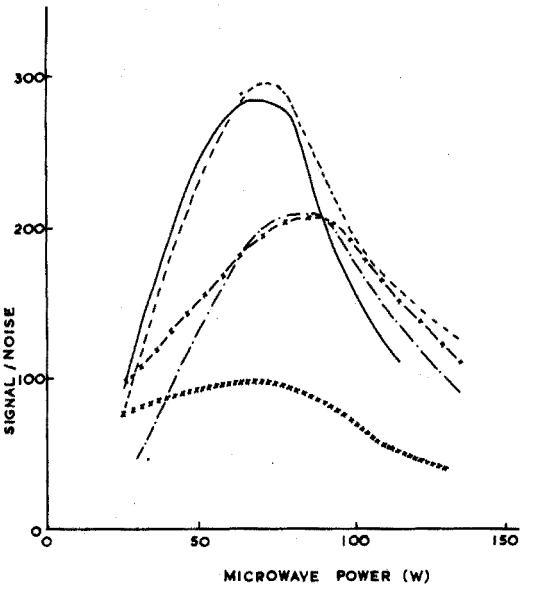

Fig. 4. Variation of peak height with microwave power for C_2/CN emission at *ca.* 388 nm. Symbols as for Fig. 2.

Fig. 5. Variation of signal-to-noise ratio with microwave power. (———) Benzene, (---------) ethyl iodide, (×–×–×) acetone, (–·–·–·–) ethanol, (× × ×) carbon disulphide.

TABLE I

MAXIMUM SIGNAL:NOISE RATIOS

Compound	*Atomic C* 247.9 *nm*	C_2 516.5 *nm*	C_2/*CN* 385–389 *nm*
Ethyl iodide	290(70)[a]	39(50)	120(160)
Benzene	280(72)	32(60)	49(160)
Acetone	205(80)	83(54)	71(160)
Ethanol	210(85)	74(63)	52(160)

[a] The figures in brackets represent the applied microwave power in W.

crease in argon flow rate (Fig. 6) may be correlated with linearly increasing residence time for the species in the plasma. The noise did not vary appreciably with flow rate, hence a flow rate as slow as possible, compatible with a convenient retention time, would give the lowest limit of detection. A flow rate of 3 l h^{-1} was generally used.

Table II shows the limits of detection (signal : noise = 2), relative sensitivity, linear range and analytical conditions for various carbon-containing compounds.

TABLE II

EMISSION CHARACTERISTICS OF SOME CARBON–CONTAINING COMPOUNDS

Compound	*Emission (nm)*	*Column*[a]	*Solvent*	*Column temperature (°)*	*Retention time (min)*	*Limit of detection (ng)*[b]	*Sensitivity* $\cdot 10^{-11}$ *g C sec*$^{-1}$	*Linear working range*
Carbon disulphide	247.9	S	Toluene	150	1.06	23.4	1.88	$>10^2$
Acetone	247.9	S	Toluene	150	4.00	7.3	1.88	$>10^3$
Methanol	247.9	S	Toluene	150	1.53	17.8	1.95	$>10^2$
Ethanol	247.9	S	Toluene	150	2.50	7.9	1.91	$>10^3$
sec-Propanol	247.9	S	Toluene	150	4.05	10.9	1.91	$>10^3$
n-Propanol	247.9	S	Toluene	150	4.30	12.7	2.00	$>10^3$
Benzene	247.9	C	Ethanol	140	3.90	6.0	1.90	$>10^3$
Toluene	247.9	C	Ethanol	150	3.30	4.0	1.90	$>10^3$
Ethyl iodide	247.9	C	Ethanol	125	3.85	31.0	1.96	$>10^3$
	206.2	C	Ethanol	125	3.85	22.4	—	$>10^3$
n-Propyl bromide	247.9	C	Ethanol	125	3.50	25.4	1.91	$>10^3$
	470.5	C	Ethanol	125	3.50	159.0	—	$>10^2$
Dichloromethane	247.9	S	Toluene	150	3.35	98.0	1.88	$>10^2$
	278.8	S	Toluene	150	3.35	*ca.* 5,000	—	—
Chloroform	247.9	C	Methanol	150	1.40	30.4	2.06	$>10^3$
	256	C	Methanol	150	1.40	41.6	—	$>10^3$
Carbon tetrachloride	247.9	C	Methanol	150	2.20	103.0	2.10	$>10^2$
	278.8	C	Methanol	150	2.20	*ca.* 4,000	—	—
	256	C	Methanol	150	2.20	96.0	—	$>10^2$

[a] C denotes Chromosorb 101; S denotes Porapak S.

[b] Limit of detection defined as signal:noise = 2.

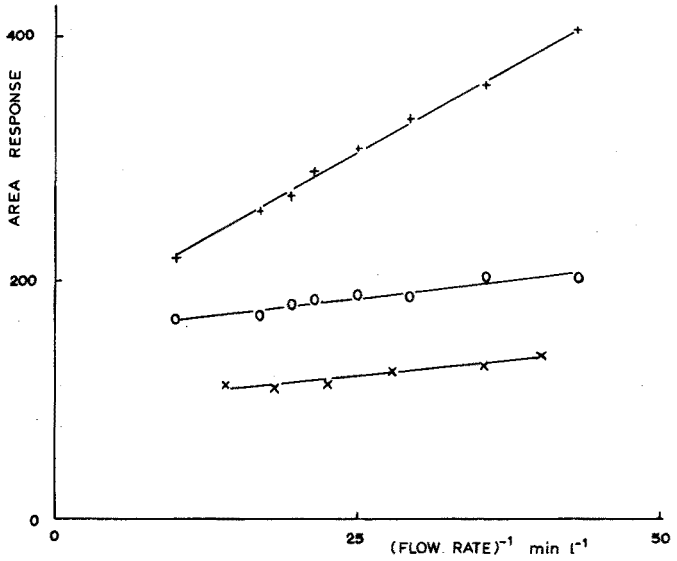

Fig. 6. Variation of area response with reciprocal of the flow rate. (+) Benzene, (○) ethyl iodide, (×) carbon disulphide.

Halogen-containing compounds

Ethyl iodide was examined alone and in admixture with benzene in ethanol at 206.2 nm (atomic iodine) and at 247.9 nm (atomic carbon) with a microwave power level of 80 W. When a low-resolution monochromator (Rank Precision Industries, Type D292) was used, the relative sensitivity for equal weights of the two compounds was 50:1 in favour of ethyl iodide. Further experiments with a higher resolution Beckman DU monochromator (slit width 0.1 mm) gave a relative sensitivity of 500:1. Because of the low noise level at 206.2 nm (compared with that at 247.9 nm), this emission line proved the most sensitive for the determination of ethyl iodide.

Bromine emission at 470.5 nm[3] was less sensitive than atomic carbon emission at 247.9 nm for the determination of *n*-propyl bromide probably because of the increased background radiation at 470.5 nm. The sensitivity for *n*-propyl bromide was 9 times greater than that for benzene and 6 times greater than that for toluene.

Difficulty was experienced in locating a sufficiently sensitive characteristic chlorine emission. No emission was found in the region of 481.9 nm[3] for dichloromethane, chloroform and carbon tetrachloride and only microgram quantities of these compounds could be detected by the CCl species at 278.8 nm (Table II). However, a band emission characteristic of these chlorine-containing compounds (possibly Cl_2) was observed at *ca.* 256 nm. The peak height *vs.* microwave power curve was quite different from that observed for atomic carbon and indicated breakdown of a molecular species with increasing microwave power (Fig. 7); this agrees with earlier work[1]. The sensitivity compared to an equivalent amount of toluene was 35:1 in favour of carbon tetrachloride and 25:1 in favour of chloroform. The sensitivity at low microwave powers for chlorinated compounds was similar to that for atomic carbon (*i.e.* at 247.9 nm) at its optimal power level.

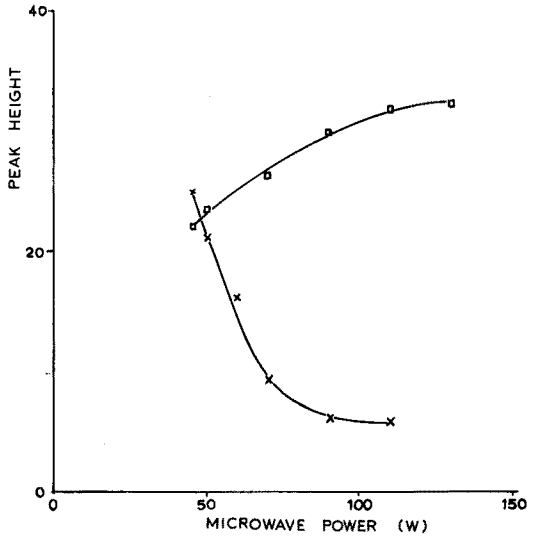

Fig. 7. Variation of detector response to emission for chloroform at 247.9 nm (□) and 256 nm (×).

Analysis of gases

For gas analysis, a Pye Chromatographic Valve fitted with a 5-μl internal sample loop was used. Gas samples were obtained in pure form and as calibrated dilutions in nitrogen (EDT Supplies Ltd., London). The gases were available in push-buttoned aerosol cans and could be readily interfaced with the sample injection system. The gases used were CH_4, C_2H_6, C_3H_8, C_4H_{10}, C_2H_4, C_3H_6, C_4H_8, C_2H_2, CO, CO_2, O_2 and N_2.

A Porapak S column was used at 150° (for C_2, C_3 and C_4 compounds) and at 50° (for C and C_2 compounds). The argon carrier gas flow rate was held at 1.5 l h^{-1} and all measurements were made at the most sensitive wavelength, 247.9 nm, with a microwave power of 70 W. The experimental parameters were as previously noted and the response of the detector system was found to be very similar for all hydrocarbons studied; an average limit of detection of $7.6 \cdot 10^{-11}$ g C sec^{-1} with a maximum variation from this of 8.5% was obtained. No difference in response was found for saturated or unsaturated species and there was no change in area response with increase in column temperature. Each series of hydrocarbons, *e.g.* C_2, C_3, C_4 compounds, gave an approximately linear response (Fig. 8) over the concentration range investigated; the maximum difference between the curves was 8.5%.

The limit of detection for carbon dioxide was $8.0 \cdot 10^{-11}$ g C sec^{-1} at 247.9 nm and $1.6 \cdot 10^{-10}$ g C sec^{-1} at *ca.* 193 nm. The corresponding limits of detection for carbon monoxide were $7.7 \cdot 10^{-11}$ g C sec^{-1} and $4.3 \cdot 10^{-11}$ g C sec^{-1}.

Nitrogen could be measured at 336 nm (N_2 and NH band emission). Under the conditions used above, oxygen is not separated from nitrogen and causes a negative interference. Separation was achieved on a 2-m molecular sieve column at −40° and the limit of detection for nitrogen was then $1.5 \cdot 10^{-11}$ g N sec^{-1}. The signal: noise ratio was independent of microwave power, indicating that breakdown is only to the N_2 molecule.

Oxygen is one of the few gases which cannot be directly determined in argon

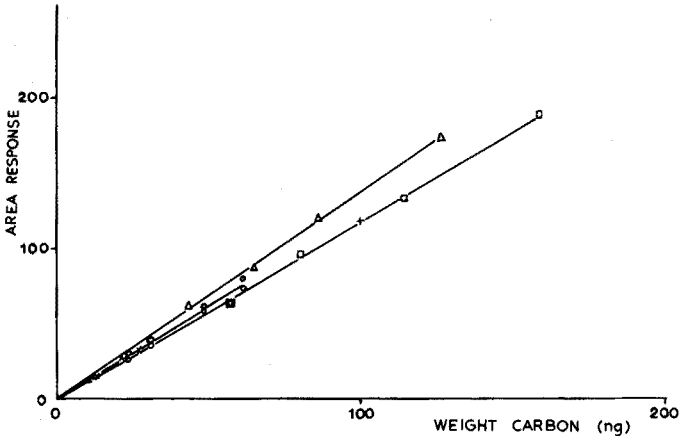

Fig. 8. Area response *vs.* carbon content for hydrocarbon gases. (×) Methane, (○) ethane and ethylene, (△) propane and propylene, (□) butane and butene-1.

plasmas; it usually causes a lower background level and so a negative interference. Similar behaviour was found at low pressures with both argon and helium plasmas.

The "open" plasma detector

An alternative form of microwave detector was evaluated with an argon plasma extending above the top of the 2 mm i.d. quartz tubing. This system has been used in other studies in this laboratory[7] and has the advantage that no carbon deposition or devitrification of the tubing is possible. A discharge under these conditions can only be maintained, however, with the more efficient quarter-wave cavity which can create an intense localized field immediately above the top of the tube. A further requirement is a relatively high flow rate of carrier gas (*ca.* 21 min^{-1}) which is not generally compatible with gas-chromatographic applications. Hence an auxiliary argon flow rate was led into the base of the detector tube together with the main chromatographic flow.

The experimental parameters were found to be similar to those described above, except that large sample volumes could be admitted to the plasma without risk of contamination or of extinguishing it. However, probably because of the high flow rate, the absolute sensitivity was reduced by *ca.* 50 fold in all cases.

CONCLUSIONS

The atmospheric plasma detector systems described above are simple in design and operation. They may be used as general detectors as well as for multi-element and qualitative analysis. Because the signal output is a well defined current pulse from a photomultiplier, it may be readily amplified and integrated for analogue or digital representation. At low light levels use may also be made of techniques such as photon counting which give a direct integrated digital output; this technique will be described at a later date. A low-resolution monochromator was used in the present study, but the use of filters would probably be better for multi-element applications.

With the experimental system described, emission at 247.9 nm from atomic carbon provides a sensitive and general region of measurement for many compounds.

The use of other wavelengths of measurement, *e.g.* 206.2 nm (atomic iodine), 470.5 nm (atomic bromine), 278.8 nm (CCl), 256 nm (for chlorine-containing compounds), 336 nm (N_2 and NH band emission), allows a certain degree of selectivity to be achieved. The limits of detection reported here are sometimes not as low as those quoted by others; this may be readily explained by the nature of the read-out system used. An advantage of the photoemissive system is that the limit of detection may be lowered by increasing the solid angle of measurement or the photomultiplier gain.

SUMMARY

An atmospheric pressure microwave-excited emissive argon plasma is evaluated for use as a detector in conventional gas-chromatographic analysis. A range of carbon-, oxygen-, nitrogen- and halogen-containing compounds was investigated in order to optimize the sensitivity, linear working range and plasma operating conditions. For the non-selective determination of carbon-containing compounds, the atomic carbon emission at 247.9 nm was found to be most useful. At this wavelength the sensitivities for all the compounds investigated were directly proportional to the amount of carbon in the compounds. The limit of detection for these compounds at 247.9 nm was $1.94 \cdot 10^{-10}$ g of carbon per sec. The atomic lines at 206.2 nm (I) and 470.5 nm (Br) were the best for the selective determination of iodine- and bromine-containing compounds respectively, and a new band emission at 256 nm, characteristic of chlorine-containing compounds, gave good sensitivity.

RÉSUMÉ

Un détecteur est examiné en vue de son utilisation pour l'analyse chromatographique gazeuse conventionnelle. Divers composés contenant carbone, oxygène, azote et halogène ont permis d'établir les conditions opératoires optima. Pour un dosage non-sélectif de composés renfermant du carbone, l'émission atomique se situe à 247.9 nm, pour le carbone. A cette longueur d'onde, les sensibilités sont directement proportionnelles aux teneurs en carbone de ces substances. La limite de détection est de $1.94 \cdot 10^{-10}$ g de carbone par sec. Pour les composés contenant iode et brome, les raies sont respectivement 206.2 et 470.5 nm. Une nouvelle bande d'émission à 256 nm, pour le chlore, permet d'obtenir une bonne sensibilité.

ZUSAMMENFASSUNG

Ein mikrowellenerregtes Argonplasma von Atmosphärendruck wurde für die Verwendung als Detektor bei der konventionellen gaschromatographischen Analyse getestet. Eine Reihe von kohlenstoff-, sauerstoff-, stickstoff- und halogenhaltigen Verbindungen wurde im Hinblick auf die Optimierung von Empfindlichkeit, linearem Arbeitsbereich und Plasma-Betriebsbedingungen untersucht. Für die nichtselektive Bestimmung von kohlenstoffhaltigen Verbindungen erwies sich die atomare Kohlenstoff-Emission bei 247.9 nm als die günstigste. Bei dieser Wellenlänge waren die Empfindlichkeiten für alle untersuchten Verbindungen der Menge des Kohlenstoffs in den Verbindungen direkt proportional. Die Nachweisgrenze für diese Verbindungen bei 247.9 nm war $1.94 \cdot 10^{-10}$ g Kohlenstoff pro sec. Die Atomlinien bei 206.2

nm (J) und 470.5 nm (Br) waren die besten für die selektive Bestimmung von jod- bzw. bromhaltigen Verbindungen, und eine neue Banden-Emission bei 256 nm, die für chlorhaltige Verbindungen charakteristisch ist, zeigte eine gute Empfindlichkeit.

REFERENCES

1 A. J. McCormack, S. C. Tong and W. D. Cooke, *Anal. Chem.*, 37 (1965) 1470.
2 C. A. Bache and D. Lisk, *Anal. Chem.*, 37 (1965) 1477; 38 (1966) 783, 1757.
3 C. A. Bache and D. Lisk, *Anal. Chem.*, 39 (1967) 786.
4 H. A. Moye, *Anal. Chem.*, 39 (1967) 1441.
5 R. M. Dagnall, S. J. Pratt, T. S. West and D. R. Deans, *Talanta*, 16 (1969) 797; 17 (1970) 1009.
6 C. H. Hartmann, *Anal. Chem.*, 43 (1971) 113A.
7 K. M. Aldous, R. M. Dagnall, B. L. Sharp and T. S. West, *Anal. Chim. Acta*, 54 (1970) 233.

Analytica Chimica Acta
Elsevier Publishing Company, Amsterdam
Printed in The Netherlands

THE ANALYSIS OF NORMAL PARAFFINS IN KEROSENE BY DIFFERENTIAL GAS CHROMATOGRAPHY

O. F. FOLMER, JR.
Continental Oil Company, Ponca City, Okla. (U.S.A.)

(Received 23rd December 1971)

There is considerable interest in the analysis of normal paraffins in kerosene-type mixtures[1-3]. The later techniques involve the use of Linde molecular sieves to separate normal paraffins from non-normal paraffins. These techniques are generally complex, involving several steps. For example, in one gas-chromatographic method, normal paraffins are sorbed by the molecular sieve and the non-normals are detected and recorded. After this, the flow is reversed, and the sorber is heated so that the normal paraffins are desorbed, detected, and recorded. In another method, which also uses molecular sieve, the normal paraffins are recovered by destroying the molecular sieve with mineral acid. Yet another method uses essentially two chromatographs in tandem. The first chromatograph contains separating columns from which the effluent flows into a thermal conductivity detector. The exhaust from this detector is connected to a molecular sieve sorber contained in a second chromatograph. The effluent from this recorder flows through a second thermal conductivity detector. The first detector records total signal, both normals and non-normals; the second detector records only the non-normal paraffins, the normal paraffins having been sorbed by the molecular sieves. The *n*-paraffins are determined by physically placing the chromatogram of the total sample over the chromatogram of the non-normal paraffin portion so that the non-normal peaks match and the normal paraffin peaks stand out.

Procedures such as these are either complex in operation or tedious in interpretation. This paper will describe a somewhat quicker, simpler method which also uses molecular sieves, but in which the signal representing the non-normal paraffins is electrically subtracted from the signal representing the total paraffins to give a difference signal representing only the normal paraffins. This is achieved by splitting the effluent from the separating column of a gas chromatograph into two equal streams. One stream flows through a molecular sieve sorber into detector A; the second stream flows through a dummy sorber into detector B. Figure 1 shows a diagram of such an apparatus. If the apparatus is properly adjusted, the result of the injection of a non-sorbed substance is no signal. One-half of the non-sorbed substance flows through the sorber to give rise to a signal in detector A, and the other half flows through the dummy sorber to give rise to an equal signal in detector B. Since detector A is connected to detector B so that the signals from the two detectors oppose each other, then the resultant difference signal is zero.

If a sorbed substance is injected, half of it flows through the dummy sorber into detector B, giving rise to a signal. The other half is sorbed in the sorber, and no

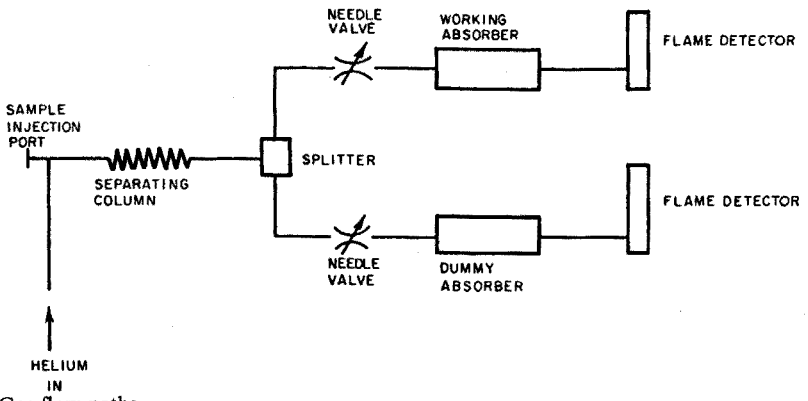

Fig. 1. Gas flow paths.

signal is produced at detector A. The resultant difference signal from the two detectors is the signal representing the unsorbed substance. Thus, it can be seen that if a kerosene sample containing both normal and non-normal paraffins is injected, then a difference signal representing only the normal paraffins will be produced. Since this method depends on the difference signal, it is called *differential gas chromatography.*

The technique of obtaining a difference signal by electrically subtracting one signal from another has been mentioned previously in the literature. Folmer *et al.*[4] suggested this technique for cancellation of thermal conductivity signals from a catalytic combustion detector, and Gayle[5] reported having accomplished this. Andreatch[6] suggested such a technique, using a scrubber or absorber to remove olefins from an olefin paraffin mixture; the paraffin signal was subtracted from the paraffin + olefin signal to provide a difference signal representing only olefins. Later, Innes *et al.*[7,8] published experimental verification of this procedure for use in exhaust gas analysis.

EXPERIMENTAL

Instrumentation

A modified Varian Aerograph 660 chromatograph with a dual/differential electrometer and dual flame ionization detectors was used. The electrometer was used in the dual mode (*i.e.* essentially two electrometers). In the attenuator of one electrometer channel a fixed resistor was replaced by a 10-turn potentiometer (Beckman Instruments, Inc.) so that the signal amplitudes from the two electrometer channels could be exactly balanced.

The outputs of the two electrometer channels were connected to the input of a Cohu Model 114C differential amplifier (Cohu Electronics, Inc., Box 623, San Diego, Calif.) and the output of this amplifier was connected to the input of a 10-mV Minneapolis-Honeywell strip chart recorder.

Figure 2 is a diagram showing the signal paths from the flame ionization detectors to the recorder.

The chromatograph was further modified by connecting the downstream end of the column to a flow splitter which divided the effluent into two nominally equal

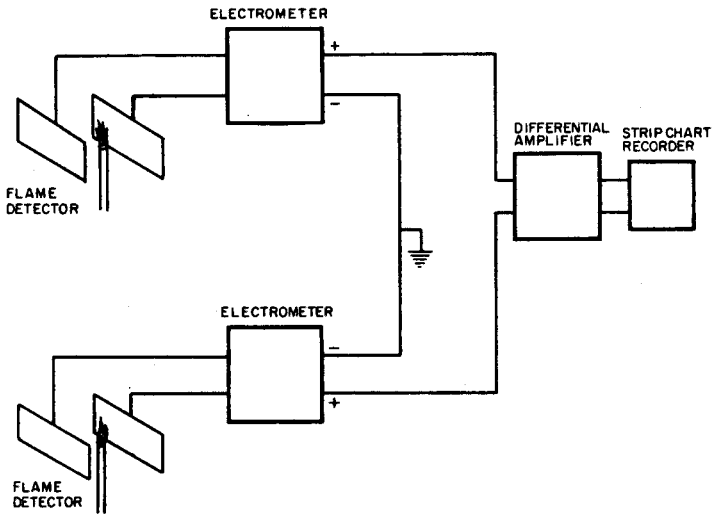

Fig. 2. Signal paths.

streams (see Fig. 1). One stream passed through a short column of 5A Linde Molecular Sieve (Union Carbide Corp., Linde Div.) to a flame detector (detector A). The other stream passed through a dummy sorber to a second flame detector (detector B).

A Whitey 22RS2 316 precision needle valve (Whitey Research Tool Co., 5525 Marshall St., Oakland 8, Calif.) was placed in the line upstream from each sorber and used in balancing the flows of gas through each sorber.

Gas chromatographic conditions

A 6-ft, 3/16-in. o.d. aluminum column, packed with 70–80 mesh Anakrom ABS coated with 20% by weight of SE-52 silicone gum rubber, was used at 170° with a carrier flow rate of 50–60 ml min^{-1}. The sorber and dummy sorber were one-inch sections of 1/4-in. o.d. aluminum tubing. The sorber contained 30–60 mesh 5A Molecular Sieve, and the dummy sorber contained 30–60 mesh untreated Celite; both sorbers were contained in an oven maintained at 320°. Wherever possible, connecting tubing with an inside diameter of 0.04 in. was used; the remainder of the connecting tubing was standard-wall stainless steel tubing with an o.d. of 1/8 in. and an i.d. of *ca.* 0.06 in. Care was taken in matching this tubing for length so that the two separate flow paths should be as nearly identical as possible. Tubing of small i.d. helped to minimize such mismatches in addition to contributing small dead volume.

The injection port was operated at 320° and in the early work the detectors were operated at 320°, because the sorbers were located in the detector oven. Later the sorbers were relocated and the detector was then operated at 200°, which improved the signal-to-noise ratio.

Hydrogen flow rate to each burner was monitored with one of a pair of identical flow meters (Emerson Electric Co., 407 W. Vine St., Hatfield, Pa.) and the flow was optimized for the operating condition used, subject to the constraint that the same flow rate was used for both burners. Burner air came from an air pump

(Aerograph). The air flow rate was not measured since previous work had shown that the amount of air supplied was well above the minimum required.

The hydrocarbons used were Phillips pure grade (Phillips Petroleum Company, Chemical Dept., Special Products Div., Bartlesville, Okla.) or the equivalent, except for the non-normal paraffins which were a mixture (Universal Oil Products).

As Fig. 2 shows, the apparatus was set up to read out the difference between the signals from the two electrometer channels. This difference signal represented the normal paraffins since the signal from non-normal paraffins was cancelled. In order to adjust the apparatus so that such a condition maintained, 2,2,5-trimethylhexane was repetitively injected and the relative flow rates through the sorbers, the relative amplitudes of the signals from the two electrometer channels, and to some extent the lengths of the split paths (following the splitter) were adjusted until a minimum signal resulted. This was taken to indicate the best approximation of balance attainable. Perfect balance would be indicated by a null signal.

RESULTS AND DISCUSSION

To obtain a null signal from a non-sorbed substance (perfect balance), it is

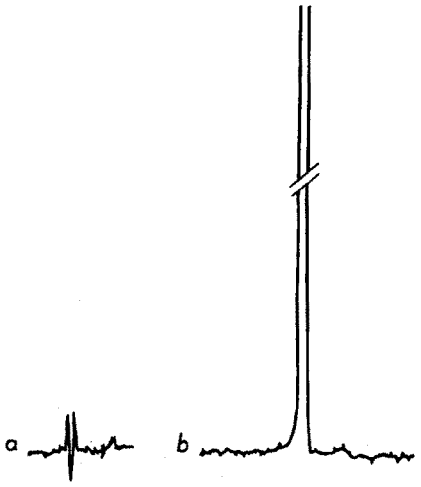

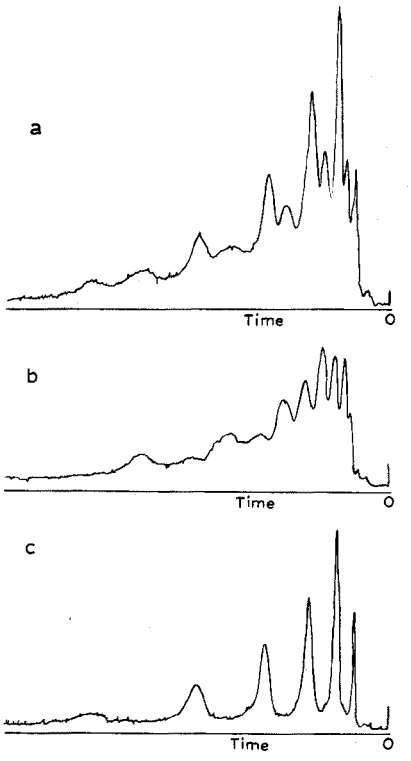

Fig. 3. Signals resulting from injection of a non-absorbed substance, 2,2,5-trimethylhexane. (a) Residual difference signal; (b) one of the two signals from which the difference signal is obtained.

Fig. 4. Kerosene sample. (a) Signal from detector following dummy absorber (total sample); (b) signal from detector following working absorber (non-normal paraffins); (c) difference between (a) and (b) (normal paraffins).

necessary to match exactly the retention times of the two parts of the substance eluting from the working and dummy sorbers, to match exactly the peak amplitudes, and to match exactly the peak shapes. Matching peak shapes is the most difficult of the three, and as Fig. 3 shows, a perfect balance was not obtained.

Several artificial mixtures similar to kerosene were prepared from Phillips pure-grade normal paraffins and a mixture of non-normal paraffins obtained by removing normal paraffins from kerosene with "molecular sieve".

Figure 4 shows the signals obtained from each detector separately and the resultant difference signal. The difference signal chromatogram is typical of the chromatograms used in the reported analyses. Normal nonane was added as an internal standard. Percentages of normal paraffins were calculated by comparing the measured area of each normal paraffin peak to the measured area of the internal standard peak. The non-normal paraffins had been effectively removed, and so could be ignored. Typical results of analyses of mixtures of normal and non-normal paraffins are shown in Table I.

TABLE I

ANALYSIS OF MIXTURES OF NORMAL AND NON-NORMAL PARAFFINS FOR NORMAL PARAFFINS

Normal paraffins	*Wt.% found*	*95% Confidence limits, relative*	*Wt.% actual*	*Error*	*Relative error (%)*
a. Mixture containing 13.40% normal paraffins[a]					
C_{10}	1.38	± 5.5%	1.25	+0.13	−10.4
C_{11}	1.99	± 3.8%	1.96	+0.03	+ 1.5
C_{12}	2.69	± 6.1%	2.99	−0.30	−10.0
C_{13}	3.16	± 5.1%	2.79	+0.37	+13.3
C_{14}	2.34	± 5.9%	2.14	+0.20	+ 9.3
C_{15}	1.54	±14.5%	2.27	−0.73	−32.2
Total	13.10	± 1.0%	13.40	−0.30	− 2.2
b Mixture containing 6.75% normal paraffins[b]					
C_{10}	0.64	± 4.1%	0.63	+0.01	+ 1.6
C_{11}	0.91	± 4.8%	0.99	−0.08	− 8.1
C_{12}	1.52	± 5.9%	1.51	+0.01	+ 0.7
C_{13}	1.69	±10.1%	1.41	+0.28	+19.9
C_{14}	1.06	± 8.9%	1.08	−0.02	− 1.9
C_{15}	0.65	±15.9%	1.14	−0.49	−43.0
Total	6.47	± 4.99%	6.75	−0.28	− 4.1
c. Mixture containing 2.62% normal paraffins[c]					
C_{10}	0.25	±21.0%	0.24	+0.01	+ 4.2
C_{11}	0.30	± 9.5%	0.38	−0.08	−21.1
C_{12}	1.06	± 8.1%	0.59	+0.47	+79.7
C_{13}	1.13	±12.9%	0.54	+0.59	+109.3
C_{14}	0.48	±16.8%	0.42	+0.06	+14.3
C_{15}	0.14	±21.0%	0.44	−0.30	−68.2
Total	3.35	± 6.6%	2.62	+0.73	+27.9

[a] Mean of 7 runs.
[b] Mean of 6 runs.
[c] Mean of 3 runs.

The absolute errors for a particular normal paraffin do not seem to be a function of the concentration of that paraffin, *i.e.*, the absolute error does not seem to increase or decrease systematically with decrease in the peak size. This error is probably due to the incomplete cancellation of the non-normal paraffin signals and indicates that the lower limit of detection of normal paraffins is dependent on the amount of the residual signal from the non-normal paraffins.

To determine the effects of changes in non-normal compositions on the analysis of normal paraffins, several kerosene-type mixtures were made up containing different amounts of a single non-normal paraffin, heptamethylnonane. These results are shown in Table II.

TABLE II

EFFECT ON NORMAL PARAFFIN ANALYSIS OF CHANGE IN COMPOSITION OF NON-NORMAL PARAFFINS

Paraffin	*Original mixture, Mean of 4 runs, Wt. % n-paraffin*	*With 8.4 % heptamethylnonane added, Mean of 3 runs, Wt. % n-paraffins*	*With 48 % heptamethylnonane added, Mean of 3 runs, Wt. % n-paraffins*
C_{10}	1.25	1.26	1.15[a]
C_{11}	1.73	1.87[a]	1.67
C_{12}	2.40	2.46	2.60
C_{13}	2.23	2.06	1.40[a]
C_{14}	1.75	2.08	1.16[a]
C_{15}	1.26	1.34	1.33
Total	10.62	11.07	9.31[a]

[a] These means are significantly different from the corresponding means in the original mixture.

Since the accuracy of the analysis depends on the degree of balance (*i.e.* the closeness of the approach to complete cancellation of the signals due to non-normal paraffins), changes in composition of the non-normal portion from one sample to another might have a deleterious effect on accuracy. The results shown in Table II indicate this is not the case. The presence of 8.4% of heptamethylnonane only causes a loss of accuracy on one component; the total percentage of normal paraffins is not significantly different from that found in the original mixture. This amount (8.4%) of heptamethylnonane makes it one of the larger non-normal components of the mixture. A really massive amount of heptamethylnonane (48%) causes considerable loss of accuracy. However, it should be mentioned that in this case a catastrophic disruption of the baseline occurs at the retention time of heptamethylnonane, between normal tridecane and normal tetradecane.

The results obtained from differential gas-chromatographic analysis of normal paraffins seemed to be as accurate and precise as those obtained by any other method. The differential method offers some advantages in that it requires less time and presents a simpler signal for interpretation. Setting up and adjusting the apparatus is a somewhat complex task; however, once done, it is relatively simple to maintain in adjustment.

Some work has also been done with thermal conductivity detectors. Early attempts with a conventional bridge with the reference filament opposed to the sensing filament gave "S"- or "W"-shaped peaks even though the carrier stream was

split evenly right at the detector. This was probably due to mismatch in such filament characteristics as total resistance and change in resistance with temperature. Different operating temperatures can produce different peak shapes because of different response time constants[9], and, of course, filament temperature is directly related to the amplitude of the signal produced. With the two filaments in one bridge, attempts to alter the operating characteristics of one filament also altered those of the other filament. The net result was that changes which decreased the mismatch also decreased the final signal; it was quickly obvious that when a matched condition was achieved, a condition of zero signal was also reached.

The necessity of being able to adjust the operating conditions of each filament independently from the other led to the device of using two separate bridges. The two bridges were connected so that the output signal from one bridge opposed that from the other, and yet the bridges were electrically isolated so that internal adjustments of one did not affect the internal balance of the other. Two separate power supplies were required so that this degree of isolation was maintained. Figure 5 is a diagram of such a dual bridge network.

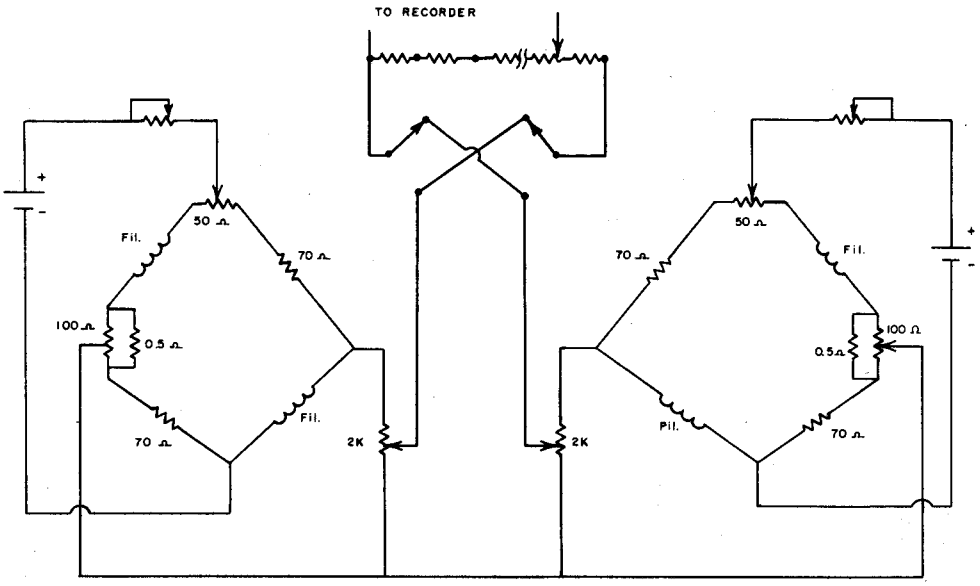

Fig. 5. Dual thermal conductivity bridge for differential gas chromatography.

It was found that when sufficient balance of signals had been obtained, only a small signal remained from an injection of 2,2,5-trimethylhexane and that an essentially null signal could be obtained if the injection was made slowly over a period of about 10 sec. Such a slow injection did not cause appreciable peak broadening with a packed column. Figure 6a shows the difference signal from a normal "fast" injection and Figure 6b shows the difference signal from a "slow" injection.

Figure 7 shows the difference signal (normal paraffins only) from a slow injection of a synthetic kerosene mixture containing 13.4% normal paraffins. Figure 8 shows the signal from the detector following the dummy sorber; this signal represents

a. "FAST" INJECTION
b. "SLOW" INJECTION

Fig. 6. Residual difference signals with thermal conductivity detector, showing effect of injection time duration.

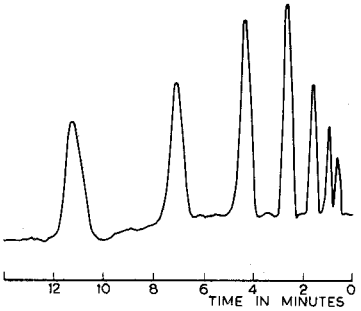

Fig. 7. Difference signal (representing normal paraffins) from thermal conductivity detector.

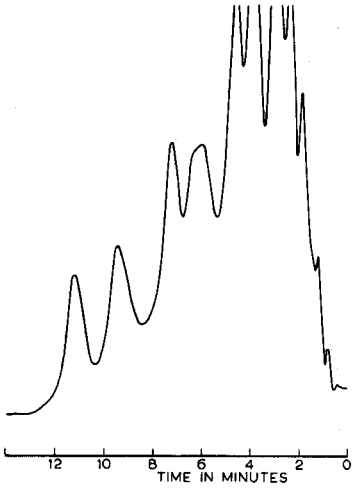

Fig. 8. Signal representing total sample from thermal conductivity detector. This is the signal from which the non-normal signal is subtracted to give the difference signal in Fig. 7.

the total sample, both normal and non-normal paraffins. The match of the two signals from the unsorbed substances is quite good as evidenced by the relatively flat baseline between peaks in Fig. 7. However, the lack of reference filaments is shown by the drifting baselines in Figs. 7 and 8. Further modification of the dual bridge network to include reference filaments would be desirable for anyone pursuing the thermal conductivity mode of operation.

Future developments

It is possible that the method may be further generalized in that the sorber may be replaced by a reactor. In this context, the reactor is defined as something which changes a particular type of substance so that the detectors in use respond differently to the altered substance as compared with the unaltered substance. Thus, it may not be necessary to remove the substances to be detected. It may be sufficient to alter the properties by which the substance is detected so that the detectors can distinguish between the altered and the unaltered forms.

If differential gas chromatography can be so generalized, it will enable gas chromatography to be used for analyses of mixtures of molecular types which hitherto were not generally possible.

SUMMARY

A differential gas-chromatographic method which offers a rapid, reasonably precise and simple technique for the analysis of normal paraffins in kerosene is described. Normal paraffins are removed on Linde molecular sieve and a dual detector system is provided; the arrangements necessary to match peak amplitudes and peak shapes with flame ionization detectors, so that only normal paraffins are measured, are discussed. The use of thermal conductivity detectors complicates the achievement of the required signal balance. The technique offers a means of determining a particular molecular type in the presence of other types; this is important with complex samples which cannot be readily separated into individual components. The prime requirement is an agent which will remove the required molecules selectively, so that a differential signal can be obtained.

RÉSUMÉ

On décrit une méthode de dosage de paraffines dans le kérosène, par chromatographie gazeuse différentielle. Cette technique offre un moyen de déterminer un type moléculaire particulier, en présence d'autres types; ceci est important pour des échantillons complexes ne pouvant pas être séparés facilement en composants individuels. Il faut avant tout un agent qui déplacera sélectivement les molécules considérées, de façon à obtenir un signal différentiel.

ZUSAMMENFASSUNG

Es wird eine Methode der Differential-Gaschromatographie beschrieben, die eine schnelle, ziemlich genaue und einfache Analyse von Normalparaffinen in Kerosin ermöglicht. Normalparaffine werden auf einem Linde-Molekularsieb entfernt. Es wird ein Dual-Detektorsystem verwendet, und es werden die Anordnungen diskutiert, die notwendig sind, damit Peakamplituden und Peakformen Flammenionisationsdetektoren so angeglichen sind, dass nur Normalparaffine gemessen werden. Die Verwendung von Wärmeleitfähigkeitsdetektoren erschwert die Erzielung des benötigten Signal-Gleichgewichts. Das Verfahren bietet die Möglichkeit zur Bestimmung einer besonderen Molekülart in Gegenwart von anderen Molekülarten; dies ist bei komplexen Proben von Bedeutung, die nicht leicht in einzelne Komponenten zerlegt werden können. Es wird hauptsächlich ein Agens benötigt, das die entsprechenden Moleküle selektiv entfernt, so dass ein Differentialsignal erhalten werden kann.

REFERENCES

1 G. C. Blytas and D. L. Peterson, *Anal. Chem.*, 39 (1967) 1434.
2 H. S. Knight, *Anal. Chem.*, 39 (1967) 1452.

3 J. R. Marquart, G. B. Dellow and E. R. Freitas, *Anal. Chem.*, 40 (1968) 1633.
4 O. F. Folmer, Jr., Kang Yang and G. Perkins, Jr., *Anal. Chem.*, 35 (1963) 454.
5 T. M. Gayle, *J. Gas Chromatogr.*, 2 (1964) 332.
6 A. J. Andreatch, *Arch. Environ. Health*, 4 (1962) 317.
7 W. B. Innes, W. E. Bambrick and A. J. Andreatch, *Anal. Chem.*, 35 (1963) 1198.
8 W. B. Innes and W. E. Bambrick, *Rapid Hydrocarbon Analysis by Chromatography and Chemical Absorption*, paper presented in the Division of Analytical Chemistry, 145th National Meeting, ACS, New York, Sept. 8–13, 1963.
9 S. D. Nogare and R. S. Juvet, Jr., *Gas Chromatography*, Interscience, New York, 1962, p. 190.

Analytica Chimica Acta
Elsevier Publishing Company, Amsterdam
Printed in The Netherlands

THE DETERMINATION OF NORMAL PARAFFINS IN KEROSENE AND CRUDE OIL HEAVY DISTILLATES BY PROGRAMMED-TEMPERATURE DIFFERENTIAL GAS CHROMATOGRAPHY

CHARLES L. STUCKEY
Continental Oil Company, Ponca City, Okla. (U.S.A.)

(Received 23rd December 1971)

The direct analysis of normal paraffin hydrocarbons in light and heavy distillate fractions of petroleum crude oils by gas–liquid chromatography is usually unsatisfactory because of the complexity of the samples and the resolution problems that arise from such mixtures. Several methods employing molecular sieves or urea adduction followed by a gas–liquid chromatography finish have been proposed. These can be classified by the following illustrations.

1. Urea adduction methods involve the removal of normal paraffins as a urea clathrate and recovery of the normal paraffins by destroying the clathrate. Methods have been proposed for gasoline and kerosene fractions[1,2] as well as for heavier distillates[3-5].

2. Sorption and re-elution gas–liquid chromatography techniques[6,7] involve removing the normal paraffins on a molecular sieve pre-column and then eluting the normal paraffins from the sieve bed at elevated temperatures. These methods are limited to kerosene-range distillates, as the heavier normal paraffins cannot be readily removed from the sieves by heating.

3. The molecular sieve methods used for heavy distillates[8-10] involve heating the petroleum distillates with an excess of sieves, washing the sieves to remove all the non-normal hydrocarbons and subsequent destruction of the sieves by hydrofluoric acid. The resulting extract is then chromatographed by routine methods. These techniques are not only laborious but also require the use of a highly reactive agent.

4. Subtractive g.l.c. methods involve duplicate chromatograms of the distillate with and without a molecular sieve pre-column. These methods essentially use two chromatographs in tandem. The first contains a separating column and thermal conductivity detection. The second chromatograph takes the effluent from the first detector through a molecular sieve absorber and a thermal conductivity detector. The chromatogram of the whole sample is placed over that of the absorber effluent and from the contours of the latter a baseline is drawn in under the normal paraffin peaks which allows a calculation of their area.

This paper will describe the application of differential gas chromatography (d.g.c.), as described by Folmer[11], to the analysis of kerosene and heavy distillates with a column temperature-programmed gas chromatograph.

EXPERIMENTAL

The instrument used was similar to that described by Folmer[11] with the following modifications.

1. The single detector block was replaced with a pair of four-filament detectors to increase the sensitivity. The difference in internal volume of these two detectors necessitated plumbing and wiring changes which placed all of the detecting filaments in one block and all of the reference filaments in the second. The carrier gas flow system is shown graphically in Fig. 1. The dual detector and control circuit are shown in Fig. 2.

2. A column oven temperature-programmer was incorporated into the instrument to facilitate the work reported here. The recorder was a Honeywell Model

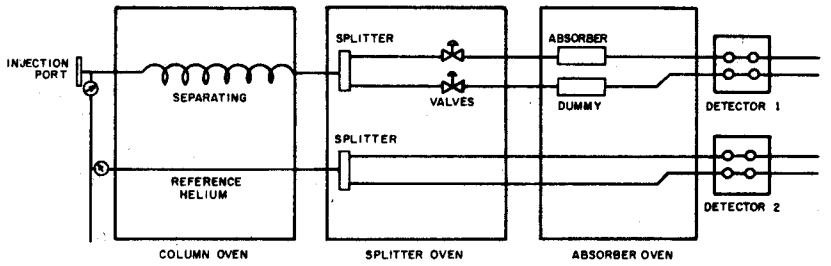

Fig. 1. Modified flow system.

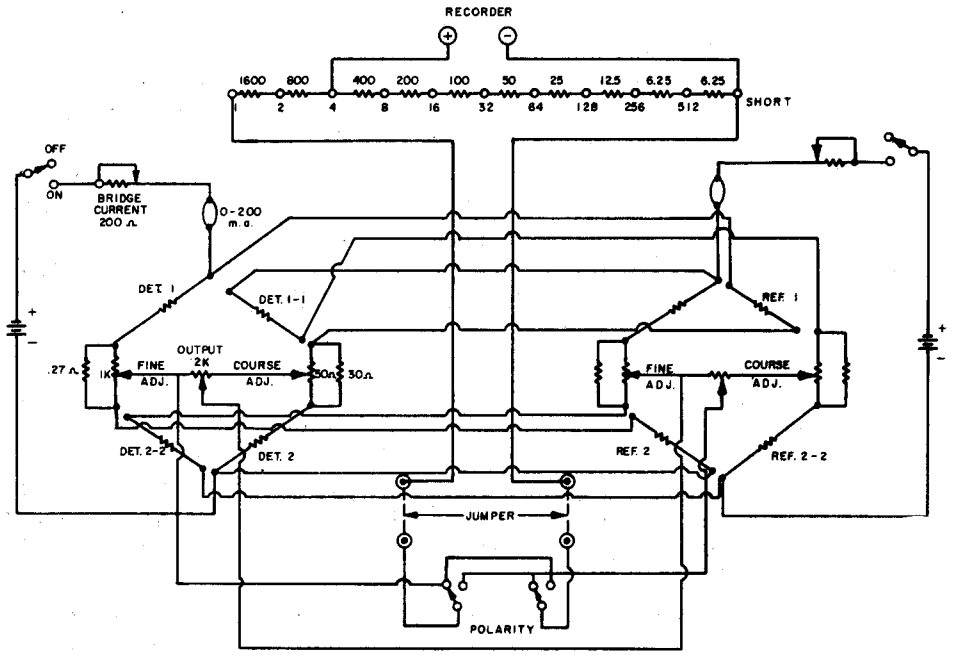

Fig. 2. Dual detector and control circuit for differential chromatograph.

15, 1-mV, 1-sec full-scale-response instrument. An Infotronics Model CRS-11HSB/42 printing integrator was used to obtain peak areas.

Standard weight-percent normal paraffin mixtures were prepared by weighing individual normal paraffins into a sample of non-normal hydrocarbons boiling within the temperature range to be studied. The normal paraffin standards were obtained from the Phillips Petroleum Company, Bartlesville, Okla., and the Chemical Samples Company, Columbus, Ohio. The non-normal hydrocarbon samples were prepared by refluxing kerosene with molecular sieves. One standard mixture was used to obtain weight response factors and the second to check the accuracy. Each normal paraffin was analyzed by capillary gas chromatography to allow correct calculations of the standard blends.

Standard weight percent blends were also prepared for the gas oil boiling ranges samples. The non-normal stock was prepared by removing the normal paraffins by urea adduction[4] and recovering the oil from the alcohol wash. These blends were used to obtain weight response factors and accuracy data.

The analytical column was a stainless steel tube, 366 cm long by 0.6 cm o.d., packed with 10% UCW-98 silicone gum rubber on 70–80 mesh Anakrom ABS. The absorber column was a stainless steel tube, 5 cm long by 1.5 mm d_c, packed with 60–80 mesh 5A molecular sieves. The dummy column had the same dimensions and was packed with 60–70 mesh Anakrom P.

Different operating conditions were used for the kerosene and heavy gas oil fractions. These conditions were as follows:

Variable		*Set I* *Kerosene*	*Set II* *Heavy gas oil*
Helium flow:	Absorber—Molecular sieves	67 cc/min	100 cc/min
	Absorber—Dummy	80 cc/min	71 cc/min
	Reference detectors	40 cc/min	52 cc/min
Temperature:	Absorber oven	608°K	608°K
	Splitter oven	573°K	573°K
	Column oven:		
	Initial	423°K	498°K
	Final	498°K	553°K
Program rate		12.5° min^{-1}	10° min^{-1}
Initial period		1 min	3 min
Sample size		4 μl	5 μl

The instrument was balanced for a null signal with 2-methyldecane for kerosene, and 2,6,10,14-tetramethylpentadecane for the heavy gas oils.

DISCUSSION

Several methods have been proposed to yield the analysis of normal paraffins in kerosene or gas oils. These procedures, although accurate, are quite laborious,

making them inconvenient for routine analysis. In contrast, the method proposed here is rapid, requiring less than 10 min per analysis, and uses the normal syringe injection technique for introduction of the sample.

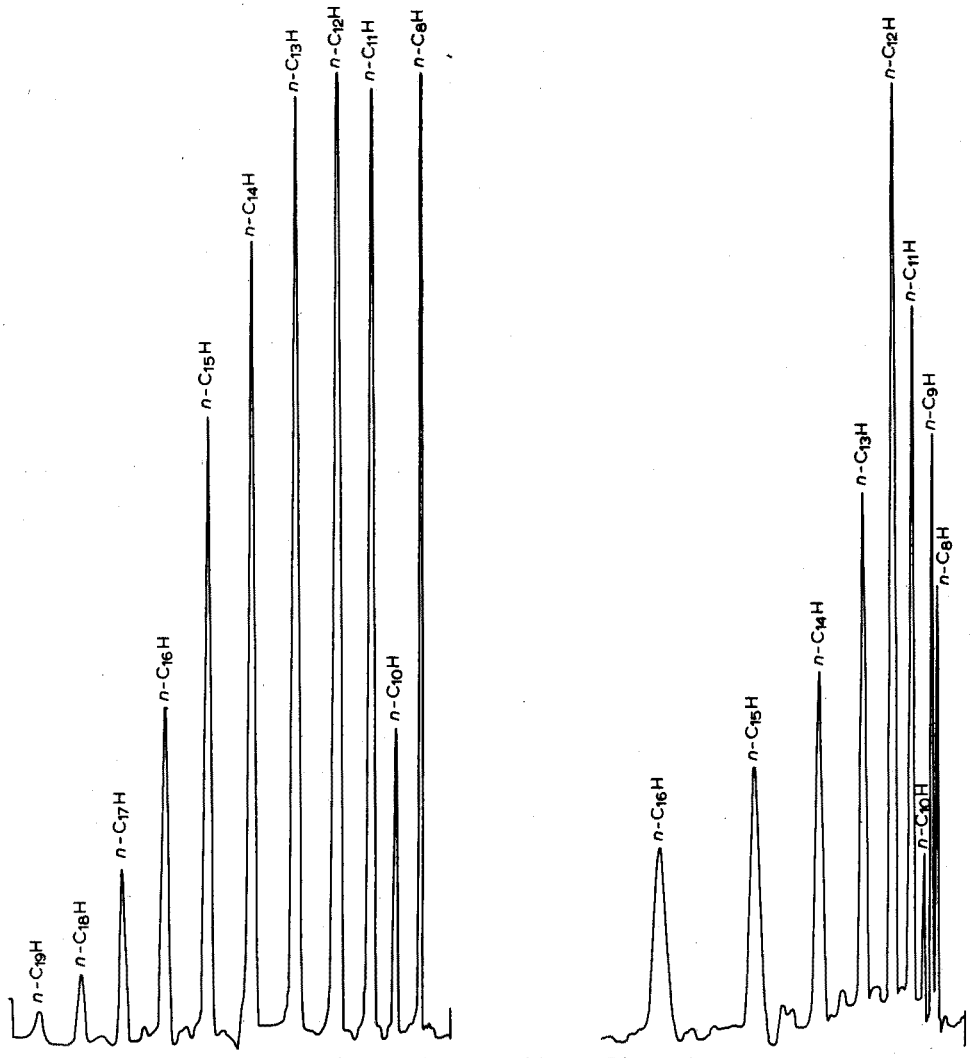

Fig. 3. Differential chromatogram of a heavy kerosene with n-C_8H internal standard.

Fig. 4. Differential chromatogram of sample No. L-2646-99-3. Column temperature 448°K isothermal.

The resolution of the normal paraffins from each other is very good (Fig. 3). This chromatogram also clearly demonstrates the chromatographic neatness of this technique when applied to the analysis of a kerosene containing roughly 18% normal paraffin hydrocarbons.

Figures 4–7 are chromatograms of a synthetic blend of normal paraffins in a non-normal kerosene base. Figure 4 is a differential chromatogram obtained under isothermal column oven operation. Figure 5 is a differential chromatogram of the

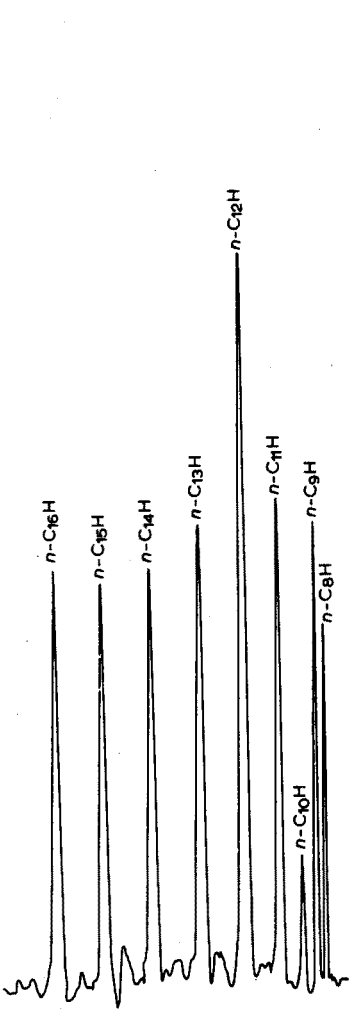

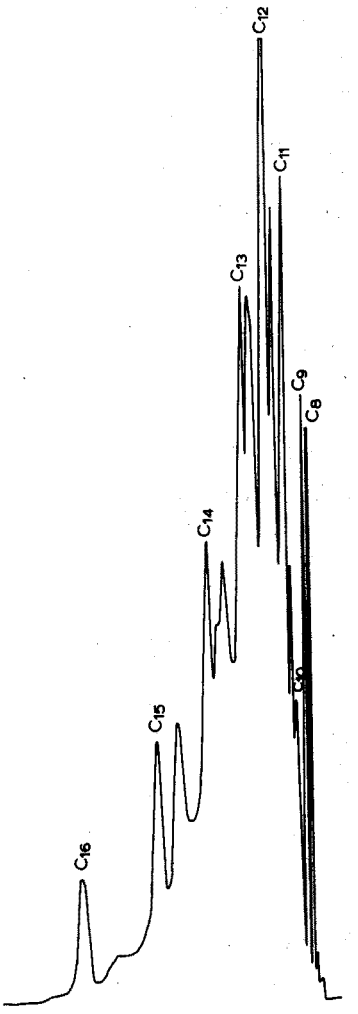

Fig. 5. Differential chromatogram of sample No. L-2646-99-3. Column temperature program 423° K to 498° K

Fig. 6. Chromatogram of full sample No. L-2646-99-3. Column temperature 448° K isothermal.

same sample, with column-temperature programming. A comparison of the chromatograms clearly demonstrates the advantages in column-temperature programming. Figures 6 and 7 are chromatograms of the whole sample. The large envelope points out the complexity of the samples when the detector signals are not electronically subtracted.

Figures 8–11 are chromatograms of a gas oil sample and are displayed in the same order as those discussed above for kerosene.

Table I lists the conversion factors obtained by dividing the area percent by the known weight percent of a synthetic blend of kerosene. The repeatability of the

TABLE I REPEATABILITY OF CONVERSION FACTORS—KEROSENE

(6 runs were done for each sample)

Carbon no.	$\bar{X}$	S	$U=50\%$	$U=99\%$
8	1.01	±0.010	±0.003	±0.02
9	1.00	±0.012	±0.004	±0.02
10	1.02	±0.022	±0.006	±0.04
11	1.00	±0.010	±0.003	±0.02
12	1.00	±0.005	±0.001	±0.01
13	0.99	±0.008	±0.002	±0.01
14	1.02	±0.010	±0.003	±0.02
15	0.93	±0.014	±0.004	±0.02
16	1.06	±0.006	±0.002	±0.01

TABLE II REPEATABILITY OF CONVERSION FACTORS—GAS OILS

(4 runs were done for each sample)

Carbon no.	$\bar{X}$	S	$U=50\%$	$U=99\%$
14	1.14	±0.013	±0.005	±0.04
15	0.98	±0.010	±0.004	±0.03
16	0.89	±0.005	±0.002	±0.01
17	0.68	±0.006	±0.002	±0.02
18	0.78	±0.039	±0.015	±0.11
19	1.20	±0.013	±0.005	±0.04
20	1.16	±0.022	±0.008	±0.06
21	1.20	±0.010	±0.004	±0.03
22	1.24	±0.005	±0.002	±0.01
23	1.29	±0.016	±0.006	±0.05
24	1.24	±0.068	±0.026	±0.20

TABLE III ACCURACY DATA—KEROSENE

(Experimental weight percent data obtained by multiplying the area percent data by the factors listed in Table I)

Carbon no.	*Standard weight percent*	*Experimental run no.*						S^a	$U=95\%$
		1	2	3	4	5	6		
8	1.35	1.37	1.37	1.37	1.37	1.37	1.37	±0.022	±0.02
9	1.52	1.57	1.55	1.57	1.56	1.54	1.57	±0.046	±0.04
10	0.48	0.52	0.50	0.51	0.50	0.51	0.54	±0.039	±0.04
11	2.28	2.32	2.31	2.27	2.33	2.33	2.34	±0.047	±0.05
12	4.04	4.05	4.09	4.04	4.11	4.16	4.16	±0.085	±0.08
13	2.41	2.47	2.46	2.45	2.49	2.51	2.49	±0.078	±0.08
14	2.09	2.12	2.10	2.08	2.15	2.15	2.11	±0.042	±0.04
15	2.00	2.04	1.98	2.01	2.05	2.06	1.98	±0.041	±0.04
16	2.18	2.20	2.22	2.19	2.20	2.24	2.18	±0.034	±0.03
Total	18.35	18.66	18.58	18.49	18.76	18.87	18.74	±0.391	±0.39

[a] S is the standard deviation from the blended weight percent.

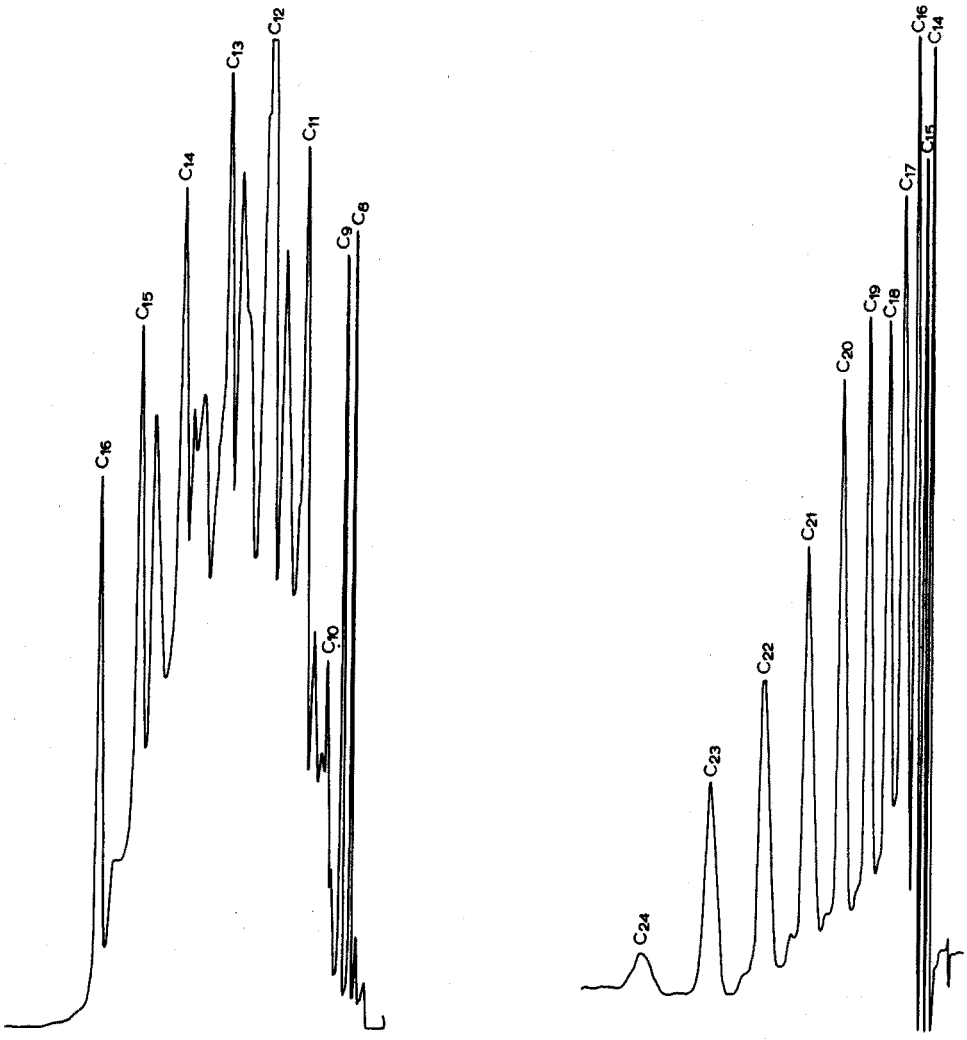

Fig. 7. Chromatogram of full sample No. L-2646-99-3. Column temperature program 423°K to 498°K.

Fig. 8. Differential chromatogram of sample No. L-2646-106-2. Column temperature 523°K isothermal.

analytical system is demonstrated here to be ±4% at the 99% confidence limit for kerosene samples. The repeatability of the gas oil procedure is not as good as the kerosene method, ranging from ±0.8–16% over the carbon number distribution. These data are shown in Table II.

Tables III and IV list the standard deviation and 95% confidence limits for standard weight percent blends of normal paraffins in non-normal petroleum stocks. These data show the method of programmed-temperature differential gas chromatography to be competitive with previously proposed methodology.

TABLE IV ACCURACY DATA—GAS OILS

(Experimental weight percent data obtained by multiplying the area percent data by the factors listed in Table I)

Carbon no.	*Standard weight percent*	*Experimental run no.*					S^a	$U=95\%$
		1	2	3	4	5		
14	0.99	0.98	0.98	0.98	0.98	0.98	±0.011	±0.01
15	1.37	1.33	1.34	1.33	1.34	1.33	±0.041	±0.05
16	2.05	1.98	1.96	1.96	1.96	1.94	±0.092	±0.10
17	1.92	1.98	1.91	1.90	1.87	1.80	±0.072	±0.08
18	1.95	1.86	1.85	1.82	1.81	1.73	±0.160	±0.18
19	1.87	1.74	1.80	1.78	1.81	1.80	±0.098	±0.11
20	1.70	1.62	1.68	1.66	1.65	1.66	±0.056	±0.06
21	1.48	1.44	1.45	1.45	1.44	1.46	±0.037	±0.04
22	1.48	1.44	1.44	1.48	1.49	1.46	±0.030	±0.03
23	1.20	1.17	1.17	1.20	1.17	1.16	±0.033	±0.04
24	0.44	0.43	0.42	0.43	0.43	0.43	±0.014	±0.02
Total	16.45	15.97	15.80	15.99	15.95	15.75	±0.633	±0.73

[a] S is the standard deviation from the blended weight percent.

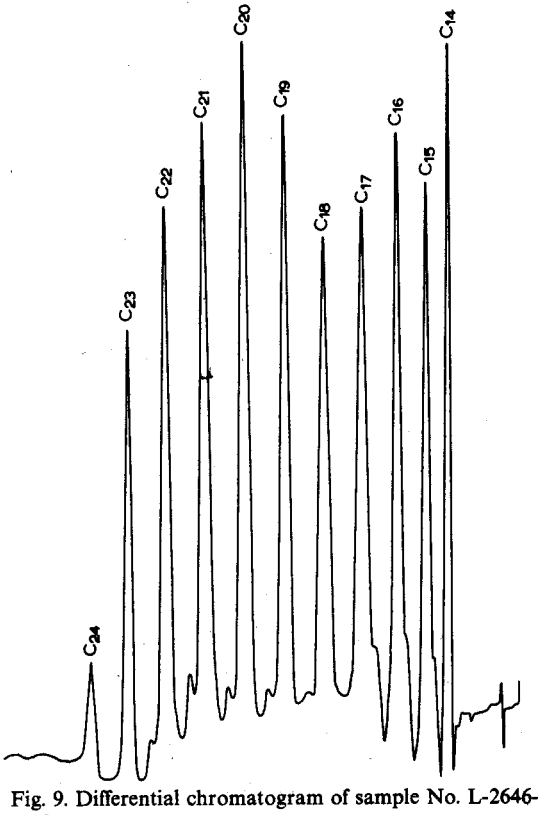

Fig. 9. Differential chromatogram of sample No. L-2646-106-2. Column temperature program 498°K to 553°K.

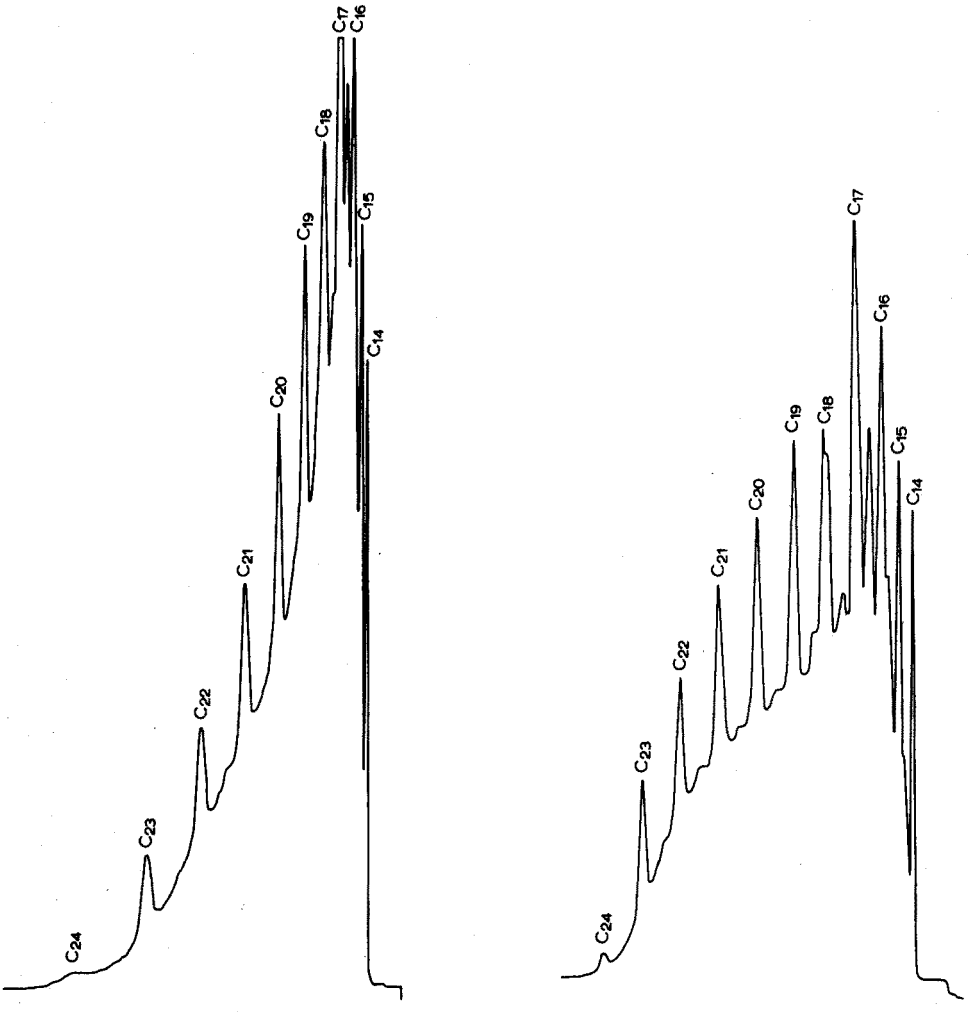

Fig. 10. Chromatogram of full sample No. L-2646-106-2. Column temperature 523°K isothermal.

Fig. 11. Chromatogram of full sample No. L-2646-106-2. Column temperature program 498°K to 553°K.

SUMMARY

A method is described which employs single injections of neat samples of petroleum kerosene and gas oils for normal paraffin analysis. Carbon number distribution as well as total normals are obtained in less than 10 min.

RÉSUMÉ

On décrit une méthode par simples injections d'échantillons de kérosène de pétrole et d'huiles minérales pour l'analyse de paraffines normales. Ces déterminations se font en moins de 10 min.

ZUSAMMENFASSUNG

Es wird eine Methode für die Analyse von Normalparaffinen beschrieben, die eine einfache Einspritzung von reinen Petroleumkerosin- und Gasölproben erfordert. Die Kohlenstoffzahlverteilung sowie die Gesamtmenge an Normalparaffinen werden in weniger als 10 min erhalten.

REFERENCES

1 I. Orszag and J. Barthory, *Acta Chim. Acad. Sci. Hung.*, 40 (1964) 367.
2 O. Frehden and G. Lazarescu, *Rev. Chim.*, 13 (1962) 491.
3 C. Karr, Jr. and J. Comberiati, *J. Chromatogr.*, 18 (1965) 394.
4 J. R. Marquart, G. B. Dellow and E. R. Freitas, *Anal. Chem.*, 40 (1968) 1633.
5 G. I. Safonova and L. M. Bulekova, *Khim. Tekhnol. Topl. Maesel*, 14, No. 10 (1969).
6 F. T. Eggertsen and S. Groenning, *Anal. Chem.*, 33 (1961) 1147.
7 G. C. Blytas and D. L. Peterson, *Anal. Chem.*, 39 (1967) 1434.
8 J. V. Brunnock, *Anal. Chem.*, 38 (1966) 1648.
9 H. S. Knight, *Anal. Chem.*, 39 (1967) 1452.
10 J. V. Mortimer and L. A. Lake, *Anal. Chim. Acta*, 38 (1967) 119.
11 O. F. Folmer, Jr., *Anal. Chim. Acta*, in press.

Analytica Chimica Acta
Elsevier Publishing Company, Amsterdam
Printed in The Netherlands

ETUDE DE L'EXTRACTION DE TITANE(IV) EN SOLUTION CHLORHYDRIQUE PAR LE TRIBUTYLPHOSPHATE EN SOLUTION DILUEE DANS LE SULFURE ET LE TETRACHLORURE DE CARBONE

G. ROLAND ET B. GILBERT*
Laboratoire de Chimie Analytique, Université de Liège au Sart Tilman, B-4000 Liège (Belgique)
(Reçu le 3 décembre 1971)

Dans une publication antérieure[1], nous avons montré que le tributylphosphate (TBP) en solution dans le sulfure de carbone ou le cyclopentane forme, avec le chlorure de titane, des composés très stables. Nous avons interprété l'influence de la concentration en complexes sur les raies Raman Ti–Cl par des associations intermoléculaires.

Nous nous sommes proposé, dans ce travail, de déterminer la nature des complexes formés lors de l'extraction du titane(IV) d'une phase aqueuse chlorhydrique par le TBP et d'étudier l'influence des associations observées en milieu anhydre sur la valeur du coefficient de distribution.

L'extraction du titane(IV) en phase organique a déjà suscité quelques travaux dont les conclusions parfois divergentes ne cadrent pas toujours avec nos résultats. S'il est difficile de résumer brièvement les conclusions des études antérieures[2-6] réalisées dans des conditions expérimentales peu comparables, deux points semblent solidement établis:

(*a*) le coefficient de distribution augmente lorsque la concentration en HCl en phase organique croît,

(*b*) le rapport $[TBP]/[Ti^{4+}]$ engagé dans le complexe extrait est égal à deux.

Alors que les travaux publiés jusqu'à présent concernaient principalement les solutions concentrées en TBP, voire le TBP pur, nous avons effectué cette étude en travaillant principalement en solution diluée dans le sulfure et le tétrachlorure de carbone ($[TBP]_t < 0.1\ M\ l^{-1}$) où les constantes des équilibres TBP–H_2O et TBP–H_2O–HCl sont connues[7].

PARTIE EXPÉRIMENTALE

Le sulfure et le tétrachlorure de carbone (p.a.) ont été distillés avant l'emploi.

Le TBP commercial a été traité par une solution de carbonate de soude à 10%, lavé à l'eau distillée avant d'être séché puis distillé sous vide.

Les solutions de titane(IV) ont été réalisées par action de l'acide chlorhydrique sur le $TiCl_4$ distillé après ébullition à reflux pendant 1 h sur P_2O_5.

Les concentrations des solutions initiales de TBP ont été déterminées soit par pesée directe en ballon jaugé, soit par dilutions exactes de solutions connues.

* Aspirant au Fonds National de la Recherche Scientifique.

L'équilibrage des solutions a été réalisé en agitant 20.0 ml de la phase organique et 10 ml de la phase aqueuse pendant 1 h à une température de $(25 \pm 0.1)°$.

Les concentrations en chlorure ont été déterminées par titrage potentiométrique au moyen d'une solution de $AgNO_3$ de normalité connue après extraction totale des ions Cl^- de la phase organique par une solution aqueuse 0.2 M l^{-1} en NaF.

Les concentrations en Ti^{4+} ont été mesurées par colorimétrie ($\lambda = 410$ nm) apres extraction du Ti^{4+} de la phase organique par une solution aqueuse (H_2SO_4 2.4 N et H_2O_2 à 10%).

Les spectres d'absorption infra-rouge et ultra-violette ont été obtenus respectivement à l'aide du spectromètre Perkin Elmer 125 et Cary 17 tandis que les spectres Raman ont été enregistrés sur un spectromètre Cary 81 équipé d'un laser hélium–neon[9]

RESULTATS EXPERIMENTAUX ET DISCUSSION

Pour chaque série d'expériences, nous avons fait varier la concentration en

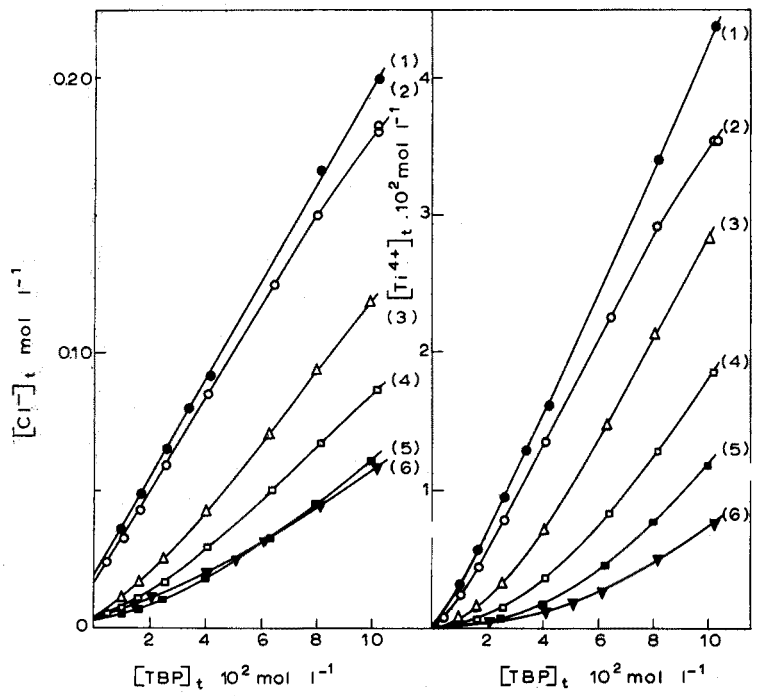

Fig. 1. Extraction de Ti^{4+} et de Cl^- par le TBP en solution dans le sulfure de carbone.

No.	$[Ti^{4+}]_{(aq.)}$ *initiale* (M l^{-1})	$[HCl]_{(aq.)}$ (M l^{-1})
(1)	0.269	11.1
(2)	0.100	11.2
(3)	0.637	9.0_5
(4)	0.272	9.2
(5)	0.540	8.3
(6)	0.102	9.2

$[TBP]_t$ en phase organique et nous avons maintenu les concentrations initiales en Ti^{4+} et en acide chlorhydrique en phase aqueuse constantes. Les résultats expérimentaux obtenus sont rassemblés sur le graphique 1.

L'examen de ces résultats montre clairement que le rapport $[TBP]/[Ti^{4+}]$ en phase organique reste toujours supérieur à deux, même en présence d'un net excès de Ti^{4+} en phase aqueuse, et que, toutes choses égales, la concentration en Ti^{4+} en phase organique augmente avec la concentration en acide chlorhydrique en phase aqueuse.

L'étude spectroscopique permet de préciser la stoechiométrie de complexes extraits:

(*a*) le spectre Raman de la phase organique après extraction du Ti^{4+} d'une phase aqueuse 11.2 *M* en acide chlorhydrique (Fig. 2, spectre 1) se caractérise dans les basses fréquences par les mêmes raies que le complexe $(TBP)_2TiCl_4$ en solution diluée, en l'absence d'acide et d'eau[1].

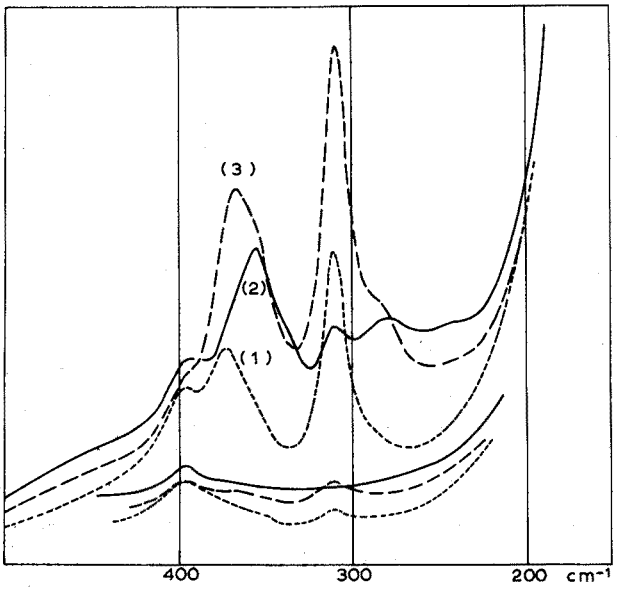

Fig. 2. Spectres Raman des complexes extraits dans le CS_2. (1) $[TBP]_t = 0.28\ M\ l^{-1}$; $[Ti^{4+}]_{(org.)} = 0.050\ M\ l^{-1}$; $[HCl]_{(aq.)} = 11.2\ M\ l^{-1}$. (2) $[TBP]_t = 0.56\ M\ l^{-1}$; $[Ti^{4+}]_{(org.)} = 0.097\ M\ l^{-1}$; $[HCl]_{(aq.)} = 9\ M\ l^{-1}$. (3) $[TBP]_t = 0.56\ M\ l^{-1}$; $[Ti^{4+}]_{(org.)} = 0.132\ M\ l^{-1}$; $[HCl]_{(aq.)} = 11.2\ M\ l^{-1}$. N.B. La raie dépolarisée située à 395 cm^{-1} est due au CS_2; la fente spectrale est de 4 cm^{-1}.

(*b*) à l'exception des bandes d'absorption caractéristiques de l'eau dissoute dans le solvant et des complexes TBP–H_2O et TBP–$H_3O^+Cl^-$ (bibl. 10), le spectre infra-rouge de cette solution ne présente, entre 4000 et 3000 cm^{-1}, aucune autre bande intense, ce qui exclut la présence de molécules d'eau d'hydratation dans le complexe (Fig. 3). Ces résultats indiquent que dans les conditions expérimentales renseignées, le titane(IV) s'extrait en phase organique en formant le complexe $(TBP)_2TiCl_4$ et excluent, du moins en solution diluée dans le sulfure de carbone, la formation, en quantités importantes, d'entités telles $(TBP)_3H_2TiCl_6$ (bibl. 2) ou

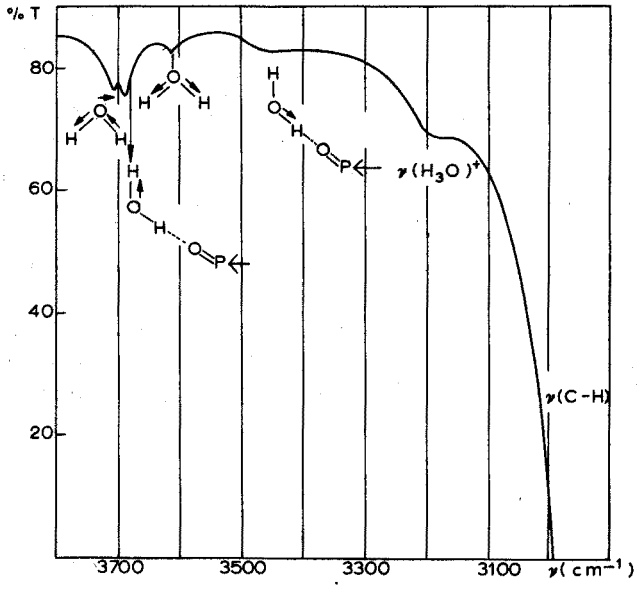

Fig. 3. Spectre infra-rouge de la phase organique après extraction du Ti^{4+} par le TBP en solution dans le CCl_4 ; $[TBP]_t = 0.041\ M\ l^{-1}$; $[TiCl_4]_{(org.)} = 1.14 \cdot 10^{-2}\ M\ l^{-1}$; $[HCl]_{(aq.)} = 11.2\ M\ l^{-1}$. Cellule en quartz de 5.00 mm, fente spectrale de 1.6 cm^{-1}.

$(TBPH_3O^+)_2Ti(OH)_2Cl_4$ (bibl. 4). L'analyse chimique de la phase organique confirme d'ailleurs les données spectroscopiques (voir plus loin).

En présence d'un complexe 2:1, en portant $\log_{10}E$, où E est le coefficient de partage, en fonction de $\log_{10}\{[TBP]_t - 2[Ti]^{4+}\}$, nous devons obtenir des droites de pente égale à deux. Expérimentalement, cette relation ne se vérifie qu'approximativement, les points expérimentaux se situant sur des droites de pente supérieure à 2.0 ou sur des courbes (Fig. 4). Cette divergence peut s'interpréter par l'effet conjugué de deux réactions secondaires en phase organique: une association et une hydrolyse partielle du complexe formé.

L'association des molécules du complexe extrait

En milieu anhydre, nous avons montré[1] que le spectre Raman du complexe $(TBP)_2TiCl_4$ en solution dans le sulfure de carbone dépendait fortement de la concentration en complexes et nous avons attribué les modifications observées à une association partielle du complexe 2:1 à lui-même. Cette interprétation permet d'expliquer directement l'augmentation anormale du coefficient de distribution et corrobore les résultats obtenus par Sevast'yanov *et al.*[5] qui proposent une polymérisation des complexes du Ti^{4+} extrait par le TBP pur pour interpréter leurs observations expérimentales.

L'hydrolyse partielle du complexe extrait

Les concentrations en Cl^- engagées dans le complexe $[Cl^-]_c$ ont été déterminées par la méthode de calcul utilisée précédemment[7] et portées en graphique en fonction de $[Ti^{4+}]_c$ (Fig. 5). La valeur du rapport $[Cl^-]_c/[Ti^{4+}]_c$ vaut 4.0 pour les faibles concentrations en $[Ti^{4+}]_{(org.)}$ et lorsque la phase aqueuse est fortement

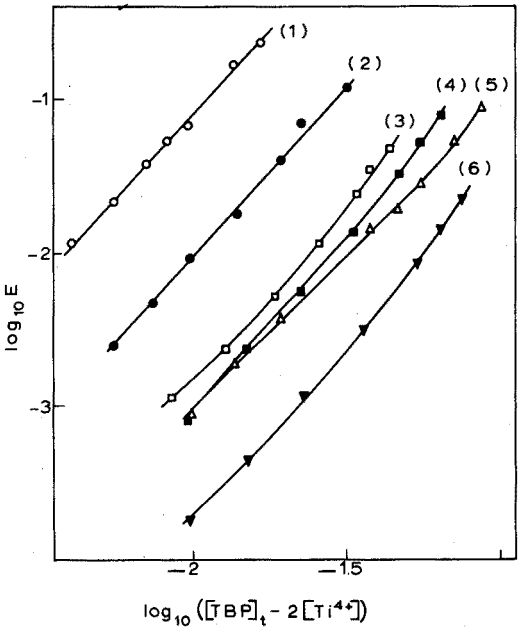

Fig. 4. Coefficient de partage en fonction de $\log_{10}\{[TBP]_t - 2[Ti]^{4+}\}$ (solvant CS_2).

No.	$[Ti^{4+}]_{(aq.)}$ *initiale* ($M\ l^{-1}$)	$[HCl]_{(aq.)}$ ($M\ l^{-1}$)
(1)	0.100	11.2
(2)	0.269	11.1
(3)	0.637	9.0_5
(4)	0.272	9.2
(5)	0.102	9.2
(6)	0.540	8.3

acide ($[HCl] \approx 11\ N$). Ce rapport diminue lorsque la concentration en Ti^{4+} en phase organique croît et cette influence est d'autant plus marquée que la concentration en acide en phase aqueuse est plus faible. Ces observations semblent indiquer qu'il y a, en plus du complexe $(TBP)_2TiCl_4$, d'autres entités caractérisées par un rapport $[Cl^-]_c/[Ti^{4+}]_c < 4.0$.

L'extraction du Ti^{4+} sous la forme $(TBP)_2TiCl_4$ semble limitée aux concentrations faibles en TBP ($[TBP]_t < 0.1\ M\ l^{-1}$) car, dès que la concentration en $[TBP]_t$ augmente, on observe une modification importante des spectres Raman et ultra-violet: les raies Raman caractéristiques du complexe $(TBP)_2TiCl_4$ disparaissent progressivement lorsque la concentration en TBP augmente et il apparaît de nouvelles raies dont les fréquences dépendent de l'acidité de la phase aqueuse (Fig. 2, spectres 2 et 3). Le spectre visible et ultra-violet du complexe $(TBP)_2TiCl_4$ présente deux bandes d'absorption intenses dont les maxima sont situés à 278 et 340 nm (Fig. 6). Lorsque la concentration en TBP augmente, le maximum d'absorption se déplace régulièrement vers les basses longueurs d'onde et se situe à 315 nm lorsqu'on utilise le TBP pur. Tout comme dans les spectres Raman, la position des bandes d'absorption est influencée par l'acidité de la phase aqueuse. D'après ces résultats, il semble bien établi que pour des concentrations en TBP supérieures à $0.1\ M\ l^{-1}$, le Ti^{4+} ne s'extrait

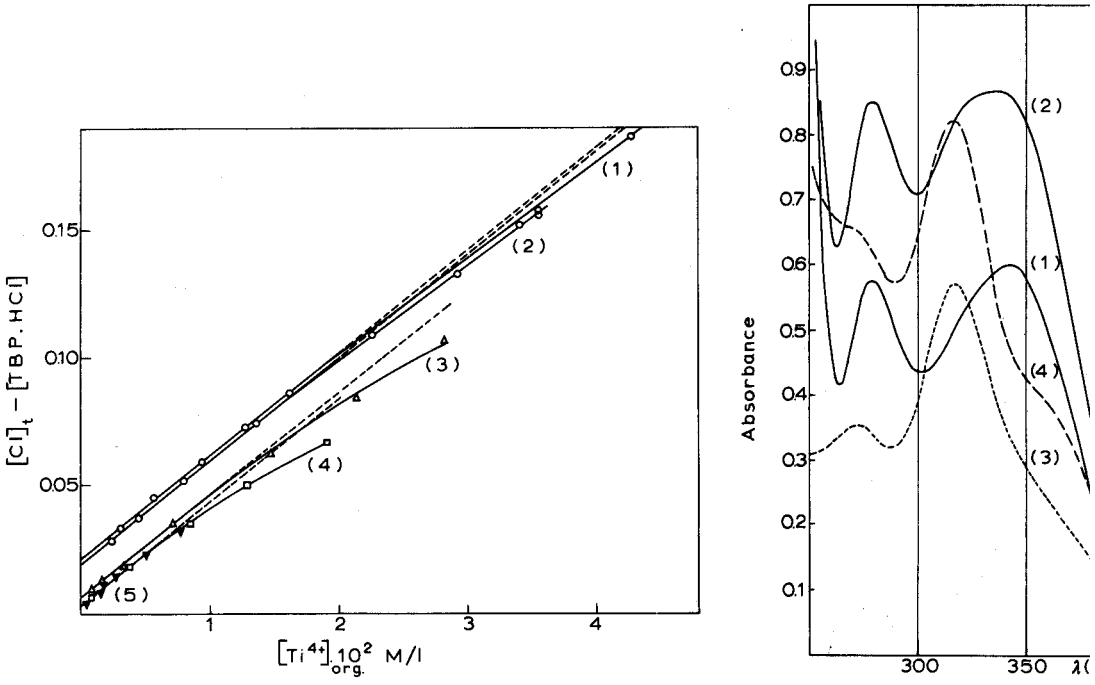

Fig. 5. Concentrations en Cl^- engagées dans le complexe.

No.	$[Ti^{4+}]_{(aq.)}$ *initiale* ($M\ l^{-1}$)	$[HCl]_{(aq.)}$ ($M\ l^{-1}$)
(1)	0.269	11.1
(2)	0.100	11.2
(3)	0.637	9.05
(4)	0.272	9.2
(5)	0.102	9.2

L'ordonnée à l'origine correspond à la concentration en HCl à saturation dans le CS_2. Les droites en traits interrompus ont une pente de 4.0.

Fig. 6. Spectres ultra-violets de la phase organique après extraction du Ti^{4+}. (1) $[TBP]_t = 0.067_4\ M\ l^{-1}$ dans CCl_4; $[TiCl_4]_{(org.)} = 5 \cdot 10^{-4}\ M\ l^{-1}$; $[HCl]_{(aq.)} = 11\ M$; cellule de 0.100 cm. (2) $[TBP]_t = 0.375\ M\ l^{-1}$ dans CCl_4; $[TiCl_4]_{(org.)} = 10^{-3}\ M\ l^{-1}$; $[HCl]_{(aq.)} = 11\ M$; cellule de 0.100 cm. (3) TBP* pur; $[Ti^{4+}] = 5 \cdot 10^{-4}\ M\ l^{-1}$; $[HCl]_{(aq.)} = 12\ M$; cellule de 0.100 cm. (4) TBP* pur; $[Ti^{4+}] = 6 \cdot 10^{-5}\ M\ l^{-1}$; $[HCl]_{(aq.)} = 12\ M$; cellule de 1.00 cm. * Le TBP utilisé a été prééquilibré avec l'acide chlorhydrique; la cellule de référence contient CH_3OH.

plus uniquement sous la forme $(TBP)_2TiCl_4$.

La complexité des équilibres encore mal connus pour le système TBP–H_2O–HCl aux concentrations élevées en TBP et les difficultés d'enregistrement des spectres Raman de solutions diluées dans le sulfure de carbone ne permettent pas de préciser la nature exacte de ces composés. Bien qu'on n'ait aucune preuve formelle, on peut cependant supposer que les complexes formés en solutions concentrées en TBP résultent de l'association du TBP à la molécule $TiCl_4$ partiellement hydrolysée par l'eau extraite en phase organique. La concentration en acide chlorhydrique extrait et destiné à empêcher l'hydrolyse du complexe en phase organique s'avèrerait insuffisante pour maintenir le Ti^{4+} sous forme de $TiCl_4$. Il semblerait qu'il existe un

parallélisme étroit entre le comportement du Ti^{4+} en phase organique et le fait que l'existence en phase aqueuse saturée en HCl des molécules $TiCl_4$ et H_2TiCl_6 proposées par certains auteurs[11-13] n'a pas toujours pu être vérifiée avec certitude[14,15].

Nous avons recherché si la coloration des complexes TBP–Ti^{4+} permettait le dosage colorimétrique de ce métal par mesure directe de l'absorbance de la phase organique. Les premiers essais que nous avons effectués se sont cependant heurtés aux difficultés expérimentales suivantes:

(*a*) l'extraction du Ti^{4+} n'est quantitative qu'aux fortes concentrations en HCl et en TBP; il est donc préférable d'utiliser le TBP pur.

(*b*) le profil des bandes d'absorption varie très fort avec la concentration en HCl en phase aqueuse; si l'extraction par le TBP pur est totale[6] lorsque $[HCl] > 5\ M\ l^{-1}$ les complexes colorés ne semblent se former qu'en milieux fortement acides ($[HCl] > 11\ M\ l^{-1}$).

(*c*) l'absorption du solvant prééquilibré avec la solution chlorhydrique n'est pas toujours reproductible et n'est pas négligeable pour des trajets optiques de 1 cm.

Malgré ces difficultés expérimentales, le dosage colorimétrique du Ti^{4+} après extraction par le TBP devrait être possible, mais, à l'heure actuelle, nous ne pouvons pas encore préciser les conditions optimales pour le dosage précis et exact de ce métal.

Nous remercions le Fonds National de la Recherche Scientifique pour l'intérêt constant apporté à nos travaux et le soutien financier accordé à notre laboratoire.

RÉSUMÉ

Nous avons étudié l'extraction du Ti^{4+} d'une solution chlorhydrique par le tributylphosphate (TBP) en solution dans le sulfure et le tétrachlorure de carbone. Les spectres Raman, infra-rouge et ultra-violet et l'analyse chimique de la phase organique ont montré que la stoechiométrie des complexes extraits dépend de la concentration en TBP en phase organique et de l'acidité de la phase aqueuse. En solution diluée ($[TBP]_t < 0.1\ M$) et en milieu acide ($[HCl] \approx 11\ M$), le composé extrait est le complexe $(TBP)_2TiCl_4$ identique au complexe formé en milieu anhydre. Lorsque l'acidité de la phase aqueuse diminue, le complexe $(TBP)_2TiCl_4$ s'hydrolyse partiellement et on doit admettre la présence de composés où le rapport $[Cl^-]/[Ti^{4+}]$ est inférieur à 4.0. Le Ti^{4+} en solution diluée s'extrait par les solutions concentrées en TBP (ou le TBP pur) sous une forme différente de $(TBP)_2TiCl_4$.

SUMMARY

The extraction of titanium(IV) from hydrochloric solutions by tributylphosphate (TBP) in carbon disulphide or carbon tetrachloride has been studied. Raman, infrared and ultraviolet spectra and chemical analysis of the organic phase have shown that the stoichiometry of the extracted complexes depends on the TBP concentration in the organic phase and on the acidity of the aqueous phase. In dilute solutions ($[TBP]_t < 0.1\ M$) and in acid media ($[HCl]_{(aq.)} \approx 11\ M$), the compound extracted is $(TBP)_2TiCl_4$, identical with the complex formed in anhydrous

media. When the acidity of the aqueous phase decreases, the $(TBP)_2TiCl_4$ complex is partially hydrolysed and the existence of species characterized by a $[Cl^-]/[Ti^{4+}]$ ratio inferior to 4.0 must be considered. Titanium(IV) in dilute solutions is extracted by concentrated TBP solutions (or pure TBP) as an entity different from $(TBP)_2TiCl_4$.

ZUSAMMENFASSUNG

Die Extraktion von Titan(IV) aus salzsauren Lösungen durch mit Schwefelkohlenstoff oder Tetrachlorkohlenstoff verdünntes Tributylphosphat (TBP) wurde untersucht. Die Raman-, Infrarot- und Ultraviolettspektren sowie die chemische Analyse der organischen Phase zeigten, dass die Stöchiometrie der extrahierten Komplexe von der TBP-Konzentration in der organischen Phase und der Säurekonzentration der wässrigen Phase abhängt. In verdünnten Lösungen ($[TBP]_t < 0.1$ *M*) und in sauren Medien ($[HCl]_{(aq.)} \approx 11$ *M*) ist die extrahierte Verbindung $(TBP)_2TiCl_4$; sie ist mit dem in wasserfreien Medien gebildeten Komplex identisch. Wenn die Säurekonzentration der wässrigen Phase abnimmt, wird der $(TBP)_2TiCl_4$-Komplex teilweise hydrolysiert, und es muss die Existenz von Spezies berücksichtigt werden, deren $[Cl^-]/[Ti^{4+}]$-Verhältnis kleiner als 4.0 ist. Die aus verdünnten Lösungen durch konzentrierte TBP-Lösungen (oder reines TBP) extrahierte Verbindung ist nicht $(TBP)_2TiCl_4$.

BIBLIOGRAPHIE

1 G. ROLAND, B. GILBERT ET G. DUYCKAERTS, *Spectrochim. Acta*, à paraître.
2 V. N. STARTSEV, E. I. KRYLOV ET YU. A. KOZ'MIN, *Russ. J. Inorg. Chem.*, 10 (1965) 1285.
3 V. N. STARTSEV, E. I. KRYLOV ET YU. A. KOZ'MIN, *Russ. J. Inorg. Chem.*, 11 (1966) 1239.
4 V. N. STARTSEV, YU. I. SANNIKOV, G. N. BEN'YASH ET E. I. KRYLOV, *Russ. J. Inorg. Chem.*, 13 (1968) 586.
5 Y. G. SEVAST'YANOV, B. Z. IOFA, A. N. NESMEYANOV ET V. G. VINOGRADA, *Radiokhim.*, 12 (1970) 33.
6 A. A. YADAV ET S. M. KHOPKAR, *Anal. Chim. Acta*, 45 (1969) 355.
7 G. ROLAND ET G. DUYCKAERTS, *Anal. Chim. Acta*, 54 (1971) 423.
8 R. MITAMURA, I. TOKURA, S. NISHIMURA, Y. KONDO ET N. G. LI, *J. Inorg. Nucl. Chem.*, 30 (1968) 1019.
9 B. GILBERT ET G. DUYCKAERTS, *Spectrochim. Acta*, 26A (1970) 2197.
10 E. V. KOMAROV, M. E. OBUKHOVA ET M. F. PUSHLENKOV, *Russ. J. Inorg. Chem.*, 12 (1967) 116.
11 W. v. KOWALEVSKY, *Z. Anorg. Chem.*, 25 (1900) 189.
12 M. E. P. RUMPF, *C.R.*, (1936) 202–950.
13 M. CRAIU ET G. GRUDER, *Rev. Roum. Chim.*, 13 (1968) 1581.
14 J. E. D. DAVIES ET D. A. LONG, *J. Chem. Soc. (A)*, (1968) 2560.
15 G. ROLAND, B. GILBERT ET G. DUYCKAERTS, travail non publié.

Analytica Chimica Acta
Elsevier Publishing Company, Amsterdam
Printed in The Netherlands

A COMPARISON OF METHODS FOR THE DETERMINATION OF GALLIUM IN ORES

G. N. LYPKA and A. CHOW
Department of Chemistry, University of Manitoba, Winnipeg, Manitoba (Canada)
(Received 8th December 1971)

The determination of gallium in minerals and rocks has been accomplished by a few techniques involving various degrees of difficulty. The most sensitive technique reported for determination of gallium is the use of a rhodamine B complex with a detection limit of 0.01 μg by fluorescence in a benzene extract[1,2]. Rhodamine B has been applied to analysis of rocks and minerals for gallium[2-4]; the complex formation was studied in more detail and the advantage of using titanium(III) chloride was emphasized. Previously, Sandell[5] had utilized the fluorescence of gallium 8-hydroxyquinolinate in analysis of silicate rocks over a range of 0.05–67 p.p.m. gallium. Other dyes have also been used for the colorimetric determination of gallium[6].

Atomic absorption spectrophotometry would appear to offer several advantages over the fluorimetric methods for determining gallium although only a few studies have been reported. Gallium and indium lamps were evaluated by Mulford[7] and the absorption characteristics evaluated by Popham and Schrenk[8]. The determination of gallium by atomic absorption has been reported[9]; gallium perchlorate was used, as well as a 4:1 mixture of methyl isobutyl ketone and 1-pentanol to extract gallium 8-hydroxyquinolinate for direct aspiration. Pollock[10] applied atomic absorption to the determination of gallium in limonite, using methyl isobutyl ketone and titanium(III) chloride to extract gallium from limonite in hydrochloric acid solution for direct aspiration. This technique gave similar values to an unstated spectrophotometric method.

The use of atomic absorption for the determination of gallium in ores has not been fully investigated or utilized. The present report details a comparison of the determination of gallium in several ore products by atomic absorption both directly with solutions of the ore and indirectly with a solvent extraction system, and by a spectrophotometric method with rhodamine B.

EXPERIMENTAL

Apparatus

A Beckman DU spectrophotometer was used. For atomic absorption, a Perkin Elmer Model 306 atomic absorption spectrophotometer was used with digital and chart recorder readouts.

Chemicals

Gallium standards were prepared by dissolving pure metal (Baker Chemicals)

in 20 ml of concentrated hydrochloric acid and diluting to a 1048 p.p.m. gallium solution. Suitable standards were prepared by dilution with water or 7 *M* hydrochloric acid.

Isopropyl ether was purified by distilling reagent-grade ether from sodium hydroxide.

Rhodamine B solution. A 0.5% dye solution in 7 *M* hydrochloric acid was used.

Chlorobenzene–carbon tetrachloride mixture. 25% carbon tetrachloride in chlorobenzene.

Titanium(III) chloride solution. 1% titanium(III) chloride was prepared by dilution of 20% titanium(III) chloride with 7 *M* hydrochloric acid.

Gallium containing ores and mill products were obtained through the courtesy of the Tantalum Mining Corporation of Canada Ltd., Bernic Lake, Manitoba.

Procedures

Preparation of ore solution. The finely ground ores and mill products were subdivided by rolling each material on a large cellophane sheet, spreading it to form a large level area and taking a portion from each 1″ square area to form the sample.

Ore samples of 4–5 g were weighed into 250-ml polyethylene beakers and 20 ml of concentrated sulfuric acid were added to each. Concentrated hydrofluoric acid was added until the foaming ceased (about 40 ml) and the covered sample was then heated on a steambath overnight. The cover was then removed and the sample heated for a day to remove hydrofluoric acid. The contents of the plastic beaker were transferred to a 250-ml glass beaker and heated with stirring to fume off sulfuric acid. The residue was redissolved by heating in 50–100 ml of 7 *M* hydrochloric acid which was just sufficient to dissolve the samples when the acid was hot. Little or no residue resulted after this treatment.

The ore solution was transferred to a 250-ml separatory funnel and 10 ml of 20% titanium(III) chloride solution were added. After allowing the ore solution to stand for 5 min, 30 ml of purified isopropyl ether were added and the separatory funnel shaken. The aqueous phase was transferred to a second separatory funnel and again shaken with 30 ml of isopropyl ether. The ether extracts were combined in the first funnel. The second funnel was rinsed with a small amount of 7 *M* hydrochloric acid and with 10 ml of isopropyl ether and both rinsings were added to the ether extracts. The extracts and washings were then shaken and the aqueous phase drawn off. After the organic phase had been drained into a 150-ml beaker and the separatory funnel washed twice with 10 ml of isopropyl ether, the combined solutions were evaporated to dryness on a steam bath. The residue was dissolved in 7 *M* hydrochloric acid and diluted to 25 ml in a volumetric flask.

Spectrophotometric determination. The spectrophotometric method used was a modification of the determination with rhodamine B[4] after several unsuccessful attempts to utilize the 8-hydroxyquinolinate fluorimetric method for gallium. A suitable aliquot of an ore sample prepared by acid dissolution and isopropyl ether extraction was placed in a 60-ml separatory funnel with 5 ml of 1% titanium(III) chloride solution, 8 ml of chlorobenzene–carbon tetrachloride solution and 0.5 ml of 0.5% rhodamine B solution. After 1 min of manual shaking, the phases were allowed to separate and the organic layer was removed through a glass wool plug

(to eliminate a fine suspension in the organic layer) into a 10-ml volumetric flask containing 1 ml of absolute ethanol (to eliminate any water suspension). The aqueous phase was washed with an additional 1 ml of chlorobenzene–carbon tetrachloride and the washings were added to the flask. The organic extract was made up to volume with chlorobenzene–carbon tetrachloride and the absorbance measured at 558 nm. It was found that the gallium complex produced was not stable to exposure to light and so all samples were measured as soon as possible after the formation of the rhodamine B complex.

Standards were measured with aliquots of a dilute gallium solution over the range of 1–10 μg and a calibration curve was prepared. Blanks gave an average absorbance of 0.006 when treated similarly. Because of some instability in the reagents it was necessary to prepare one or more standards with each sample run and to correct the calibration graph accordingly.

Atomic absorption determination. A preliminary atomic absorption method was attempted with an ore solution prepared as described above by acid dissolution, evaporation, fuming and dissolution in 7 *M* hydrochloric acid. The values obtained were 50% or more higher than those obtained by the rhodamine B spectrophotometric method. The addition of known amounts of gallium to the ore solution before atomic absorption analysis resulted in values 15% or more, higher than would be expected. Other attempts to extract gallium selectively from the ores with HCl, HNO_3, H_2SO_4, HF, 1 *M* NaOH, $HCl+HNO_3$ or $HF+HNO_3$ produced values varying from 0 to 100% extraction when the filtered solution was diluted and determined by atomic absorption, with hydrofluoric or sulfuric acid being the most efficient.

TABLE I

EFFECT OF VARIOUS METALS ON GALLIUM ABSORBANCE

(41.6 p.p.m. gallium taken; 600 p.p.m. diverse metal added)

Metal salt added	*Value ± average deviation*	*Metal salt added*	*Value ± average deviation*
None	1000± 8	$CoCl_2$	961±10
$FeCl_3$	965± 6	K_2CrO_4	985±19
$CuSO_4$	1009± 7	$Pb(NO_3)_2$	985±16
$Ni(NO_3)_2$	1001±11	Na_2MoO_4	920±10
$Zn(NO_3)_2$	950± 6	$Bi(NO_3)_3$	1073±10
$CdCl_2$	950±13	$SnCl_2$[a]	902±14

[a] 10,000 p.p.m. Sn added.

A study of the effect of various metals on the absorbance obtained for a standard gallium solution in 5.5 *M* hydrochloric acid indicated little effect (Table I). The source of these positive errors was not determined as it was considered that the more generally applicable solvent extract–atomic absorption technique would be more acceptable.

Initial studies with gallium standards indicated a strong dependence of absorbance on hydrochloric acid content. A series of values was obtained for a 41.6-p.p.m. gallium solution in a variety of acids and bases of different concentration (Table II).

TABLE II

EFFECT OF VARIOUS SOLUTIONS ON GALLIUM ABSORBANCE

(41.6 p.p.m. gallium taken)

Additive	*Final concentration (M)*	*Value ± average deviation*	*Additive*	*Final concentration (M)*	*Value ± average deviation*
H_2O	—	1000±15		6.4	1006±11
HCl	0.012	1009± 9		9.6	1020±13
	0.05	1011±13	H_2SO_4	0.01	1012± 5
	0.12	976±16		0.06	1003±14
	0.5	945±17		0.12	1020± 4
	1.2	953±11		0.6	1061±11
	2.4	930± 6		3.6	1060±10
	4.8	862±14		7.2	1059±18
	7.2	815± 4		14.4	962±18
HNO_3	0.016	1002±13		21.6	734±18
	0.08	994±15	NaOH	0.01	1028± 9
	0.16	973±13		0.06	947±28
	0.8	978±13		0.12	911±20
	1.6	994±21		0.6	760± 6
	3.2	1000±12	NH_4Cl	1.0	950±11

The conditions used for determination of gallium by atomic absorption with the Perkin Elmer 306 were an air–acetylene flame set to be lean, a 0.7-nm slit, a current of 7 mA on the Varian gallium hollow-cathode lamp and a wavelength setting of 287.4 nm. A linear response was obtained over the range 0–100 p.p.m. gallium in the unexpanded absorbance mode and over the range 0–20 p.p.m. in an expanded mode.

For convenience of comparison, gallium concentration was determined in ore samples with 7 *M* hydrochloric acid and therefore all standards were prepared at this acidity. A series of ore samples was prepared by the dissolution and solvent extraction method described. An aliquot of the ore solution was then analyzed by the rhodamine B spectrophotometric method and a second aliquot by the solvent extraction–atomic absorption method.

RESULTS AND DISCUSSION

The results obtained by the two methods for various ores and mill products are reported in Table III.

The values obtained by the rhodamine B spectrophotometric method and by the atomic absorption method are in reasonable agreement, although they show some deviations which might be expected of ore samples. The difficulties of determining gallium by atomic absorption spectrophotometry have not been appreciated in the literature. The wide variation in absorbance with hydrochloric acid concentration suggests that adequate attention must be paid to this effect in any determination.

The strong positive influence of components of the ore solution indicates that serious consideration must be given to the matrix composition or that a separation

TABLE III

A COMPARISON OF GALLIUM ASSAY BY SPECTROPHOTOMETRIC AND ATOMIC ABSORPTION METHODS

Sample		*Value found*			
		Spectrophotometric (p.p.m.)	*Average ± avg. deviation*	*Atomic absorption (p.p.m.)*	*Average ± avg. deviation*
R. T. Tails	13-A	187		225	
	14-A	176		199	
			181 ± 6		212 ± 13
Sand Tail Rougher	5B	237		274	
	6B	253		250	
	7B	259		275	
			250 ± 9		266 ± 11
Slime Rougher Tail	1C	321		343	
	2C	310		297	
	3C	310		298	
			314 ± 5		313 ± 20
Ilmenite	1D	53.4		59.9	
	2D	56.7		58.1	
	3D	57.5		59.9	
			55.9 ± 1.6		59.3 ± 0.8
	1E	98.1		96.8	
	2E	89.7		79.7	
	3E	94.1		97.6	
			94.0 ± 2.9		91.4 ± 7.8

method, such as the solvent extraction scheme described, must be used. The solvent extraction–atomic absorption method of analysis provides a sensitive and consistent method for gallium in a variety of ore and mill products. This method provides similar values, and is a convenient alternative, to the rhodamine B spectrophotometric method which shows some difficulties caused by complex instability.

The authors wish to express their thanks to the National Research Council of Canada and to the Manitoba Research Council and Manitoba Department of Industry and Commerce for their financial support.

SUMMARY

Gallium was determined in a series of ores and mill products by acid dissolution of the ore and solvent extraction of gallium with isopropyl ether. A comparison of the determination of gallium by a rhodamine B spectrophotometric method and by an atomic absorption method based on preliminary solvent extraction, indicated similar results. The dependence of gallium atomic absorbance on acid strength and matrix was noted.

RÉSUMÉ

Le gallium est dosé dans une série de minerais et de produits de broyage; on

procède par dissolution acide et extraction du gallium au moyen d'isopropyléther. Un dosage spectrophotométrique au moyen de Rhodamine-B et un dosage par absorption atomique, basé sur une extraction préliminaire dans un solvant, ont donné des résultats similaires. On examine l'influence de la force en acide et de la matrice.

ZUSAMMENFASSUNG

Gallium wurde in einer Reihe von Erzen und Hüttenprodukten durch Säureaufschluss des Erzes und durch Extraktion des Galliums mit Isopropyläther bestimmt. Ein Vergleich der Bestimmung von Gallium nach einer spektrophotometrischen Methode mit Rhodamin B und nach einer Atomabsorptionsmethode nach vorausgehender Extraktion ergab ähnliche Werte. Die Abhängigkeit der atomaren Extinktion des Galliums von Säurestärke und Matrix wurde festgestellt.

REFERENCES

1 H. Onishi, *Anal. Chem.*, 27 (1955) 832.
2 H. Onishi and E. B. Sandell, *Anal. Chim. Acta*, 13 (1955) 159.
3 H. Onishi and E. B. Sandell, *Geochim. Cosmochim. Acta*, 2 (1951) 1.
4 F. Culkin and J. P. Riley, *Analyst*, 83 (1958) 208.
5 E. B. Sandell, *Anal. Chem.*, 19 (1947) 63.
6 I. A. Sheka, I. S. Chaus and T. T. Mityureva, *Chemistry of Gallium*, Elsevier, Amsterdam, 1966, p. 266.
7 C. E. Mulford, *At. Absorpt. Newsl.*, 5 (1966) 28.
8 R. E. Popham and W. G. Schrenk, *Spectrochim. Acta*, 24B (1969) 223.
9 H. K. L. Gupta, F. J. Amore and D. F. Boltz, *At. Absorpt. Newsl.*, 7 (1968) 107.
10 E. N. Pollock, *At. Absorpt. Newsl.*, 10 (1971) 77.

Analytica Chimica Acta
Elsevier Publishing Company, Amsterdam
Printed in The Netherlands

EXTRACTION–SPECTROPHOTOMETRIC DETERMINATION OF TRACES OF PALLADIUM WITH AZIDE AND METHYLENE BLUE

ROKURO KURODA, NOBUTAKA YOSHIKUNI and YOSHIHIRO KAMIMURA
Laboratory for Analytical Chemistry, Faculty of Engineering, University of Chiba, Chiba (Japan)
(Received 18th December 1971)

Metal complexes containing the azide ion have been known for some time, but it is only recently that the preparation and properties of azido complexes of transition metals have been extensively studied[1,2]. Correspondingly, use of the azide ion as a spectrophotometric reagent for metals is still rare.

Clem and Huffman have reported extraction–spectrophotometric methods for the determination of palladium[3] and gold[4], based on the formation of tetraazidopalladium and tetraazidogold complexes, respectively. They also have investigated the efficiency of extraction into chloroform of pyridine azide complexes of eleven metals, presenting spectrophotometric methods for copper, nickel and palladium[5]. A procedure for the extraction and spectrophotometric determination of iron as an *o*-phenanthroline-azide mixed ligand complex has appeared recently[6].

Ion-association complexes of palladium involving its azido complex and methylene blue have apparently not been reported previously. In the work described here, it was found that the ternary complex involving palladium(II), azide and methylene blue can be easily extracted into chloroform, providing a basis for a highly sensitive spectrophotometric method for palladium. The molar absorptivity is about $5.8 \cdot 10^4$, which is high enough compared to those reported recently for palladium complexes with PAR[7] ($1.3 \cdot 10^4$), 3-nitroso-2,6-pyridinediol[8] ($2.6 \cdot 10^4$), 1-(2-carboxy-4-sulphonatophenyl)-3-hydroxy-3-phenyltriazene[9] ($2.0 \cdot 10^4$), thiocyanate and zephiramine[10] ($3.7 \cdot 10^4$), etc.

EXPERIMENTAL

Apparatus

Spectrophotometric measurements were made with a Hitachi Perkin-Elmer 139 u.v.–vis. Spectrophotometer in 1-cm quartz cells. The pH measurements were made with a Hitachi Horiba pH meter Model 5-M.

Reagents

Reagent grade chemicals were used unless otherwise mentioned.

Palladium(II) stock solution. Dissolve 0.1064 g of spectroscopically pure palladium black in hot aqua regia, evaporate nearly to dryness, and treat with 5-ml portions of hydrochloric acid to convert to chloride. Finally evaporate the hydrochloric acid solution to dryness and take up the residue with 0.1 *M* hydrochloric acid, diluting exactly to 100 ml with the same acid to yield a 0.01 *M* palladium(II) stock solution.

Sodium azide solution. Dissolve 65 g of sodium azide in 1 l of deionized water to give a 1.0 *M* stock solution.

Methylene blue solution (0.001 *M*). Dissolve 0.0374 g of methylene blue in 100 ml of deionized water.

Buffer solutions. Prepare acetate buffer solutions of pH 3–6 by mixing 0.1 *M* sodium acetate and 0.1 *M* acetic acid in varying proportions. Prepare phosphate buffer solutions by mixing 0.1 *M* disodium hydrogenphosphate and 0.1 *M* potassium dihydrogenphosphate in proper proportions to cover the pH range 4–9.

Procedure

Place the sample solution containing 1–15 μg of palladium(II) in a 100-ml separatory funnel. Add 5.0 ml of 0.01 *M* sodium azide solution, 10 ml of acetate buffer solution (pH 4.5) and 2.0 ml of 0.001 *M* methylene blue solution. Adjust the volume to 30 ml. Add 10.0 ml of chloroform and extract for 3 min by shaking mechanically. Withdraw the organic layer and centrifuge it for 3 min to remove water droplets. Measure the absorbance of the organic phase at 653 nm against a reagent blank which has been carried through the same procedure. Obtain the calibration curve by carrying aliquots containing 1–15 μg of palladium(II) through the same procedure.

RESULTS AND DISCUSSION

Absorption spectra

The spectrum of the palladium(II)–azide–methylene blue complex is illustrated in Fig. 1 along with that of methylene blue in aqueous solution. The respective spectra of the ternary complex and methylene blue are almost identical in shape, although the absorption maximum of the ternary complex (653 nm) shifts a little towards shorter wavelength.

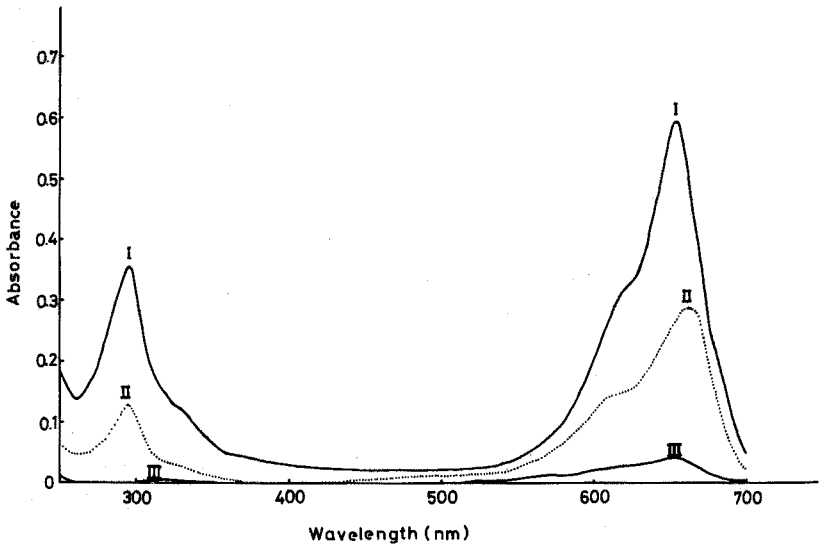

Fig. 1. Absorption spectra. (I) Palladium(II)–azide–methylene blue complex in chloroform against reagent blank. Aqueous phase: Pd(II) $1.00 \cdot 10^{-7}$ mole taken, pH 4.5. (II) Methylene blue in deionized water, $1.0 \cdot 10^{-5}$ *M*. Reference: deionized water. (III) Reagent blank against chloroform.

Unless otherwise mentioned, the following tests were made with 10.6 μg of palladium(II) by the procedure above. The amount of chloride introduced together with palladium(II) was 0.1 mmole, thus yielding *ca.* 0.003 *M* chloride solution; the amount of chloride contributed from the methylene blue solution was low enough except when increasing amounts of methylene blue were added to see the effect of methylene blue concentration.

Effect of pH

The effect of pH on the color development was examined in the pH range 3–6 (acetate buffer). Absorbance was constant over the pH range 4.0–5.5, decreasing at both higher and lower pH values. Hydrazoic acid is a weak acid (p*K* 4.72) and at lower pH values gives poor color development because of the suppression of dissociation of the hydrazoic acid. Hydrolysis may account for the lower absorbance at higher pH region.

The choice of the buffer system is highly important. The acetate buffer system was finally chosen because it gave the lowest blank absorbance among the buffer systems tested. When the phosphate buffer system was used, the pH range 3.5–6 was found to give the highest absorbance, but the blank level was generally high, increasing sharply with increasing pH values; it became as high as 0.25 (absorbance) at pH 7.

Effect of shaking time

The shaking time was varied from 1 min to 10 min. The absorbance remained constant after 3-min extraction.

Effect of azide and methylene blue concentrations

A constant absorbance was obtained by adding 2–6 ml of 0.01 *M* sodium azide solution with other variables held constant. When less than 2 ml was added, a lower absorbance resulted.

The amount of methylene blue solution (0.001 *M*) added was varied from 0.5 to 10 ml, a constant absorbance being obtained when more than 1 ml of the solution was added. An excess of methylene blue should be avoided, because increasing amounts increase the level of the blank absorbance, which amounts to 0.1 when 10 ml of the solution is used.

Stability of colored solution

The absorbance of the complex extracted into chloroform remained unchanged for at least 24 h.

Volume ratio

Under the conditions in the procedure, the volume of chloroform was held constant at 10.0 ml and the volume of the aqueous phase was varied from 30 to 75 ml. Constant absorbance was found up to a volume ratio of 4.5 : 1 of aqueous to organic phase. The absorbance then decreased very gradually down to 87% of the initial absorbance at the ratio of 7.5 : 1.

Calibration curve

The palladium(II)–azide–methylene blue system obeyed Beer's law in the

range 1–15 μg of palladium(II) in the 10.0-ml chloroform extract for 1.00-cm cells. The apparent molar absorptivity was about $5.8 \cdot 10^4$.

Effect of complexing cations

Instead of methylene blue, zephiramine (tetradecyldimethylbenzylammonium chloride) was used successfully. From the phosphate buffer solution (pH 5–8), palladium(II)–azide–zephiramine complex was easily extracted into chloroform, giving an absorbance maximum at 328 nm. Although the sensitivity of the zephiramine method was much less than that of the methylene blue method, the pH range for extraction was wider and the blank absorbance was extremely low. Beer's law was obeyed over the range 1–50 μg or more in the 10.0-ml chloroform extract for 1.00-cm cells. The molar absorptivity was $2.0 \cdot 10^4$.

Usually palladium(II) can be extracted from 10–100 ml of the phosphate buffer solution containing 0.05 mmole of sodium azide and 0.005 mmole of zephiramine by shaking with 10.0 ml of chloroform for 3 min. The absorbance of the zephiramine complex was stable for 24 h.

Tetraphenylarsonium chloride was also tested, but the color sensitivity was inferior to the zephiramine method.

Partial composition of the methylene blue complex

It is difficult to confirm the empirical formula of the extracted palladium(II)–azide–methylene blue complex in the presence of excess of azide ion along with chloride ion. Job's method of continuous variation was applied keeping the total chloride concentration in the aqueous phase less than $4 \cdot 10^{-4}$ *M*. In the presence of an excess of azide ($5 \cdot 10^{-2}$ mmole) equimolar solutions of palladium(II) and methylene blue ($4 \cdot 10^{-5}$ *M*) were mixed in varying amounts, the total volume being kept at 10.0 ml. These solutions were adjusted to pH 4.5, diluted to 30 ml, extracted with 10.0 ml of

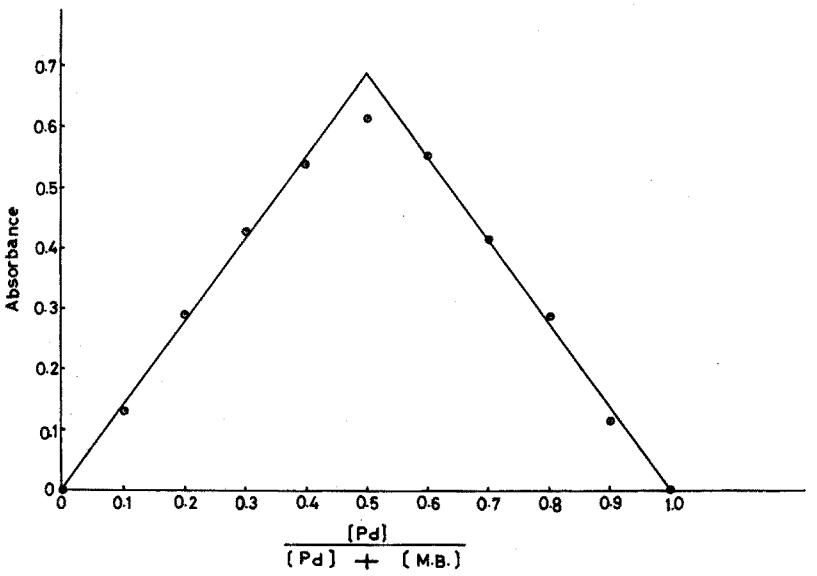

Fig. 2. Job's method of continuous variation. Total molarity in aqueous phase $1.3 \cdot 10^{-5}$ *M*.

chloroform, and measured at 653 nm. The result (Fig. 2) indicates a palladium(II): methylene blue ratio of 1:1. When palladium(II) sulfate solution was prepared and used as the starting material, the same ratio was obtained.

Interference study

In order to determine the effect of various ions on the methylene blue method, solutions containing palladium(II) and the ion in question were treated exactly as in the procedure above. The amount of palladium(II) added in anion interference study was 5.32 μg ($5.00 \cdot 10^{-8}$ *M*), and varying concentrations of anions were added as indicated in Table I. Significant interferences were observed for perchlorate, iodide and thiocyanate. High concentrations of phosphate, sulfate and tartrate did not interfere. This provides a favorable condition for the determination of palladium-(II). Interfering volatile acids such as hydrochloric, hydroiodic, nitric acid, etc. can be removed by fuming with sulfuric acid and perhaps with phosphoric acid. Secondly, tartrate may be used as the buffer and masking agent for interfering cations. Because of this, 1 ml of 0.3 *M* sodium tartrate was added to the sample solution (30 ml) as the masking agent in the cation interference study.

The metals investigated were added as chloride, sulfate or oxyanion. When the chloride was used, the final chloride concentration was kept below $3 \cdot 10^{-3}$ *M*. The amount of palladium(II) was mostly 10.6 μg ($1.00 \cdot 10^{-7}$ *M*). In the presence of tartrate, 500 μg each of aluminum(III), beryllium(II), bismuth(III), copper(II),

TABLE I

EFFECT OF FOREIGN ANIONS[a]

Anion	*Added as*	*Concn. (M)*	*Pd(II) recovered (%)*
$B_4O_7^{2-}$	$Na_2B_4O_7$	$1 \cdot 10^{-2}$	88.8
		$1 \cdot 10^{-3}$	100.0
Cl^-	NaCl	$3.3 \cdot 10^{-2}$	118.3
		$6 \cdot 10^{-3}$	100.4, 100.8
ClO_4^-	$NaClO_4$	$3 \cdot 10^{-6}$	108.3
		$3 \cdot 10^{-7}$	100.0
F^-	NaF	$1 \cdot 10^{-1}$	50.9
		$1 \cdot 10^{-2}$	102.8
I^-	KI	$1 \cdot 10^{-5}$	115.4
		$1 \cdot 10^{-6}$	98.9
		$1 \cdot 10^{-7}$	100.3
NO_3^-	$NaNO_3$	$3 \cdot 10^{-3}$	108.7
		$3 \cdot 10^{-4}$	100.8
PO_4^{3-}	KH_2PO_4	$1 \cdot 10^{-1}$	104.2
		$1 \cdot 10^{-2}$	100.5
SCN^-	NaSCN	$3 \cdot 10^{-6}$	109.5
		$3 \cdot 10^{-7}$	100.4
SO_4^{2-}	Na_2SO_4	$1 \cdot 10^{-1}$	100.0
		$1 \cdot 10^{-2}$	100.9
Citrate	Sodium salt	$1 \cdot 10^{-2}$	91.6
		$1 \cdot 10^{-3}$	101.0
Tartrate	Sodium salt	$1 \cdot 10^{-1}$	97.2
		$1 \cdot 10^{-2}$	100.0

[a] 5.32 μg of Pd(II) taken.

iron(III), gallium(III), mercury(II), indium(III), lanthanum(III), manganese(II), antimony(III), tin(IV), thorium(IV) and tungsten(VI) did not interfere. Even in the absence of tartrate 500 μg each of arsenic(III), calcium(II), cadmium(II), cobalt(II), nickel(II), selenium(IV), tellurium(IV) and zinc(II) did not interfere; 50-μg levels of uranium(VI), vanadium(IV) and zirconium(IV) did not interfere in the presence of tartrate. However, gold(III), chromium(VI), molybdenum(VI) and rhenium(VII) interfered with the determination of palladium(II) even at the level of 5 μg in the presence of tartrate. Only 5 μg each of iridium(IV), platinum(IV) and ruthenium(III) could be tolerated in the presence of tartrate. The criterion for interference was a recovery of palladium(II) which varied more than 4.0% from the expected value.

SUMMARY

A sensitive extraction–spectrophotometric method is described for the determination of palladium(II). This is based on the formation of a palladium(II)–azide–methylene blue ternary complex, which is extracted in chloroform from the acetate buffered solution at pH 4.0–5.5. The color develops rapidly and is stable for at least 24 h. The complex system conforms to Beer's law up to 15 μg of palladium(II) in the 10-ml chloroform extract at 653 nm. The apparent molar absorptivity is about $5.8 \cdot 10^4$. Few metals interfere in the presence of tartrate; gold(III), chromium(VI), molybdenum(VI), platinum group metals and rhenium(VII) interfere seriously. Sulfate and phosphate do not interfere even in excess.

RÉSUMÉ

On décrit une méthode sensible par extraction–spectrophotométrie pour le dosage du palladium(II). Elle est basée sur la formation d'un complexe ternaire: palladium(II)–azoture–bleu de méthylène, pouvant s'extraire dans le chloroforme, en milieu tampon acétate (pH 4.0–5.5). La coloration se développe rapidement; elle est stable 24 h au moins. La loi de Beer s'applique jusqu'à 15 μg de palladium(II) dans un extrait de 10 ml de chloroforme, à 653 nm. Coefficient d'extinction molaire apparent: env. $5.8 \cdot 10^4$. En présence de tartrate, il y a peu d'interférences métalliques; cependant l'or(III), le chrome(VI), le molybdène(VI), les métaux du groupe du platine et le rhénium(VII) gênent considérablement. Sulfate et phosphate ne gênent pas, même en excès.

ZUSAMMENFASSUNG

Es wird eine empfindliche extraktions–spektrophotometrische Methode für die Bestimmung von Palladium(II) beschrieben. Sie beruht auf der Bildung eines ternären Komplexes Palladium(II)–Azid–Methylenblau, der aus acetatgepufferter Lösung bei pH 4.0–5.5 mit Chloroform extrahiert wird. Die Färbung entwickelt sich schnell und ist mindestens 24 h beständig. Das Komplexsystem gehorcht dem Beerschen Gesetz bis zu 15 μg Palladium(II) in 10 ml Chloroformextrakt bei 653 nm. Der scheinbare molare Extinktionskoeffizient ist etwa $5.8 \cdot 10^4$. In Gegenwart von Tartrat stören nur wenige Metalle; Gold(III), Chrom(VI), Molybdän(VI), Metalle der Platingruppe und Rhenium(VII) stören erheblich. Sulfat und Phosphat stören auch im Überschuss nicht.

REFERENCES

1 H.-H. Schmidtke and D. Garthoff, *J. Amer. Chem. Soc.*, 89 (1967) 1317.
2 K. Bowman and Z. Dori, *Inorg. Chem.*, 9 (1970) 397.
3 R. G. Clem and E. H. Huffman, *Anal. Chem.*, 37 (1965) 86.
4 R. G. Clem and E. H. Huffman, *Anal. Chem.*, 37 (1965) 1155.
5 R. G. Clem and E. H. Huffman, *Anal. Chem.*, 38 (1966) 926.
6 V. P. R. Rao and P. V. R. B. Sarma, *Mikrochim. Acta*, (1970) 783.
7 K. K. Saxena, B. V. Agarwala and A. K. Dey, *Mikrochim. Acta*, (1969) 694.
8 C. W. McDonald and J. H. Bedenbaugh, *Mikrochim. Acta*, (1970) 474.
9 A. K. Majumdar and D. Chakraborti, *Anal. Chim. Acta*, 53 (1971) 393.
10 H. Matsuo, S. Chaki and K. Akabori, *Bunseki Kagaku*, 20 (1971) 226.

Analytica Chimica Acta
Elsevier Publishing Company, Amsterdam
Printed in The Netherlands

SPECTROPHOTOMETRIC DETERMINATION OF PALLADIUM WITH PONTACHROME AZURE BLUE B

KATSUYA UESUGI
Laboratory of Chemistry, Himeji Institute of Technology, Himeji (Japan)
TSUNENOBU SHIGEMATSU and MASAYUKI TABUSHI
Institute for Chemical Research, Kyoto University, Uji (Japan)
(Received 22nd September 1971)

Many organic reagents for the spectrophotometric determination of palladium have been reviewed by Beamish[1]. More recently, procedures based on the palladium complexes with 2,2′-dipyridylketoxime[2], 2,1,3-benzoselenadiazole[3], chromazurol S[4], and tropaeolin O and its analogues[5], have been suggested. Pontachrome azure blue B (sodium-2″, 6″-dichloro-4′-hydroxy-3,3′-dimethylfuchsone-5,5′-dicarboxylate; Color Index 43830), a triphenylmethane dye, has been used as a spectrophotometric reagent for beryllium[6], iron(III)[6], copper(II)[6], uranium(VI)[7], and scandium[8].

It has been found that microgram amounts of palladium also react with this reagent in a weakly acidic medium to form a complex. This paper describes a method for the determination of palladium based on the formation of a colored complex of palladium with pontachrome azure blue B. Several conditions under which microgram amounts of palladium can be determined, the influences of diverse ions and the composition of the complex are discussed. The proposed method for palladium offers the advantages of simplicity, good sensitivity, and high precision without the need for extraction; reasonable selectivity can be achieved by means of making agents.

EXPERIMENTAL

Apparatus

All absorbance measurements were made with a Hitachi spectrophotometer, model 139, in 1.00-cm matched quartz cells. The pH measurements were carried out using a Hitachi–Horiba glass electrode pH meter, model M-5.

Reagents

All chemicals were of analytical-reagent grade in quality.

Standard palladium solution. A standard stock solution was prepared by dissolving palladium chloride in distilled water, and then adding small amounts of hydrochloric acid. The palladium content of this stock solution (1.17 mg ml^{-1}) was established gravimetrically by the dimethylglyoxime method[9]. The working solutions were made by suitable dilution of this stock solution, as required.

Pontachrome azure blue B solution. Pontachrome azure blue B (E. I. du Pont de Nemours & Co. Inc., U.S.A.) was further purified by recrystallization from

methanol before use, and an aqueous 0.2% (w/v) solution was prepared. The solution was stable for at least 3 weeks.

Buffer solution (*pH* 5.5). 0.1 *M* Potassium dihydrogenphosphate solution and 0.1 *M* disodium hydrogenphosphate solution were mixed.

Standard procedure

Transfer the sample solution containing 2.5–60 μg of palladium to a 25-ml volumetric flask. Add 2.5 ml of the reagent solution and 5 ml of the phosphate buffer solution to adjust the pH to 5.5. If the pH of the resulting solution is not between 5.2 and 5.7, it may be preneutralized with hydrochloric acid or sodium hydroxide solution. Dilute the solution to the mark with distilled water and mix. After 10 min, measure the absorbance at 605 nm against a reference solution containing the same amounts of reagents. Calculate the palladium concentration of the sample solution by means of a calibration curve.

RESULTS AND DISCUSSION

Absorption spectra

The absorption spectra of pontachrome azure blue B have been presented previously[8]; maximal absorbance occurs at 480 nm below pH 4.5, at 430 nm over the pH range from 5.5 to 10, and at 590 nm above pH 10.5. The absorption spectra of pontachrome azure blue B and its palladium complex are presented in Fig. 1; the solutions were adjusted to pH 5.5 with the phosphate buffer solution. The maximal

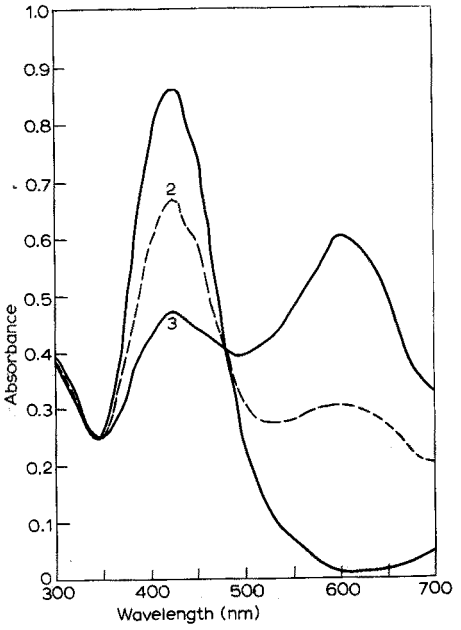

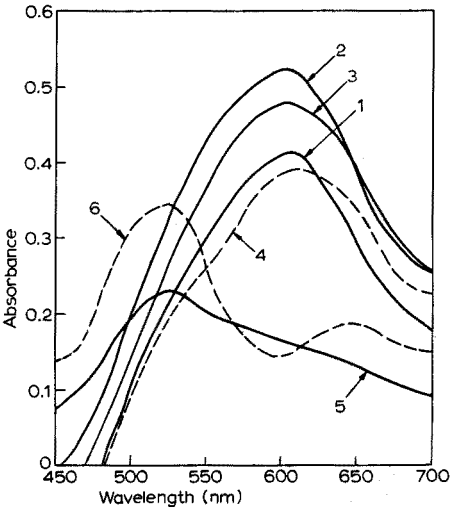

Fig. 1. Absorption spectra of pontachrome azure blue B and its palladium complex at pH 5.5. Reagent 40 p.p.m.; Pd: (1) 0, (2) 0.9, (3) 1.8 p.p.m.

Fig. 2. Absorption spectra of palladium complex at various pH values. Reagent 200 p.p.m.; Pd 1.17 p.p.m.; pH: (1) 4.0, (2) 5.2–5.5, (3) 6.0, (4) 7.0, (5) 8.0, (6) 10.0.

absorption of the palladium complex is found at 605 nm, at which point the reagent does not absorb appreciably.

In order to observe the spectral changes on varying the pH, absorption curves for the palladium complex were prepared at different pH values (Fig. 2). These curves were obtained by measuring the absorbance of colored solutions containing 1.17 p.p.m. of palladium and 200 p.p.m. of pontachrome azure blue B at various pH values against a reagent blank containing the same amount of reagents. Below pH 7.5, the maximal absorbance of the complex was found at 605 nm; above pH 8.0, maximal absorbance was shifted to shorter wavelengths. Below pH 3, the complex partly precipitated.

Effect of pH

The effect of pH on the color development of the complex was examined by measuring, at 605 nm, the absorbance of a solution containing palladium and the reagent at different pH value from 3.5 to 8.0. Maximal absorbance of the complex was observed between pH 5.2 and 5.7 and a pH of 5.5 was, therefore, maintained in subsequent work. The reagent curve was obtained in the same manner, with the same amount of the reagent. A 0.1 *M* phosphate buffer pH 5.5 was found to be satisfactory. The volume of the buffer solution used was found to have no effect on the absorbance of a 0.9-p.p.m. palladium solution over the range 3–10 ml.

The order of addition of the buffer and the reagent had no effect on the intensity of the complex color.

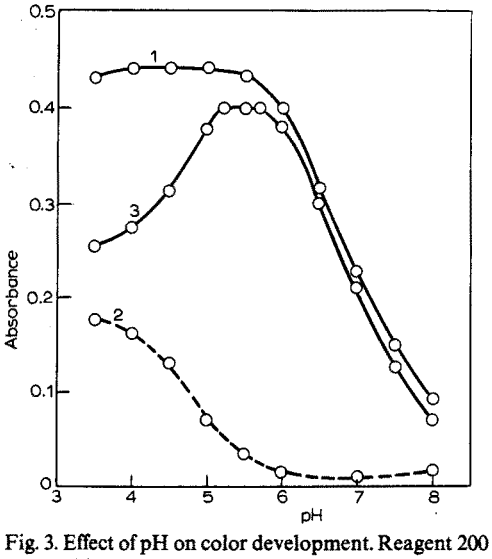

Fig. 3. Effect of pH on color development. Reagent 200 p.p.m.; Pd 0.9 p.p.m.; (1) reference: water, (2) reagent blank; (3) reference: reagent blank.

Stability of color

The color of the complex was fully developed in a few min after mixing, and an essentially constant absorbance reading was obtained over a period of at least 2 h.

Effect of reagent concentration

The effect of the reagent concentration was examined by measuring the

absorbance at 605 nm of solutions containing a constant concentration of palladium and varying amount of the reagent. A 15-fold molar excess of the reagent over palladium was required in order to obtain maximal absorbance. With only a small excess of reagent, the colored complex was slow to develop. Large amounts of the reagent, *e.g.* 35-molar excess, did not affect either the rate or the color intensity of the complex. The optimal amount of the reagent was 2.5 ml of a 0.2% reagent solution in a final volume of 25 ml, which sufficed for less than 2.5 p.p.m. of palladium.

Effect of temperature

The absorbance was independent of the temperature of the color development over the range 10–40°. Above 40°, the absorbance gradually decreased with rise of temperature. Hence, normal laboratory temperature changes introduce no error.

Calibration, range, and sensitivity

The palladium–pontachrome azure blue B complex obeys Beer's law over the concentration range of 0.1 to at least 2.5 p.p.m. of palladium (2.5–62.5 μg per 25 ml). The optimal working range was about 0.2–2 p.p.m. of palladium. At 605 nm the molar absorptivity was $4.79 \cdot 10^4$ l mole^{-1} cm^{-1}. The spectrophotometric sensitivity was estimated to be $2.2 \cdot 10^{-3}$ μg Pd cm^{-2}.

The sensitivity of the present method is compared with those of other methods in Table I.

TABLE I

COMPARISON WITH OTHER REAGENTS FOR PALLADIUM

Reagent	*Sensitivity* ($\cdot 10^{-3}$ $\mu g\ cm^{-2}$)	*Molar absorptivity* ($\cdot 10^4$)
2,2′-Dipyridylketoxime[2]		1.2 (410 nm)
N,N′-bis-(2-sulfoethyl)dithio-oxamide[10]	8.3 (425 nm)	1.286
N,N′-bis-(3-dimethylamino-propyl)dithio-oxamide[11]	8 (427 nm)	
4-(2-Thiazolylazo)-1-naphthol[12]	7 (635 nm)	1.61
Chromazurol S[4]	5.8 (596 nm)	1.86
α-Furildioxime[13]	5 (380 nm)	
Didodecyldithio-oxamide[14]	5 (450 nm)	
2,1,3-Benzoselenadiazole[3]		1.9 (330 nm)
Xylenol orange[15]	4 (518 nm)	2.6
3-Hydroxy-1-*p*-sulfonatophenyl-3-phenyltriazine[16]	3.6 (420 nm)	
Pontachrome azure blue B	2.2 (605 nm)	4.79

Reproducibility

In a test of the reproducibility of the method, 10 samples, each containing 1.0 p.p.m. of palladium, were prepared according to the standard procedure and measured at 605 nm. The average absorbance was 0.425, with a standard deviation of 0.005 absorbance unit or 1.2%.

Effect of diverse ions

Beryllium, copper(II), iron(III), uranium(VI), scandium, aluminum, yttrium, and rare earth elements also form colored complexes with pontachrome azure blue B in weakly acidic solutions[6-8]. These ions were therefore included in a study of possible interference with the determination of palladium. Some common ions, including these cations, were added individually to a solution containing 29.2 μg of palladium, and their effect was examined under the conditions of the standard procedure. The results are summarized in Table II. It can be seen that some diverse cations, especially aluminum, beryllium, copper(II), and iron(III), interfered seriously with the determination of palladium. Scandium, uranium(VI), yttrium, and rare earth elements did not form colors in a phosphate-buffered solution. Chloride, sulfate, acetate, nitrate, phosphate, and fluoride were without effect even in large amounts. The following metallic ions did not interfere up to 10 p.p.m.: magnesium, calcium, strontium, barium, cadmium, lead, zinc, mercury(II), cobalt(II), and nickel. Cyanide and EDTA prevented the formation of the palladium complex.

TABLE II

EFFECT OF DIVERSE IONS ON THE DETERMINATION OF PALLADIUM

(Palladium taken: 29.2 μg)

Ion	*Added (μg)*	*Pd found (μg)*	*Ion*	*Added (μg)*	*Pd found (μg)*
Beryllium(II)	20	68.2	Rhodium(III)	1000	28.9
Copper(II)	30	45.9	Gold(III)	1000	29.0
Iron(III)	30	29.4	Platinum(IV)	1000	28.9
	60	36.7	Germanium(IV)	100	29.0
Aluminum(III)	10	30.5	Titanium(IV)	100	28.8
	30	52.8	Uranium(VI)	100	29.2
Scandium(III)	100	29.0	Molybdenum(VI)	100	28.9
Yttrium(III)	100	28.8	Fluoride	20000	29.2
Lanthanum(III)	100	28.7	Sulfate	1000	29.2
Cerium(III)	100	28.6	Chloride	1000	28.9
Neodymium(III)	100	28.9	Phosphate	1000	29.3
Gadolinium(III)	100	28.6	Acetate	1000	28.7
Dysprosium(III)	100	29.0	Nitrate	1000	28.9
Erbium(III)	100	29.2	EDTA	1000	20.3
Ruthenium(III)	1000	29.0			

Fluoride was investigated as a masking agent for the more seriously offending ions. Aluminum and beryllium were effectively masked by fluoride and can be tolerated without further separation (Table III). However, the interference by copper(II) and iron(III) cannot be eliminated by the addition of fluoride. Therefore, these ions must be separated completely, by ion exchange[17], solvent extraction[18], or other suitable procedures.

Complex formation

The method of continuous variations[19] was applied; a series of solutions was prepared from equimolar concentration of palladium and pontachrome azure blue B. The color was developed and measured in the usual way. A plot of absorbance at

TABLE III

EFFECT OF FLUORIDE AS A MASKING AGENT

(Palladium taken: 29.2 μg; fluoride added: 5 ml of 0.1 *M* NaF solution)

Ion added (μg)		*Pd found* (μg)	*Error* (%)
Beryllium(II)	250	28.9	− 0.3
	500	29.2	0
Copper(II)	30	38.9	+33.2
Aluminum(III)	250	29.0	− 0.7
	500	28.8	− 1.4
Iron(III)	30	29.3	+ 0.3
	50	34.5	+18.2

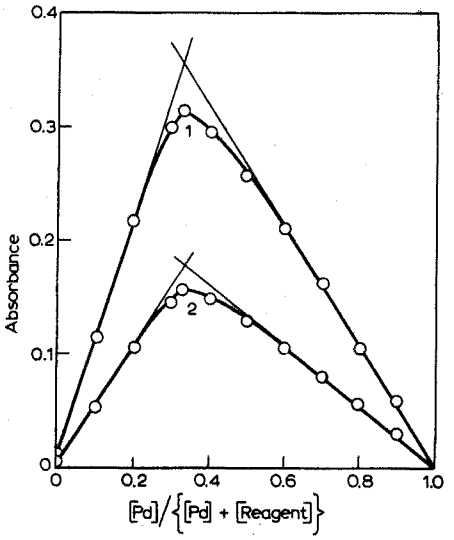

Fig. 4. Continuous variation method. pH 5.5; [Pd] + [Reagent]: (1) $4.4 \cdot 10^{-5}$ *M*, (2) $2.2 \cdot 10^{-5}$ *M*.

605 nm against mole fraction of palladium is shown in Fig. 4. The maximum corresponds to a 1:2 reaction ratio between palladium and pontachrome azure blue B. These results were confirmed by the mole ratio method[20]. Similar relations were also observed for the beryllium[6]–, copper(II)[6]–, and scandium–pontachrome azure blue B complexes[8] formed in a slightly acidic medium.

The formation constant of the palladium complex was determined spectrophotometrically. The conditional formation constant for the complex at pH 5.5 and 25° was calculated, from the curves of the continuous variation, to be $5.0 \cdot 10^{10}$.

It is expected that this reagent will find many applications where a highly sensitive reaction for palladium is desired.

The present work was supported in part by a Grant for Scientific Research from the Ministry of Education, Japan Government.

SUMMARY

A new spectrophotometric method for the determination of palladium with pontachrome azure blue B (Color Index 43830) as reagent is described. The palladium complex has maximal absorbance at pH 5.2–5.7 and at 605 nm. Beer's law is obeyed up to at least 2.5 p.p.m. of palladium; the molar absorptivity is $4.79 \cdot 10^4$ l mole^{-1} cm^{-1} and the sensitivity is $2.2 \cdot 10^{-3}$ μg Pd cm^{-2}. The mole ratio of palladium and reagent in the complex is estimated to be 1:2. The formation constant of the complex is $5.0 \cdot 10^{10}$ under these conditions. Only copper(II) and iron(III) interfere with the determination of palladium when sodium fluoride is used as a masking agent.

RÉSUMÉ

Une nouvelle méthode spectrophotométrique est décrite pour le dosage du palladium, au moyen de Bleu pontachrome azuré B (index 43830). L'absorption maximale se situe à 605 nm, au pH 5.2–5.7. La coloration suit la loi de Beer jusqu'à 2.5 p.p.m. de palladium; coefficient d'extinction molaire, $4.79 \cdot 10^4$ l mole^{-1} cm^{-1}; sensibilité, $2.2 \cdot 10^{-3}$ μg Pd cm^{-2}; constante de formation du complexe, $5.0 \cdot 10^{10}$. En présence de fluorure de sodium, seuls cuivre(II) et fer(III) gênent.

ZUSAMMENFASSUNG

Es wird eine neue spektrophotometrische Methode für die Bestimmung von Palladium mit Pontachromazurblau B (Farbindex 43830) als Reagenz beschrieben. Der Palladiumkomplex hat eine maximale Extinktion bei pH 5.2–5.7 und 605 nm. Das Beersche Gesetz ist mindestens bis 2.5 p.p.m. Palladium erfüllt; der Extinktionskoeffizient ist $4.79 \cdot 10^4$ l mol^{-1} cm^{-1} und die Empfindlichkeit $2.2 \cdot 10^{-3}$ μg Pd cm^{-2}. Das Molverhältnis von Palladium und Reagenz im Komplex wurde zu 1:2 ermittelt.

Die Bildungskonstante des Komplexes ist unter diesen Bedingungen $5.0 \cdot 10^{10}$. Wenn Natriumfluorid als Maskierungsmittel verwendet wird, stören nur Kupfer(II) und Eisen(III) die Bestimmung von Palladium.

REFERENCES

1 F. E. Beamish, *Talanta*, 12 (1965) 743.
2 W. J. Holland and J. Bozic, *Anal. Chem.*, 40 (1968) 433.
3 T. G. Bunting and C. E. Meloan, *Anal. Chem.*, 40 (1968) 435.
4 R. Ishida, *Bull. Chem. Soc. Jap.*, 42 (1969) 1011.
5 K. K. Saxena and A. K. Dey, *Anal. Chem.*, 40 (1968) 1280.
6 Y. Katsube, K. Uesugi and J. H. Yoe, *Bull. Chem. Soc. Jap.*, 34 (1961) 72.
7 Y. Katsube, K. Uesugi and J. H. Yoe, *Bull. Chem. Soc. Jap.*, 34 (1961) 826.
8 T. Shigematsu, K. Uesugi and M. Tabushi, *Jap. Anal.*, 12 (1963) 267.
9 A. I. Vogel, *A Text-book of Quantitative Inorganic Analysis*, 3rd Ed., Longmans Green, London, 1961, p. 511.
10 A. Goeminne, M. Herman and Z. Eeckhaut, *Anal. Chim. Acta*, 28 (1963) 512.
11 W. D. Jacobs, *Anal. Chem.*, 32 (1960) 512.
12 A. Kawase, *Jap. Anal.*, 12 (1963) 714.
13 O. Menis and T. C. Rains, *Anal. Chem.*, 27 (1955) 1932.
14 W. D. Jacobs, C. M. Wheler and W. H. Waggoner, *Talanta*, 9 (1962) 243.

15 M. Otomo, *Bull. Chem. Soc. Jap.*, 36 (1963) 889.
16 N. C. Sogani and S. C. Bhattacharya, *Anal. Chem.*, 29 (1957) 397.
17 A. G. Marks and F. B. Beamish, *Anal. Chem.*, 30 (1958) 1464.
18 K. L. Cheng, *Anal. Chem.*, 26 (1954) 1894.
19 P. Job, *Ann. Chim.*, 9 (1928) 113.
20 J. H. Yoe and H. L. Jones, *Ind. Eng. Chem., Anal. Ed.*, 16 (1944) 11.

Analytica Chimica Acta
Elsevier Publishing Company, Amsterdam
Printed in The Netherlands

THE SPECTROPHOTOMETRIC DETERMINATION OF THALLIUM(III) BY TERNARY COMPLEX FORMATION

R. S. RAMAKRISHNA and M. E. FERNANDOPULLE
Department of Chemistry, University of Ceylon, Colombo 3 *(Ceylon)*
(Received 14th January 1972)

The existence of two comparatively stable oxidation states for thallium has resulted in a larger number of analytical methods for thallium than for gallium and indium. In aqueous solution thallium(I) is distinctly more stable with a redox potential of 1.25 V for the Tl(III)/Tl(I) couple[1], which is very dependent on pH as well as on the presence of complexing anions such as chloride. The analytical chemistry of thallium is based on the precipitation of thallium(I), on the oxidation of Tl(I) to Tl(III) and on the reduction of Tl(III) to Tl(I). Thallium(I) and thallium(III) ions are known to differ markedly in many of their properties.

Although many methods for the determination of thallium have been based on reactions of thallium(I), little attention has so far been paid to analyses based on reactions of thallium(III). Such reactions, particularly those involving complex formation, could be of interest in the development of new methods which may overcome some of the existing inadequacies in the determination of thallium. Thallium(III) shows pronounced oxidative properties and a tendency to form complexes with both inorganic and organic ligands. The hydroxo, nitrato, sulphato, cyano and halogeno complexes[2] of thallium(III) are well known. The halogenothallate complexes are known to be precipitated with organic bases such as pyridine[3], 1,10-phenanthroline[4], etc.

Although extensive studies on the reaction of thallium(I) with thiocyanate have been reported, little is known of the thallium(III)–thiocyanate system. Hume *et al.*[5] reported that lead(II) and thallium(I) show relatively little tendency to form complexes with thiocyanate in solution, as evidenced by the close correspondence of the half-wave potentials in dilute thiocyanate solutions with those in "non-complexing" electrolytes. However, Bell and George[6] have shown from solubility measurements the existence of "ion-pair" thallium–thiocyanate species in solution, although the shifts in the half-wave potentials of thallium(I) in solutions of thiocyanate are quite small, suggesting that complex formation if any is weak; they reported that the existence of TlSCN as a complex species is not clearly evident. Bell and George also reported that the use of potassium thiocyanate above 0.04 *M* resulted in precipitation of thallium(I) thiocyanate. However, thallium(I) is one of the few univalent cations which can associate appreciably with anions of low charge; the existence of covalent bonded TlOH has been demonstrated in the literature.

In an extended study[7] of the chemistry of thallium, evidence was found for the formation of a mixed ligand complex of thallium(III) with thiocyanate and pyridine in a metal-to-ligand ratio of 1 : 2 : 2. Its quantitative study was of interest because

of the formation of a ternary complex of thallium(III) in solution, as the only mixed ligand complexes reported for thallium(III) are those with halide ions and ammonia[8], ethylenediamine, 2,2′-bipyridine and 1,10-phenanthroline[4] and these have only been obtained as solids for purposes of analytical study. Furthermore, its formation is of value in the development of selective analytical procedures for thallium where the +3 oxidation state is of interest.

The addition of thiocyanate to an aqueous solution of thallium(III) resulted in the formation of a yellow colour which was unstable and became colourless within a few minutes; a white precipitate was obtainable when concentrations greater than 0.05 *M* were used. This colour change and precipitation were evidently due to the reduction of Tl(III) to Tl(I) and the formation of insoluble TlSCN at the concentration of thiocyanate employed. However, the addition of an aqueous solution of thallium(III) to a solution of thiocyanate in the presence of pyridine gave a yellow colour which showed a stable absorbance in diffuse light for over 24 h, thus indicating the formation of a mixed ligand complex of thallium(III). This complex was characterized by two absorption maxima at 320 nm and 405 nm (Fig. 1).

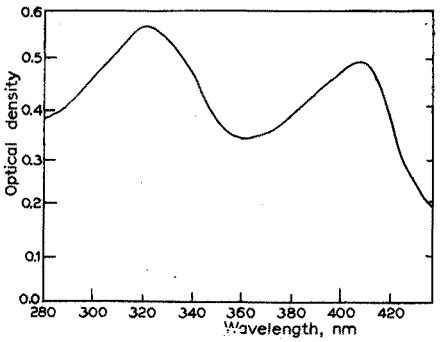

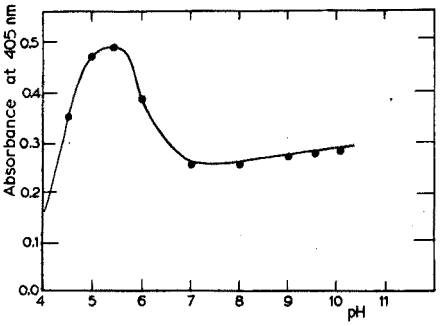

Fig. 1. Absorption spectrum of the ternary complex, $1.20 \cdot 10^{-3}$ *M* thallium(III).

Fig. 2. Effect of pH on the absorbance of the complex.

Effect of pH

The dependence of the formation of this complex on the pH value was investigated by measurement of the absorbance at 405 nm of solutions containing the same concentrations of thiocyanate, pyridine and thallium(III), adjusted to varying pH by the use of 0.1 *M* hydrochloric acid or 0.1 *M* sodium hydroxide; absorbances were measured after about 30 min, when full development of colour was obtained. Figure 2 shows that the range of constant maximum absorbance was between 5.2 and 5.5. The complex was not stable below pH 4; above pH 6 there was slight turbidity resulting in lower absorbance and above pH 9 precipitation of thallium(III) hydroxide occurred. In the formation of the complex, the order in which the reagents were added was significant, for the addition of thiocyanate to thallium(III) before the addition of pyridine gave no colour, suggesting that no complex was formed, possibly because of the reduction of thallium(III) to thallium(I) in the presence of thiocyanate. However, the addition of a solution of thallium(III) to one containing pyridine and thiocyanate gave a yellow colour which was stable for over 24 h in diffuse light.

Stoicheiometry

The composition of the complex in solution was established by the molar ratio method[9] and by Job's method of continuous variation[10]. The thallium(III)–thiocyanate and thallium(III)–pyridine ratios were determined by maintaining constant concentrations of thallium and either pyridine or thiocyanate, while the concentration of the third component was varied. The solutions were all adjusted to pH 5.2–5.5; absorbances were measured at 405 nm against water in the reference cell. The stoicheiometry of the ternary complex was shown to be 1:2:2, corresponding to the formation of the $[Tl(py)_2(SCN)_2]^+$ cationic complex species.

In a study of the concentration range of the method, it was shown that the thallium complex followed Beer's law at 405 nm over a concentration of 20–300 μg Tl(III) ml^{-1}, when the general procedure given below was used.

Inteference from diverse ions

In examining the interference of various diverse ions, those which normally occur with thallium or are usually present in important alloys, natural sources and bio materials and those of importance to the chemistry of thallium were considered. In addition, the interference caused by a variety of other ions was also established.

The results given in Table I show that the presence of similar or even larger amounts of Tl(I), Zn(II), Pb(II), Cd(II), Ba(II), nitrate, sulphate or chloride caused little or no interference. The presence of small amounts of antimony, cobalt and nickel also showed no interference. However, gross interference was observed in the presence of Ga^{3+}, In^{3+}, Al^{3+}, Cu^{2+}, Ag^+, Fe^{3+}, UO_2^{2+}, Mo(VI), VO^{2+} and Br^-.

The use of cupferron in 1 *M* mineral acid solution is known[11] to extract cupferrates of a number of metals, including Fe(III), Sb(III), Ga(III), Ti(IV), Mo(VI), U(IV), Zr and V(V), into chloroform and thus effect a separation of these interfering ions from thallium(III). A 1:1 mixture of benzene and amyl alcohol has been used by

TABLE I

INTERFERENCE FROM DIVERSE IONS[a]
(Concentration of Tl^{3+} = 5.608 mg)

Ion added	*Amount added (mg)*	*Tl^{3+} found (mg)*	*Ion added*	*Amount added (mg)*	*Tl^{3+} found (mg)*
Tl^+	12.50	5.608	VO^{2+}	0.251	4.907
Zn^{2+}	6.25	5.608	Ag^+	0.252	4.711
Pb^{2+}	6.25	5.592	UO_2^{2+}	0.250	6.349
Cd^{2+}	6.25	5.500	TiO^{2+}	0.250	4.867
Ca^{2+}	50.20	5.608	Fe^{3+}	0.252	7.127
Ba^{2+}	20.04	5.650	Mo^{6+}	0.251	4.132
Sb^{3+}	2.48	5.580	Cl^-	625	5.608
Co^{2+}	0.501	5.900	NO_3^-	625	5.608
Ni^{2+}	0.501	5.608	SO_4^{2-}	400	5.608
Ga^{3+}	6.25	4.04	Br^-	6.25	6.730
In^{3+}	6.25	4.48	Mn^{2+}	0.250	Ppt.
Al^{3+}	6.25	2.24	Bi^{3+}	0.250	Ppt.
Cu^{2+}	0.233	15.57			

[a] Cations were added as their nitrate, sulphate or chloride salt and anions as their sodium or potassium salt. Antimony was added as potassium antimony tartrate and titanium as potassium titanyl oxalate.

Fritz *et al.*[12] to extract the cupferrates of Cu(II), Co(II), Ni(II) and Mn(II) below pH 5.

Extraction with diethyl ether from solutions 4 *M* in hydrochloric acid is known[2] to extract Fe, Ga, Hg, Sb and Mo, as well as thallium, and thus could be used to separate Tl from In and Al as well as to concentrate thallium in solution. As the presence of large amounts of chloride caused no interference, silver could be removed by precipitation with chloride from acid solutions.

The use of such methods would thus enable the separation of thallium(III) from interfering ions, as these suggested methods are compatible with the recommended procedure for the determination of thallium(III). The non-interference of thallium(I) is a particularly significant feature of these studies. With anions, the presence of more than 100-fold amounts of chloride, nitrate and sulphate was found not to cause any interference. Marked interference was shown in the presence of small quantities of bromide, possibly because of the formation of coloured species such as $TlBr^{2+}$, $TlBr_2^+$, $TlBr_3$ and $TlBr_4^-$ whose existence has been reported by Benoit[13] whereas the corresponding chloro complexes have been reported colourless in aqueous solutions.

EXPERIMENTAL

Analar chemicals were used throughout.

Thallium(III) solution was prepared from Tl_2O_3 and standardized gravimetrically. Absorption measurements were made with a Unicam SP 500 spectrophotometer with matched silica cells.

Recommended procedure for the determination of thallium(III)

Add an aqueous solution of thallium(III) containing *ca.* 5 mg of thallium(III) to a solution containing 2.5 ml of 10^{-1} *M* pyridine and 7.5 ml of $2 \cdot 10^{-2}$ *M* potassium thiocyanate. Adjust the pH of the resulting solution to *ca.* 5.2 by the addition of a few ml of 0.1 *M* hydrochloric acid and dilute the solution to the final volume (25 ml). Measure the absorbance of the solution at 405 nm against a water blank after keeping the solution in diffuse light for *ca.* 30 min.

Stoicheiometry of the ternary complex

Thallium(III): pyridine ratio. Method (*i*). A series of solutions was prepared from 7.50 ml of $2 \cdot 10^{-2}$ *M* potassium thiocyanate, *x* ml of $1 \cdot 10^{-1}$ *M* pyridine solution, and 3.00 ml of $1 \cdot 10^{-2}$ *M* thallium(III) solution, adjusted to pH 5.2 for complex formation and made up to 25 ml with water. The recommended procedure was then followed.

The results showed that maximal absorbance occurred at a molar ratio of 1:1.96 for thallium(III) to pyridine in the complex.

Method (*ii*). Solutions containing 7.50 ml of $2 \cdot 10^{-2}$ *M* potassium thiocyanate, *x* ml of $1 \cdot 10^{-2}$ *M* pyridine and $(10-x)$ ml of $1 \cdot 10^{-2}$ *M* thallium(III) solution were adjusted to pH 5.2 and made up to 25 ml with water. The recommended procedure was then followed. The absorbance of the reagents alone was negligible. The measured absorbance thus corresponded to values for the Job ordinate A_j. The Job plot confirmed the ratio of 1:2 for thallium(III) to pyridine in the ternary complex (Fig. 3).

Thallium(III): thiocyanate ratio. Method (*i*). Solutions containing 2.50 ml of

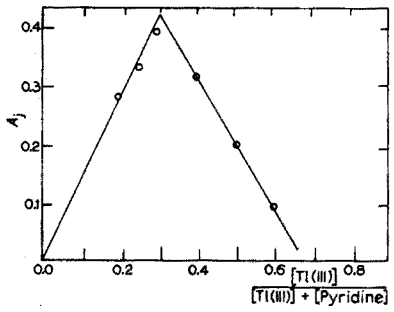

Fig. 3. Continuous variation plot for the determination of the Tl:pyridine ratio in the complex, total concentration (Tl + pyridine) = 4×10^{-3} *M*.

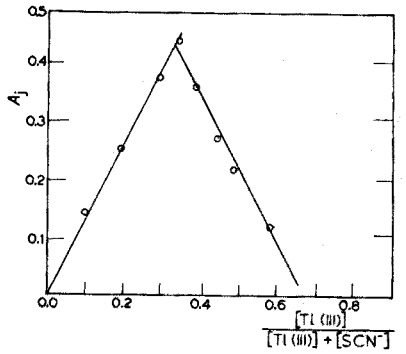

Fig. 4. Continuous variation plot for the determination of the Tl:CNS^- ratio in the complex, total concentration ($Tl + CNS^-$) = 4×10^{-3} *M*.

$1 \cdot 10^{-1}$ *M* pyridine, *x* ml of $2 \cdot 10^{-2}$ *M* thiocyanate solution, and 3.00 ml of $1 \cdot 10^{-2}$ *M* Tl(III) solution, were treated as described for Method (*i*) above.

Maximal absorbance was obtained at a molar ratio of 1:2.08 for thallium(III) to thiocyanate in the complex.

Method (ii). Solutions containing 2.50 ml of $1 \cdot 10^{-1}$ *M* pyridine, *x* ml of $1 \cdot 10^{-2}$ *M* thiocyanate solution and $(10 - x)$ ml of $1 \cdot 10^{-2}$ *M* thallium(III) were treated as in the recommended procedure.

The resulting Job plot confirmed the molar ratio 1:2 for thallium(III) to thiocyanate in the complex (Fig. 4).

Interference from other ions

Solutions containing 7.50 ml of $2 \cdot 10^{-2}$ *M* thiocyanate solution, 2.50 ml of $1 \cdot 10^{-1}$ *M* pyridine, 3.00 ml of $1 \cdot 10^{-2}$ *M* thallium(III) and *x* ml of a solution containing the interfering ion were taken through the recommended procedure.

The authors thank the University of Ceylon, Colombo, for providing a research grant. They are also very grateful to Miss P. S. S. Perera for checking the method and completing the interference study.

SUMMARY

If thallium(III) is added to an aqueous solution of potassium thiocyanate containing a large amount of pyridine in the pH range 5.2–5.5, a yellow solution which is stable in diffuse light is obtained. The yellow colour can be measured at 405 nm for the colorimetric determination of thallium(III) in the range 20–300 μg Tl ml^{-1}. The complex is a mixed ligand complex with a metal–ligand ratio of 1:2:2. Thallium(I) does not interfere. The interference of various other metal ions and anions is discussed.

RÉSUMÉ

On observe la formation d'une coloration jaune lorsqu'on ajoute du thallium-

(III) à une solution aqueuse de thiocyanate de potassium, contenant une forte quantité de pyridine (pH 5.2–5.5). Cette coloration peut être mesurée à 405 nm et permet un dosage du thallium(III), de 20 à 300 μg Tl ml^{-1}. Le thallium(I) ne gêne pas. On examine l'influence de divers autres ions métalliques et anions.

ZUSAMMENFASSUNG

Bei Zugabe von Thallium(III) zu einer wässrigen Kaliumthiocyanatlösung, die eine grosse Menge Pyridin im pH-Bereich 5.2–5.5 enthält, wird eine gelbe Lösung erhalten, die in diffusem Licht beständig ist. Die gelbe Färbung kann bei 405 nm für die kolorimetrische Bestimmung von Thallium(III) im Bereich 20–300 μg Tl ml^{-1} gemessen werden. Der Komplex enthält gemischte Liganden in einem Metall–Liganden-Verhältnis von 1:2:2. Thallium(I) stört nicht. Die Störungen durch verschiedene andere Metallionen und Anionen werden diskutiert.

REFERENCES

1 J. R. Partington and H. J. Stonehill, *Trans. Faraday Soc.*, 31 (1935) 1365.
2 A. I. Busev and V. G. Tiptsova, *Russ. Chem. Rev.*, 29 (1960) 479.
3 G. Sandri, *Mikrochim. Acta*, 2 (1958) 253.
4 G. J. Sutton, *Aust. J. Chem.*, 11 (1958) 120.
5 G. W. Leonard, M. E. Smith and D. N. Hume, *J. Phys. Chem.*, 60 (1956) 1493.
6 R. P. Bell and J. H. B. George, *Trans. Faraday Soc.*, 49 (1953) 619.
7 R. S. Ramakrishna and M. E. Fernandopulle, *J. Inorg. Nucl. Chem.*, 33 (1971) 1940.
8 A. P. Kochetkova and V. G. Tronev, *Zh. Neorg. Khim.*, 2 (1957) 2043.
9 A. E. Harvey and D. L. Manning, *J. Amer. Chem. Soc.*, 72 (1950) 4488.
10 P. Job, *Ann. Chim.*, 9 (1928) 113.
11 E. B. Sandell, *Colorimetric Determination of Traces of Metals*, 3rd Ed., Interscience, New York, 1959.
12 J. S. Fritz, M. J. Richard and A. S. Bystroff, *Anal. Chem.*, 29 (1957) 578.
13 R. Benoit, *Bull. Soc. Chim. Fr.*, 16 (1949) 518.

Analytica Chimica Acta
Elsevier Publishing Company, Amsterdam
Printed in The Netherlands

A MICROMETHOD FOR THE DETERMINATION OF NITRITE IN BLOOD

H. SHECHTER, N. GRUENER and H. I. SHUVAL

Environmetal Health Laboratory, Department of Medical Ecology, Hebrew University, Hadassah Medical School, Jerusalem (Israel)

(Received 11th January 1972)

The determination of nitrite in blood may have to be carried out in cases of intoxication by nitrite-containing drugs or ingestion of food containing nitrite or nitrate[1]. Ingested nitrates may be reduced by the intestinal flora to nitrites. Nitrite, when absorbed into the bloodstream, oxidizes haemoglobin to methaemoglobin and if sufficient haemoglobin is converted, the oxygen-carrying capacity of the blood may be markedly reduced. Cases of nitrite intoxication are also known[2,3], especially in infants, arising from drinking water with a high nitrate content. This problem has become of current interest because of the increasing contamination of water sources by waste water, solid organic wastes and possibly by chemical fertilizers, which can lead to a rather high nitrate content in drinking water.

Investigations carried out in this laboratory[4] concerning the relationship between the amount of nitrate in drinking water and the content of methaemoglobin in blood[5] emphasized the need for a method of estimating low nitrite levels in the circulatory blood of laboratory animals fed with nitrate or nitrite. The method was also required for planned field studies of infants consuming water high in nitrate concentration.

The existing methods for nitrite determination in blood[6-8] were not found to be satisfactory for the determination of very low concentrations of nitrite, especially in the small blood sample volumes available in these investigations.

In this work, different factors were investigated that may influence nitrite determination in blood by a spectrophotometric method, based on diazotization and coupling reactions, involving sulphanilic acid and Cleve's acid. The modifications and refinements developed in order to reach a detection limit of 0.01 μg N in 0.1 ml blood are described in this paper. The advantages of the micromethod presented are high selectivity, wide range, accuracy and lack of photosensitivity of the final colour obtained.

EXPERIMENTAL

Apparatus

A Zeiss PMQ II spectrophotometer equipped with 10-mm cells (Hellma 105/4 microcell) and an Eppendorf Microfuge 3200 centrifuge providing 15,000 rev min^{-1} with the special 1.5-ml microtubes were used. A conventional clinical centrifuge may also be used.

Reagents

All chemicals used were of analytical-reagent grade. Nitrite-free distilled water was used in the preparation of all solutions.

Sulphanilic acid solution. Dissolve 0.5 g of sulphanilic acid in 150 ml of a 20% (v/v) solution of glacial acetic acid in water. Store in a brown bottle.

Cleve's acid solution. Dissolve 0.2 g of Cleve's acid (1-naphthylamine-7-sulphonic acid) in 120 ml of water, warming in a water-bath. Filter the solution, cool and add 30 ml of glacial acetic acid. Store in a brown bottle in a refrigerator.

Stock nitrite solution. Dissolve 0.4928 g of sodium nitrite and dilute to 1 l with water (1 ml = 100 μg of nitrite as nitrogen). Preserve with 1 ml of purified chloroform. Interfering substances present in the chloroform can be removed by extracting 100 ml of chloroform with four 20-ml portions of 0.1 *M* hydrochloric acid.

Standard nitrite solution. Dilute 10 ml of stock solution to 1 litre (1 ml = 1 μg NO_2^-–N). Prepare this solution immediately before use.

Zinc sulphate solution. Dissolve 4.31 g of zinc sulphate heptahydrate in water and make up to 100 ml.

Recommended procedure

Collection of samples. Adequate precautions must be taken during collection of blood samples for the determination of nitrite because it is rapidly oxidizable *in vitro*. Blood samples should be analyzed within the shortest possible time. However, the sample may be stored at 4° for about 1 h without significant loss of the nitrite content.

Deproteinization. Add 0.1 ml of blood to a 1.5-ml microtube containing 0.6 ml of zinc sulphate solution. Add 0.4 ml of bidistilled water and mix well, preferably using a Vortex-Genie apparatus. To this add 0.1 ml of aqueous 4% (w/v) sodium hydroxide solution and mix again. Keep on ice for 1 h. Remove the precipitated proteins by centrifugation (2 min at 15,000 rev min^{-1}).

Colour reaction. Take 0.6 ml of clear supernate in a 100/10 test-tube and add 0.4 ml of bidistilled water; mix well, add 0.1 ml of sulphanilic acid solution and leave on ice for 15 min for the diazotization to take place. Add 0.1 ml of Cleve's acid solution and leave for 60 min at room temperature for the coupling reaction. If nitrite is present a red-violet diazo complex is formed. The absorbance is read at 520 nm.

Preparation of standard curve. Add several aliquots (up to 0.5 ml) of standard sodium nitrite solution (1 ml = 1 μg NO_2^-–N) to Eppendorf centrifuge microtubes containing 0.6 ml of the zinc sulphate solution. Thereafter follow the technique as described under *Recommended procedure.*

Double-distilled water was substituted for nitrite solution for the reagent blank.

RESULTS AND DISCUSSION

The variables which may influence the results of nitrite determination in such a complex matrix as blood were investigated and different procedures for removing blood proteins were tested. The precision and accuracy of the method were evaluated statistically.

Removal of blood proteins

One of the problems of the method for nitrite determination in blood is the

choice of a deproteinizing agent that will not inhibit colour development. Most protein precipitants are active in acidic media, which are not suitable here, because of the instability of the nitrite ion. Therefore, only protein precipitants acting in slightly alkaline or neutral media may be considered. In the present work, two deproteinizing systems were compared: zinc sulphate with either barium hydroxide or sodium hydroxide. Figure 1 shows the recovery curves between 0 and 0.5 μg of nitrite-nitrogen in standard solutions and after treatment with both the above-mentioned protein precipitants. It appears that the zinc sulphate–sodium hydroxide deproteinizing system is superior to the other system and does not inhibit colour development.

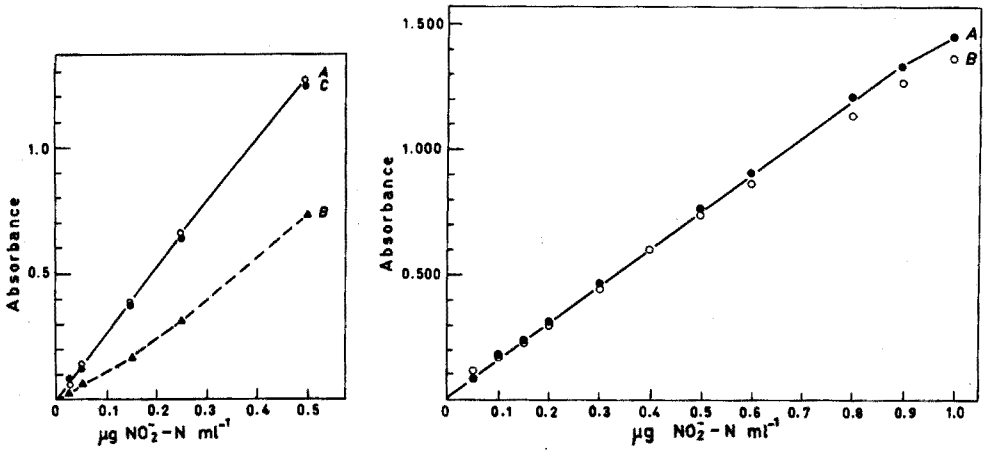

Fig. 1. Influence of deproteinizing reagents on nitrite recovery. (A) Blank; (B) $Ba(OH)_2 + ZnSO_4$; (C) $NaOH + ZnSO_4$.

Fig. 2. Standard curves for nitrite determination. Comparison of two coupling agents. (A) Cleve's acid; (B) naphthylethylenediamine.

The colour reaction

Coupling reagent. The classical coupling reagent in the Griess–Ilosvay reaction is α-naphthylamine[9]. This substance has been shown to be carcinogenic[10]. Among the other known non-carcinogenic coupling agents, the following two were chosen for investigation: 1-naphthylethylenediamine[11] and 1-naphthylamine sulphonic acid (Cleve's acid)[12]. A comparison of these two coupling agents under the proposed experimental conditions showed that both reagents gave good results, but Cleve's acid was preferable; it provides a colour of higher intensity, Beer's law is obeyed over a wider range and the colour is less dependent on the temperature. The results are presented in Fig. 2.

Diazotization time and coupling time. The time factor is important in the reactions involved in this method. Different diazotization times were tried: 0, 5, 10, 15 and 20 min; and the coupling time was varied concomitantly between 20 and 90 min. The results obtained under these various conditions for a concentration of 0.2 μg NO_2^-–N per ml are presented in Fig. 3 and are summarized as follows: with a diazotization time of zero, when the coupling agent is added immediately after the diazotization agent, the colour developed is of low intensity, and increases with time without

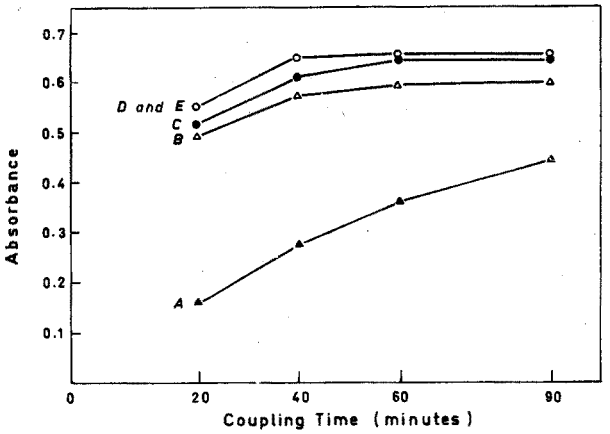

Fig. 3. Effect of diazotization time and coupling time. Diazotization time: (A) 0 min; (B) 5 min; (C) 10 min; (D) 15 min; (E) 20 min.

levelling off after 60 min; with diazotization times of 5, 10, 15, or 20 min, the strength of the colour formed increases with the increasing diazotization time and becomes more stable after 40–60 min.

Diazotization times longer than 15 min led to no further improvement. Thus, the optimal diazotization time was established to be 15 min and the coupling time 60 min.

The effect of temperature. The effect of temperature on the final colour development was studied. During the diazotization time a temperature of about 1° is necessary. When the diazotization is done at 20°, the final absorbance is decreased by about 10%. During the coupling time, temperature variation between 20° and 30° does not affect the intensity of absorbance. In parallel determinations with naphthylethylenediamine and Cleve's acid, the influence of temperature was found to be somewhat greater with the former reagent.

Evaluation of method

Limit of detection. Under the experimental conditions and with the aforementioned optical system, the limit of detection is 0.01 μg of nitrite-nitrogen in 0.1 ml of blood, which yields an absorbance of 0.012. This sensitivity was adequate for the research on residual nitrite in the blood of rats with induced methaemoglobinaemia. Other known methods[6-8] are less sensitive and need at least 1 ml of blood for each determination. The method of Litchfield[8], which requires less than 1 ml of blood, has a sensitivity similar to the proposed method, but needs special apparatus.

Precision. Precision was determined by 36 replicate analyses of standard solutions in distilled water with 1, 4 and 5.5 μg of nitrite-nitrogen per ml. Standard deviations and 95% confidence limits were calculated at the various levels. The results are shown in Table I. The standard deviation varied between 0.025 and 0.110, and the 95% confidence limits between ± 0.01 and ± 0.06.

Accuracy. The accuracy of the method was evaluated by determining the recovery of different amounts of nitrite added to plasma. Recovery data from whole blood were not evaluated because haemoglobin reacts immediately with nitrite. Ten

TABLE I

PRECISION OF THE METHOD FOR NITRITE DETERMINATION IN BLOOD

(12 determinations were done at each level)

NO_2^-–N taken ($\mu g\ ml^{-1}$)	Mean value found ($\mu g\ ml^{-1}$)	Range	Standard deviation	95% Confidence limit
1.00	0.99	0.97–1.04	0.025	0.99 ± 0.01
4.00	3.99	3.96–4.04	0.025	3.99 ± 0.01
5.50	5.52	5.40–5.68	0.110	5.52 ± 0.06

TABLE II

RECOVERY OF NITRITE FROM BLOOD PLASMA

(10 determinations were done at each level)

NO_2^-–N added ($\mu g\ ml^{-1}$)	Mean NO_2^-–N found ($\mu g\ ml^{-1}$)	Standard deviation	Mean recovery (%)	Recovery range (%)
0.40	0.39	0.06	97.5	82–112
1.00	0.99	0.04	99.0	95–103
2.50	2.48	0.07	99.4	96–104
4.00	4.01	0.08	100.2	99–102
6.00	5.95	0.16	99.1	96–102

determinations were carried out at each concentration in plasma and in distilled water; the results are presented in Table II. The mean recovery varied between 97.5 and 100.2%.

Some applications of the method

The proposed method was specially developed for the determination of small amounts of free nitrite in the blood of experimentally nitrite-intoxicated rats in connection with the levels of methaemoglobin formed. Since haemoglobin reacts with nitrite, the determination of residual nitrite in blood is a necessary parameter in the study of this reaction. At the first contact between nitrite and blood, some nitrite reacts and haemoglobin is partially converted to methaemoglobin. The partition of residual nitrite among the different blood components is a particular feature of interest.

Different amounts of nitrite-nitrogen between 1 and 100 $\mu g\ ml^{-1}$ were added to human blood *in vitro* and simultaneously, for reference, to distilled water. After the blood had been mixed, part of it was centrifuged and the plasma separated. Residual nitrite was determined in total blood and, in parallel, in plasma. The results obtained are presented in Table III. With nitrite concentrations varying between the above limits, the initial drop of nitrite in blood represents 76–90% of the amount added. The concentration of nitrite in plasma was about twice that found in blood. In Table III the amount of nitrite was calculated for 0.53 ml of plasma, since plasma represents $53 \pm 5\%$ of the total blood volume[13]. The total residual nitrite in 0.53 ml of

TABLE III

RESIDUAL NITRITE PARTITION IN BLOOD AND PLASMA

NO_2^-–N added to blood ($\mu g\ ml^{-1}$)	NO_2^-–N found			
	in blood		in plasma	
	($\mu g\ ml^{-1}$)	(%)	($\mu g\ ml^{-1}$)	(μg 0.53 ml^{-1}[a])
100.0	24.0	24.0	46.0	24.40
60.0	13.0	21.7	25.0	13.20
30.0	7.0	23.3	14.0	7.40
21.0	4.0	19.0	7.8	4.10
10.0	1.8	18.0	3.6	1.90
1.0	0.1	10.0	0.2	0.11

[a] Plasma represents 53% of the total blood volume[13].

plasma indicates figures very close to those obtained in 1 ml of whole blood. Therefore, it can be assumed that most of the residual nitrite in blood is found in the plasma fraction.

The described method was applied to urine nitrite determinations as well; in this test mercury(II) chloride(5%) was used as deproteinizing agent.

The recommended method is now used in this laboratory in experiments concerning parallel nitrite and methaemoglobin kinetics[14] in the blood of nitrite-intoxicated rats.

This study was carried out under Research Agreement No. 06-012-3 Environmental Protection Agency, U.S.A.

SUMMARY

The diazotization–coupling reaction for the determination of nitrite is modified and adapted for micro-analysis of blood and plasma. The limit of detection by the proposed method is 0.01 μg of nitrite-nitrogen and only 0.1 ml of blood is needed for analysis. The results showed high reproducibility; the standard deviation at nitrite concentrations of 1–6 $\mu g\ ml^{-1}$ varied from 0.025 to 0.110. Some applications of the method showing the recovery of nitrite from blood and its components are discussed.

RÉSUMÉ

La réaction de copulation–diazotation pour le dosage des nitrites est modifiée et appliquée à la micro-analyse du sang et du plasma. La limite de détection obtenue par la méthode proposée est de 0.01 μg d'azote-nitrite, en n'utilisant que 0.1 ml de sang. Les résultats obtenus présentent une excellente reproductibilité. La déviation standard varie de 0.025 à 0.110 pour des concentrations de l'ordre de 1 à 6 $\mu g\ ml^{-1}$.

ZUSAMMENFASSUNG

Die Diazotierungs–Kupplungs-Reaktion für die Bestimmung von Nitrit wurde modifiziert und der Mikroanalyse von Blut und Plasma angepasst. Die Nachweisgrenze der vorgeschlagenen Methode ist 0.01 μg Nitrit-Stickstoff; für die Analyse

wird nur 0.1 ml Blut benötigt. Die Ergebnisse zeigen eine hohe Reproduzierbarkeit; die Standardabweichung bei Nitritkonzentrationen von 1–6 μg ml^{-1} variierte zwischen 0.025 und 0.110. Einige Anwendungen der Methode, die den erfassbaren Anteil von Nitrit in Blut und seinen Bestandteilen zeigen, werden diskutiert.

REFERENCES

1 J. D. Orgeron, J. D. Martin, C. T. Caraway, R. M. Martine and G. H. Hauser, *Publ. Health Rep.*, 72 (1957) 189.
2 W. A. B. Campbell, *Br. Med. J.*, 2 (1952) 371.
3 Z. Knotek and P. Schmidt, *Pediatr.*, 34 (1964) 78.
4 N. Gruener and H. I. Shuval, *Developments in Water Quality Research*, Humphrey Science Publishers, Ann Arbor–London, 1970, p. 89.
5 E. Hegesh, N. Gruener, S. Cohen, R. Bochkovsky and H. I. Shuval, *Clin. Chim. Acta*, 30 (1970) 679.
6 E. J. Stieglitz and A. E. Palmer, *J. Pharmacol. Exp. Ther.*, 11 (1934) 398.
7 R. H. Diven, W. J. Pistor, R. E. Reed, R. J. Trautman and R. E. Watts, *Amer. J. Vet. Res.*, 23 (1962) 94.
8 M. H. Litchfield, *Analyst*, 92 (1967) 132.
9 *Standard Methods for the Examination of Water and Wastewater*, 12th Ed., American Public Health Association, New York, 1965, p. 205.
10 *Precautions for Laboratory Workers who handle Aromatic Amines*, Chester Beatty Research Institute, London, 1965.
11 B. E. Saltzmann, *Anal. Chem.*, 26 (1954) 1949.
12 N. G. Bunton, N. T. Crosby and S. J. Patterson, *Analyst*, 94 (1969) 585.
13 M. M. Wintrobe, *Clinical Hematology*, 6th Ed., Lea Febiger, Philadelphia, 1967, p. 86.
14 N. Gruener and H. I. Shuval, *Environmental Quality and Safety*, Vol. II, Academic Press, London–New York, 1972, in press.

Analytica Chimica Acta
Elsevier Publishing Company, Amsterdam
Printed in The Netherlands

LA CHELATION DES IONS FER(III) PAR L'ACIDE PYROCATECHOLDISULFONIQUE-3,5

M. MORIN et J. P. SCHARFF
Chaire de Chimie Minérale, Université Claude Bernard, Lyon I, 69-Villeurbanne (France)
(Reçu le 13 janvier 1972)

Ayant entrepris une étude générale des complexes mixtes formés par les ions fer(III) avec différents coordinats multidentés, nous avons signalé dans un précédent Mémoire[1] les raisons pour lesquelles nous étions amenés à préciser les données relatives aux systèmes simples.

Le problème se pose de façon encore plus nette dans le cas du système Fe(III)–acide pyrocatécholdisulfonique-3,5 (H_4L) pour lequel les données bibliographiques demeurent encore discutables. Certains auteurs[2-4] ne signalent en milieu acide que l'existence du complexe FeL^-, alors que d'autres comme Schwarzenbach et Willi[5] puis McBryde[6] admettent l'existence d'une forme protonée FeHL sans toutefois pouvoir déterminer le site de protonation et les propriétés d'absorption d'une telle espèce. Enfin il n'existe pas à notre connaissance d'étude potentiométrique de ce système alors que la sensibilité d'une telle méthode garantit généralement une précision excellente.

Nous avons donc repris cette étude à la fois par une méthode protométrique très précise et par une méthode spectrophotométrique, obtenant ainsi les valeurs β_{pqr} des constantes de stabilité ionique

$$\beta_{pqr} = \frac{[M_pH_qL_r]}{m^p h^q l^r}$$

où m, l, h sont les concentrations des constituants libres et des ions H^+.

Les faisceaux de spectres d'absorption obtenus nous ont permis également de déterminer les coordonnées trichromatiques des différentes espèces mettant ainsi en évidence leur formation successive et leur domaine d'existence.

Toutes nos mesures furent effectuées à la température de $25° \pm 0.1°$ en milieu de force ionique 0.5 M, maintenue constante par du nitrate de sodium.

PARTIE EXPÉRIMENTALE

Techniques

Leur principe en a été décrit dans notre précédent Mémoire[1].

Réactifs

Nous avons utilisé le nitrate ferrique commercial ($Fe(NO_3)_3 \cdot 9H_2O$ p.a.).

L'acide pyrocatécholdisulfonique-3,5 sous forme de son sel disodique (Tiron ; $C_6H_4Na_2O_8S_2 \cdot H_2O$ p.a.) dont la pureté a été vérifiée par potentiométrie. Néanmoins nous n'avons pas préparé de solution mère car nous avons constaté que ces solutions

n'étaient pas stables au cours du temps. Nous avons donc, pour chaque manipulation, pesé la quantité nécessaire de réactif qui était introduite en solution juste avant le début des mesures. Nous avons également constaté une oxydation des solutions aussi bien en milieu fortement acide (HNO_3) qu'en milieu fortement alcalin où les diphénols (en particulier les dérivés *ortho* et *para*) s'altèrent assez vite à l'air et à la lumière.

LES CONSTANTES D'IONISATION

Les constantes d'ionisation $K_n^H = [H_{n-1}L][H]/[H_nL]$ de l'acide pyrocatéchol-disulfonique-3,5 ont été déterminées potentiométriquement. Les deux groupements sulfoniques se comportent comme des acides forts et sont totalement dissociés; nous négligerons donc K_3^H et K_4^H. Les courbes de neutralisation par la soude de solutions 0.5 *M* en $NaNO_3$ et respectivement $1.000 \cdot 10^{-2}$, $1.025 \cdot 10^{-2}$, $1.910 \cdot 10^{-2}$ et $2.050 \cdot 10^{-2}$ *M* en Tiron permettent de tracer la courbe représentant le nombre moyen $\bar{p}$ de protons liés par coordinat en fonction du pH. On constate que les différents essais donnent une courbe $\bar{p} = f$ (pH) (Fig. 1) unique jusqu'à des pH de l'ordre de 11 ($\bar{p} \neq 0.88$). Pour des pH > 11 les courbes tracées sous atmosphère normale et sous atmosphère d'azote ne sont plus confondues et ceci est dû à l'oxydation du coordinat. Ce fait explique à notre avis le peu de précision des résultats antérieurs où l'on trouve pour pK_1^H des valeurs allant de 11.6[7] à 12.6[5]. Nous nous sommes donc limités pour l'exploitation de cette courbe (par la méthode de Bjerrum) à la détermination de $pK_2^H = 7.31$.

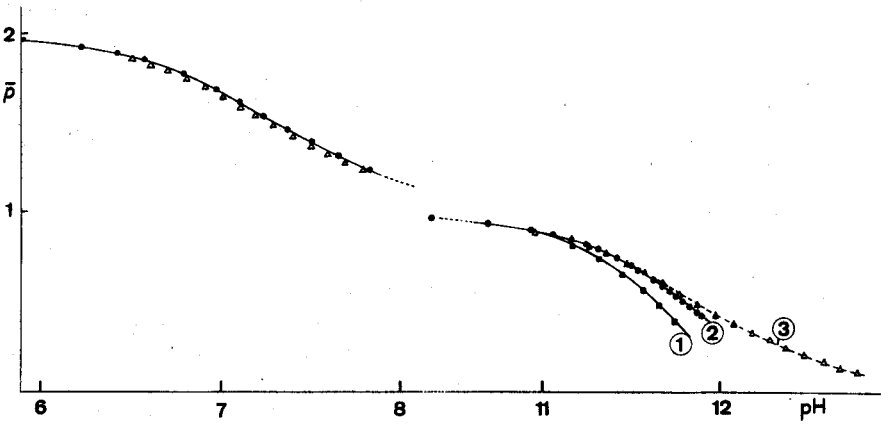

Fig. 1. Courbe de formation $\bar{p} = f(pH)$. (1) Titrage à l'air (■); (2) titrage sous azote (●); (3) courbe calculée (△).

Cependant afin d'utiliser un nombre maximum de données, nous avons calculé les deux constantes pour tous les points des courbes de titrage jusqu'à pH = 11.50. Nous avons obtenu ainsi les valeurs suivantes que nous adopterons par la suite:

$pK_1^H = 11.85 \pm 0.05$ (moyenne de 35 valeurs)

$pK_2^H = 7.29 \pm 0.04$ (moyenne de 43 valeurs)

La courbe $\bar{p} = f$ (pH) est recalculée à partir de ces données et l'on constate la bonne concordance avec le tracé expérimental sur la Fig. 1.

ÉTUDE POTENTIOMÉTRIQUE DE LA STABILITÉ IONIQUE

Nous avons neutralisé par la soude des solutions contenant l'ion métallique et le coordinat à différents rapports R (Tableau I) en présence d'acide nitrique.

TABLEAU I

RAPPORTS DE L'ION MÉTALLIQUE ET DU TIRON

$R=[L]_T/[Fe]_T$	$[Fe(III)]_T$	$[L]_T$	$[HNO_3]_T$
5	$1.007\cdot10^{-3}$	$5.000\cdot10^{-3}$	$1.035\cdot10^{-2}$
10	$1.007\cdot10^{-3}$	$1.000\cdot10^{-2}$	$1.035\cdot10^{-2}$
20	$1.007\cdot10^{-3}$	$2.000\cdot10^{-2}$	$1.035\cdot10^{-2}$

Pour les trois rapports examinés, nous avons calculé $\bar{n}$ et 1, nécessaires au tracé des courbes de formation $\bar{n}=f(-\log 1)$, à l'aide d'un ordinateur IBM 360* en fournissant comme données les concentrations initiales des différents constituants, les constantes d'ionisation du coordinat, le volume de soude ajouté et le potentiel correspondant de l'électrode en verre.

Les différents rapports examinés conduisent à une courbe de formation unique (Fig. 2) pour des valeurs de $\bar{n}$ comprises entre 1 et 3. Il est difficile d'obtenir des valeurs correctes pour $\bar{n}<1$ car les valeurs du pH sont alors très faibles et la précision des mesures peu satisfaisante.

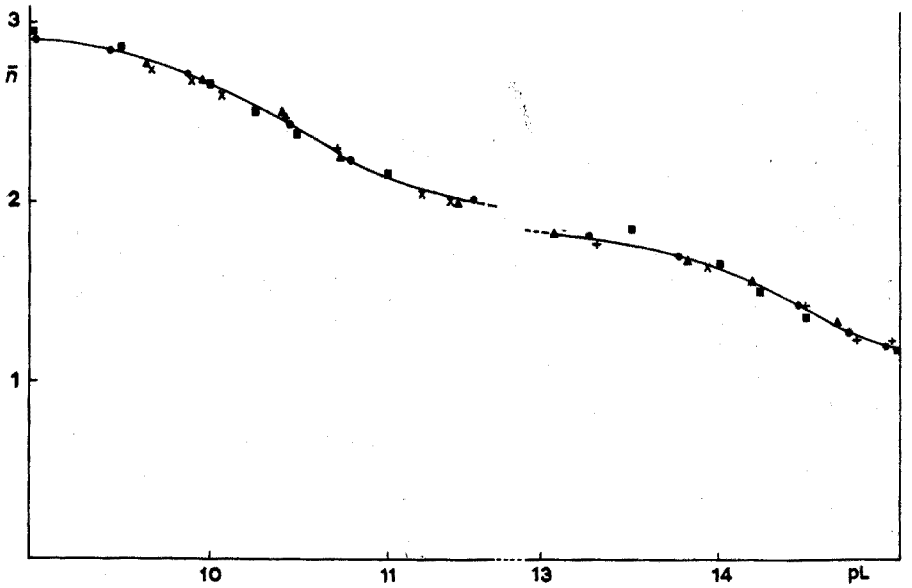

Fig. 2. Courbe de formation du système Fe(III)–acide pyrocatécholdisulfonique-3,5. (●) Rapport 5; (+) rapport 10; (▲) rapport 20; (■) points recalculés.

* Tous les calculs de ce travail ont été effectués par l'intermédiaire du Centre Inter-disciplines Régional de calcul électronique d'Orsay.

On peut alors appliquer la méthode des moindres carrés aux données $\bar{n}$ et 1 et obtenir des valeurs affinées des constantes de stabilité $K_n = [ML_n]/[ML_{n-1}] \cdot 1$. C'est ainsi que l'on obtient les valeurs ci dessous qui sont constantes après 3 itérations successives:

$\log K_2 = 14.23$
$\log K_3 = 10.28$

ÉTUDE SPECTROPHOTOMÉTRIQUE

La constante d'équilibre k_n pour la réaction

$$ML_{n-1} + H_2L \rightleftarrows ML_n + 2H$$

est définie par la relation

$$k_n = \frac{[ML_n]h^2}{[ML_{n-1}][H_2L]} \quad (1)$$

Il est possible de déterminer le rapport $a_n = [ML_n]/[ML_{n-1}]$ à partir des données spectrophotométriques et ceci pour différentes longueurs d'onde[6,8]:

$$a_n = \frac{\varepsilon_{n-1} - \varepsilon_M}{\varepsilon_M - \varepsilon_n}$$

ε_M, ε_n, ε_{n-1} representant respectivement les coefficients d'extinction moléculaire de la solution métal–coordinat, du complexe ML_n et du complexe ML_{n-1}. On dispose également des équations:

$$\bar{n} = (n-1) + a_n/a_{n+1}$$
$$[H_2L] = (1 - \bar{n}m)(1 + K_2^H/h)$$

Nous nous sommes limités en ce qui nous concerne à la détermination de k_1, les constantes d'ordre supérieur ayant été déterminées par potentiométrie. Il faut remarquer alors que a_1 représente le rapport de la concentration de l'espèce complexe ML sur la concentration du fer aussi bien sous sa forme libre Fe^{3+} que sous sa principale forme hydroxydée $FeOH^{2+}$. Pour calculer k_1 à l'aide de l'éqn. (1) nous avons donc multiplié le terme de droite par $(1 + K_H/[H])$ où K_H représente la constante d'hydrolyse de $FeOH^{2+}$. La valeur utilisée est celle déterminée par Wilson et Taube[9] en milieu de force ionique 0.5 M et à 25°.

Nous avons donc tracé deux faisceaux de spectres

$([L]_T/[M]_T = 5 \text{ et } 10)$

dans un domaine de longueurs d'onde allant de 400 nm à 750 nm. Ces faisceaux présentent chacun deux points isosbestiques bien définis à 675 nm et 530 nm où se trouvent respectivement à l'équilibre les espèces ML–ML_2 et ML_2–ML_3. Les calculs de a_1 sont effectués pour les spectres représentatifs de la seule espèce ML, c'est à dire pour tous les spectres passant en dessous du point isosbestique (675 nm). Pour un pH donné les valeurs de a_1 obtenues sont remarquablement constantes pour différentes longueurs d'onde comme le montre le Tableau II.

Cependant le calcul de k_1 montre une variation indiscutable de cette valeur en fonction du pH. Ce fait doit être attribué à l'existence d'une forme protonée MHL. Comme il n'existe aucun changement dans les spectres d'absorption dans la zone de

TABLEAU II

EXEMPLE DE CALCUL DE a_1 POUR $R=5$

pH	$\lambda=410$ *nm*	$\lambda=530$ *nm*	$\lambda=590$ *nm*	$\lambda=675$ *nm*
1.512	2.355	2.354	2.354	2.354
1.575	2.666	2.667	2.667	2.667
1.694	3.660	3.660	3.662	3.661
1.804	4.769	4.767	4.770	4.769
1.909	6.302	6.299	6.299	6.300
1.999	7.506	7.504	7.506	7.505

pH où cette protonation apparait nous sommes conduit à l'alternative: ou l'espèce MHL possède le même coefficient d'extinction moléculaire que l'espèce ML ou bien l'espèce protonée n'absorbe pas dans cette région.

Nous avons examiné ces deux hypothèses:

Dans le premier cas a_1 représente alors le rapport $[ML]+[MHL]/m$ et l'on est conduit à la relation

$$\frac{a_1 h^2}{[H_2L]} = k_1 + \frac{k_1}{k_H} h \text{ avec } k_H = \frac{[ML]h}{[MHL]} \tag{2}$$

Dans le deuxième cas $a_1=[ML]/(m+[MHL])$ et

$$\frac{[H_2L]}{a_1 h^2} = \frac{1}{k_1} + \frac{[H_2L]}{k_H h} \tag{3}$$

Ces deux relations peuvent donner lieu à une représentation graphique linéaire conduisant aux valeurs de k_1 et k_H. Nos calculs pour les deux rapports $R=5$ et 10 montrent que seule la relation (2) conduit à une concordance valable (Fig. 3). En effet la relation (3) conduit à deux droites (correspondant aux deux rapports envisagés) de pentes non conformes aux conditions expérimentales, et d'ordonnées à l'origine différentes. L'hypothèse selon laquelle l'espèce protonée possède le même coefficient d'extinction moléculaire que l'espèce ML est donc vérifiée; nous verrons qu'elle n'est pas contredite par la méthode trichrome.

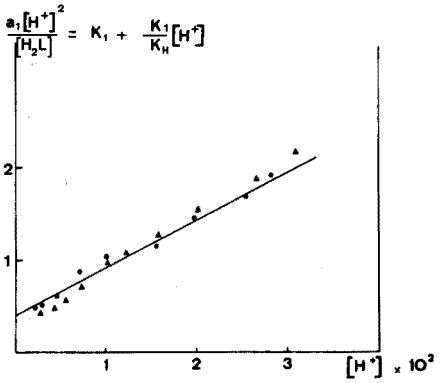

Fig. 3. Détermination de k_1 et k_H. (●) Rapport 10; (▲) rapport 5.

Les résultats retenus sont $pk_1 = 0.40$; $pk_H = 2.12$ soit $\log \beta_{101} = 18.74$; $\log \beta_{111} = 20.86$.

Nous sommes alors en possession de toutes les valeurs des constantes β_{pqr} du système Fe(III)–acide pyrocatécholdisulfonique-3,5 et nous avons rassemblé nos résultats dans le Tableau III où nous avons fait figurer également les données bibliographiques.

MÉTHODE TRICHROME

Nous ne reviendrons pas sur le principe de la méthode trichrome[10-13] brèvement exposée dans notre précédent Mémoire[1]. Nous avons effectué des essais pour trois rapports différents de réactifs engagés.

$R = [L]_T/[M]_T = 5$	$[M]_T = 2.517 \cdot 10^{-4} M$	$[L]_T = 1.250 \cdot 10^{-3} M$
$R = 10$	$[M]_T = 2.517 \cdot 10^{-4}$	$[L]_T = 2.500 \cdot 10^{-3}$
$R = 20$	$[M]_T = 2.517 \cdot 10^{-4}$	$[L]_T = 5.000 \cdot 10^{-3}$

Après avoir tracé les spectres d'absorption en fonction du pH, trois intervalles spectrophotométriques (410–510, 510–610 et 610–710 nm) sont utilisés pour étudier les courbes d'absorption et calculer les coordonnées trichromatiques u, v, w.

On obtient des résultats semblables dans les trois cas et nous donnons à titre d'exemple, sur la Fig. 4, les courbes u, v, w = f(pH) pour $R = 10$. Nous avons égale-

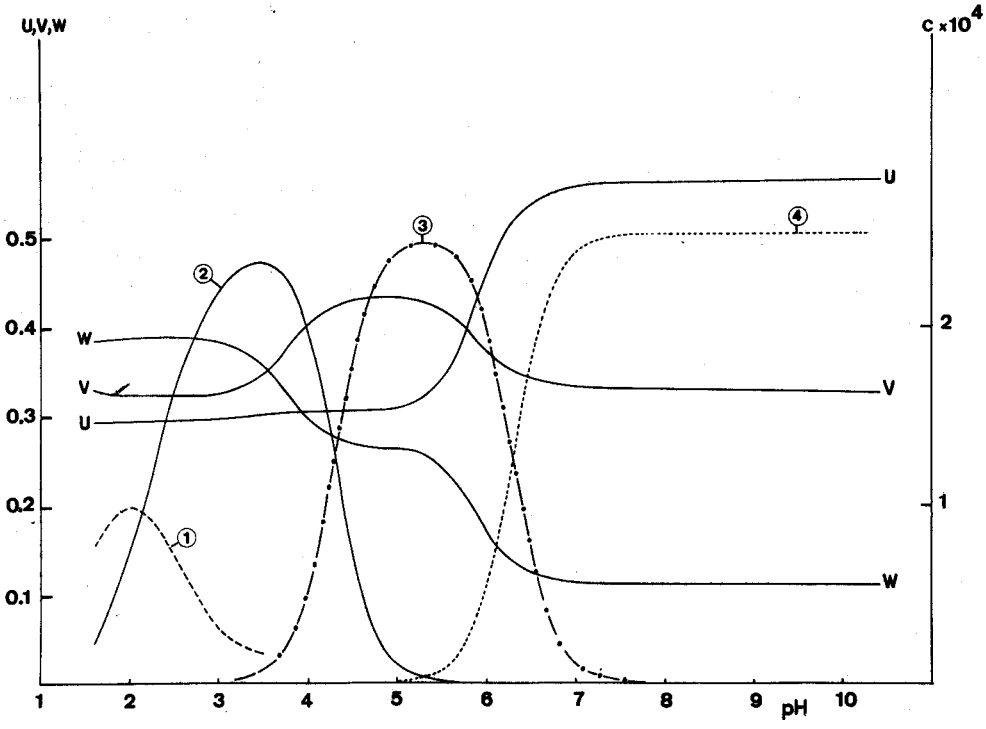

Fig. 4. Méthode trichrome (u, v, w) et courbes de répartition (1, 2, 3, 4) pour le rapport 10. ① FeHL; ② FeL; ③ FeL_2; ④ FeL_3.

TABLEAU III

COMPARAISONS DE NOS VALEURS DE CONSTANTES AVEC LES DONNÉES BIBLIOGRAPHIQUES

	Schwarzenbach et Willi[5]	*McBryde*[6]	*Nos valeurs*
$\log \beta_{111}$	22.5	—	20.86
$\log \beta_{101}$	20.7	19.50[a]	18.74
$\log \beta_{102}$	35.9	34.60	32.97
$\log \beta_{103}$	46.9	46.18	43.25

[a] Moyenne de différentes valeurs dépendant du pH.

ment tracé sur la même Fig. les courbes de répartition de toutes les espèces présentes simultanément en solution, calculées au moyen des constantes obtenues précédemment et pour les conditions de concentration indiquées ci-dessus.

On observe un premier palier pour des pH < 3. Or les courbes de répartition montrent que dans cette zone de pH coexistent les deux espèces MHL et ML^- (coloration bleu-vert); on a donc une confirmation du fait que ces deux complexes ont des coefficients d'extinction moléculaire identiques car autrement les graphes ne seraient pas parallèles à l'axe des pH. Au dela de pH = 3 apparait l'espèce ML_2^{5-}, on a donc en équilibre plusieurs espèces colorées distinctes ce qui explique que le premier palier des courbes u, v, w soit limité à cette valeur.

On constate également que l'on observe pas de palier correspondant à l'espèce ML_2^{5-} (bleu-violet). Ici encore les courbes de répartition expliquent ce fait puisque l'on voit que cette espèce n'existe jamais seule en solution mais qu'elle est en équilibre soit avec le deuxième complexe (pH < 5.6) soit avec le quatrième (pH > 5.0).

Enfin on remarque que l'on observe le palier correspondant à l'espèce ML_3^{9-} (rouge) pour des pH supérieurs à 7.50 en accord avec la courbe de répartition qui montre qu'à partir de cette valeur la concentration en ML_2^{5-} devient négligeable. Il faut noter d'autre part que cette quatrième espèce demeure stable pour des pH très élevés (pH > 10).

CONCLUSION

Notre étude avait pour objet de lever les indéterminations relatives aux complexes des ions ferriques avec l'acide pyrocatécholdisulfonique-3,5 et notamment en ce qui concerne la stabilité ionique et le domaine d'existence de l'espèce protonée FeHL.

Pour la première fois des mesures protométriques précises ont été effectuées sur ce système et la courbe de formation déterminée sans ambiguité pour $1 < \bar{n} < 3$.

En associant à ces mesures une méthode spectrophotométrique nous avons pu déterminer les constantes de stabilité globales β_{pqr} de toutes les espèces présentes en solution et montrer que les espèces FeHL et FeL^- possédaient le même coefficient d'extinction moléculaire. Il faut remarquer que si les valeurs de nos constantes diffèrent sensiblement de celles obtenues précedemment par d'autres auteurs, ceci est dû en grande partie au peu de précision avec laquelle avait été déterminée jusqu'àlors la constante d'ionisation K_1^H du coordinat en raison de l'oxydation importante des solutions de Tiron en milieu alcalin.

Nous avons pu calculer la répartition des diverses espèces complexées en fonction du pH montrant aussi que l'espèce protonée existe en quantité notable jusqu'à environ pH 3.50.

Cette répartition a été confirmée par la spectrophotométrie trichrome mettant en évidence la formation successive et les domaines d'existence des différentes espèces colorées.

Nous remercions vivement le Professeur R. A. Pâris pour ses conseils et l'aide précieuse qu'il nous a apportée dans la réalisation de ce travail.

RÉSUMÉ

Les auteurs étudient au moyen de méthode potentiométrique et spectrophotométrique, la complexation des ions fer(III) avec l'acide pyrocatécholdisulfonique-3,5. A coté des trois espèces simples FeL_n ($1 \leqslant n \leqslant 3$), une espèce protonée FeHL est mise en évidence, dont le coefficient d'extinction moléculaire est identique à celui de l'espèce FeL. Les domaines d'existence, les compositions et les constantes de stabilité des espèces formées sont donnés.

SUMMARY

The complex formation of iron(III) with 3,5-pyrocatecholdisulfonic acid (Tiron) has been studied by potentiometric and spectrophotometric measurements. In addition to three simple species FeL_n ($1 \leqslant n \leqslant 3$), the results indicate the formation of a protonated complex FeHL having the same, molar absorptivity as the unprotonated species FeL. The ranges of formation, the composition and the stability constants of all the species formed have been determined.

ZUSAMMENFASSUNG

Die Komplexbildung zwischen Eisen(III) und Brenzcatechindisulfonsäure-(3,5) (Tiron) wurde durch potentiometrische und spektrophotometrische Messungen untersucht. Ausser drei einfachen Spezies FeL_n ($1 \leqslant n \leqslant 3$) weisen die Ergebnisse auf die Bildung eines protonierten Komplexes FeHL hin, der denselben molaren Extinktionskoeffizienten wie der nichtprotonierte Komplex FeL hat. Die Bildungsgebiete, die Zusammensetzung und die Stabilitätskonstanten aller gebildeten Spezies wurden ermittelt.

BIBLIOGRAPHIE

1 M. Morin, M. R. Pâris et J. P. Scharff, *Anal. Chim. Acta*, 57 (1971) 123.
2 L. Vareille, *Bull. Soc. Chim. Fr.*, (1955) 1496.
3 K. S. Klausen, *Anal. Chim. Acta*, 44 (1969) 377.
4 J. Canonne, G. Nowogrocki et G. Tridot, *Bull. Soc. Chim. Fr.*, (1971) 1121.
5 G. Schwarzenbach et A. Willi, *Helv. Chim. Acta*, 61 (1951) 528.
6 W. A. E. McBryde, *Can. J. Chem.*, 42 (1964) 1917.
7 R. Nasanen, *Suom. Kem.*, 33 (1960) 111.
8 W. A. E. McBryde, J. L. Rohr, J. S. Penciner et J. A. Page, *Can. J. Chem.*, 48 (1970) 2574.
9 A. S. Wilson et H. Taube, *J. Amer. Chem. Soc.*, 74 (1952) 3509.
10 C. N. Reilley, H. A. Flaschka, S. Laurent et B. Laurent, *Anal. Chem.*, 32 (1960) 1218.
11 C. N. Reilley et A. Smith, *Anal. Chem.*, 32 (1960) 1233.
12 H. Flaschka, *Talanta*, 7 (1960) 90; 8 (1961) 8 et 342.
13 M. Petit-Ramel et M. R. Pâris, *Commun. Soc. Chim. Fr. Rouen*, 7b (1970) 34.

Analytica Chimica Acta
Elsevier Publishing Company, Amsterdam
Printed in The Netherlands

VOLATILE ALKALINE EARTH CHELATES OF FLUORINATED ALKANOYLPIVALYLMETHANES

A THERMOGRAVIMETRIC, GAS CHROMATOGRAPHIC AND MASS SPECTRAL STUDY*

R. BELCHER, C. R. CRANLEY, J. R. MAJER, W. I. STEPHEN and P. C. UDEN**
Department of Chemistry, University of Birmingham, P.O. Box 363, Birmingham B15 2TT (England)

(Received 31st January 1972)

Considerable attention has been paid to the study of metal chelate systems suitable for gas chromatographic analysis. Techniques such as thermogravimetric analysis and mass spectrometry help to predict and explain the gas chromatographic behaviour of many chelates. Such studies on alkaline earth chelates, have, until recently, been confined to the acetylacetonates. Yamakawa *et al.*[1] chromatographed these, but lack of characterisation of the eluates has led to doubts that the peaks observed were in fact due to the chelates[2]. Hyper-pressure gas chromatography which has proved successful for the elution of many metal acetylacetonates, leads to decomposition of the alkaline earth chelates[3].

The tendency of the alkaline earth β-diketonates to show increased coordination through solvolysis[4] or possibly polymerisation[5,6] is a contributory factor in determining their thermal stability and suitability for gas chromatography. For certain systems, *e.g.* the alkali metals[7], lead[8], and the rare earths[9,10], the sterically crowded ligand, dipivalylmethane and some fluorinated alkanoylpivalylmethanes, give chelates with more favourable gas chromatographic characteristics than the simple acetylacetonates. For the rare earths this property may be attributed to the fact that these ligands give unsolvated, monomeric chelates which have the necessary stability for successful gas chromatography.

Accordingly, this group of fluorinated ligands was chosen in the hope of preparing alkaline earth chelates whose properties would permit quantitative gas chromatographic analysis. The present paper describes the preparation and characterisation of the alkaline earth chelates of trifluoroacetylpivalylmethane, pentafluoropropanoylpivalylmethane and heptafluorobutanoylpivalylmethane, their mass spectra including identified polymeric ions, and some proposals about their fragmentation behaviour. Information on their relative volatility and thermal stability is gained from thermogravimetric analysis. Finally the results of a preliminary gas chromatographic study are described.

Recently, Schwarberg *et al.*[11] have reported the gas chromatographic properties

---

* This paper is dedicated to Professor Clément Duval on the occasion of his seventieth birthday.
** Present address: Department of Chemistry, University of Massachusetts, Amherst, Mass. 01002, U.S.A.

of the alkaline earth dipivalylmethanates. Although the individual chelates had different retention times, resolution of mixtures was not achieved.

EXPERIMENTAL

General nomenclature

The β-diketones are referred to by the trivial names given below, which in the metal chelates refer to the enolate ion of the parent β-diketone.

2,2,6,6-Tetramethylheptane-3,5-dione (dipivalylmethane), DPM*.

1,1,1-Trifluoro-5,5-dimethylhexane-2,4-dione (trifluoroacetylpivalylmethane), TPM.

1,1,1,2,2-Pentafluoro-6,6-dimethylheptane-3,5-dione (pentafluoropropanoylpivalylmethane), PPM.

1,1,1,2,2,3,3-Heptafluoro-7,7-dimethyloctane-4,6-dione (heptafluorobutanoylpivalylmethane), HPM.

Synthesis of β-diketones

DPM was prepared by the condensation of methyl pivalate and pinacolone with sodium hydride as condensing agent. TPM, PPM, and HPM were prepared by the sodium hydride condensation of pinacolone with ethyl trifluoroacetate, ethyl pentafluoropropionate and ethyl heptafluorobutyrate, respectively.

Synthesis of the metal chelates

The magnesium and strontium derivatives of trifluoroacetylpivalylmethane, pentafluoropropanoylpivalylmethane and heptafluorobutanoylpivalylmethane were formed by addition of the ligand to an aqueous solution of the metal chloride. Adjustment of the pH of the solution to *ca.* 7.0 with ammonia (4 *M*) produced white oily precipitates which were extracted into ether, the chelates being recovered on evaporation.

The calcium derivatives were prepared by addition of the ligand to a suspension of calcium hydroxide in methanol. The chelate was precipitated by the addition of water to the methanolic solution, previously reduced to 2–3 ml by rotary evaporation. This precipitate was extracted into ether, the ethereal layer then being evaporated to yield the chelate.

The barium chelates were prepared from barium hydroxide, after any barium carbonate impurity had been removed by filtration from aqueous solution. The ligand was added to an aqueous solution of the hydroxide and the white precipitate was filtered off, washed with water and air-dried.

The chelates prepared by these procedures were generally contaminated with an excess of ligand. This was removed by washing with *n*-hexane. Microanalytical results for these alkaline earth chelates are shown in Table I and correspond in most cases to hydration of the chelates by two water molecules.

---

* We prefer the group $(CH_3)C \cdot CO$ to be called "pivalyl" from the trivial name, pivalic acid, by analogy with acetyl from acetic acid. The term "pivaloyl" is not strictly correct, the "oyl" ending being a systematic one for acids ending in "oic".

TABLE I

MICROANALYTICAL, THERMOGRAVIMETRIC AND GAS CHROMATOGRAPHIC DATA FOR THE ALKALINE EARTH CHELATES

	Carbon–hydrogen (%)				*Thermogravimetric data*	*Gas chromatographic data*
	Calcd.		*Found*		*Weight loss (%)*	*Retention time*
	C	*H*	*C*	*H*		
$Mg(TPM)_2 \cdot 2H_2O$	42.6	5.4	43.2	5.3	100	1 min 36 sec
$Mg(PPM)_2 \cdot 2H_2O$	39.3	4.4	39.5	4.3	100	20–30 sec
$Mg(HPM)_2 \cdot 2H_2O$	36.9	3.7	36.8	3.8	100	20–30 sec
$Ca(TPM)_2 \cdot 2H_2O$	41.2	5.2	41.6	4.8	100	8 min 34 sec
$Ca(PPM)_2 \cdot 2H_2O$	38.2	4.3	38.6	3.9	100	4 min 45 sec
$Ca(HPM)_2 \cdot 2H_2O$	36.0	3.6	36.1	3.6	100	1 min 24 sec
$Sr(TPM)_2 \cdot 2H_2O$	37.4	4.7	36.8	4.7	98	8 min 55 sec
$Sr(PPM)_2 \cdot 2H_2O$[a]	35.2	4.0	36.9[a]	3.7[a]	100	6 min 10 sec
$Sr(HPM)_2 \cdot 2H_2O$	33.6	3.4	33.2	3.3	96	1 min 50 sec
$Ba(TPM)_2 \cdot 2H_2O$	34.1	4.3	34.3	4.1	76	9 min 12 sec
$Ba(PPM)_2 \cdot 2H_2O$	32.6	3.7	32.6	3.3	94	5 min 15 sec
$Ba(HPM)_2 \cdot 2H_2O$	31.5	3.2	31.8	3.0	95	2 min 24 sec

[a] Corresponds to $Sr(PPM)_2$, C = 37.4 and H = 3.5.

Sublimation

The chelates were sublimed at 0.1 torr in a sublimation apparatus immersed in an oil bath, the sublimates being collected on a cold finger. The magnesium chelates were all sublimed rapidly at 140–150° giving a clear melt on the finger which slowly solidified to a glassy solid. The calcium chelates sublimed rapidly at 190–195° giving white crystalline sublimates. The strontium and barium chelates were sublimed at temperatures between 190 and 220°; some yellowing of the sublimates was seen to occur, especially for barium trifluoroacetylpivalylmethanate.

Mass spectrometry

The mass spectra of the dehydrated alkaline earth chelates were recorded on an A.E.I. MS 9 double focussing mass spectrometer. The source temperature was maintained at about 200° and samples were evaporated into the source from the direct insertion probe. Mass measurements were made with heptacosafluorotri-*n*-butylamine as the reference compound.

Thermogravimetric analysis

Thermogravimetric data were recorded with the Perkin-Elmer TGS 1 Thermobalance for *ca.* 1.8-mg samples at a scan rate of 20° min^{-1} from 30° to 650° in an atmosphere of dry nitrogen.

Gas chromatography

A Philips PV 4000 (Pye R) chromatograph with hydrogen flame ionisation

detection was used. A Teflon column (3/16 inch o.d. and 2 feet in length) packed with 2.5% E. 301 silicone rubber on Universal B (60–85 mesh) was operated at 230°. The injection port and detector temperatures were maintained at 260° and the nitrogen flow was 46 ml min^{-1}. Injections of *ca.* 1% w/v solutions in sodium-dried ether were made.

RESULTS AND DISCUSSION

Mass spectra

A typical example of the spectra obtained for the magnesium chelates is shown in Fig. 1a for magnesium trifluoroacetylpivalylmethanate. The fragmentation pattern is consistent with that from a chelate where no metal valency change is possible. The molecular ion $[Mg(TPM)_2]^+$ initially loses odd electron fragments, *tert.*-butyl or TPM, to form the $[Mg(TPM)]^+$ ion followed by loss of the even electron, CF_2 fragment. Similar patterns have been reported for some fluorinated aluminium β-diketonates[12–14]. Only one peak with an *m/e* value higher than that of the molecular ion is observed, that corresponding to the $[Mg_2(TPM)_3]^+$ ion.

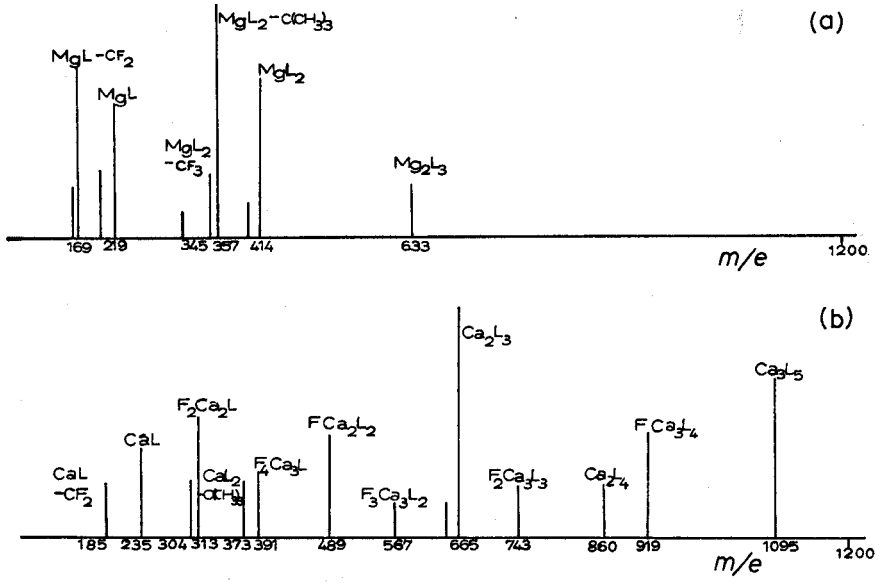

Fig. 1. Major features of the mass spectra of magnesium and calcium trifluoroacetylpivalylmethanates.

In contrast, the mass spectra of the calcium, strontium and barium chelates are much more complex, their main feature being a large number of peaks arising from polymeric ions extending to *m/e* values of well above 1500. A typical mass spectrum showing peaks up to *m/e* 1200 is shown in Fig. 1b. Although not shown, peaks of higher *m/e* values were obtained corresponding to $[Ca_4TPM_7]^+$, $[Ca_5TPM_9]^+$, etc. In the spectra of all these alkaline earth chelates, the molecular ion peak, $[ML_2]^+$, (M = Ca, Sr, Ba; L = TPM, PPM, HPM) was either very small or was not observed at all. However, peaks arising from the loss of odd electron species like *tert.*-butyl, CF_3 and L from this ion were evident. The peaks corresponding to the

ions $[M_2L_3]^+$ and $[M_3L_5]^+$ were more abundant than those from the ions of polymeric structure $[M_2L_4]^+$, $[M_3L_6]^+$, from which they are derived. Previous work on the mass spectra of alkaline earth acetylacetonates[5,6] revealed the same general trends as described above.

The $[M_2L_3]^+$ ion was the most predominant in the spectra, probably being derived from the $[M_2L_4]^+$ ion by loss of L. This ion fragmented by losing the even electron species CF_2, accompanied by migration of the remaining fluorine atom to the metal giving the $[FM_2L_2]^+$ ion. Further breakdown occurred, again by loss of CF_2 and transfer of the fluorine atom, to give the $[F_2M_2L]^+$ ion. These fragmentation steps were confirmed by the existence of metastable peaks, and by mass measurement of the $[M_2L_3]^+$, $[FM_2L_2]^+$, $[F_2M_2L]^+$ ions. A similar series of ions and reactions also appeared to occur as a result of fragmentation of the $[M_3L_6]^+$ ion. The following steps are postulated although not confirmed by mass measurement.

$$[M_3L_6]^+ \rightarrow [M_3L_5]^+ \rightarrow [FM_3L_4]^+ \rightarrow [F_2M_3L_3]^+ \rightarrow [F_3M_3L_2]^+ \rightarrow [F_4M_3L]^+$$

Loss of CF_2 with rearrangement of the remaining fluorine atoms to the metal has been reported for some fluorinated metal β-diketonates[12-16], but such reactions in the breakdown of polymeric chelate species have not previously been described.

It is as yet uncertain whether the polymeric species exist in the alkaline earth chelate vapour or if they are formed in the source of the mass spectrometer on evaporation and ionisation. There are, however, indications that some polymerisation occurs in the source, for the area under the integrated ion-current curve for the $[M_2L_3]^+$ ion increased with an increase in the temperature of the source.

Thermal analysis

The thermograms recorded for the hydrated alkaline earth chelates (Fig. 2) show that for each ligand there is a significant difference in volatility (taken as the position of the sublimation curve with respect to temperature) between the alkaline earth metals. Schwarberg *et al.*[11] reported a similar difference in the thermograms of the alkaline earth dipivalylmethanates.

Decomposition of the chelates as indicated by the percentage weight loss of sample (see Table I) did not occur for the magnesium and calcium chelates, was slight for most of the strontium and barium chelates, and was only significant for barium trifluoroacetylpivalylmethanate. The sublimation thermograms are sometimes

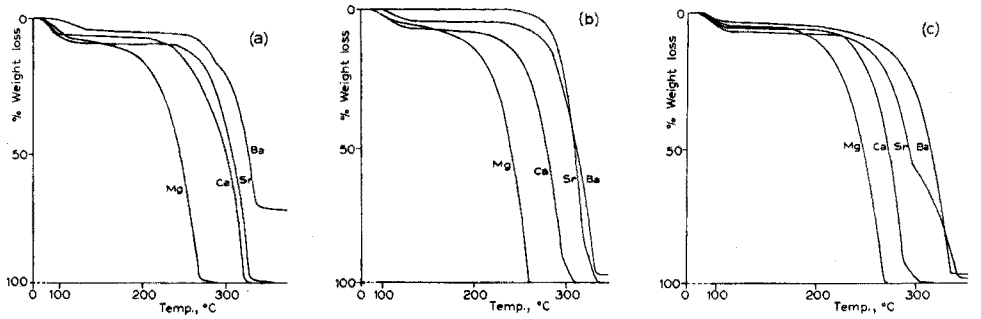

Fig. 2. Thermograms of the alkaline earth trifluoroacetylpivalylmethanates (a), pentafluoropropanoylpivalylmethanates (b), and heptafluorobutanoylpivalylmethanates (c). Heating rate 20° min^{-1}.

irregular. Thus, for calcium pentafluoropropanoylpivalylmethanate and heptafluorobutanoylpivalylmethanate, the final 10% of sample loss occurred over a wider temperature range than for the other chelates. A shoulder occurred in the thermogram of strontium heptafluorobutanoylpivalylmethanate. In most cases this behaviour was not attributed to decomposition, for quantitative weight losses were recorded. However, these curves could indicate the presence of several species of differing volatility resulting from polymer formation. Schwarberg *et al.*[11] from molecular weight data, concluded that the alkaline earth dipivalylmethanates were polymeric in benzene solution. The thermograms of these chelates were, however, regular.

The initial weight losses at 70–100° were attributed to the loss of hydrated water molecules. Strontium pentafluoropropanoylpivalylmethanate gave an anomalous result, showing no weight loss for several different preparations, and microanalytical data confirmed the absence of water. The other chelates were dehydrated by heating over P_2O_5 at 100° under vacuum for 1–2 h. Removal of water was confirmed by thermal analysis and microanalysis. The thermogravimetric curves were identical with those of the hydrated chelates after the loss of water, as were the percentage weight losses. Dehydration of these chelates therefore appears to take place without decomposition, a property also exhibited by the rare earth derivatives of these ligands[9,10].

Gas chromatography

The retention times of the alkaline earth chelates given in Table I were similar for the different metals with the same ligand, with the exception of magnesium. Figure 3 is illustrative of the chromatograms obtained; the best peak shapes were given by the trifluoroacetylpivalylmethane derivatives whereas those of the heptafluorobutanoylpivalylmethane chelates were broader than expected for such short retention times. Confirmation that the peak was due to the elution of the chelate

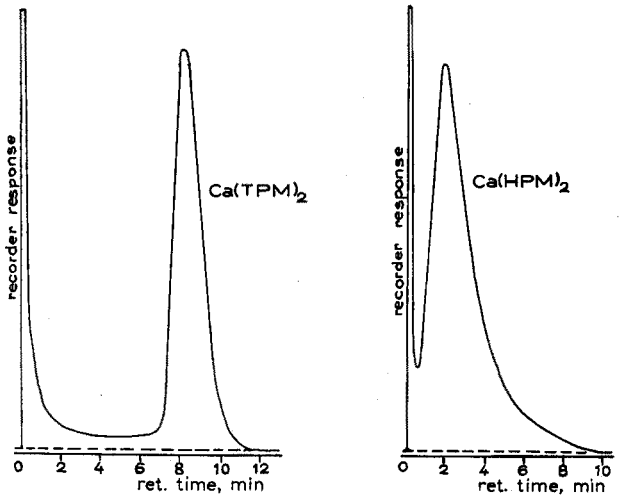

Fig. 3. Chromatograms of the Ca–TPM and Ca–HPM chelates on a 2-ft. Teflon column (3/16 in. o.d.) packed with 2.5% E.301 Silicone Rubber on Universal B (60–85 mesh). Column temperature 230°. Nitrogen flow 46 ml min^{-1}.

was given by microanalysis of the calcium heptafluorobutanoylpivalylmethanate eluted from the column.

An important feature of the gas chromatography of these chelates was their adsorption by the column. The tendency of the dehydrated chelates to increase their metal co-ordination number probably leads to bonding with the support through free OH groups. Adsorption and displacement effects[17], similar to those reported for other chelates, were evident. Thus, one alkaline earth chelate (*e.g.* $Mg(HPM)_2$) absorbed on the column was readily displaced by subsequent injections of another alkaline earth chelate (*e.g.* $Ca(TPM)_2$). Such effects tended to make retention time measurements unreliable, and may have contributed to the observed broadness of the peaks.

Although thermogravimetric analysis suggested a significant difference in the volatility of the alkaline earth chelates, the retention times on this column were too similar and the peaks were too broad to give any separation of mixtures of the calcium, strontium and barium derivatives of any of the three ligands. Schwarberg *et al.*[11] were unable to separate mixtures of alkaline earth dipivalylmethanates; this failure was attributed to the formation of heteronuclear polymeric species giving a peak with a retention time between the retention times of the individual chelates. In this study. however, no such species were evident but the retention times were probably too similar for such an effect to be noticeable.

These preliminary gas chromatographic results showed that the alkaline earth chelates may be eluted with minimal decomposition. The peak shapes of the trifluoroacetylpivalylmethane derivatives, with the exception of barium, were probably good enough to allow development of quantitative determinations of single alkaline earths. Future attempts to separate mixtures of alkaline earths may achieve greater success if column substrates can be found offering more specific interactions with individual chelates.

We wish to thank the United Kingdom Atomic Energy Authority for the maintenance grant for one of us (C.R.C.) and the Science Research Council for a grant towards the purchase of the Perkin Elmer TGS-1 thermobalance.

SUMMARY

The synthetic details and characterisation of some alkaline earth chelates of fluorinated alkanoylpivalylmethanes are given. The mass spectra of the calcium, strontium and barium compounds exhibit peaks due to polymeric ions, and some fragmentation steps of these ions are postulated. The thermogravimetric properties of the hydrated and dehydrated chelates are described in terms of relative volatility and stability. The results of a preliminary gas chromatographic study are discussed; elution appears to occur without decomposition but no separation of the calcium, strontium, and barium chelates is achieved.

RÉSUMÉ

Divers renseignements sont donnés sur la caractérisation de quelques chélates alcalino-terreux de fluoroalcanoylpivalylméthanes. Les spectres de masse obtenus

pour les dérivés de calcium, de strontium et de baryum présentent des pics dus à des ions polymériques. Les propriétés thermogravimétriques des chélates hydratés et deshydratés sont décrites, selon leur volatilité relative et leur stabilité. Une étude préliminaire par chromatographie gazeuse est effectuée.

ZUSAMMENFASSUNG

Einige Erdalkalimetall-Chelate von fluorierten Alkanoylpivalylmethanen werden dargestellt und charakterisiert. Die Massenspektren der Calcium-, Strontium- und Bariumverbindungen ergeben Peaks, die von polymeren Ionen herrühren; es werden einige Fragmentierungsstufen dieser Ionen postuliert. Die thermogravimetrischen Eigenschaften der hydratisierten und nichthydratisierten Chelate werden hinsichtlich relativer Flüchtigkeit und Stabilität beschrieben. Die Ergebnisse einer vorläufigen gaschromatographischen Untersuchung werden diskutiert; die Elution scheint ohne Zersetzung möglich zu sein, jedoch wird keine Trennung der Calcium-, Strontium- und Bariumchelate erreicht.

REFERENCES

1 K. Yamakawa, K. Tanikawa and K. Arakawa, *Chem. Pharm. Bull.* (*Tokyo*), 11 (1963) 1405.
2 R. W. Moshier and R. E. Sievers, *Gas Chromatography of Metal Chelates*, Pergamon, Oxford, 1965, p. 18.
3 N. M. Karayannis and A. H. Corwin, *J. Chromatogr. Sci.*, 8 (1970) 251.
4 B. Morosin, *Acta Crystallogr.*, 22 (1967) 315.
5 C. G. Macdonald and J. S. Shannon, *Aust. J. Chem.*, 19 (1966) 1545.
6 J. Macklin and G. Dudek, *Inorg. Nucl. Chem. Lett.*, 2 (1966) 403.
7 R. Belcher, J. R. Majer, R. Perry and W. I. Stephen, *Anal. Chim. Acta*, 45 (1969) 305.
8 R. Belcher, J. R. Majer, W. I. Stephen, I. J. Thomson and P. C. Uden, *Anal. Chim. Acta*, 50 (1970) 423.
9 K. J. Eisentraut and R. E. Sievers, *J. Amer. Chem. Soc.*, 87 (1965) 5254.
10 C. S. Springer, D. W. Meek and R. E. Sievers, *Inorg. Chem.*, 6 (1967) 1105.
11 J. E. Schwarberg, R. E. Sievers and R. W. Moshier, *Anal. Chem.*, 42 (1970) 1828.
12 C. Reichert, J. B. Westmore and H. D. Gesser, *Chem. Commun.*, (1967) 782.
13 R. Perry, *Ph.D. Thesis*, University of Birmingham, 1968.
14 C. R. Jenkins, *Ph.D. Thesis*, University of Birmingham, 1970.
15 G. M. Bancroft, C. Reichert, J. B. Westmore and H. D. Gesser, *Inorg. Chem.*, 8 (1969) 474.
16 A. L. Clobes, M. L. Morris and R. D. Koob, *J. Amer. Chem. Soc.*, 91 (1969) 3087.
17 P. C. Uden and C. R. Jenkins, *Talanta*, 16 (1969) 893.

Analytica Chimica Acta
Elsevier Publishing Company, Amsterdam
Printed in The Netherlands

FRACTIONAL SUBLIMATION OF VARIOUS METAL CHELATES OF DIPIVALOYLMETHANE

EUGENE W. BERG and NICOLAS M. HERRERA*
Coates Chemical Laboratories, Louisiana State University in Baton Rouge, Baton Rouge, La. 70803 (*U.S.A.*)
(Received 1st November 1971)

The fractional sublimation technique developed by Berg and Hartlage[1,2] has proven to be an effective tool for the study of the volatility and separability of various β-diketone metal chelates. Berg and Chiang[3,4] reported on the volatility and fractional sublimation of the dipivaloylmethane (DPM) chelates of the lanthanides and related elements and Berg and Reed[5,6] reported on the fractional sublimation of some metal chelates of thenoyltrifluoracetone.

The present investigation was undertaken to extend the study of the volatility of dipivaloylmethane chelates to include the more common normal and transition elements so that comparisons might be made between the volatilities observed for the metal chelates of dipivaloylmethane and other β-diketone ligands.

Hartlage's studies[2] demonstrated both qualitatively and quantitatively that fractional sublimation data collected for individual chelates could be used to predict accurately the separability of various metal chelate mixtures. Similar criteria have been employed in this study to predict the separability by fractional sublimation of numerous mixtures of dipivaloylmethane metal chelates.

EXPERIMENTAL

Reagents

Dipivaloylmethane (2,2,6,6-tetramethyl-3,5-heptanedione, Peninsular Chem Research, Inc.) and the platinum metal salts (A. D. Mackay, Inc.) were used without further purification. All other metal salts and reagents were analytical-reagent grade.

Preparation of the metal chelates of dipivaloylmethane

The chelates were prepared by methods[2,7] routinely used for the preparation of various β-diketone chelates. These methods are described briefly below.

Method A[2]. A 15% dipivaloylmethane–ethanol solution was added, while stirring, to an aqueous solution of the metal salt which had been buffered with an excess of potassium acetate. The chelate was recovered by filtration and purified by sublimation.

Method B[7]. Pure dipivaloylmethane was added to a 50% ethanol–water solution of the metal salt, then concentrated aqueous ammonia was added while stirring until the chelate precipitated. The chelate was recovered by filtration and

* Present address: Department of Chemistry, St. Bernard College, St. Bernard, Ala. 35138, U.S.A.

purified by recrystallization from aqueous ethanol.

Method C. An aqueous 10% (w/v) solution of potassium hydrogen carbonate was added to an aqueous 5% solution of the metal salt until the solution reached a pH just below that required for the precipitation of the hydroxide. This solution then was treated with a slight excess of a 15% dipivaloylmethane–ethanol solution and stirred for 5 h. The chelate was recovered by filtration and purified by sublimation.

Method D[7]. A solution of 3 g of chromium(III) chloride hexahydrate, 20 g

TABLE I

GENERAL DATA ON THE METAL CHELATES OF DIPIVALOYLMETHANE[1]

Compound	*Crystals*	*Method of preparation*	*M.p. [lit.] (°)*	*Formula*	*Analysis*			
					Calculated		*Found*	
					%C	%H	%C	%H
$Al(DPM)_3$	White, needles	A	265–266[264–265]	$AlC_{33}H_{57}O_6$	68.72	9.96	68.29	9.95
$Ba(DPM)_2$	White, needles	B	171–172[171]	$BaC_{22}H_{38}O_4$	52.44	7.60	----	----
$Be(DPM)_2$	White, needles	B	95–97[93–97]	$BeC_{22}H_{38}O_4$	70.36	10.20	70.20	10.28
$Ca(DPM)_2$	White, needles	B	222–225[224]	$CaC_{22}H_{38}O_4$	64.98	9.42	----	----
$Cd(DPM)_2$	White, needles	C	228[a]	$CdC_{22}H_{38}O_4$	55.17	8.00	54.97	8.05
$Cr(DPM)_3$	Purple	D	228–229[229]	$CrC_{33}H_{57}O_6$	65.86	9.77	65.56	9.67
$Co(DPM)_2$	Purple	B	142–143[143]	$CoC_{22}H_{38}O_4$	62.10	9.00	60.14	9.14
$Co(DPM)_3$	Dark green	A	244–245[245]	$CoC_{33}H_{57}O_6$	65.11	9.45	65.17	8.81
$Cu(DPM)_2$	Deep blue	A	198–199[198]	$CuC_{22}H_{38}O_4$	61.44	8.91	61.00	8.81
$Fe(DPM)_3$	Red, needles	A	164–165[163]	$FeC_{33}H_{57}O_6$	65.44	9.48	64.67	9.46
$Mg(DPM)_3$	White, needles	B	94–95[94]	$MgC_{22}H_{38}O_4$	67.60	9.80	----	----
$Mn(DPM)_3$	Black	C	164–165[165]	$MnC_{33}H_{57}O_6$	65.54	9.50	65.32	9.56
$Ni(DPM)_2$	Pink, needles	B	223–225[225]	$NiC_{22}H_{38}O_4$	61.84	8.96	60.99	9.17
$Hg(DPM)_2$	White, needles	A	190–192[192]	$Hg_2C_{22}H_{38}O_4$	34.39	5.01	34.04	4.97
$Pd(DPM)_2$	Yellow	C	228[b]	$PdC_{22}H_{38}O_4$	55.86	8.10	55.77	8.19
$Pt(DPM)_2$	Yellow	C	230[b]	$PtC_{22}H_{38}O_4$	47.05	6.54	46.98	6.81
$Rh(DPM)_3$	Orange yellow	C	185	$RhC_{33}H_{57}O_6$	61.19	8.79	64.10	9.50
$Sr(DPM)_2$	White, needles	B	199–201[200]	$SrC_{22}H_{38}O_4$	58.18	8.43	----	----
$Zn(DPM)_2$	White, needles	B	143–144[144]	$ZnC_{22}H_{38}O_4$	60.89	8.82	60.90	8.82
$Zr(DPM)_4$	Yellow	A	330–332	$ZrC_{44}H_{76}O_8$	64.09	9.31	63.85	9.34

[a] Decomposes.
[b] Sublimes with partial decomposition.

of urea and 5 g of dipivaloylmethane in a 65% ethanol–water solvent, was heated at 90° for 5 h. The solution was cooled to room temperature and 100 ml of water was added. The chelate was recovered by filtration and purified by sublimation.

Each of the chelates prepared was characterized by its melting point, a carbon–hydrogen analysis, an infrared absorption spectrum and a n.m.r. spectrum. Melting point data were collected on a Mel-Temp melting point apparatus. Infrared spectra were recorded on a Perkin-Elmer Infracord instrument with solid chelate samples powdered and suspended in potassium bromide pellets. The n.m.r. spectra were recorded on a Varian A-60A spectrometer with saturated solutions of the chelates in carbon tetrachloride.

The dipivaloylmethane chelates prepared in this study are listed in Table I with an indication of the method of preparation employed and certain of their physical properties. The infrared and n.m.r. data for the various chelates are summarized in Table II.

TABLE II

INFRARED AND n.m.r. DATA OF VARIOUS METAL DIPIVALOYLMETHANE CHELATES

Metal chelate	*Infrared frequency maxima for selected absorption bands* [a] *(cm^{-1})*		*N.m.r. chemical shifts (CCl_4)* $-\delta$ *tert.-Butyl*	$-\delta \gtrless CH$
	$C{=}{=}C$	$C{=}{=}O$		
$Al(DPM)_3$	1600	1570	1.08	5.60
$Ba(DPM)_2$	1590	1575	1.01	5.55
$Be(DPM)_2$	1550	1515	1.19	5.80
$Ca(DPM)_2$	1570	1570	1.06	5.60
$Cd(DPM)_2$	1590	1570	1.19	5.72
$Co(DPM)_2$	1555	1520	1.10	5.65
$Co(DPM)_3$	1570	1515	----	----
$Cr(DPM)_3$	1595	1560	----	----
$Fe(DPM)_3$	1540	1510	----	----
$Mg(DPM)_2$	1549	1525	1.19	5.80
$Mn(DPM)_3$	1570	1525	----	----
$Hg(DPM)_2$	1598	1680	----	----
$Ni(DPM)_2$	1575	1560	1.17	5.35
$Pd(DPM)_2$	1540	1540	1.15	5.62
$Pt(DPM)_2$	1545	1545	1.14	5.60
$Rh(DPM)_3$	1545	1545	1.13	5.60
$Sr(DPM)_2$	1590	1560	1.05	5.59
$Zn(DPM)_2$	1550	1550	1.21	5.74
$Zr(DPM)_4$	1575	1540	----	----

[a] Accuracy of values: $\pm 10\ cm^{-1}$.

Fractional sublimation apparatus and procedure

Specifications for the fractional sublimator used in this work were reported earlier[1,2]. Briefly, the apparatus consists of a 1-m (12 mm o.d.) pyrex tube with a continuous temperature gradient maintained along its length and evacuated to 1 mm of mercury pressure with a carrier gas (air) flowing from the high temperature to the low temperature end of the sublimator. Samples were placed in small aluminum

boats and inserted between glass-wool plugs into the high temperature end of the sublimation tube before the pressure was reduced. The samples then were heated for 2 h at reduced pressure. The volatilized chelate was entrained in the stream of air and carried through the tube until condensation occurred. The recrystallized (sublimed) chelates were found in discrete and reproducible temperature condensation zones. Individual chelates were recovered by cutting the sublimation tube into selected segments and dissolving the chelate in an appropriate solvent. The sublimation recrystallization temperature zones for the various chelates studied are reported in Fig. 1. Where the recrystallization zones were divided into distinct parts the solid line represents the major concentration of the chelate and the dotted line represents a diffuse zone in which trace amounts of the chelate were found.

Mixtures of various chelates were sublimed under the same conditions and the sublimation recrystallization temperature zones for the components of the mixtures studied are given in Fig. 2.

DISCUSSION AND RESULTS

Five alkaline earth metal chelates of dipivaloylmethane were prepared and characterized but only the Be(II) and Mg(II) chelates were volatile; the Ca(II), Sr(II) and Ba(II) chelates were not volatile under the experimental conditions used. A problem arose in the characterization of the Ca(II), Sr(II) and Ba(II) chelates because the carbon–hydrogen analyses were completely erratic, although the compounds were readily recrystallized from aqueous ethanol solutions and gave i.r. and n.m.r. spectra which left little doubt as to their purity and β-diketone chelate character; the melting point data agreed closely with that for previously reported preparations. It was assumed that the Ca(II), Ba(II) and Sr(II) compounds were indeed the non-volatile chelates. Schwarberg *et al.*[8] have reported the gas-chromatographic properties of these chelates, and have shown that they are not significantly volatile below 300°.

An evaluation of the data in Fig. 1 shows that the beryllium(II) chelate is the most volatile chelate of those studied and that the dipivaloylmethane chelates of the lanthanides and actinides are among the least volatile. The relatively low volatility of the lanthanide chelates is not completely apparent unless one compares the data presented here with earlier data[3,4], Chiang's data on the lanthanide dipivaloylmethane chelates were not collected under exactly the same conditions as the data reported here, hence for comparison purposes the most volatile and least volatile lanthanide chelates (Y(III) and La(III), respectively) were sublimed to establish the temperature range over which the lanthanides would sublime. The temperature condensation range reported here for the lanthanide chelates compares very favorably with that reported by Chiang, thus one can conclude that the lanthanide dipivaloylmethane chelates are among the least volatile studied. Similarly, a comparison of the observed volatility of the thorium(IV) dipivaloylmethane chelate with that reported by Chiang for throrium(IV) and related elements suggests that the actinides exhibit a relatively low volatility comparable to that of the lanthanide chelates.

All previous work done with the fractional sublimator has shown that once the temperature condensation zone has been established for a pure compound under certain prescribed conditions, this zone is reproducible and predictable even if other

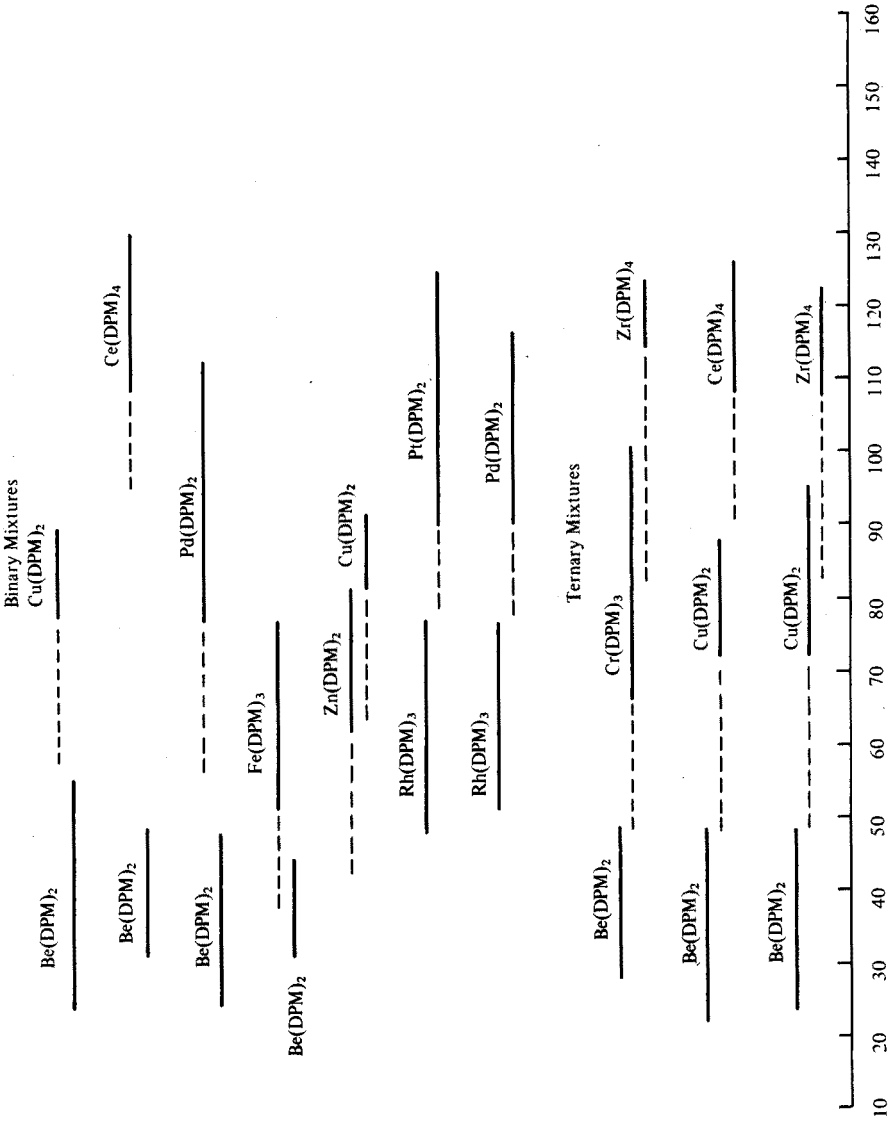

Fig. 1. Individual sublimation–condensation temperature zones for the metal chelates of dipivaloylmethane.

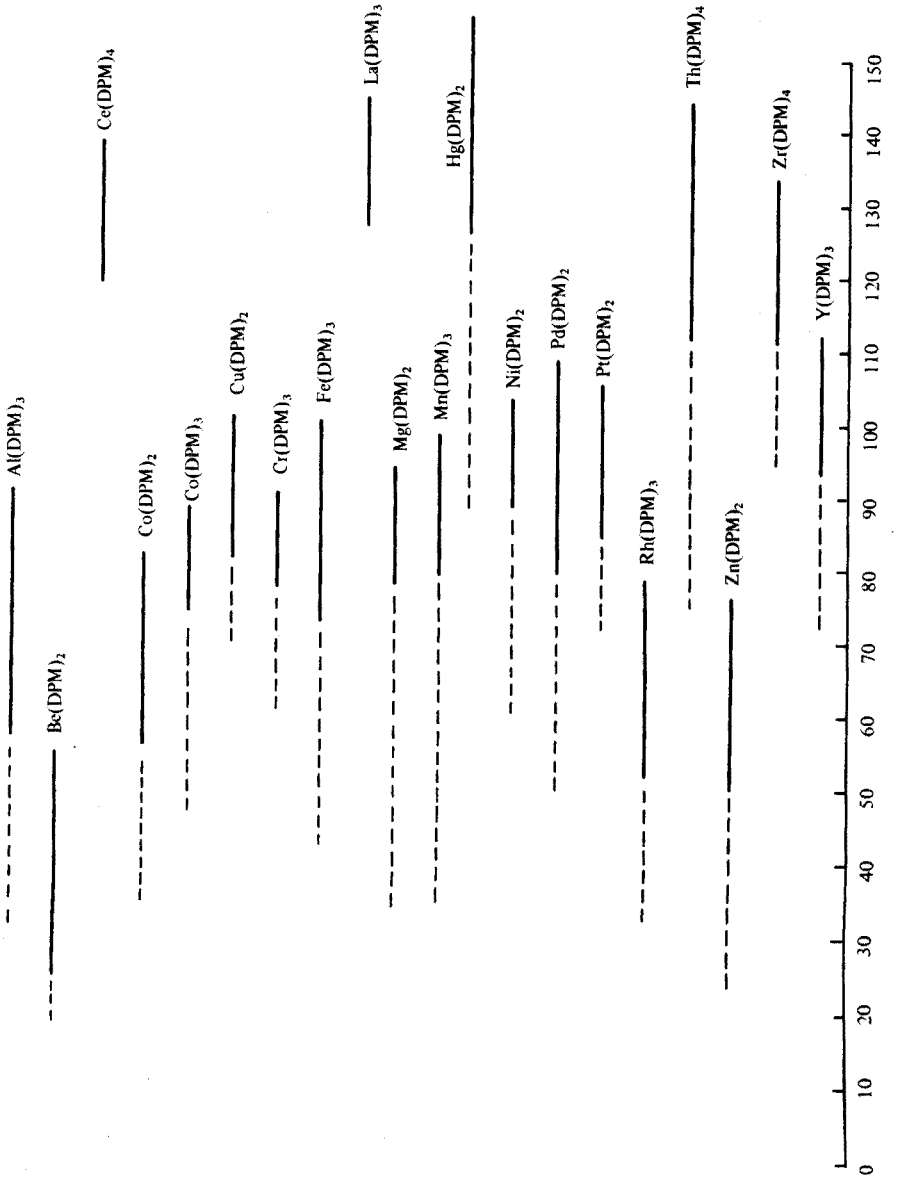

Fig. 2. Data on the fractional sublimation of mixtures of metal dipivaloylmethane chelates.

volatile components are present in the sample. Advantage is taken of this reproducibility of temperature condensation zones to predict numerous separations from the data provided in Fig. 1. It is proposed that the various binary and ternary mixtures of dipivaloylmethane chelates listed in Table III can be quantitatively separated by fractional sublimation. Seven binary and three ternary mixtures of various metal dipivaloylmethane chelates were separated by fractional sublimation and the results are shown in Fig. 2. The separations are in close agreement with prediction from the data in Fig. 1.

TABLE III

MIXTURES OF VARIOUS METAL DIPIVALOYLMETHANE CHELATES WHICH PROBABLY CAN BE QUANTITATIVELY SEPARATED BY FRACTIONAL SUBLIMATION

Binary mixtures

Al(III) –Ce(IV)	Cr(III) –Hg(II)	Fe(III) –Zr(IV)	Rh(III)–La(III)
Al(III) –La(III)	Co(II) –La(III)	Mg(II) –Ce(IV)	Rh(III)–Hg(II)
Al(III) –Hg(II)	Co(II) –Hg(II)	Mg(II) –La(III)	Rh(III)–Th(IV)
Be(II) –Ce(IV)	Co(II) –Th(IV)	Mg(II) –Hg(II)	Rh(III)–Zr(IV)
Be(II) –Cu(II)	Co(II) –Zr(IV)	Mn(III)–Ce(IV)	Zn(II) –Ce(III)
Be(II) –Cr(III)	Co(III)–Ce(IV)	Mn(III)–La(III)	Zn(II) –La(III)
Be(II) –La(III)	Co(III)–La(III)	Mn(III)–Hg(II)	Zn(II) –Hg(II)
Be(II) –Hg(II)	Co(III)–Hg(II)	Ni(II) –Ce(IV)	Zn(II) –Th(IV)
Be(II) –Ni(II)	Cu(II) –Ce(IV)	Ni(II) –La(III)	Zn(II) –Zr(IV)
Be(II) –Th(IV)	Cu(II) –La(III)	Pd(II) –La(III)	Zr(IV) –Al(III)
Be(II) –Y(III)	Fe(III) –Ce(IV)	Pt(II) –Ce(IV)	Zr(IV) –Cr(III)
Cr(III) –Ce(IV)	Fe(III) –La(III)	Pt(II) –La(III)	Zr(IV) –Co(III)
Cr(III) –La(III)	Fe(III) –Hg(II)	Rh(III) –Ce(IV)	Zr(IV) –Mg(II)
			Zr(IV) –Mn(II)

Ternary mixtures

Be(II)–Cr(III)–Ce(IV)	Be(II)–Cu(II)–La(III)
Be(II)–Cr(III)–La(III)	Be(II)–Ni(II) –Ce(IV)
Be(II)–Cr(III)–Hg(II)	Be(II)–Ni(II) –La(III)
Be(II)–Cr(III)–Zr(IV)	Be(II)–Pd(II)–La(III)
Be(II)–Cu(II) –Ce(IV)	Be(II)–Pt(II) –Ce(IV)
	Be(II)–Pt(II) –La(III)

A comparison of the data presented in Fig. 1 with earlier data[1,2] shows that the dipivaloylmethane chelates possess volatilities similar to those of the corresponding metal acetylacetonates but less than those of the chelates of trifluoroacetylacetone and hexafluoroacetylacetone. The chelates of benzoylacetone, benzoyltrifluoroacetone[1,2] and thenoyltrifluoroacetone[6] are less volatile than the corresponding chelates of dipivaloylmethane.

The infrared absorption frequency assignments given the C=C and C=O bonds in Table II are those made by Nakamoto[9] for β-diketone chelates. The absorption frequencies of the two bonds are lower than those of the corresponding acetylacetonates of the same metals, which may mean that these bonds are weaker in the dipivaloylmethane chelates than in the corresponding metal acetylacetonates. The infrared absorption data suggest that all of the compounds studied possessed similar types of bonds with the possible exception of the mercury(II) chelate which

absorbed at a much higher frequency than was expected for the C=O bond.

As was to be expected, there was no significant difference in the n.m.r. chemical shifts for the *tert.*-butyl or >CH protons in the chelates regardless of what metal ion was bound to the ligand.

This work was supported in part by a National Science Foundation Science Faculty Fellowship and an Academic Year Extension of the NSF Research Participation Program for College Teachers awarded N.M.H.

SUMMARY

Twenty different metal chelates of dipivaloylmethane were prepared and characterized by melting points, carbon–hydrogen analyses, and infrared and n.m.r. absorption data. The pure chelates were sublimed in the Berg fractional vacuum sublimator and the temperature condensation (sublimation) zones were recorded for each chelate under standardized conditions. The beryllium(II) chelate was the most volatile and the lanthanide and actinide chelates among the least volatile dipivaloylmethanates. The only volatile alkaline earth metal chelates were those of Be(II) and Mg(II); the Ca(II), Sr(II) and Ba(II) chelates were not volatile under the conditions used. Overall it was found that the chelates of dipivaloylmethane exhibited volatilities similar to those of the corresponding metal acetylacetonates but less than those of the trifluoroacetylacetonates and the hexafluoroacetylacetonates. The chelates of benzoylacetone, benzoyltrifluoroacetone and thenoyltrifluoroacetone are less volatile than the corresponding chelates of dipivaloylmethane. The data suggest that some 64 different binary and ternary mixtures of metal dipivaloylmethane chelates can be quantitatively resolved. Seven binary and three ternary mixtures of the metal chelates were resolved satisfactorily.

RÉSUMÉ

Vingt chélates métalliques du dipivaloylméthane ont été préparés et caractérisés par leur point de fusion, leur analyse carbone–hydrogène, leur absorption infrarouge et r.n.m. On a procédé à leur sublimation dans le dispositif à vide fractionné de Berg; les températures des zones de condensation ont été enregistrées pour chaque chélate. Le chélate de béryllium est le plus volatil; ceux des lanthanides et des actinides sont les moins volatils. 64 mélanges binaires et ternaires de dipivaloylméthanates métalliques peuvent être résolus quantitativement par sublimation fractionée.

ZUSAMMENFASSUNG

Zwanzig verschiedene Metallchelate von Dipivaloylmethan wurden dargestellt und durch Schmelzpunkte, Kohlenstoff–Wasserstoff–Analysen, Infrarot- und n.m.r.-Absorptionsdaten charakterisiert. Die reinen Chelate wurden im Berg-Vakuum-sublimationsapparat fraktioniert sublimiert, und die Temperatur-Kondensations (Sublimations)-Zonen wurden für jeden Chelat unter standardisierten Bedingungen aufgezeichnet. Der Beryllium(II)-Chelat zeigte die grösste Flüchtigkeit, während die

Chelate der Lanthaniden und Aktiniden zu den am wenigsten flüchtigen Dipivaloylmethanaten gehörten. Die einzigen flüchtigen Chelate der Erdalkalimetalle waren die von Be(II) und Mg(II); die Chelate von Ca(II), Sr(II) und Ba(II) waren unter den angewendeten Bedingungen nicht flüchtig. Im ganzen zeigten die Chelate von Dipivaloylmethan Flüchtigkeiten, die ähnlich denen der korrespondierenden Metallacetylacetonate, aber geringer als die der Trifluoracetylacetonate und der Hexafluoracetylacetonate waren. Die Chelate von Benzoylaceton, Benzoyltrifluoraceton und Thenoyltrifluoraceton sind weniger flüchtig als die korrespondierenden Chelate von Dipivaloylmethan. Die Ergebnisse lassen erkennen, dass etwa 64 verschiedene binäre und ternäre Gemische von Metall–Dipivaloylmethan-Chelaten quantitativ aufgespalten werden können. Sieben binäre und drei ternäre Gemische der Metallchelate wurden befriedigend aufgespalten.

REFERENCES

1 E. W. Berg and F. R. Hartlage, Jr., *Anal. Chim. Acta*, 33 (1965) 173; 34 (1966) 46.
2 F. R. Hartlage, Jr., *Sublimation Separation Studies of Various Metal β-Diketone Chelate Compounds*, Ph.D. Dissertation, Louisiana State University, Baton Rouge, La., 1964.
3 J. J. Chiang A., *A Study on the Volatility of the β-Diketone Chelates of Group III B Elements*, Ph.D. Dissertation, Louisiana State University, Baton Rouge, La., 1967.
4 E. W. Berg and J. J. Chiang A., *Anal. Chim. Acta*, 40 (1968) 101.
5 K. P. Reed, *Thio-β-Diketones and Methylene Alkylated β-Diketones—Their Synthesis and Chelates*, Ph.D. Dissertation, Louisiana State University, Baton Rouge, La., 1968.
6 E. W. Berg and K. P. Reed, *Anal. Chim. Acta*, 42 (1968) 207.
7 G. S. Hammond, D. C. Nonhebel and S. W. Chin-Hua, *Inorg. Chem.*, 2 (1963) 73.
8 J. E. Schwarberg, R. E. Sievers and R. W. Floshier, *Anal. Chem.*, 42 (1970) 1828.
9 K. Nakamoto, *Infrared Spectra of Inorganic and Coordination Compounds*, John Wiley, New York, 1968.

Analytica Chimica Acta
Elsevier Publishing Company, Amsterdam
Printed in The Netherlands

"QUASI-ISOTHERMAL" AND "QUASI-ISOBARIC" THERMOGRAVIMETRY

F. PAULIK AND J. PAULIK
Institute for General and Analytical Chemistry, Technical University, Budapest (Hungary)
(Received 1st December 1971)

Recently, a new thermoanalytical method called "quasi-isothermal" thermogravimetry has been developed[1,2]. The derivatograph[3,4] has been slightly modified and a heating control device has been constructed. With this additional control, the temperature of the sample is raised in the usual way at a uniform heating rate (0.5–5.0° min^{-1}) so long as the weight of the sample remains constant, but as soon as the weight of the sample begins to change, the temperature increase is stopped automatically. Thereafter the regulator system switches out the heating current whenever the rate of the weight change exceeds a very small value and switches it on again when, owing to the small temperature drop, the rate of the weight change decreases below the preselected value. This alternating process, which requires only a few seconds, is repeated continuously until the end of the thermal decomposition.

The results obtained even in the initial experiments were surprisingly good. The TG curves of calcium carbonate shown in Fig. 1 were obtained in different types of sample holder, partly with the help of the new method (curves 1–4), and partly with the dynamic 10° min^{-1} heating program (curves 5–8). When the dynamic heating program was used, the thermal decomposition of calcite took place in the temperature interval between 200° and 300° (curves 5–7). However, the temperature of the sample remained constant during the reaction—with the exception of the small

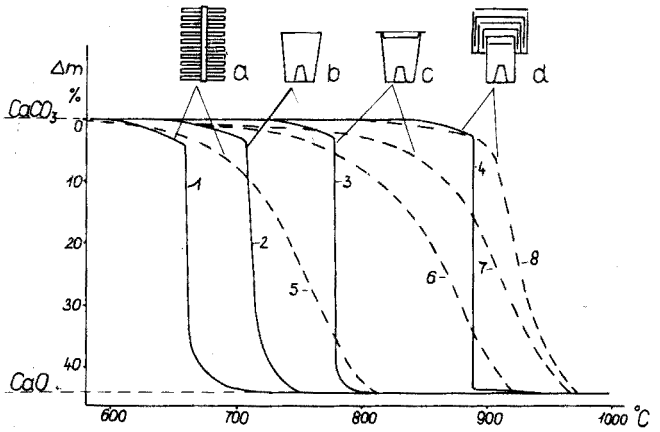

Fig. 1. TG curves of the decomposition of calcium carbonate. Sample holders: (a) polyplate sample holder[9]; (b) crucible without lid[4]; (c) crucible with lid; (d) the new type of crucible covered with the six-fold lid. Quasi-isothermal heating program: curves 1–4. Dynamic heating program 10° min^{-1}: curves 5–8.

initial and final periods of the reaction—when the new heating regulator was applied (see curves 2 and 3). Accordingly, the device establishes, though in an indirect way, "quasi-isothermal"conditions during the time that transformations connected with weight change are taking place in the sample.

It was also observed that the decomposition temperatures are always dependent on the experimental conditions, *i.e.* according to the composition of the gas phase present in the space between the grains. Accordingly, when the experiments were carried out with covered crucibles, the decomposition temperatures were always higher (see curves 3 and 7) than when open crucibles (curves 2 and 6) were used. This observation suggested the desirability of constructing a special sample holder so that a self-generated atmosphere could be established in the surroundings of the sample; this would render the decomposition temperatures independent of changes in experimental conditions.

The purposeful application of self-generated atmospheres was first made by Garn and Kessler[5] and by Forkel[6], but numerous other experiments have also been carried out along these lines[7].

Experience has shown that it is rather difficult to establish a self-generated atmosphere of perfect purity even if a high heating rate (5–10° min^{-1}) is applied; under the conditions of the lengthy "quasi-isothermal" examination, it is particularly difficult to establish pure atmospheres. However, in spite of the many difficulties, appropriate results were finally achieved by using a platinum crucible covered with a six-fold lid[2,8] the construction of which is shown in Fig. 2. As can be seen the specially shaped crucible is covered by six well-fitting lids in such a way that the gaseous decomposition products are forced to pass through a long and narrow labyrinth when leaving the sample. The gaseous decomposition products streaming through the labyrinth are able to hinder the diffusion of air from the opposite direction, even when the evolution of the gases is very slow, as in the case of the decomposition of calcite where the carbon dioxide is evolved at a rate of 0.5 ml min^{-1}. At certain positions, the channels of the labyrinth form bottlenecks, and there are sudden changes in direction or forks which also assist in hindering the back-flow of air.

The thermal decomposition of calcium carbonate under "quasi-isothermal" conditions was also studied by using this new type of crucible with the six-fold lid. Figure 3 shows the curves of the temperature change (T) and weight change (TG) of the 0.4-g sample as functions of time. According to these curves, the temperature of the sample increased at a rate of 4.5° min^{-1} until it reached 892°. The thermal decomposition of calcium carbonate began only at this temperature, taking place very slowly, over a period of about 200 min, *i.e.* with a speed of 1 mg min^{-1}.

The result of this same experiment is also shown by curve 4 in Fig. 1, which demonstrates the changes not as a function of time but as a function of temperature. The TG curve was obtained by means of an X-Y recorder. At the beginning of this curve, between 840° and 890°, a slightly sloping horizontal section can be seen. This can be interpreted by assuming that only 2% of the sample has decomposed in this temperature interval to produce carbon dioxide in sufficient amount to expel completely the air not only from the crucible but also from the space between the grains.

After the section mentioned, the curve shows a sharp vertical turn. In this interval of the decomposition, the temperature of the sample becomes spontaneously 892° and the sample is maintained at this temperature until the end of the decomposi-

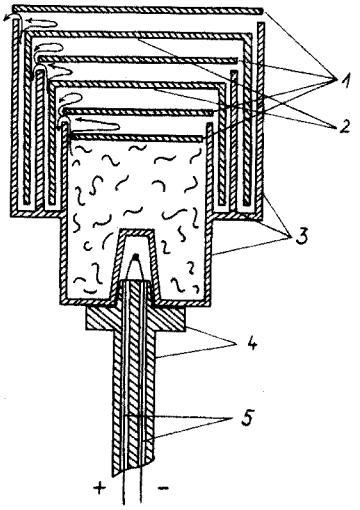

Fig. 2. Crucible covered with the six-fold lid. (1) Lid of type I; (2) lid of type II; (3) crucible; (4) corundum tube; (5) thermocouple.

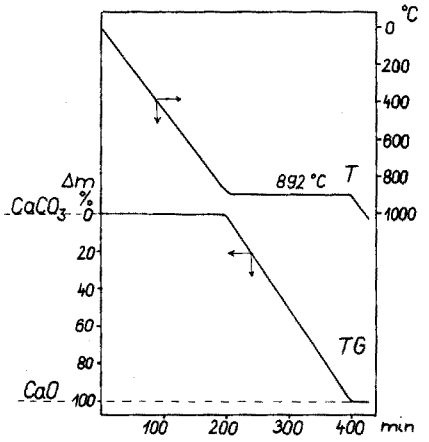

Fig. 3. Thermal decomposition of calcium carbonate under quasi-isothermal and quasi-isobaric conditions.

tion. The fact that the temperature becomes constant spontaneously, is noteworthy, since the heating control applied provides only for the constancy of the rate of the weight change and not for that of the temperature.

According to the literature, the decomposition pressure of calcium carbonate under equilibrium conditions attains one atmosphere at 895°. Because the value of the decomposition temperature obtained (892°) lies near the above value and because stabilization of the decomposition temperature occurs spontaneously, it can be concluded that under the given circumstances, the decomposition of the sample takes place under quasi-isothermal and quasi-isobaric (*i.e.* under quasi-equilibrium) conditions.

Curve 8 of Fig. 1 was recorded with the help of the crucible covered by the six-fold lid, but with programmed dynamic heating, *i.e.* at a heating rate of $10° \text{ min}^{-1}$. The shape of this curve is completely different from curve 4 discussed earlier. The distortion of curve 8 has probably two causes. First, if it is assumed that the rates of both the nucleus formation and the growth of nuclei of calcium oxide are slower than the rate of the temperature rise, then the decomposition process will be determined by the rate of formation of the new solid phase. Secondly, owing to the temperature drop inside the sample, which shows poor heat conductivity, the thermal decomposition takes place in successive layers of the sample at different times; this also contributes to the distortion of the curve. The significant difference between the shape of curves 4 and 8 proves that the self-generated atmosphere alone does not solve the problem of standardization, and adequate results can be obtained only if it is combined either with the proposed quasi-isothermal system or possibly with a very slow heating program.

The authors wish to thank Prof. E. Pungor for valuable discussions.

SUMMARY

The recently proposed "quasi-isothermal" thermogravimetric method has been developed further. When a specially designed crucible is used, a self-generated atmosphere surrounds the sample which then decomposes under "quasi-isobaric" conditions. For example, calcite decomposes completely at a constant temperature of 892°, which is very close to the decomposition temperature of 895° achieved by static methods in the presence of 100% carbon dioxide under equilibrium conditions.

RÉSUMÉ

Un nouveau développement a été effectué pour la méthode thermogravimétrique "quasi-isothermique" récemment proposée. Par exemple, la calcite se décompose complètement à une température constante de 892°, très voisine de la température de décomposition de 895° obtenue par des méthodes statiques, en présence de dioxyde de carbone à 100%, dans les conditions d'équilibre.

ZUSAMMENFASSUNG

Die kürzlich vorgeschlagene Methode der "quasi-isothermen" Thermogravimetrie wurde weiterentwickelt. Bei Verwendung eines speziellen Tiegels umgibt eine selbsterzeugte Atmosphäre die Probe, die sich dann unter "quasi-isobaren" Bedingungen zersetzt. Zum Beispiel zersetzt sich Calcit vollständig bei einer konstanten Temperatur von 892°, die sehr dicht an der Zersetzungstemperatur von 895° liegt, welche nach statischen Methoden in Gegenwart von 100% Kohlendioxid unter Gleichgewichtsbedingungen erhalten wird.

REFERENCES

1 J. PAULIK AND F. PAULIK, *Anal. Chim. Acta*, 56 (1971) 328.
2 F. PAULIK AND J. PAULIK, *Proc. III Int. Conf. Thermal Analysis*, in press.
3 F. PAULIK, J. PAULIK AND L. ERDEY, *Z. Anal. Chem.*, 160 (1958) 241.
4 F. PAULIK, J. PAULIK AND L. ERDEY, *Talanta*, 13 (1966) 1405.
5 P. B. GARN AND J. E. KESSLER, *Anal. Chem.*, 32 (1960) 1563.
6 W. FORKEL, *Naturwiss.*, 47 (1960) 10.
7 A. E. NEWKIRK, *Thermochim. Acta*, 2 (1971) 1.
8 J. PAULIK AND F. PAULIK, *Hungarian patent*, 1971.
9 J. PAULIK, F. PAULIK AND L. ERDEY, *Anal. Chim. Acta*, 34 (1966) 419.

Analytica Chimica Acta
Elsevier Publishing Company, Amsterdam
Printed in The Netherlands

COMPLEXIMETRIC TITRATIONS BASED ON 1:2 COMPLEX FORMATION

PART II. THE SYSTEMATIC TITRATION ERROR

F. FREESE AND G. DEN BOEF
Laboratory for Analytical Chemistry, University of Amsterdam, Amsterdam (The Netherlands)

(Received 20th December 1971)

In Part I[1] it was shown that 1:2 complex formation, though of little practical consequence in potentiometric or visually indicated titrations, is more promising in combination with "linear" indication methods such as amperometry and photometry. For the titration reaction of a metal ion M of analytical concentration c_M, with a ligand L, according to the reaction

$$M + 2\,L \rightleftarrows ML_2\,,$$

mathematical expressions were derived for the relative concentrations m, ml, ml_2 and l ($m=[M]/c_M$, etc.) as a function of the titration parameter $f=c_L/c_M$.

In the present paper expressions are given for the systematic titration error.

General

In practical work the end-points of these titrations are found by the intersection of two tangents drawn to the titration curve. As a model of this procedure, for each of the possible four titration curves, tangents can be drawn at a point $f=0$ and at a point near $f=3$, which is taken as the point where $l=1$. When considerable 1:2 complex formation occurs, $l=1$ nearly corresponds with $f=3$. As is obvious from the previous paper, this is the case when $Z_2 \gg 1$.

However, this is not the only requirement. Although the stability constant of the first step of the complexation reaction K_1 is usually much larger than that of the second step K_2, exceptions occur. Moreover, the conditional stability constant K'_1 may become much smaller than K'_2 when the metal ion undergoes a side-reaction. Such a side-reaction, *e.g.* a reaction with hydroxyl ions, affects K'_1 but not K'_2. The influence of a side-reaction on K'_1 may be so large that the overall stability constant $\beta'_2=K'_1K'_2$ becomes too small for complete or nearly complete formation of the 1:2 complex, although $Z_2 \gg 1$. In terms of Z_1 and Z_2 this means that apart from $Z_2 \gg 1$, a second condition $Z_1Z_2 \gg 1$ has to be fulfilled for nearly complete formation of ML_2 near $f=3$; this also follows from the systematic titration errors derived below.

In the following paragraphs discussion is first restricted to the normal case where $Z_1 \gg Z_2$. The special case $Z_1 \ll Z_2$ is then discussed briefly.

THE CASE $Z_1 \gg Z_2$

For the f–l and f–m curves, the intersection of the tangents at $f=0$ and $f\simeq 3$

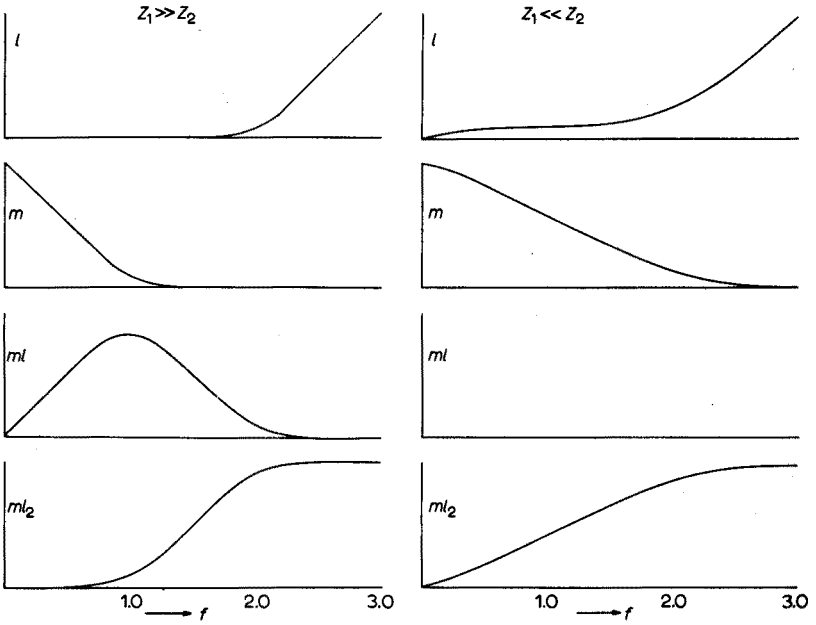

Fig. 1. $f-l, f-m, f-ml$ and $f-ml_2$ curves for $Z_1 \gg Z_2$ and $Z_1 \ll Z_2$.

($l=1$) produces an end-point at $f=2$ and $f=1$ respectively. In the case of indication by means of ML or ML_2, a third tangent has to be drawn at the inflection point of the f–ml or f–ml_2 curve. This tangent produces intersections with the tangents at $f=0$ and $f=3$ corresponding to end-points at $f=1$ and $f=2$ respectively. For convenience the four cases are presented in Fig. 1.

The general equation of a tangent to the curve $f=f(x)$ at a point x_t, f_t is

$$f = \left(\frac{df}{dx}\right)_t (x-x_t) + f_t$$

and the value of f for the point of intersection of two tangents in x_0 and x_1 is given by

$$f_s = \frac{\left(\frac{df}{dx}\right)_0 \left[f_1 - \left(\frac{df}{dx}\right)_1 (x_1-x_0)\right] - f_0 \left(\frac{df}{dx}\right)_1}{\left(\frac{df}{dx}\right)_0 - \left(\frac{df}{dx}\right)_1} \qquad (1)$$

The indices 0, 1 and i are used for tangents at $f=0$, $f\simeq 3$ ($l=1$) and at the inflection points, respectively.

The $f-l$ curve

Tangents at $f=0$ and $l=1$ are needed. From the preceding paper[1]:

$$f = l + \frac{Z_1 l + 2Z_1 Z_2 l^2}{1 + Z_1 l + Z_1 Z_2 l^2} \qquad (2)$$

At $f=0$, also $l=0$.

At $l=1$, the value of f can be calculated by means of eqn. (2)

$$f_1 = 1 + \frac{Z_1 + 2Z_1Z_2}{1 + Z_1 + Z_1Z_2} \quad \text{or} \quad f_1 = 1 + \frac{2 + \frac{1}{Z_2}}{1 + \frac{1}{Z_2} + \frac{1}{Z_1Z_2}}$$

It is supposed that $Z_2 \gg 1$ and $Z_1Z_2 \gg 1$. This results in:

$$f_1 = 1 + \left(2 + \frac{1}{Z_2}\right)\left(1 - \frac{1}{Z_2} - \frac{1}{Z_1Z_2}\right)$$

which leads to

$$f_1 = 3 - \frac{1}{Z_2}$$

Thus $f_0 = 0, l_0 = 0$ and $f_1 = 3 - \frac{1}{Z_2}, l_2 = 1.$

It is easily found by means of eqn. (2) that

$$\left(\frac{df}{dl}\right)_0 = 1 + Z_1, \quad \text{and} \quad \left(\frac{df}{dl}\right)_1 = 1 + \frac{1}{Z_2}$$

Inserting these values in eqn. (1) leads to:

$$f_s = 2 - \frac{2}{Z_2}$$

and to a systematic titration error for indication on L at $f = 2$ of

$$\Delta_l = -\frac{2}{Z_2}.$$

The f–m curve

Tangents at $f = 0$ and $f = 1$ are needed. From the preceding paper[1]:

$$f = 2(1-m) + \left(\frac{1}{Z_2} - Rm\right) W_m \quad \text{with} \tag{3}$$

$$W_m = \tfrac{1}{2}\left\{\left(1 + \frac{4}{R}\,\frac{1-m}{m}\right)^{\frac{1}{2}} - 1\right\}$$

As $m = (1 + Z_1 l + Z_1Z_2 l^2)^{-1}$ it is easily seen that

$$m_0 = 1;\ f_0 = 0 \text{ and } f_1 = 3 - \frac{1}{Z_2};\ m_1 = \frac{1}{Z_1Z_2}$$

The general equation of the tangent is

$$\frac{df}{dm} = -2 - \left\{\frac{1}{Z_2} - Rm\right\} \frac{1}{Rm^2\left(1 + \frac{4}{R}\,\frac{1-m}{m}\right)^{\frac{1}{2}}} - RW_m$$

Thus

$$\left(\frac{df}{dm}\right)_0 = -\left(1+\frac{1}{Z_1}\right) \text{ and } \left(\frac{df}{dm}\right)_1 = -\tfrac{1}{2}Z_1Z_2$$

The intersection is found by means of eqn. (1):

$$f_s = 1 + \frac{1}{Z_1}$$

and for the systematic titration error at $f=1$:

$$\Delta_m = \frac{1}{Z_1}.$$

The f–ml curve

Tangents at $f=0$, $l=1$ and at the inflection point are needed to find the systematic errors at the end-points at $f=1$ and $f=2$.

According to the previous paper the rising part of the curve is given by

$$f_{(-)} = ml + \left\{\frac{1}{Z_1} + \frac{2\,ml}{R}\right\}\frac{ml}{1-ml} \tag{4}$$

Thus $f_0=0$ and $ml_0=0$, and it can easily be derived that

$$\left(\frac{df_{(-)}}{dml}\right)_0 = 1 + \frac{1}{Z_1}.$$

The descending branch of the $f-ml$ curve can be approximated by

$$f_{(+)} = 2 - ml + \frac{1}{Z_2}\frac{1-ml}{ml} - \left\{\frac{1}{Z_1} + \frac{2\,ml}{R}\right\}\frac{ml}{1-ml} \tag{5}$$

At $l=1$, $ml_1 = \dfrac{1}{Z_2}$ and $f_1 = 3 - \dfrac{1}{Z_2}$.

Furthermore

$$\frac{df_{(+)}}{dml} = -1 - \left\{\frac{1}{Z_1} + \frac{2\,ml}{R}\right\}\frac{1}{(1-ml)^2} - \frac{2}{R}\frac{ml}{1-ml} - \frac{1}{Z_2} - \frac{1}{(ml)^2}. \tag{6}$$

Substitution of ml gives

$$\left(\frac{df_{(+)}}{dml}\right)_1 = -Z_2$$

From eqn. (6) the coordinates of the inflection point can be found by differentiating once again and putting

$$\frac{d^2f_{(+)}}{(dml)^2} = 0$$

It follows that

$$ml_i = \frac{1}{1+\left(\dfrac{1+2Z_2}{R}\right)^{\frac{1}{3}}} \tag{7}$$

It is possible to find a general equation for the titration errors in both end-points expressed in Z_1, Z_2 and R, but the mathematics is very cumbersome. It is better to calculate, for each special case, ml_i by means of eqn (7), f_i by means of eqn. (5) and $(df_{(+)}/dml)_i$ by means of eqn. (6), and then insert these values in eqn. (1).

An example is given below for illustration.

Example for $Z_1 = 10^4$ *and* $Z_2 = 10^2$, $R = 10^2$

From eqn. (7), $ml_i = 0.4420$ and from eqns. (5) and (6), $f_{(+)i} = 1.5635$ and $(df_{(+)}/dml)_i = -1.0952$.

In combination with the values

$$f_0 = 0 \qquad f_1 = 3$$
$$ml_0 = 0 \qquad \text{and} \qquad ml_1 = 0.01$$
$$\left(\frac{df}{dml}\right)_0 = 1.00 \qquad \left(\frac{df}{dml}\right)_1 = -100,$$

eqn. (1) yields for the first point of intersection ${}_1f_s = 0.9773$, corresponding to a systematic titration error of -2.3%, and for the second point of intersection ${}_2f_s = 2.0470$, corresponding to a relative systematic titration error of $+2.4\%$.

The f–ml_2 curve

Tangents at $f = 0$, $l = 1$ and at the inflection point are needed to find the systematic errors at $f = 1$ and $f = 2$. It can easily be seen that for $f = 0$, $(ml_2)_0 = 0$ and $(df/dml_2)_0$ is infinite, which means that the tangent at $f = 0$ is the f-axis. At $l = 1$ we have again $f_1 = 3 - 1/Z_2$.

$$\text{As } ml_2 = \frac{Z_1 Z_2 l^2}{1 + Z_1 l + Z_1 Z_2 l^2}$$

then for $l = 1$, $(ml_2)_1 = 1 - 1/Z_2$. The tangent at $l = 1$ can be found from the approximate equation from the previous paper[1]

$$f = \left(1 + \frac{1}{Z_1} + \frac{1}{R}\right) + \left(1 - \frac{1}{R}\right) ml_2 + \frac{1}{Z_2}\,\frac{ml_2}{1 - ml_2} - \frac{1}{R}\,\frac{1 - ml_2}{ml_2} \qquad (8)$$

$$\frac{df}{dml_2} = 1 - \frac{1}{R} + \frac{1}{Z_2}\,\frac{1}{(1 - ml_2)^2} + \frac{1}{R}\,\frac{1}{(ml_2)^2}$$

Substitution of $(ml_2)_1 = 1 - 1/Z_2$ leads to

$$\left(\frac{df}{dml_2}\right)_1 = Z_2$$

Between $f = 1$ and $f = 2$, the $f - ml_2$ curve shows an inflection point, which is found by differentiating eqn. (8) twice with respect to ml_2. This leads to

$$(ml_2)_i = \frac{1}{1 + \left(\frac{R}{Z_2}\right)^{\frac{1}{3}}}$$

As in the case of the f–ml curve, in any special case, f_i and $(df/dml_2)_i$ can be calculated to find the data necessary for calculating the theoretical end-points. In this case,

however, an attempt to find general expressions for the two end-points as a function of Z_1, Z_2 and R is more successful and leads to the simple equations

$$ {}_1f_s = 1 + \frac{1}{Z_1} - \frac{3}{(RZ_1)^{\frac{1}{2}}} $$

and

$$ {}_2f_s = 2 + \frac{1}{Z_1} - \frac{1}{Z_2} + \frac{3}{(Z_1Z_2)^{\frac{1}{2}}} $$

which leads to the following titration errors:

$$ {}_1\Delta_{ml_2} = -\frac{3}{(RZ_1)^{\frac{1}{2}}} + \frac{1}{Z_1}, $$

in which the second term is usually negligible and

$$ {}_2\Delta_{ml_2} = -\frac{1}{Z_2}. $$

THE CASE $Z_1 \ll Z_2$

It can be shown that for $R=(Z_1/Z_2)<4$, not only the $f-ml$ and $f-ml_2$ curves but also the $f-l$ and $f-m$ curves have a point of inflection. For $R \ll 1$ which, as $ml_{max} = R^{\frac{1}{2}}/(2+R^{\frac{1}{2}})$, implies that ml during the titration is negligible, the situation becomes mathematically simpler than in the normal case treated above. In this extreme case the three curves f *vs.* m, l and ml_2 can be found from the equations:

$$ Z_1Z_2 = \frac{ml_2}{m \cdot l^2}, \qquad m+ml_2 = 1, \text{ and } l+2ml_2 = f. $$

From the last two stoicheiometric relations, it can be inferred that the inflection points in the three curves are situated at the same value of f, *viz.* $f_i = 1 + (3Z_1Z_2)^{-\frac{1}{2}}$ at values of $l=(3Z_1Z_2)^{-\frac{1}{2}}$, $m=\frac{3}{4}$ and $ml_2=\frac{1}{4}$.

Furthermore it can be seen that there exists a simple linear relation between the three curves, because in all cases $ml_2 = 1-m$ and $l = f-2ml_2 = (f-2)-2m$.

Because of these simple relationships, the same systematic titration error can be found from each curve if the tangents are drawn at the same pair of f-values. If the first tangent is drawn at the point of inflection of the curve and the second, as before, at $f=3-1/Z_2$ ($l=1$), the tangents will intersect at $2+3/(3Z_1Z_2)^{\frac{1}{2}}$, and the systematic titration error becomes

$$ \Delta = 3^{\frac{1}{2}}/(Z_1Z_2)^{\frac{1}{2}}. $$

DISCUSSION

Some general rules can be given for the titration error. When an end-point occurs at $f=2$, which is the more common case, the titration error will be of the order of $1/Z_2$, unless $Z_1 \ll Z_2$. Then the error will be of the order $(Z_1Z_2)^{-\frac{1}{2}}$. For end-points near $f=1$ the value of R has to be large. The error is $1/Z_1$ in the case of indica-

tion by means of M, and a function of RZ_1 in the case of indication by means of ML or ML_2.

It should be emphasized that this paper deals with systematic errors for those cases where indication by means of only one of the compounds involved in the reaction is possible. In practice an instrumental signal generally stems from more than one of the compounds. If the sensitivities of the signals of the individual compounds do not differ very much, the angles between the linear parts of the resulting titration curve may be very obtuse. For optimal titration conditions, the signal from one of the compounds should predominate as much as possible.

In fact, the points where tangents were drawn were chosen arbitrarily. Taking other points of the curves for drawing tangents leads to titration errors governed by the same general rules mentioned in this discussion.

SUMMARY

Expressions are given for the systematic titration errors in linear compleximetric titrations of a metal M with a ligand L resulting in a complex of the type ML_2.

RÉSUMÉ

Des expressions ont été calculées pour les erreurs systématiques des titrages complexiométriques linéaires du type $M+2L \rightarrow ML_2$.

ZUSAMMENFASSUNG

Es werden Ausdrücke abgeleitet für die systematischen Fehler bei der linearen komplexiometrischen Titration von einem Metall M dass mit einem Ligand L das Komplex ML_2 bildet.

REFERENCE

1 F. FREESE, G. DEN BOEF AND G. J. VAN ROSSUM, *Anal. Chim. Acta*, 58 (1972) 429.

Analytica Chimica Acta
Elsevier Publishing Company, Amsterdam
Printed in The Netherlands

STUDIES ON THE CHEMISTRY OF THE DETERMINATION OF BORON WITH CURCUMIN

DAVID W. DYRSSEN, YURI P. NOVIKOV* and LEIF R. UPPSTRÖM
Department of Analytical Chemistry, University of Gothenburg, Fack, S-402 20 Göteborg 5 (Sweden)
(Received 24th January 1972)

Curcumin is the most sensitive and reliable reagent for the determination of small quantities of boric acid and in recent years the analytical procedure with curcumin has been considerably simplified[1-3]. Present knowledge of the chemical properties of the reagent and its complexes with boric acid is, however, still unsatisfactory, and statements in the literature are somewhat contradictory[4-9]. The analyst is often confused by the fact that two different species, one called rubrocurcumin and another called rosocyanin are used for the determinations, but both procedures are in the literature referred to as "the Curcumin Method". Rubrocurcumin is formed by the reaction between boric acid, curcumin and oxalic acid in a 1:1:1-complex; the structure has been discussed by Spicer and Strickland[4], by Bellamy *et al.*[5] and later by Roth and Miller[6]. The formation of rosocyanin by the reaction between boric acid and curcumin in the presence of strong sulphuric acid is for different reasons the superior method in analytical procedures, *e.g.* the molar absorptivity is about twice that for rubrocurcumin and it has also a higher stability toward hydrolysis. The ratio boric acid : curcumin has been stated[4,6,7] to be 1:2, but a 1:3 ratio has also been suggested[8].

In an early work Korenman[9] had the opinion that rosocyanin was a 1:1 complex. Recently, Umland and Pottkamp[10] state that the 1:2 complex can only be formed from heated samples in the solid state obtained through precipitation or evaporation. In solution they only observed the 1:1 complex formation.

In this paper we wish to report studies on the stability of the reagent in the sulphuric acid–acetic acid medium both in the presence and absence of boric acid, as well as investigations of the following equilibria in aqueous–ethanolic media (curcumin is denoted $RCOCH_2COR$ or H_3A, where R is the $C_6H_3(OH)(CH_3O)CH{=}CH-$ radical of the substituted β-diketone):

$$H_3A \rightleftharpoons H^+ + H_2A^- \quad (1)$$

$$B(H_2A)_2^+ \rightleftharpoons H^+ + B(H_2A)(HA) \quad (2)$$

$$B(H_2A)_2^+ + Cl^- \rightleftharpoons B(H_2A)_2^+Cl^- \text{ (chloroform)} \quad (3)$$

$$B(H_2A)(HA) \rightleftharpoons B(H_2A)(HA) \text{ (chloroform)} \quad (4)$$

Rosocyanin can be isolated as a salt, usually from some sulphuric acid medium, and may be denoted as $B(H_2A)_2^+HSO_4^-$. In the sulphuric acid–acetic acid medium curcumin is mainly in the protonated form H_4A^+. The equilibrium $H_4A^+ \rightleftharpoons H^+ + H_3A$ has not been studied in the present work, nor has the deprotonation of the

* Present address: Vernadsky Institute of Geochemistry and Analytical Chemistry, Moscow, U.S.S.R.

phenolic groups at higher pH whereby HA^{2-} and A^{3-} may be formed; β-diketones generally decompose in alkaline solutions.

EXPERIMENTAL

Reagents

Curcumin solution. Curcumin (British Drug Houses Ltd), 10^{-4} *M* in glacial acetic acid.

Boric acid solution. Boric acid (Merck suprapur), 10^{-4} *M* in glacial acetic acid.

Sulphuric acid–acetic acid reagent. One volume of sulphuric acid (s.g. 1.84) was mixed with three volumes of glacial acetic acid. Both chemicals were of Merck reagent grade.

Rosocyanin. The different rosocyanin solutions were made from rosocyanin synthesized by the method of Spicer and Strickland[11], dissolved in ethanol or glacial acetic acid.

Acetate buffer solution was made by mixing 90 ml of ethanol (96%), 180 g of ammonium acetate, and 135 ml of glacial acetic acid; the final volume was made up to 1 l with redistilled water.

Buffer solutions for the determination of the acid dissociation constants were made by mixing KH_2PO_4, H_3PO_4, NaCl and NaOH in required amounts keeping the ionic strength at 0.1 *M*.

The spectra were obtained by a Beckman DB at a temperature of $23 \pm 1°$. The pH was measured by a Radiometer pH 25. The calculations were performed by an Hewlett-Packard 2114 B minicomputer.

EXPERIMENTS IN SULPHURIC ACID–ACETIC ACID MEDIUM

Decay of protonated curcumin

To 0.5 ml of a solution of 10^{-4} *M* curcumin in acetic acid, 6 ml of the sulphuric–acetic acid reagent were added and the volume was made up to 16 ml with glacial acetic acid. The absorbance was measured at different time intervals and the data treatment was based on a work by Wilkinson[12]. If the decomposition of the protonated curcumin is investigated with the assumption that the decay is proportional to some degree n of its own concentration c the rate law can be written

$$-\mathrm{d}c/\mathrm{d}t = kc^n \tag{5}$$

which in integrated form

$$\int_{c_0}^{c} \mathrm{d}c/c^n = k \int_0^t \mathrm{d}t \tag{6}$$

yields the general solution for $n \neq 1$

$$\frac{1}{n-1}\left(\frac{1}{c^{n-1}} - \frac{1}{c_0^{n-1}}\right) = kt \tag{7}$$

If $p = (c_0 - c)/c_0 = 1 - c/c_0$ where p is the fraction which has reacted at time t and $K = kc_0^{n-1}$, for convenience eqn. (7) can be transformed to

$$(1-p)^{1-n} = Kt(n-1) + 1 \tag{8}$$

Development according to the binomial theorem and rejection of powers of p higher than 2 gives eqn. (8) as:

$$\frac{t}{p} = \frac{1}{K} + \frac{np}{2K} \tag{9}$$

As finally p/K can be set approximately equal to t we get

$$\frac{t}{p} = \frac{1}{K} + \frac{nt}{2} \tag{10}$$

By plotting t/p-data against t in a diagram we obtain, if the approximations hold, a straight line with a slope of $n/2$ and an intercept of $1/K$. As soon as n is determined, an approximate value of k can be calculated. The result of this experiment is shown in Fig. 1. The slope was found to be 1.03, that is, the rate can be looked upon as second order. The k_2-value was found to be 0.0805 $M^{-1}h^{-1}$. Introducing $n=2$ in eqn. (7)

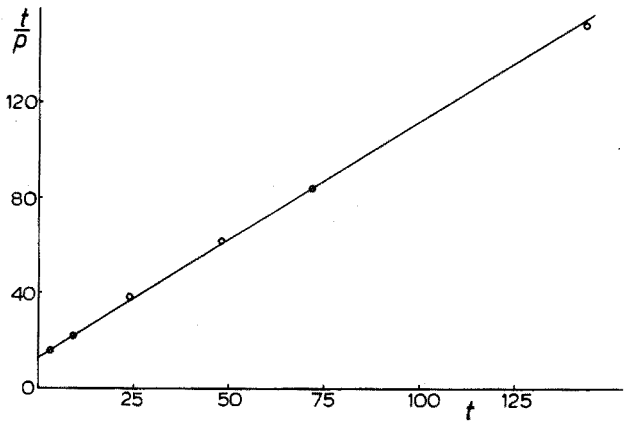

Fig. 1. Plot according to eqn. (10) for the determination of the reaction order of the decomposition of protonated curcumin.

we get

$$\frac{1}{c} - \frac{1}{c_0} = k_2 t \tag{11}$$

A plot of $1/c$ against t gives a straight line and a k_2-value of 0.10 $M^{-1}h^{-1}$. The decomposition of the protonated curcumin thus follows the law

$$-\mathrm{d}[H_4A^+]/\mathrm{d}t = k_2[H_4A^+]^2 \tag{12}$$

Inhibition of the decay by boric acid

A series of seven solutions was prepared to contain 0.0, 0.1, 0.2, 0.3, 0.4, 0.5, 0.6 ml of 10^{-4} M boric acid and 9.6, 9.5, 9.4, 9.3, 9.2, 9.1, 9.0 ml of glacial acetic acid, respectively; to each were added 0.4 ml of 10^{-4} M curcumin and 6.0 ml of sulphuric–acetic acid mixture. The blank solution (0.0 ml of boric acid) is denoted as a in Figs. 2–4, and the strongest solution (0.6 ml of boric acid) as b. The absorbances were measured at different times: 5 min, 3, 9, 24, 48, 72, 144, and 216 h. The results are illustrated by the

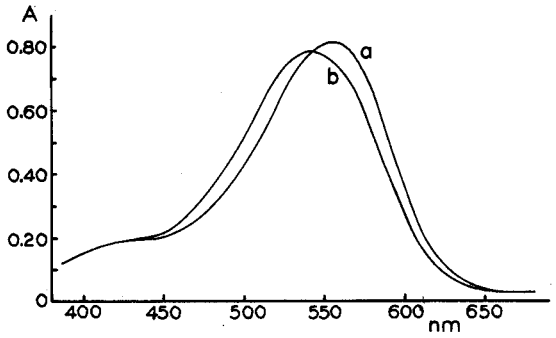

Fig. 2. Absorbance curves of the curcumin solutions containing no boric acid (a) and with the highest concentration of boric acid (b) 5 min after the preparation of the samples. In the absorbance curves of intermediate boric acid concentrations (not shown in the Figure) the maximum is shifted toward lower wavelength and the maximum is lowered as the boric acid concentration increases. All the curves are situated between a and b.

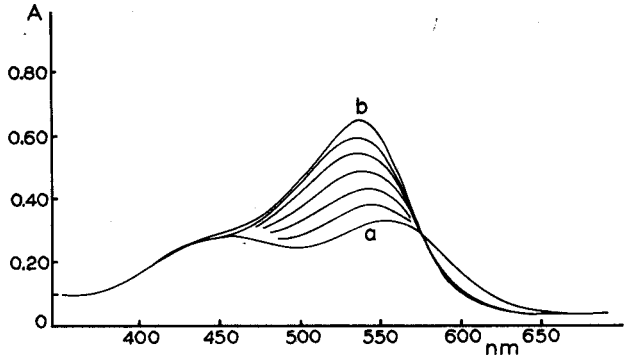

Fig. 3. Absorbance curves of the solutions after 24 h at 23°. The boric acid inhibits the decomposition of the protonated curcumin almost proportionally to the boric acid concentration.

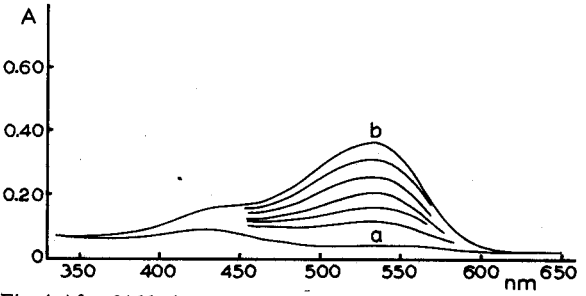

Fig. 4. After 216 h the protonated curcumin without boric acid present (curve a) is completely decomposed whereas the boric acid-containing solutions still have maxima proportional to their concentrations.

spectra in Figs. 2–4. The 5-min spectra show that the solution with no boric acid (Fig. 2, curve a) has a higher absorbance than the solutions containing boric acid and the solution with the highest concentration of boric acid has the lowest value of absorbance (Fig. 2, curve b). Furthermore, the maximum of absorption is moved toward shorter wavelength for higher boric acid concentrations. In the next spectra (Fig. 3) the picture is changed. The decomposition of the zero solution is faster and one can now see that the solution with the highest concentration of boric acid (curve b) has the highest absorbance followed by the next highest, etc. The absorbance values of the boric acid-containing solutions are also almost directly proportional to the boric acid concentrations. The boric acid inhibits strongly the decomposition of the protonated curcumin by a complex formation, but the complexes formed decompose slowly themselves. After 216 h, practically all H_4A^+ has been decomposed in the absence of boric acid (Fig. 4, curve a); the boric acid solutions however, still have an absorbance between 0.12–0.37.

Determination of the complex formed

If an acetate buffer solution is added to the strongly acidic solutions of curcumin and boric acid so that the pH is changed to around 4, the curcumin–proton complex disappears but the boric acid–curcumin complex remains and its decomposition practically stops. This neutralisation procedure has been used in the determination of boron[1,3,13]. Through elimination of the proton complex in this way for a series of solutions with varying curcumin concentrations and a constant amount of boric acid, the composition of the complex can be determined by spectrophotometric measurements.

Briefly, the procedure was performed in the following way. To solutions with constant amounts of concentrated sulphuric acid (0.5 ml) and boric acid (0.3 ml of 10^{-4} *M*) were added different amounts of a curcumin solution (0.1–0.9 ml of 10^{-4} *M*) and all solutions were then brought to the same final volume (16 ml) with glacial acetic acid. After a reaction time of 1 h in order to establish equilibrium conditions, the acetate buffer solution was added to eliminate the interfering colour of H_4A^+. The absorbance of the boric acid–curcumin complex was measured at 540 nm. The calculations used are based on the following equation:

$$K_n = \frac{A/\varepsilon}{(C_M - A/\varepsilon)(C_L - nA/\varepsilon)^n} \tag{13}$$

where

A = measured absorbance with 1-cm cuvettes,
ε = molar absorptivity for the boric acid complex with n curcumin,
$C_M = 0.3 \cdot 10^{-4}/16$ = total concentration of boric acid,
$C_L = v \cdot 10^{-4}/16$ = total concentration of curcumin.

This is based on the following equilibria in the sulphuric acid–acetic acid mixture:

$$B(OH)_3 + nH_4A^+ \rightleftharpoons B(OH)_xA_nH_y^{N+} + (3-x)H_2O + (4n-y-3+x)H^+ \tag{14}$$

where the charge $N+ = 3-x-3n+y$.

As the constant concentrations of water and H^+ in the mixture are not determined, the complex formation constant is expressed as

$$K_n = \frac{[B(OH)_xA_nH_y]}{[B(OH)_3][H_4A^+]^n} \quad (15)$$

and the total concentrations of boric acid and curcumin as

$$C_M = [B(OH)_3] + [B(OH)_xA_nH_y] \quad (16)$$

$$C_L = [H_4A^+] + n[B(OH)_xA_nH_y] \quad (17)$$

The most likely complexes are

$B(OH)H_2A^+$ or $B(OH)_2H_2A$ with $n=1$, $y=2$, and $x=1$ or 2

and

$B(H_2A)_2^+$ or $B(HA)(H_2A)$ with $n=2$, $x=0$, and $y=4$ or 3.

From the value $\varepsilon = 180{,}000$ which has been reported by several authors[8,14,15], K_1 and K_2 were calculated from eqn. (13). The results are shown in Table I. Although the precision decreases with increasing n, it is obvious that K_2 is rather independent of v, while K_1 increases steadily. This strongly supports the formation of the 1:2 complex. The mean value of K_2 is $2.8 \cdot 10^{11}$ while the mean value with reasonable weighting is $3.0 \cdot 10^{11}$. This constant K_2 can be used to calculate the suitable excess of curcumin for the analysis of boron.

TABLE I

THE MEASURED ABSORBANCE AT 540 nm AS A FUNCTION OF v ml CURCUMIN SOLUTION AND CALCULATED VALUES OF K_1 AND K_2 (eqn. 13) WITH $\varepsilon = 180{,}000$

A	v	$K_1 \cdot 10^{-5}$	$K_2 \cdot 10^{-11}$	*Approx. weight*
0.012	0.1	0.66	1.52	1
0.038	0.2	1.22	1.85	2
0.086	0.3	2.45	4.04	4
0.111	0.4	2.60	3.05	6
0.148	0.5	3.39	3.56	8
0.174	0.6	3.82	3.22	10
0.191	0.7	3.93	2.57	9
0.222	0.8	5.10	2.99	8
0.237	0.9	5.47	2.63	7

Precipitation of the complex formed

If water or a slightly basic aqueous solution is added to a solution containing the above-mentioned complex in acidic solution, the complex precipitates. After rinsing with water and ether a dark green powder with metallic lustre is obtained. It was found to be identical with rosocyanin prepared as described by Spicer and Strickland[11]. Furthermore, the precipitate found after the addition of water to the reaction solution in the boron determination method of Uppström[1] had the same quality. The colour of the salt and its solutions in alcohol and acetic acid, the solubility in alcohol, the spectra of the solutions and the speed of decomposition in different solutions were all identical with the rosocyanin results. Molar absorptivities calculat-

ed from calibration curves according to Uppström[1] show the same high values ($\varepsilon =$ 180,000 mole^{-1} cm^{-1}) as were obtained by Spicer and Strickland[15] in their method where the reactants are evaporated to dryness, and by Hayes and Metcalfe[8]. The conclusion is that a 1:2 boric acid–curcumin complex is formed in the solutions investigated and it is highly probable that the complex is rosocyanin.

Final results

The following formulae conclude the results obtained in the acidic medium (H_3A = curcumin).

$$H_3A + H^+ \rightleftharpoons H_4A^+ \tag{18}$$

$$2H_4A^+ \xrightarrow[\text{second order}]{k_2} \text{decomposition products} \tag{19}$$

$$2H_4A^+ + B(OH)_3 \rightleftharpoons B(H_2A)_2^+ + 3H_2O + H^+ \tag{20}$$

The equilibrium (18) is in highly acidic solutions moved far to the right, whereas the amount of $B(H_2A)_2^+$ found in the same medium depends on the concentrations of curcumin and boric acid according to the value of K_2 reported above. The acidic medium creates a reactive form of curcumin, but counteracts the formation of the boron complex according to equilibrium (20), which also explains the necessity of water exclusion and excess of curcumin in the analytical methods. On neutralization of the sulphuric acid–acetic acid medium, the conditions for the establishment of equilibrium (20) cease and the amount of $B(H_2A)_2^+$ formed is obviously stable (inert) in the acetate buffer. The red H_4A^+, on the contrary, is rapidly deprotonized to H_3A, the yellow colour of which does not interfere with the determination of the red $B(H_2A)_2^+$. On addition of water the solubility product of the ion-pair between the boron–curcumin complex and the hydrogensulphate ion is exceeded and it precipitates. Thus the water prevents the formation of the rosocyanin complex, but the latter, once formed, is not easily hydrolyzed. The ethanol used in the acetate buffer solution keeps the complex in solution.

EXPERIMENTS IN AQUEOUS ETHANOLIC MEDIA

The acid dissociation constant of curcumin

The spectra at different pH values for a 10^{-5} M curcumin solution in a 1:1

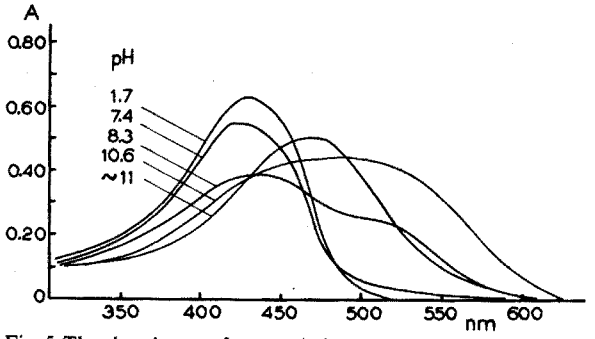

Fig. 5. The absorbance of curcumin in a 1:1 water–ethanol solution measured at different pH values.

ethanol–water solution are shown in Fig. 5. The shifts indicate that several acid–base equilibria must be involved. Starting with the neutral form (H_3A) we have a maximum at 430 nm for a pH of 3–7. When more acid is added a maximum forms at 555 nm (see Fig. 2) and an isosbestic point at 470 nm. If, instead, alkali is added to the neutral solution, another maximum appears at about 520 nm. Owing to decomposition, the isosbestic point in the vicinity of 470 nm, is not very pronounced. Further addition of alkali shifts the maximum to shorter wavelength, *ca.* 480 nm, the curcumin being quite unstable. Addition of acid to a solution of pH 12 does not reverse the last reaction. The behaviour of curcumin at different pH stages can be summarized as follows:

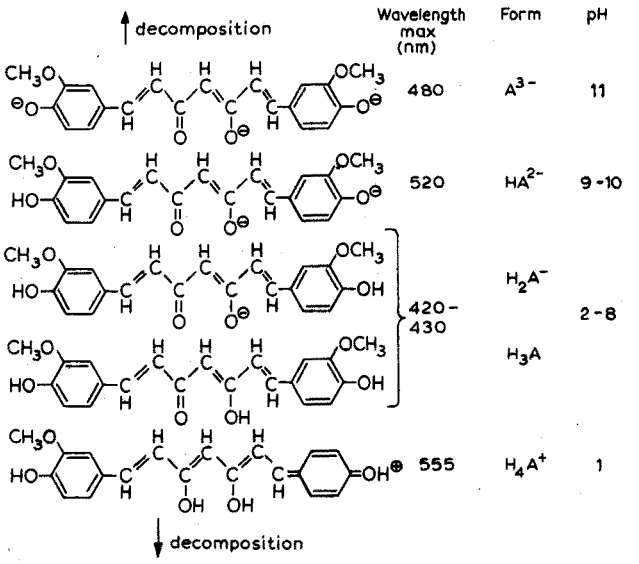

For analytical purposes there is an interest in extraction of the rosocyanin complex formed as described previously, and its separation from the excess of curcumin. Therefore it is necessary to have an accurate knowledge of the composition of the solution at a certain pH interval which in this case is where the equilibrium $H_3A \rightleftharpoons H_2A^- + H^+$ predominates. The pK_a value was determined in the following way. To a volume of $2 \cdot 10^{-5}$ *M* curcumin in 96% ethanol solution an equal volume of a 0.1 *M* buffer solution was added and after equilibration for 5 min a spectrum was obtained at 425 nm and the pH measured. The absorbance was plotted against pH (corrected to aqueous solution) in the interval pH 5–8.5. The absorbance A_{425} could be regarded as the sum of the absorbance contributions from both H_3A and H_2A^-:

$$A = a_{H_3A}[H_3A] + a_{H_2A^-}[H_2A^-] \tag{21}$$

the total concentration was:

$$C = [H_3A] + [H_2A^-] \tag{22}$$

and

$$K_a = [H^+][H_2A^-]/[H_3A] \tag{23}$$

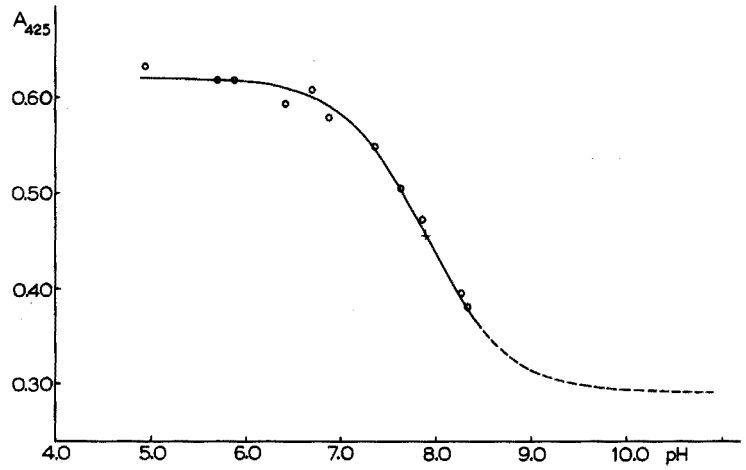

Fig. 6. The absorbance at 425 nm of curcumin in a 1:1 water–ethanol solution plotted against pH. The curve fitted to the points was calculated as described in the text.

From these equations we get the expression

$$A(K_a/[H^+]+1) = Ca_{H_3A} + Ca_{H_2A^-}(K_a/[H^+]) \quad (24)$$

The value of K_a was calculated in the following way. First an approximate value of a_{H_3A} was obtained from A/C at pH 5. If then K_a is guessed to a first approximation from the experimental results, $Ca_{H_2A^-}$ could be found as the slope when $A(K_a/[H^+]+1)$ is plotted against $K_a/[H^+]$.

With the experimental value of Ca_{H_3A} and by varying the experimental value of $Ca_{H_2A^-}$ $\pm 30\%$, values for pK_a were found to be in the range 7.93 ± 0.05. With the mean value of pK_a and the value of Ca_{H_3A}, a multitude of curves were generated by a minicomputer with different values of $Ca_{H_2A^-}$. The experimental points were then fitted to the best curve, which is shown in Fig. 6. From this fit the value of pK_a was found to be 7.9. It should be observed that the pH values were only approximately corrected to aqueous phase conditions by standardizing the pH meter in phosphate buffers with and without 50% ethanol.

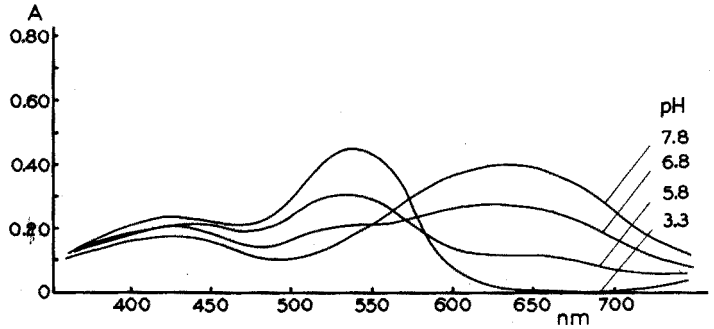

Fig. 7. Absorbance curves of rosocyanin dissolved in a 1:1 water–ethanol solution obtained at different pH values.

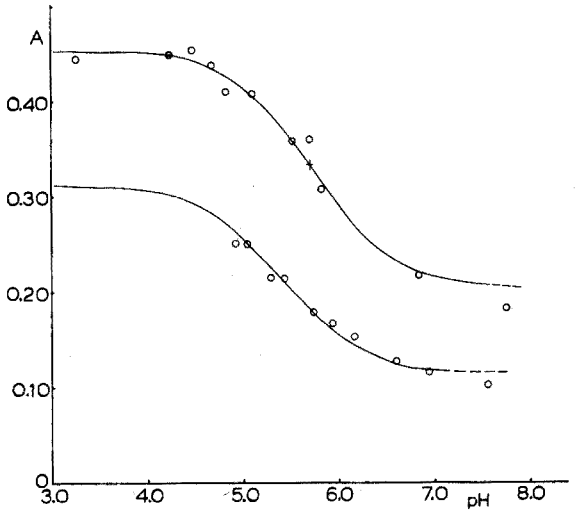

Fig. 8. The absorbance at 550 nm of rosocyanin in a 1:1 water–ethanol solution (upper curve) and in chloroform (lower curve) plotted against pH. The curves fitted to the points were calculated as described for curcumin in the text.

The acid dissociation constant of rosocyanin

Spectra for rosocyanin in water–ethanol solutions at different pH values are given in Fig. 7. The acidic form $B(H_2A)_2^+$ has its maximum at 540 nm. In more alkaline solution a maximum is found at 630 nm. According to Spicer and Strickland[11] this maximum is reached through a two-stage neutralization step with the following approximate K_a values: $K_{a_1} \approx 3 \cdot 10^{-7}$, $K_{a_2} \approx 2 \cdot 10^{-8}$. In quite alkaline solutions a maximum was found at about 685 nm which they ascribed to the simultaneous loss of the phenolic hydrogens with $K_{a_{3,4}} \approx 5 \cdot 10^{-10}$. A′ curve (Fig. 8) was now obtained for the pH range 3–8 in the same way as for curcumin. Rosocyanin solutions (10^{-5} *M*) in ethanol were mixed with equal volumes of buffer solutions and the absorbance values at 550 nm were plotted against the pH values. No two-stage reaction could be observed. The curve fitted to the points was calculated in the same way as for curcumin. Because of the decomposition, less weight was given to the final point on the alkaline side. Curves generated on the assumption that two protons are dissociated in the pH interval 3–8 do not at all fit the experimental points. The acid dissociation constant determined from our curve is $K_a = 10^{-5.7}$ corrected to aqueous solution. The observed colour changes, crimson red → purple and blue → green, on which Spicer and Strickland[11] based their calculations, were probably partly influenced by the decomposition of rosocyanin whereby yellow curcumin was formed in the solution. If an alkaline blue-green solution of rosocyanin is treated with chloroform a blue compound remains in the aqueous phase whereas a yellow compound is extracted into the organic phase. Spicer and Strickland[11] have themselves confirmed the findings by Clarke and Jackson[16] that curcumin is the main product when rosocyanin solutions are hydrolyzed in the presence of water.

Extraction of rosocyanin with chloroform

To solutions (5 ml) of 10^{-5} *M* rosocyanin in ethanol were added 5 ml buffer solutions of different pH in the region 5–8 and 10 ml of chloroform. After equilibration

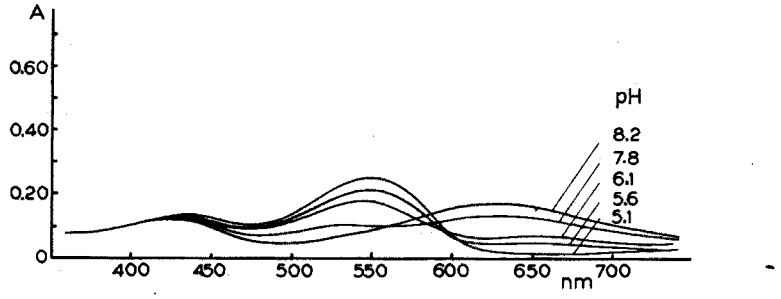

Fig. 9. Absorbance curves of rosocyanin in chloroform obtained at different pH values. Comparison with the curves in Fig. 7 shows the same general picture although the absorbance is lower in chloroform.

and centrifugation, spectra were obtained from the organic solutions (Fig. 9); the aqueous phase was colourless. The acid form of rosocyanin, which is probably extracted as an ion pair with chloride, $B(H_2A)_2^+Cl^-$, dissolves just as well in chloroform as the neutral form, $B(H_2A)(HA)$. This can be seen from Fig. 8 even if the molar absorptivities are lower in chloroform. If the neutral form were considerably more soluble in chloroform than the ion-pair, then the two sigmoid curves would be in separate pH regions. This indicates that the charge of $B(H_2A)_2^+$ is delocalized over the entire molecule.

CONSEQUENCES FOR THE ANALYSIS OF BORON

Water elimination in analytical procedures

It has been shown that water prohibits the formation of the reaction product rosocyanin and it is clear that water elimination is an important part of the determination process. Evaporation, distillation and extraction processes are generally tedious and it is obvious that direct methods are much more convenient especially if the procedure should be automated[3]. In the method of Uppström[1] propionic anhydride catalyzed by oxalyl chloride is used for direct elimination of water. It was found that propionic anhydride should not be added in excess because of its preferred reaction with the protonated curcumin, probably with the hydroxyl groups. This requirement is fulfilled in the procedures recommended for aqueous solutions in the work mentioned. Should the sample contain a high amount of salt or be low in water, one has to observe the necessary decrease of the amount of anhydride. As a rule of thumb: do not add a larger volume of propionic anhydride than 7 times the estimated volume of the water in the sample.

The decay of the protonated curcumin

The relatively fast decomposition of the protonated curcumin shows that longer reaction times are of no advantage. In the previous work[3], it was found that for a reaction temperature of 40° the maximal gain was reached in 12 min. The decay of the protonated curcumin could, of course, be applied for a kinetic determination of the boric acid content in a sample solution, based on the fact that boric acid inhibits the decomposition. It is, however, doubtful if such a method can compete with the usual spectrophotometric procedures.

Extraction processes

Methods for the extraction of the rosocyanin followed by spectrophotometric determination have previously been described by some authors[1,7]. Those procedures allow determinations in the nanogram range. Curcumin and rosocyanin are not easily separated and there is little advantage to such a separation for a spectrophotometric analysis. Very small amounts of boric acid can be extracted and concentrated by simple diols like 2,2-diethyl-1,3-hexanediol[17] and determined directly in the organic phase or transferred to an aqueous phase before applying the analytical method described.

This investigation was supported by the Swedish Natural Science Research Council and Knut and Alice Wallenbergs Foundation which we gratefully acknowledge. Thanks are also due to Dr. Louis Henderson, who revised the English text of this paper. Dr. Yuri Novikov's visit was arranged according to the agreement on exchange of scientists between the Royal Swedish Academy of Sciences, the Royal Swedish Academy of Engineering Sciences and the Academy of Sciences of the USSR.

SUMMARY

The stability of the reagent curcumin (H_3A) in sulphuric acid–acetic acid medium both in the presence and absence of boric acid has been studied. Kinetic measurements show that protonated curcumin decomposes according to a second-order rate law. The decomposition is inhibited by the addition of boric acid which forms a complex with curcumin. This complex has a much slower decay rate. The complex was analyzed and found to be a 1:2 boric acid–curcumin compound. The chemical behaviour as well as the physical data are in good agreement with results from the investigation of rosocyanin synthesized as described by Spicer and Strickland. The necessity of water removal and the use of curcumin in excess in the analytical procedures is explained. The acid dissociation constant of curcumin in water–ethanol solution has been determined and $K_a = ([H^+][H_2A^-])/[H_3A] = 10^{-7.9}$. For rosocyanin, $B(H_2A)_2^+$, the acid dissociation constant for the equilibrium $B(H_2A)_2^+ \rightleftharpoons H^+ + B(H_2A)(HA)$ was found to be $10^{-5.7}$ in the same medium. From two-phase experiments with chloroform, rosocyanin in the form of an ion-pair with chloride was found to dissolve in the organic phase just as well as the neutral form. The consequences of the results for analytical purposes are discussed.

RÉSUMÉ

Une étude est effectuée sur la stabilité du réactif curcumine (H_3A), en milieu acide sulfurique–acide acétique, soit en présence, soit en absence d'acide borique. Le comportement chimique, de même que les constantes physiques correspondent bien aux résultats décrits par Spicer et Strickland concernant la rosocyanine synthétique. On examine les conséquences des résultats obtenus pour l'analyse.

ZUSAMMENFASSUNG

Die Beständigkeit des Reagenzes Curcumin (H_3A) in Schwefelsäure–Essigsäure-Medium wurde sowohl in Gegenwart als auch in Abwesenheit von Borsäure

untersucht. Kinetische Messungen zeigen, dass das protonierte Curcumin sich nach einem Geschwindigkeitsgesetz zweiter Ordnung zersetzt. Die Zersetzung wird durch Zusatz von Borsäure gehemmt, die einen Komplex mit Curcumin bildet. Dieser Komplex hat eine viel geringere Zerfallsgeschwindigkeit. Der Komplex wurde analysiert; er enthält Borsäure und Curcumin im Verhältnis 1:2. Das chemische Verhalten und die physikalischen Eigenschaften stimmen gut mit den Ergebnissen der Untersuchung von Rosocyanin überein, das nach der Methode von Spicer und Strickland synthetisiert worden ist. Die Notwendigkeit der Entfernung von Wasser und der Verwendung von überschüssigem Curcumin bei den analytischen Verfahren wird erklärt. Die Säure-Dissoziationskonstante von Curcumin in Wasser–Äthanol-Lösung wurde bestimmt: $K_a = ([H^+][H_2A^-])/[H_3A] = 10^{-7.9}$. Die Säure-Dissoziationskonstante von Rosocyanin, $B(H_2A)_2^+$, für das Gleichgewicht $B(H_2A)_2^+ \rightleftharpoons H^+ + B(H_2A)(HA)$ im selben Medium beträgt $10^{-5.7}$. Aus Zweiphasen-Versuchen mit Chloroform ergab sich, dass sich Rosocyanin in der organischen Phase sowohl in der Form eines Ionenpaars mit Chlorid als auch in der neutralen Form auflöst. Die Folgerungen aus den Ergebnissen in analytischer Hinsicht werden diskutiert.

REFERENCES

1 L. Uppström, *Anal. Chim. Acta*, 43 (1968) 475.
2 F. Umland and A. Janssen, *Z. Anal. Chem.*, 249 (1970) 186.
3 P. Hulthe, L. Uppström and G. Östling, *Anal. Chim. Acta*, 51 (1970) 31.
4 G. S. Spicer and J. D. H. Strickland, *J. Chem. Soc.*, (1952) 4650.
5 L. J. Bellamy, G. S. Spicer and J. D. H. Strickland, *J. Chem. Soc.*, (1952) 4653.
6 H. J. Roth and B. Miller, *Arch. Pharm.*, 297 (1964) 660.
7 D. Thierig and F. Umland, *Z. Anal. Chem.*, 211 (1965) 161.
8 M. R. Hayes and J. Metcalfe, *Analyst*, 87 (1962) 956.
9 I. M. Korenman, *Zh. Anal. Khim.*, 2 (1947) 153.
10 F. Umland and F. Pottkamp, *Z. Anal. Chem.*, 241 (1968) 223.
11 G. S. Spicer and J. D. H. Strickland, *J. Chem. Soc.*, (1952) 4644.
12 R. W. Wilkinson, in A. A. Frost and R. G. Pearsson, *Kinetics and Mechanism*, John Wiley, New York, 1961.
13 R. R. Grinstead and S. Snider, *Analyst*, 92 (1967) 532.
14 F. Umland and D. Thierig, *Z. Anal. Chem.*, 197 (1963) 151.
15 G. S. Spicer and J. D. H. Strickland, *Anal. Chim. Acta*, 18 (1958) 231.
16 L. Clarke and C. L. Jackson, *Amer. Chem. J.*, 39 (1908) 696.
17 D. Dyrssen, L. Uppström and M. Zangen, *Anal. Chim. Acta*, 46 (1969) 55.

Analytica Chimica Acta
Elsevier Publishing Company, Amsterdam
Printed in The Netherlands

A STANDARD ADDITION TITRATION METHOD FOR THE DETERMINATION OF FLUORINE IN SILICATE ROCKS

DANIEL JAGNER
Department of Analytical Chemistry, University of Göteborg, Fack 402 20 *Göteborg* 5 (*Sweden*)

VIOLETA PAVLOVA
Geological Institute, Bulgarian Academy of Science, Sofia (*Bulgaria*)

(Received 24th January 1972)

The determination of fluorine in rocks is normally carried out spectrophotometrically. In order to avoid interference, fluorine is first separated by different variations[1] of the well-established distillation method of Willard and Winter[2] although some recent methods use pyrohydrolysis for this purpose[3-5].

The introduction of the fluoride-selective electrode has made it possible to determine the fluorine content without previous separation. Excess of complexing agent must be added to the sample solution so that the amount of fluoride bound to metal may be neglected. Methods employing fluoride-selective electrodes for rock analysis[6-9], have hitherto been of the "single-point" type, with subsequent evaluation of the fluoride concentration from a calibration curve[9]. Too large an excess of complexing agent may, however, affect the Nernstian behaviour of the electrode, owing to complexation with lanthanum from the electrode membrane[10].

In this paper a standard addition titration, employing the graphical method of evaluation first suggested by Gran[11], is proposed. The procedure exploits several potential measurements for a single fluoride determination, thus yielding results of high precision. Since the method is self-calibrating at the time of analysis, it is applicable in the presence of the slow potential drift caused by the necessarily high concentration of complexing agent. Moreover, errors arising from different ionic strengths in test and calibration solutions are eliminated.

THEORY

If v ml of t M sodium fluoride solution are added to v_0 ml of a solution which is x M in total fluoride, then

$$(v_0+v)([F^-]+[HF])=v_0x+vt \quad (1)$$

provided that the amount of fluoride bound in metal complexes can be neglected. Introducing the stability constant, β_{HF}, for the formation of hydrofluoric acid,

$$(v_0+v)[F^-](1+\beta_{HF}[H^+])=v_0x+vt \quad (2)$$

At constant pH eqn. (2) can be written:

$$F_1=(v_0+v)[F^-]\propto v_0x+vt \quad (3)$$

If F_1, or a value proportional to F_1, is plotted against v ml of titrant added, a straight line will be obtained, which, when extrapolated to $F_1 = 0$, intersects the v-axis at $v = -v_0 x/t$. From the known values of v_0 and t the value of x can then be determined.

A value proportional to F_1 is obtained directly from the potentiometric readings, *e.g.* as

$$F_1 = (v_0 + v)[F^-] \propto (v_0 + v)\, 10 \exp (EF/RT \ln 10) \quad (4)$$

assuming that the electrode follows the Nernst law, *i.e.*

$$E = E^0 + RT \ln 10 \log (f[F^-])/F + E_j \quad (5)$$

and that the activity coefficient, f, and the sum of the liquid junction potentials, E_j,

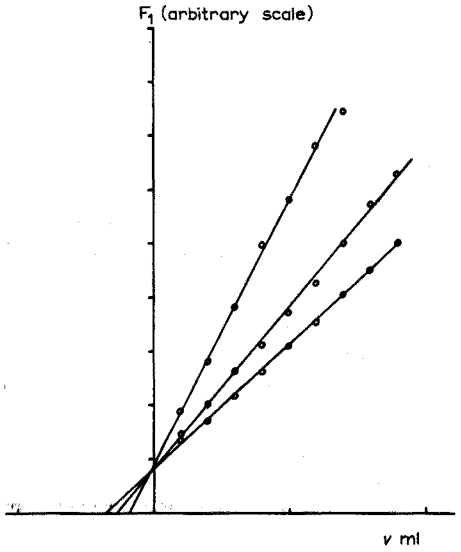

Fig. 1. Example of a determination by the standard addition titration technique (100, 150 and 200 mg of reference sample 1, see Table II). F_1 (eqn. 4) is plotted against v ml of 20 p.p.m. sodium fluoride solution added.

are constant throughout a titration. The evaluation procedure is illustrated in Fig. 1 where F_1 has been plotted on an arbitrary scale for the titrations of 100, 150 and 200 mg of the same silicate rock sample, pretreated by the procedure described below.

EXPERIMENTAL

Equipment

Orion Research Inc. Model 94-09 fluoride electrode and Radiometer K 401 saturated calomel reference electrode were used, with an Orion Research Inc. Digital pH meter Model 501.

Reagents

All reagents were of analytical grade. A stock fluoride solution (1000 p.p.m.)

was prepared by dissolving sodium fluoride, dried at 105°, in doubly distilled water. This solution was diluted to 20 p.p.m. for use as titrant.

The complexing solution was made 0.2 *M* in trisodium citrate and 0.2 *M* in potassium nitrate[9]. This solution was checked for fluoride impurities by the titration procedure described below.

Decomposition of the rock samples

Form each finely ground rock sample, carefully mix 100-, 150- or 200-mg samples with sodium carbonate (0.50, 0.75 or 1.00 g, respectively) and zinc oxide (0.10, 0.15 or 0.20 g, respectively) in 10-ml platinum crucibles, and sinter for 30 min at 900°. After cooling, place the crucibles in 50-ml borosilicate glass beakers. Add 30 ml of distilled water, cover the beakers with watch glasses, and digest the samples for 12 h on a steam bath. The sintered cakes can then easily be broken up. After leaching with 0.1% sodium carbonate solution and filtering, wash the solid residue several times with the carbonate solution and finally discard. Collect the filtrates in 100-ml polyethylene volumetric flasks and add 2 ml of 6 *M* hydrochloric acid to each. Expel carbon dioxide, and adjust the volume to 100 ml.

Potential measurements

To 40 ml of the filtrate solution, add 40 ml of complexing solution, yielding a final pH value of *ca.* 6.5. Make the first potential reading after 5–10 min. The lower the initial fluoride concentration, the longer is the time needed to obtain a steady potential reading. Then add titrant increments of 0.4–4.0 ml of 20 p.p.m. sodium fluoride solution to the titration vessel until a total potential change of 40–60 mV is obtained. Owing to the increase in fluoride concentration, the potential reading corresponding to each increment of titrant can be made after considerably less than 5 min. Evaluate the fluoride concentration according to eqn. (4) and Fig. 1.

Electrode storage

Long exposure to solutions of low fluoride concentrations and high concentrations of complexing agents have been shown to have a fatal effect on the electrode response[10]. If, however, the electrode is stored between successive titrations for at least 5 min in a 4-p.p.m. sodium fluoride solution, it will resume its Nernstian behaviour[10]. The citrate interference with the membrane potential was kept low by making the potential readings as soon as constant values were obtained and by storage of the electrode in sodium fluoride.

RESULTS AND DISCUSSION

The results of the analysis of seventeen different silicate rocks, two of them previously analysed by the Swedish Geological Survey, are shown in Tables I and II.

Loss of fluoride

In order to ensure that no fluorine was lost in the sintering process, three duplicate sets of sodium fluoride, corresponding to sample concentrations of 0.01, 0.05 and 0.07% fluorine, respectively, were mixed with 0.5 g of sodium carbonate and 0.10 g of zinc oxide. Three of these samples were heated at 900° for 30 min while this

TABLE I

ANALYSIS OF ROCKS OF LOW FLUORIDE CONTENT
(Results are given in % by weight)

Sample weight (mg)	*Granite 1*	*Granite 2*	*Rhyolite*	*Perlite 1*	*Perlite 2*	*Latite 1*	*Latite 2*	
100	0.081	0.064	0.024	0.038	0.046	0.064	0.076	
150	0.080	0.060	0.023	0.040	0.043	0.065	0.078	
200	0.081	0.062	0.025	0·040	0.045	0.064	0.079	
	Andesite 1	*Andesite 2*	*Basalt*	*Diabase*	*Tuff*	*Gneiss*	*Muscovite*	*Diorite*
100	0.082	0.045	0.051	0.055	0.014	0.033	0.031	0.040
150	0.084	0.046	0.053	0.053	0.014	0.032	0.031	0.040
200	0.082	0.045	0.051	0.054	0.015	—	—	0.043

procedure was omitted for their corresponding duplicates. All samples were then treated by the complete procedure described above and analysed for fluoride. No loss of fluoride could be shown within the $\pm 0.001\,\%$ level.

Fluoride impurities in the reagents

A mixture of sodium carbonate and zinc oxide was sintered at 900° for 30 min, and then analysed for fluoride by the procedure described above. The intersection of the plot F_1 on the v-axis at $v = 0$ ml showed that the reagents did not contain significant amounts of fluoride impurities and that fluoride was not transferred from the furnace walls to the samples[12]. This result also showed that hydroxyl ions do not contribute to the fluoride electrode membrane potential under the conditions used.

TABLE II

COMPARISON OF RESULTS OBTAINED BY PROPOSED METHOD AND BY PYROHYDROLYSIS METHOD
(Results are given in % by weight)

	Standard addition titration after alkaline treatment	*Calibration curve measurements after pyrohydrolysis*[a]
Reference sample 1 (mg)		
100	0.018	0.016
150	0.018	0.017
200	0.018	—
Reference sample 2 (mg)		
100	0.025	0.022
150	0.025	0.022

[a] Swedish Geological Survey.

Accuracy

After the sample has been decomposed the accuracy of the method relies mainly on:

(*a*) the electrode couple obeying Nernst's law and the choice of a relevant sample temperature (*cf.* eqn. 4);

(*b*) the amount of metal–fluoride complexes in the titration vessel being negligible in comparison with the amount of fluoride and hydrofluoric acid; and

(*c*) an accurate knowledge of the fluoride concentration of the titrant.

In order to compare the suggested analytical procedure with the results obtained by another laboratory, two samples, previously analysed by the Swedish Geological Survey (SGU), were analysed. The SGU samples had been analysed, after pyrohydrolysis, by means of a fluoride electrode and a calibration curve. The results are shown in Table II. The difference is probably mainly due to the difference in decomposition techniques of the samples.

Precision

The precision can be assessed from the results shown in Table I. Increased precision might be obtainable by including more titration points and by evaluating the experimental data by means of a suitable computer program (see *e.g.* Anfält and Jagner[13]). A straight line regression calculation of the data (*e.g.* in Fig. 1) would result in a third figure in Table I. The method described here has, however, been designed for laboratories which do not have access to computer techniques[14]. It seems very probable, moreover, that both the accuracy and the precision are largely determined by the efficiency of decomposition. The chemical meaning of a third figure in the analysis of minerals of low fluoride content is therefore rather questionable.

CONCLUSIONS

The main advantages of the suggested method are as follows. It is associated with a higher precision than the other known potentiometric methods for analysis of rocks, owing to the exploitation of a large number of independent potential measurements for each fluoride determination. The method is self-calibrating at the time of analysis which eliminates errors arising from the potential drift caused by the high concentration of complexing agent. Errors associated with separate calibration, *e.g.* caused by different ionic strengths or temperatures in test and calibration solutions, are eliminated.

No separate determination of E^0 for the electrode couple at the relevant ionic composition is necessary. The Nernstian behaviour of the electrode is checked in each determination: if the plot F_1 is not linear the results must be discarded.

The results can be evaluated either graphically, as in Fig. 1, or according to a least-squares refinement procedure, preferably with a computer.

The authors wish to express their gratitude to Professors David Dyrssen and Donald Johnson for valuable discussions and to Dr. Bengt Rönnholm, Swedish Geological Survey, for providing the rock samples.

SUMMARY

Silicate minerals have been analysed for fluoride, after decomposition with sodium carbonate and zinc oxide, by a standard addition titration technique. The main advantages of the method are its precision and the elimination of errors arising from separate preliminary calibration.

RÉSUMÉ

Le dosage des fluorures dans les silicates a pu être effectué par une méthode de titrage avec addition d'étalon, après décomposition de l'échantillon au moyen de carbonate de sodium et d'oxyde de zinc. Les principaux avantages de cette méthode sont sa précision et l'élimination d'erreurs provenant d'une séparation préliminaire.

ZUSAMMENFASSUNG

Fluorid in Silicatmineralen wurde nach Zersetzung mit Natriumcarbonat und Zinkoxid nach einem Standard-Zumischverfahren bestimmt. Die wesentlichen Vorteile der Methode sind Genauigkeit und die Ausschaltung von Fehlern, die durch eine gesonderte vorausgehende Eichung entstehen.

REFERENCES

1 W. H. Ewans and G. A. Sergeant, *Analyst*, 92 (1967) 690.
2 H. H. Willard and O. B. Winter, *Ind. Eng. Chem., Anal. Ed.*, 5 (1933) 7.
3 W. Bloxan, *Chem. Geol.*, 3 (1968) 23.
4 D. Weiss, *Chem. Listy*, 63 (1969) 1152.
5 R. L. Clements, G. A. Sergeant and P. J. Webb, *Analyst*, 96 (1971) 51.
6 J. L. Guth, *Bull. Soc. Fr. Mineral. Crystallogr.*, 92 (1969) 105.
7 C. R. Edmond, *Bull. Aust. Min. Dev. Lab.*, 7 (1969) 1.
8 C. R. Edmond, *Anal. Chem.*, 41 (1969) 1327.
9 B. L. Ingram, *Anal. Chem.*, 42 (1970) 1825.
10 T. Anfält and D. Jagner, *Anal. Chim. Acta*, 50 (1970) 23.
11 G. Gran, *Analyst*, 77 (1952) 661.
12 H. Nommik, *Acta Polytech. (Stockholm)*, (1953) 127.
13 T. Anfält and D. Jagner, *Anal. Chim. Acta*, 53 (1971) 13.
14 D. Jagner, *A Computer Treatment of Theoretical and Practical Aspects of Titration Procedures*, Abstracts of Gothenburg Dissertations in Science 25, Almqvist and Wiksell, Stockholm, 1971.

Analytica Chimica Acta
Elsevier Publishing Company, Amsterdam
Printed in The Netherlands

DETERMINATION OF NANOGRAM AMOUNTS OF BISMUTH IN ROCKS BY SUBSTOICHIOMETRIC ISOTOPE DILUTION ANALYSIS

L. PAUL GREENLAND and E. Y. CAMPBELL
U.S. Geological Survey, Washington, D.C. 20242 (*U.S.A.*)
(Received 8th October 1971)

Studies of the geochemistry of bismuth require a rapid, efficient technique applicable to the determination of 1–10 ng of bismuth in many samples of silicate rocks. The abundance of bismuth usually found in rocks is too low to be determined by common spectrophotometric, atomic absorption and spectrographic methods. Spectrographic methods[1] with ion-exchange preconcentration require large samples and have questionable accuracy and sensitivity. Neutron activation methods[2,3] have the requisite sensitivity, but require β-counting and extensive radiochemical separations, hence are not amenable to the analysis of large numbers of samples. The present paper describes a substoichiometric isotope dilution method, which can be routinely applied to determine the low concentrations of bismuth found in silicate rocks.

In recent years the principles of substoichiometric isotope dilution analysis have become well known and many analytical methods have been developed[4–7]. In brief, the method consists of reacting a known substoichiometric amount of a complexing agent with the analysis element which has been labelled with a radioactive isotope. After separation of the unreacted element by solvent extraction or ion exchange, the specific activity of the complexed fraction can be determined by counting the radioisotope and thus the abundance of the element in the original sample can be calculated. Although this method is capable of sensitivities in the nanogram range for many elements, most applications to practical analyses have been in the microgram region[8–10].

Briscoe and Dodson[11] have discussed the theory of complexing with a substoichiometric amount of EDTA followed by solvent extraction of a weaker complex of the excess element. The high stability constant of the bismuth–EDTA complex and the ready extractability of bismuth iodide suggested the use of this method for the determination of bismuth in rocks. Very recently Stary *et al.*[12] described an isotopic exchange reaction for the determination of bismuth; however, the substoichiometric method has several advantages: (*a*) greater selectivity, (*b*) two or more determinations can be made on a single solution, (*c*) only one phase need be counted.

EXPERIMENTAL

Reagents

Standard bismuth solution. Dissolve about 1 g of metallic bismuth in 50 ml

of (1+9) nitric acid. Dilute to 100 ml in a volumetric flask with (1+9) nitric acid. Determine the exact concentration by EDTA titration of an aliquot with xylenol orange as indicator[13]. Dilute an aliquot with (1+9) nitric acid to a known concentration of about 10 μg Bi ml^{-1}. Prepare more dilute standards just before use by dilution with (1+9) nitric acid.

EDTA solution. Prepare an 0.01 *M* solution by dissolving 0.372 g of disodium ethylenediaminetetraacetate in 100 ml of water. Prepare a dilute stock solution weekly by dilution of this solution to $5 \cdot 10^{-5}$ *M*. Prepare the reagent solution just before use by further dilution to $1 \cdot 10^{-7}$ *M*: 0.1 ml of the reagent solution corresponds to about 2 ng of bismuth.

Iodide solution. 0.1 % (w/v) each of potassium iodide and of hydroxyammonium chloride in water.

Sulfuric acid. Dilute 2 ml of ultra-pure sulfuric acid (J. T. Baker Co.) to 100 ml with water.

Tracer solution. Dilute commercially available ^{207}Bi solution with (1+9) nitric acid so that 0.1 ml yields about 40,000 c.p.m. From our supplier, 0.1 ml contains about 1 ng Bi; adjustment to provide 1 ng Bi may be necessary from other suppliers.

Reagent purification. All reagents except sulfuric acid were reagent grade and used without further purification. Water was singly distilled.

Counting apparatus

A 3 × 3 in. NaI (Tl) detector coupled to a single-channel analyzer was used for counting ^{207}Bi. The window of the analyzer was adjusted to encompass only the 87-keV Bi X-ray.

Procedure

To 100 mg sample (1–10 ng Bi) in a teflon beaker, add 3 ml of 72 % perchloric acid and 10 ml of 40 % hydrofluoric acid. Prepare four standards over the 1–10 ng Bi range with the same acid additions. Add 0.1 ml of tracer to each beaker and also to 5 ml of water in a counting vial as a counting standard. Dissolve the samples and expel acids by overnight evaporation on a steam bath. Dilute the residual perchloric acid solution with 15 ml of water and heat on the steam bath to obtain a clear solution. Cool to room temperature and add 1 ml of 1 % (w/v) hydroxyammonium chloride to reduce iron(III). Add 5 ml of iodide solution and extract in a separatory funnel with 20 ml of methyl isobutyl ketone (MIBK). Discard the aqueous phase and wash the organic phase with 5 ml of the diluted sulfuric acid plus 1 ml of iodide solution. Discard the aqueous phase, and wash the organic phase again with 5 ml of diluted sulfuric acid plus 1 ml of iodide solution. Discard the aqueous phase and add 5 ml of water and 1 ml of iodide solution, shake with the MIBK, and discard the aqueous phase. Add 5 ml of 0.014 *M* nitric acid and 0.10 ml of EDTA reagent to the MIBK. Mix the phases for 5 min to ensure complete reaction of the EDTA and bismuth. Without separating the phases, add 1 ml of the iodide solution and extract the uncomplexed bismuth. Drain the aqueous phase quantitatively to a counting vial for the determination of the specific activity of the bismuth in the EDTA complex. A second determination can be made by repeating the second and third washes of the MIBK, EDTA reaction, and extraction of excess bismuth.

Count the sample vials and counting standard for 2 min. Plot the ratio of the

counting rate of standard to the counting rate of sample, against the known amount of bismuth in the standard samples and determine the amount of bismuth in the unknowns by reference to this calibration curve.

RESULTS AND DISCUSSION

Substoichiometric determination of bismuth

This determination of bismuth is based on its reaction with a known substoichiometric amount of EDTA followed by the separation of the excess of bismuth. The way in which this reaction leads to the determination of bismuth is shown by the following considerations. After decomposition of the samples, the specific activity of the solutions is $A/(m+m_b)$, where A is the counting rate of the tracer aliquot, and m and m_b are the mass of bismuth in the sample and in the reagents (including tracer) respectively. This ratio is not altered by losses in the chemical separations because a proportionate amount of radio-bismuth is always lost with the inactive bismuth. Similarly, the bismuth reacting with the EDTA has the original specific activity and thus, after extraction of the excess bismuth, $A/(m+m_b) = a/(m_c)$ where a is the counting rate of the aqueous phase and m_c is the mass of bismuth complexed by EDTA. Therefore, $m=(A/a)m_c-m_b$ and plotting A/a against the known m of the standards yields a calibration curve with an intercept and slope given by the amount of bismuth in the blank and in the EDTA complex, respectively. In practice, the stability of the EDTA is such that little or no variation is found in m_c; the reagent blank, exclusive of the tracer, has varied from 1 to 3 ng of bismuth with different bottles.

Least-squares analysis of data from standard solutions taken through the entire procedure indicates a standard error of estimate of 0.2–0.3 ng bismuth.

More extended discussions of substoichiometric analyses have been given by Ruzicka and Stary[4,5] and of the separation of excess of a metal from its EDTA complex by Briscoe and Dodson[11]. It should be noted, however, that these and most other formulations of the substoichiometric isotope dilution equation differ from the present one in implicitly assuming a known blank. In practical analyses, the reagent blank will vary from run to run, and, therefore, the proposed, more explicit, formulation and the simultaneous analysis of several standards with each batch of samples are preferred.

As discussed above, chemical losses during the purification stages of the procedure do not affect the determination, if they are not so extensive that the amount of EDTA added is no longer substoichiometric. The recoveries usually amounted to 80–90% and were never observed to fall below 70%. With 1 ng of bismuth in the sample, 1 ng in the tracer, and a further 2 ng in the reagents, even a 70% recovery is comfortably above the substoichiometric limit for the amount of EDTA added.

The chemical yield would become important, however, if the reagent blank were distributed over the entire procedure. In such a case the specific activity of the bismuth would change continuously with additions of new inactive bismuth and would depend on losses before new additions; thus the final specific activity of the EDTA fraction would not equal the original sample specific activity as required by the equation given above. However, all of the reagent blank seems to be derived from the tracer solution and the acids used for sample decomposition: therefore the problem does not arise.

The reproducibility of the substoichiometric reaction was tested by reacting EDTA, equivalent to 1 ng of bismuth, with amounts of bismuth varying from 0.2 to 12 ng at constant specific activity. After separation of the excess bismuth, the counting rate of the EDTA phase increased linearly to the stoichiometric equivalence point and remained constant thereafter. The reaction of a constant amount of bismuth (4 ng) with EDTA varying from 0.2 to 8 ng bismuth equivalents was also tested; again the counting rate of the EDTA phase increased linearly to the equivalence point at which all of the activity was retained by the EDTA. These experiments show that a fixed substoichiometric amount of EDTA complexes a fixed amount of bismuth independent of the concentration of bismuth.

The extraction of bismuth iodide with MIBK[14,15] separates bismuth from all the major and minor and most trace elements in rocks. A few trace elements would be expected to accompany bismuth through the separation; the interference of 1 μg each of In, Tl, Pd, Pt, Au, Cd, Pb, Sb and of 10 μg Zn on the determination of 4 ng bismuth was examined. No significant interference was found from any of these elements. The lack of interference from iodide-extractable elements is probably due to the high stability constant of Bi-EDTA (10^{26}, Ruzicka and Stary[5]) and the acidity of the reaction media (pH 1.8 with the washing procedure and volumes given above). Agreement of the present results with neutron activation analyses of the U.S. Geological Survey standard rocks (discussed below) confirms the absence of interference from elements at their usual abundance levels in rocks.

The EDTA reaction is not sensitive to the procedural conditions. The aqueous volume has been varied from 3 to 10 ml, the organic volume from 5 to 30 ml, the iodide addition from 0.6 to 2 ml, and the pH from 1 to 2 without effect on the determination. The pH is easily maintained in the 1.5–2 region by the procedural conditions.

Losses of bismuth

No losses of bismuth by adsorption on glassware were found. Early attempts to decompose samples in platinum ware, however, led to losses of 20–90% by adsorption on the platinum; even strong fuming with perchloric acid failed to free the bismuth. Large losses of bismuth from solutions containing any trace of precipitate were also noted. The procedure given here results in clear solutions and a negligible loss of bismuth.

Decomposition of samples

The most critical part of the procedure is the mode of decomposing the sample. A strong tendency for complexes of bismuth to form with, or be catalyzed by, some constituent of rocks was found with various dissolution techniques; these complexes did not react stoichiometrically with EDTA, leading to erratic (usually high) results. For example, solutions prepared by evaporating hydrofluoric–perchloric acid and fuming the residual perchloric acid gave satisfactory results with mafic rocks and very erratic results with silicic rocks. Evaporation with hydrofluoric acid followed by repeated evaporations with fuming nitric acid was satisfactory for most samples, but produced erratic results with iron-rich materials. Several other techniques were investigated with even less success.

Hydrofluoric–perchloric acid decomposition was usually satisfactory if

steam-bath temperature was not exceeded. Occasional erratic results were still obtained, however, and routine analysis of duplicates on different days is recommended. Samples containing much organic material probably would require another technique; experience suggests that fuming nitric–hydrofluoric acid attack would be satisfactory for samples containing less than 5% iron, but this has not been studied extensively.

Analysis of rocks

The accuracy and precision of this method were tested by analyzing replicates from each of four bottles of six of the U.S. Geological Survey standard rocks and eight splits from a single bottle of two others. The replicates were run on different days to preclude any correlation of errors. These data are given in Table I which also compares previous neutron activation determinations of bismuth. From these data the analytical precision for a single analysis is 10–15% except for the two ultramafic rocks. Repeating the analysis of variance with the analyses combined as duplicates yields an analytical precision of 5–10% except for the ultramafic rocks. The large errors associated with the DTS-1 and PCC-1 analyses may be due either to the low bismuth abundance or to sampling difficulties; in either case the precision could be

TABLE I

BISMUTH (ng g^{-1}) IN U.S. GEOLOGICAL SURVEY STANDARD ROCKS

Rock	*Bismuth concn. (Splits of given bottle in parenthesis)*	*Mean*	*Standard deviation*		*Neutron activation results (ng g^{-1})*
			Bottles	*Error*[a]	
G-1, granite	(53, 42, 63, 46, 53, 50, 54, 54)	51.9	—	6.2	46
W-1, diabase	(49, 55, 41, 40, 61, 53, 52, 62)	51.6	—	8.1	44
GSP-1, granodiorite	(30, 27, 34, 40)				
	(29, 39, 37, 37)	36.7	2.4	4.3	37
	(38, 38, 46, 37)				
	(37, 39, 37, 42)				
AGV-1, andesite	(50, 57, 57, 64)				
	(53, 58, 54, 47)	55.5	1.1	5.0	56
	(57, 57, 52, 49)				
	(64, 59, 48, 62)				
G-2, granite	(41, 53, 37, 44)				
	(46, 41, 39, 39)	41.0	1.1	4.9	38
	(40, 45, 36, 33)				
	(40, 44, 36, 42)				
BCR-1, basalt	(44, 51, 53, 50)				
	(51, 52, 60, 42)	49.6	0.2	4.9	47
	(43, 46, 48, 48)				
	(50, 56, 46, 54)				
DTS-1, dunite	(3.0, 4.0) (4.8, 4.2)	5.1	1.1	3.4	4.8
	(13, 3.5) (3.9, 4.5)				
PCC-1, peridotite	(1.6, 7.7) (2.8, 6.8)	5.7	1.5	3.2	8
	(9.4, 7.2) (7.7, 2.7)				

[a] Error is the standard deviation of the replicates for G-1 and W-1; it is the square root of the mean sum of squares variance within bottles with 12 degrees of freedom for GSP-1, AGV-1, G-2, and BCR-1 and with 4 degrees of freedom for DTS-1 and PCC-1.

improved by taking samples larger than the 100 mg used here. The agreement with the neutron activation results of Laul *et al.*[2] is within the error limits of the present method, which implies that the accuracy is satisfactory.

The replicate analyses of four bottles of the standard rocks were used to test for bottle-to-bottle heterogeneity by a one-way analysis of variance. The F-test showed that the variation attributable to the four bottles was not significantly (95% confidence level) larger than the variation within bottles and thus that different bottles of the standard rocks did not differ in bismuth concentration within the limits of analytical error.

We are indebted to I. May, H. T. Millard, Jr., and J. J. Rowe for helpful comments on the manuscript and to F. Flanagan for assistance with the analysis of variance experiment. This work was partially supported by NASA contracts W-13, 130 and W-13, 276.

SUMMARY

A rapid procedure suitable for the routine determination of 1–10 ng of bismuth in a silicate rock matrix is described. Results for the U.S. Geological Survey standard rocks are presented. Rocks and minerals are dissolved in hydrofluoric–perchloric acid in the presence of ^{207}Bi tracer and the silica is removed by evaporation. The perchloric acid residue is taken up in water and bismuth iodide is extracted into methyl isobutyl ketone. After three acid–iodide washes, the bismuth is stripped into water and reacted with a substoichiometric amount of EDTA. Excess of bismuth is extracted as the iodide and the specific activity of the bismuth–EDTA complex is determined.

RÉSUMÉ

On décrit une méthode rapide de routine pour le dosage du bismuth (1 à 10 ng) dans un silicate. L'échantillon à analyser est dissous dans un mélange d'acides fluorhydrique et perchlorique, en présence de ^{207}Bi comme traceur; la silica est éliminée par évaporation. Le résidu d'acide perchlorique est repris par l'eau; le bismuth, sous forme d'iodure, est extrait dans la méthylisobutylcétone. On procède finalement à la détermination de l'activité spécifique du complexe bismuth–EDTA.

ZUSAMMENFASSUNG

Es wird ein schnelles Verfahren für die Routinebestimmung von 1–10 ng Wismut in einer Silicatgestein-Matrix beschrieben. Ergebnisse für die U.S. Geological Survey-Standardgesteine werden vorgelegt. Gesteine und Minerale werden in Fluorwasserstoff–Perchlorsäure in Gegenwart von ^{207}Bi-Tracer aufgelöst; die Kieselsäure wird durch Eindampfen entfernt. Der perchlorsaure Rückstand wird mit Wasser aufgenommen und Wismutjodid mit Methylisobutylketon extrahiert. Nach dreimaligem Waschen mit saurer Jodidlösung wird das Wismut mit Wasser re-extrahiert und mit einer unterstöchiometrischen Menge EDTA umgesetzt. Überschüssiges Wismut wird als Jodid extrahiert, und es wird die spezifische Aktivität des Wismut–EDTA-Komplexes bestimmt.

REFERENCES

1 R. R. Brookes, L. H. Ahrens and S. R. Taylor, *Geochim. Cosmochim. Acta*, 18 (1960) 162.
2 J. C. Laul, D. R. Case, F. Schmidt-Bleek and M. E. Lipschutz, *Geochim. Cosmochim. Acta*, 34 (1970) 89.
3 G. W. Reed, K. Kigoshi and A. Turkevich, *Geochim. Cosmochim. Acta*, 20 (1960) 122.
4 J. Ruzicka and J. Stary, *Talanta*, 8 (1961) 228.
5 J. Ruzicka and J. Stary, *Substoichiometry in Radiochemical Analysis*, Pergamon Press, Oxford, 1968.
6 J. Stary and J. Ruzicka, *Talanta*, 11 (1964) 697.
7 J. Stary and J. Ruzicka, *Talanta*, 18 (1971) 1.
8 A. Arnold, S. Davis and A. L. Jordan, *Analyst*, 94 (1969) 664.
9 L. T. McClendon and J. R. DeVoe, *Anal. Chem.*, 41 (1969) 1454.
10 N. K. Baishya and R. B. Heslop, *Anal. Chim. Acta*, 53 (1971) 87.
11 G. B. Briscoe and A. Dodson, *Talanta*, 14 (1967) 1051.
12 J. Stary, K. Kratzer and A. Zeman, *J. Radioanal. Chem.*, 5 (1970) 71.
13 C. J. Van Nieuwenburg and J. W. L. Van Ligten, *Quantitative Chemical Microanalysis*, Elsevier, Amsterdam, 1963.
14 J. B. Headridge and J. Richardson, *Analyst*, 95 (1970) 930.
15 C. L. Luke, *Anal. Chim. Acta*, 39 (1967) 447.

Analytica Chimica Acta
Elsevier Publishing Company, Amsterdam
Printed in The Netherlands

REDOX TITRATIONS AT MILLIMOLAR CONCENTRATION IN N,N-DIMETHYLFORMAMIDE MEDIA

ROBERT D. BRAUN and JOHN T. STOCK
Department of Chemistry, University of Connecticut, Storrs, Conn. 06268 (*U.S.A.*)

(Received 29th October 1971)

Although N,N-dimethylformamide (DMF) has been much used as a solvent for acid–base titrimetry, comparatively few oxidation–reduction (redox) studies in DMF have been reported. Copper(II) has been used as oxidizing agent in titrations that involve titanium(III)[1,2], various organic thiol compounds[3-5], chromium(II)[1,6], and iron(II)[6]. Iodine, bromine, and antimony(V) have also been examined in titrations with titanium(III) and chromium(II)[1]. The oxidant lead(IV) has been used in titrations that involve copper(I), iron(II), titanium(III), chromium(II), iodide, and various thiol compounds[7]. Most of these titrations have involved titrand concentrations of 0.01 *M* or greater. The present authors have demonstrated that copper(II) at millimolar concentration can be satisfactorily titrated with titanium(III) by the use of bimetallic and "titrant stream" electrode systems[2]. A classical-type potentiometric electrode system has been used in the present study to confirm this conclusion and to investigate various other redox titrations at millimolar concentrations.

EXPERIMENTAL

Reagents

Reagent-grade chemicals were used throughout. The average water content of the DMF (Matheson, Coleman, and Bell) as indicated by Karl Fischer titrimetry[8] was 0.02% v/v. Standard methods were used to assay anhydrous iron(III) chloride[9a], ammonium dichromate[9a], cobalt(II) hexahydrate[9b], and mercury(II) acetate[9b]. Ascorbic acid was checked iodimetrically. Titanium(III) chloride (K. and K. Laboratories) was assayed by dissolution in DMF and titration of standard copper(II) solution[2]. Thiolactic acid (Aldrich Chemical Co.) and L(+)-cysteine hydrochloride monohydrate (Matheson, Coleman, and Bell) were used as received.

Equipment

The titration cell was a capped 100-ml tall beaker equipped for magnetic stirring. Holes in the cap were provided for the jet of the microburet, tubes for entry and exit of dry nitrogen, the 0.5-mm diameter × 10-mm long platinum wire indicator electrode, and the silver–0.01 *M* silver nitrate in DMF reference electrode[10]. The latter was a silver wire that dipped into solution contained in a 14-mm o.d. glass tube that was closed at the lower end by a fine-porosity frit. A 20-mm high column of methyl cellulose gelled with 0.1 *M* ammonium nitrate in DMF separated the frit from the reference solution.

All titrations were carried out under slight positive pressure of nitrogen and with the reference electrode connected to the "glass" jack of the Leeds and Northrup type 7401 pH meter. This instrument was zeroed on the right-to-left scale. Except in the early stages of some titrations, the potential of the indicator electrode was always negative with respect to the reference electrode. Most titrations were made on 50-ml portions of *ca.* 0.001 *M* titrand with *ca.* 0.1 *M* titrant (0.01 *M* in the case of iron(III) chloride, owing to limited solubility). Exploratory titrations with copper(II) chloride of titanium(III), cobalt(II), ascorbic acid, cysteine, and thiolactic acid were made first. Solutions of these substances were then used in turn to titrate copper(II). Similar sets of forward and reverse titrations were then carried out with ammonium dichromate, iron(III) chloride, and mercury(II) chloride in place of copper(II) chloride. Titrant–titrand pairs that gave reasonable potentiometric curves were then examined more closely.

RESULTS AND DISCUSSION

Copper(II) as oxidant

As expected, acceptable results were obtained in the titration of copper(II) with titanium(III)[2]. Although rapid potential equilibration and titration curves of excellent shape were also obtained in the reverse titration, the precision (standard deviation, s.d., 4.1% for 6 runs) was poor. Because the titer decreased as successive portions of titanium(III) were titrated (Table I), it appears that millimolar solutions of this titrand lack stability under the titration conditions. Poor results obtained in the titration of cysteine (s.d., 4.7% for 5 runs) and of thiolactic acid (s.d., 3.5% for 7 runs) are probably due to similar lack of stability at low concentration, as indicated by the results in Table I. However, both of the reverse titrations gave the satisfactory curves shown in Fig. 1. The results of these and of other acceptable titrations are summarized in Table II.

Figure 2 shows typical curves obtained in the titration of ascorbic acid with copper(II) and in the reverse titration. The forward titration has two indicated end-points; the second stage requires approximately twice as much titrant as used in the first stage. However, the reproducibility of both end-points was unsatisfactory (s.d., 2.1% and 8.6% for the 1st and 2nd end-points respectively, based on the results

TABLE I

DECREASE IN COPPER(II) TITER OF CERTAIN MILLIMOLAR SOLUTIONS

Titrand	*Relative titer (1st = 100) in successive titrations*[a,b]					
	1	2	3	4	5	6
Titanium(III)	100	54[c]	53	50	49	55
Cysteine	100	96	93	90	87	—
Thiolactic acid	100	67[c]	62	57	54	—

[a] 50-ml aliquots of freshly prepared *ca.* 1 m*M* stock solutions.
[b] Made at irregular time intervals. Approximate total times for the sets of end-point locating (rapid) titrations were 100 min for titanium(III) and cysteine, and 200 min for thiolactic acid.
[c] Interval of *ca.* 60 min between 1st and 2nd titrations.

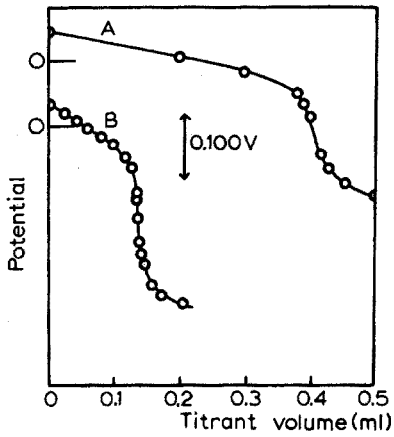

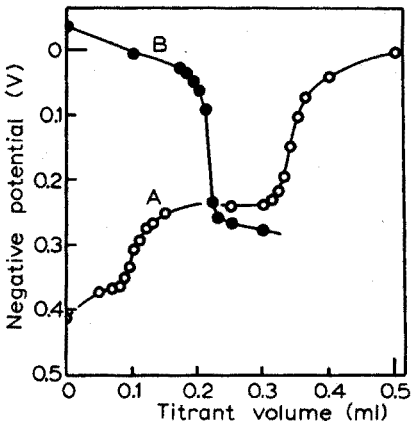

Fig. 1. Titration of 50 ml of (A) 0.00093 *M* copper(II) with 0.099 *M* cysteine; (B) 0.001 *M* copper(II) with 0.400 *M* thiolactic acid.

Fig. 2. Titration of 50 ml of (A) 0.00035 *M* ascorbic acid with 0.110 *M* copper(II); (B) 0.0011 *M* copper(II) with 0.120 *M* ascorbic acid.

TABLE II

ACCEPTABLE TITRATIONS AT MILLIMOLAR TITRAND CONCENTRATIONS

Titrant	*Titrand*	*Time (min)*[a]	*No. of runs*	*Standard dev. (%)*
Titanium(III)	Copper(II)	30	7	1.2
Cysteine	Copper(II)	35	9	0.7
Thiolactic acid	Copper(II)	15	9	0.5
Ascorbic acid	Copper(II)	60	6	0.6
Titanium(III)	Chromium(VI)	10	3	2.0
Chromium(VI)	Ascorbic acid	35	8	1.4
Titanium(III)	Iron(III)	40	6	2.2
Titanium(III)	Mercury(II)	40	5	1.2
Mercury(II)	Ascorbic acid	30	8	1.6
Ascorbic acid	Mercury(II)	10	9	0.4
Mercury(II)	Cobalt(II)	10	9	1.0
Cobalt(II)	Mercury(II)	6	9	0.5
Thiolactic acid	Mercury(II)	35	9	0.7, 0.5[b]

[a] Average time required to outline the titration curve and to locate the end-point. Equilibration of potential was almost instantaneous in titrations that averaged 10 min or less.
[b] For 1st and 2nd end-points, respectively.

of 6 runs). The reverse titration gave a curve that indicated a precise single end-point. The overall reaction in both forward and reverse titrations appears to be

$$2Cu(II) + C_6H_8O_6 = 2Cu(I) + C_6H_6O_6 + 2H^+$$

No recognizable end-point was obtained in the attempted titration of cobalt(II) with copper(II), or in the reverse titration.

Ammonium dichromate (chromium(VI)) as oxidant

The titration of titanium(III) with chromium(VI) could be done quite rapidly and yielded a curve with an end-point break of approximately 450 mV, as shown by curve A in Fig. 3. The unacceptably large s.d. of 3.1 % (10 runs) is probably due mainly to the instability of millimolar titanium(III) solutions. A typical curve obtained in the reverse titration is shown by curve B. This titration gave acceptable results.

Satisfactory results were obtained in the titration of ascorbic acid with chromium(VI). The potential equilibration was very sluggish in the reverse titration. Three runs, each of which took 2 h, indicated that the standard deviation exceeded 30 %.

Titration of cysteine with chromium(VI) showed the reaction to be sluggish and the curve to be misshapen. No end-point was found in the attempted reverse titration. No end-point was found in the titration of thiolactic acid with chromium(VI) but a rough end-point indication could be obtained in the reverse titration. The curve was however poorly shaped and unsuitable for titrimetry. No end-points were found in the titration of cobalt(II) with chromium(VI) or in the reverse titration.

Iron(III) as oxidant

The attempted titration of titanium(III) with iron(III) gave drawn-out poorly reproducible curves that were unsuitable for titrimetry. Precise and accurate results in the titration of *ca.* 0.06 *M* iron(III) with titanium(III) have been reported by Hinton and Tomlinson[1]. Curve C, Fig. 3 and the results summarized in Table II show that this titration is possible at millimolar concentrations of iron(III).

No end-points could be found in the titration with iron(III) of cobalt(II), cysteine, or thiolactic acid, nor in any of the reverse titrations. Some response was obtained when ascorbic acid was very slowly titrated with iron(III), but the process was tedious and gave imprecise results. No end-point was found in the reverse titration.

Mercury(II) as oxidant

Initially colorless 0.1 *M* mercury(II) acetate in DMF solution became yellow on standing and eventually formed a fine yellow precipitate. Color change and precipitation were inhibited by the addition of potassium chloride or of concentrated hydrochloric acid (1 drop per 50 ml of DMF solution). Some titrations were repeated with mercury(II) chloride in place of acidified mercury(II) acetate. The pairs of titration curves were essentially identical.

Mediocre results were expected in the titration of titanium(III) with mercury(II). Instead, highly irreproducible curves were obtained and the potential became *more* negative during the titration. In no case could the apparent end-point be reproduced to within 10 %. The curves obtained in the reverse titration were normal both in shape and in direction (potential becoming more negative during the titration) and led to acceptable results.

Titrations of ascorbic acid with mercury(II) and the reverse could be carried out quite rapidly. The forward titration yielded curve A, Fig. 4, with a titrant–titrand end-point ratio that suggests the reaction

$$Hg(II) + C_6H_8O_6 = Hg(0) + C_6H_6O_6 + 2H^+$$

Curve B was obtained in the reverse titration. The end-point potential break is

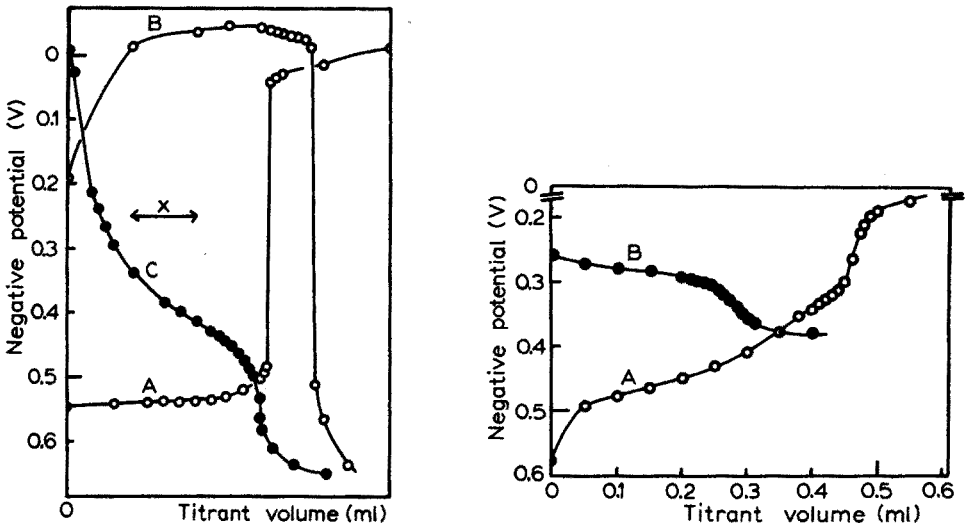

Fig. 3. Titration of 50 ml of (A) 0.0016 *M* titanium(III) with 0.100 *M* chromium(VI), $x=0.04$ ml; (B) 0.001 *M* chromium(VI) with 0.077 *M* titanium(III), $x=1.00$ ml; (C) 0.0012 *M* iron(III) with 0.097 *M* titanium(III), $x=0.20$ ml.

Fig. 4. Titration of 50 ml of (A) 0.001 *M* ascorbic acid with 0.100 *M* mercury(II); (B) 0.001 *M* mercury(II) with 0.100 *M* ascorbic acid.

smaller and its position suggests the overall reaction

$$2Hg(II)+C_6H_8O_6=2Hg(I)+C_6H_6O_6+2H^+$$

Both titrations yielded results of acceptable reproducibility.

During the titration of cobalt(II) with mercury(II), the color changed from blue through light purple to red. In the reverse titration the sequence was colorless, red, purple and violet. Because of rapid stabilization of potential, both titrations could be carried out quite quickly and reproducibly. Typical curves, shown as A and B in Fig. 5, indicate a 1:1 titrant–titrand end-point ratio.

No end-points were found in the titration of cysteine with mercury(II) or in the reverse titration. Although curves of satisfactory shape were obtained in the titration of thiolactic acid, the reproducibility of the titer was poor (s.d. 7.0% for 7 runs). The reverse titration gave curves with two breaks in potential, as shown by curve C in Fig. 5. The titration volumes indicated by both breaks were reproducible. A thiolactic acid–mercury(II) ratio of 2:1 was indicated by this second break and by the single break obtained when mercury(II) was the titrant.

Titanium(III) titrations of copper and iron in technical samples

To examine the applicability of titanium(III) titrimetry to the determination of copper in brass, 2 ml of concentrated hydrochloric acid was added to 0.15 g of brass (Thorn Smith, Troy, Mich., certified 81.46% Cu), followed by 30 ml of 30% hydrogen peroxide, which was added cautiously. When dissolution was complete, evaporation just to dryness was carried out. The residue was dissolved in *ca.* 50 ml of DMF and

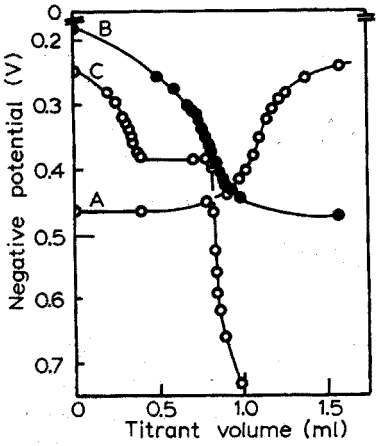

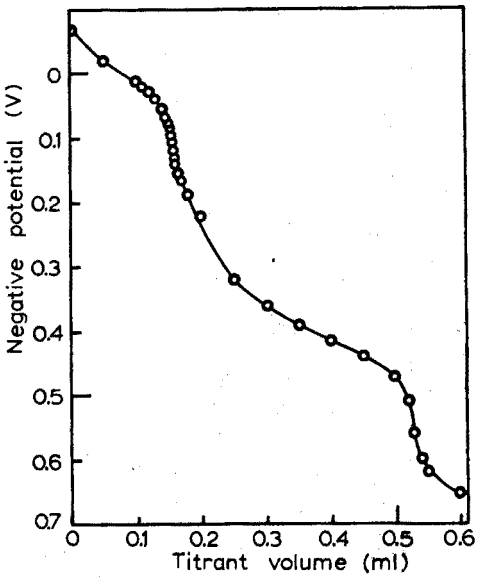

Fig. 5. Titration of 50 ml of (A) 0.00085 *M* cobalt(II) with 0.110 *M* mercury(II); (B) 0.0011 *M* mercury(II) with 0.085 *M* cobalt(II); (C) 0.001 *M* mercury(II) with 0.110 *M* thiolactic acid.

Fig. 6. Successive titration of copper(II) and iron(III) with 0.5 *M* titanium(III).

titrated with 0.5 *M* titanium(III) chloride in DMF. Triplicate runs gave 81.0±0.4% of copper.

In the triplicate titration of solutions made from National Bureau of Standards bronze No. 164 (certified 63.76% Cu), the result, 63.8±3.9% of copper, was not very precise. When continued beyond the copper end-point, the titration curve showed a second end-point. This alloy contained 2.52% of iron; the average interval between the two end-points agreed closely with this value.

Figure 6 shows a curve obtained in the titration of a solution prepared from a sample of copper matte (Thorn Smith, certified 21.64% Cu and 41.20% Fe). Results for three analyses were copper, 21.3±0.3%, and iron, 42.8±4.5%.

Although the application of redox titrations in DMF to the analysis of alloys and other technical materials shows promise, aspects such as possible interferences by sample constituents obviously need further study.

This work was carried out with the partial support of the University of Connecticut Research Foundation.

SUMMARY

Potentiometric oxidation–reduction titrations in N,N-dimethylformamide (DMF) have been shown to be valid at millimolar concentrations of titrand. Forward and reverse titrations that involve the oxidants copper(II), chromium(VI), iron(III), and mercury(II) with the reductants titanium(III), cobalt(II), ascorbic acid, cysteine, and thiolactic acid have been examined. Some preliminary results of titanium(III) in DMF titrimetry in the determination of copper and iron in alloys are presented.

RÉSUMÉ

Les titrages potentiométriques d'oxydo-réduction, dans la N,N-diméthylformamide (DMF) semblent valables pour des concentrations millimolaires de titrant. On examine divers titrages directs et en retour: cuivre(II), chrome(VI), fer(III) et mercure(II) comme oxydants et titane(III), cobalt(II), acide ascorbique, cystéine et acide thiolactique comme réducteurs. Quelques résultats préliminaires sont donnés sur le dosage du cuivre et du fer dans des alliages, par titrimétrie au moyen de titane(III) dans DMF.

ZUSAMMENFASSUNG

Potentiometrische Oxidations–Reduktions-Titrationen in N,N-Dimethylformamid (DMF) können bei millimolaren Konzentrationen des Titranden ausgeführt werden. Direkte Titrationen und Rücktitrationen mit den Oxidationsmitteln Kupfer(II), Chrom(VI), Eisen(III) und Quecksilber(II) und den Reduktionsmitteln Titan(III), Kobalt(II), Ascorbinsäure, Cystein und Thiomilchsäure wurden untersucht. Einige vorläufige Ergebnisse der Bestimmung von Kupfer und Eisen in Legierungen durch Titration mit Titan(III) in DMF werden vorgelegt.

REFERENCES

1 J. F. Hinton and H. M. Tomlinson, *Anal. Chem.*, 33 (1961) 1502.
2 J. T. Stock and R. D. Braun, *Microchem. J.*, 15 (1970) 519.
3 Z. Hladky, *Z. Chem.*, 5 (1965) 424.
4 Z. Hladky, *Wiss. Z.*, 9 (1967) 5.
5 Z. Hladky and J. Vrestal, *Collect. Czech. Chem. Commun.*, 34 (1969) 1098.
6 Z. Hladky and J. Vrestal, *Collect. Czech. Chem. Commun.*, 34 (1969) 84.
7 Z. Hladky and J. Ruza, *Chem. Zvesti*, 23 (1969) 336.
8 R. D. Braun and J. T. Stock, *Microchem. J.*, 16 (1971) 236.
9 I. M. Kolthoff, E. B. Sandell, E. J. Meehan and S. Bruckenstein, *Quantitative Chemical Analysis*, 4th Ed., MacMillan, London, 1969, (a) pp. 828, 839; (b) p. 812.
10 I. M. Kolthoff, M. K. Chantooni and H. Smagowski, *Anal. Chem.*, 42 (1970) 1622.

Analytica Chimica Acta
Elsevier Publishing Company, Amsterdam
Printed in The Netherlands

COULOMETRIC TITRATION WITH +3 URANIUM APPLICATION TO THE DETERMINATION OF URANIUM

GREGORY C. FARRINGTON AND JAMES J. LINGANE
Department of Chemistry, Harvard University, Cambridge, Mass. 02138 (U.S.A.)

(Received 20th December 1971)

The preparation of solutions of +3 uranium by reducing +4 uranium has been studied by several authors[1-3]. A previous study in this laboratory[4] demonstrated that the current efficiency is very close to 100% when the reduction is performed at controlled potential with a mercury cathode. However, the possibility of employing electrogenerated +3 uranium in a constant-current coulometric titration has not previously been investigated. Because the potential of the U^{4+}/U^{3+} couple (−0.635 V *vs.* N.H.E.) is more strongly reducing than that of any electrogenerated reagent used heretofore in coulometric titrations, it was of interest to investigate this possibility.

Because the potential of the U^{4+}/U^{3+} couple is so strongly reducing, one would expect that +3 uranium would be oxidized by hydrogen ion, and, indeed, this does occur. Fortunately, however, the rate of this reaction is remarkably small[1]. Peretrukhin *et al.*[5] measured the rate of oxidation of +3 uranium by hydrogen ion in a variety of media, and, for example, in 0.2 *M* hydrochloric acid at 25° found that the rate constant was only $1.43 \cdot 10^{-7}$ sec^{-1}, corresponding to a half-life of 1360 h. As the pH is increased to the point at which hydrolysis of +3 uranium begins, the half-life decreases, reaching a value of 1.6 h at pH 3.4. Peretrukhin *et al.* also observed that the oxidation of +3 uranium by hydrogen ion is accelerated by a high concentration of chloride ion, presumably because the chloro complex thus formed reacts more rapidly than does the aquo U^{3+} ion. For example, in 5.6 *M* lithium chloride +0.5 *M* hydrochloric acid medium, the half-life is 36 h. Thus, while it might be expected that oxidation of +3 uranium by hydrogen ion would prevent its use as a coulometric titrant, the conditions under which the reaction is minimized are convenient enough to maintain that this does not cause serious difficulty.

EXPERIMENTAL

The cell shown in Fig. 1 was used for all of the titrations. High-purity nitrogen was used to exclude air (oxygen). Potentiometric end-point detection was employed, with a small mercury indicator electrode.

Constant current was supplied by a Kepco Model 120-1-M power supply, externally programmed for constant-current operation. The instrument delivered current constant over at least 30-min periods to one part in 80,000. A DPDT mercury-wetted relay switched the current between the cell and a dummy load. Current was timed by tapping the 1 kHz output of the internal crystal oscillator into the input of a Hewlett-Packard 5245-L Electronic Counter. By this technique, time was measured with an uncertainty of only ±0.001 sec.

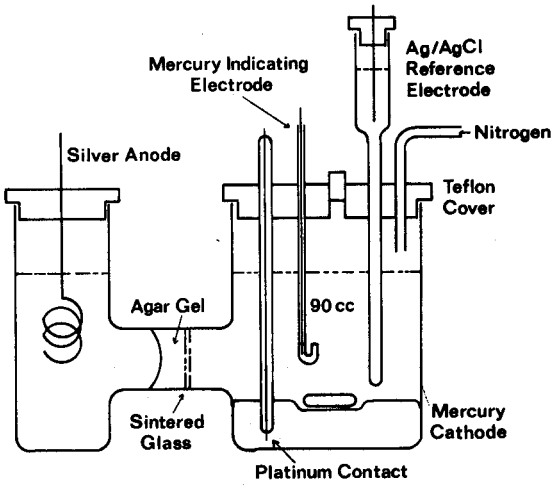

Fig. 1. Constant-current coulometric titration cell.

Potential measurements were made with a Leeds and Northrup Model 7553-A Precision Potentiometer. Current was measured by determining the voltage drop across a General Radio precision 10.002-ohm resistor, previously calibrated with a certified Leeds and Northrup 10-ohm resistor.

Standard uranium samples were prepared from National Bureau of Standards U_3O_8 (Sample No. 950a). The oxide was dissolved in hot aqua regia and the resulting solution was evaporated to dryness several times with excess of hydrochloric acid in a fused silica beaker on a steam bath.

The reagent precursor solution consisted of +4 uranium chloride in dilute hydrochloric acid. Stock solutions of 0.4 *M* uranium tetrachloride were prepared by reducing in a Jones reductor an appropriate solution of uranyl chloride, previously prepared by multiple evaporations to dryness of Mallinckrodt reagent uranyl acetate with excess of hydrochloric acid on a steam bath. Reduction of uranyl chloride with a Jones reductor produces a mixture of +3 and +4 uranium, but the former is easily oxidized to the +4 state by bubbling air through the solution until the color changes to the clear green of +4 uranium.

Solutions of +4 uranium undergo slow air oxidation to the +6 state. However, even with this complication, about two months can pass before the magnitude of the pre-titration, the technique used to insure that all the reagent precursor is in the +4 state, becomes prohibitively large. If longer storage periods are contemplated, the solution should be stored under an inert atmosphere.

In a typical titration, the reagent precursor solution was pre-titrated to the end-point, the deaerated sample was then added with a calibrated 25-cm^3 pipette, and the solution was titrated back to the end-point.

RESULTS AND DISCUSSION

Figure 2 compares the experimentally observed and theoretically predicted equilibrium titration curves for the titration of +6 uranium with +3 uranium. The

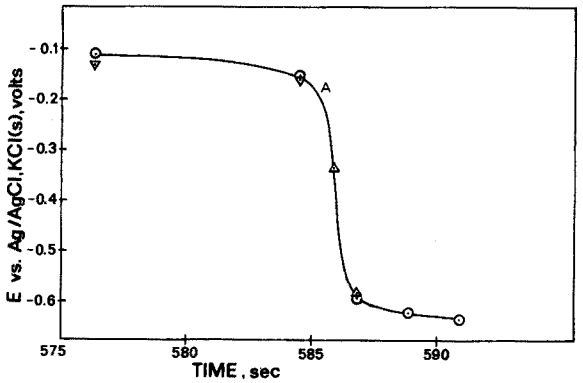

Fig. 2. Observed *vs.* calculated equilibrium titration curve. Titration of 21 mg of uranium with 30 mA generating current in 0.11 *M* hydrochloric acid, 40 m*M* in +4 uranium. (⊙) Observed; (△) calculated.

experimentally observed potentials were obtained by waiting until the potential of the mercury indicator electrode did not change more than 0.1 mV min^{-1} after successive generations of +3 uranium. The UO_2^{2+}/UO_2^{+} couple and the equilibrium data of Nelson and Kraus[6], who made an extensive study of the equilibrium between +6, +5, and +4 uranium, were used to calculate the equilibrium potentials. The excellent agreement between the two curves corroborates the data of Nelson and Kraus, and the potential–time behavior at each point on the observed titration curve demonstrates that the UO_2^{2+}/UO_2^{+} couple is potential-determining. In all cases the potentials drift upward to their equilibrium values. Since +3 uranium reacts with +6 faster than with +5 uranium, this drift reflects the disappearance of excess of +5 uranium *via* disproportionation. This decrease in the concentration of +5 uranium can cause an upward potential drift only if the UO_2^{2+}/UO_2^{+} couple is potential-determining.

Lingane[4] observed an anomalous potential rise just before the end-point in a controlled-potential coulometric titration of +6 uranium. He suggested that, at that point, the disproportionation of UO_2^{+} had a greater relative effect on the potential, causing the upward drift. However, we have found that the potential rise is caused simply by oxygen leaking into the titration cell from the agar plug. When the auxiliary electrode compartment, as well as the main compartment, was deaerated for 24 h, so that the oxygen originally dissolved in the agar plug was removed, the anomalous potential behavior disappeared.

As Fig. 2 illustrates, a potential rise was not observed in titrations in which excess of +4 uranium was present. However, the equilibrium concentration of +5 uranium in a typical constant-current coulometric titration (40 m*M* excess of +4 uranium) is 55 times greater than in a controlled-potential titration (no excess of +4 uranium) at corresponding points in the vicinity of the end-point. Both concentrations were calculated for a titration of 21 mg of uranium in 0.2 *M* hydrochloric acid. Evidently, the effect of oxygen is masked by the large concentration of +5 uranium.

The reduction of +4 uranium to the +3 state is reversible in dilute hydrochloric acid and occurs at the potential expected from the formal potential of the U^{4+}/U^{3+} couple.

Some hydrogen ion is also reduced at the generating electrode simultaneously with the reduction of +4 uranium. The amount of current arising from this reduction

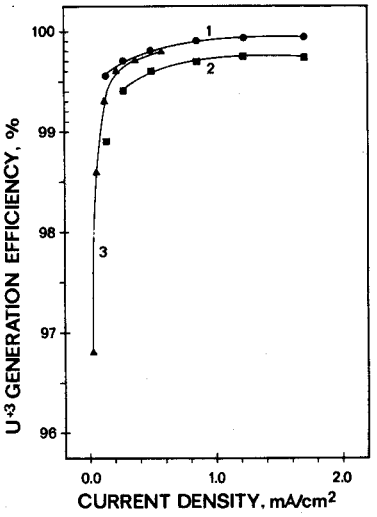

Fig. 3. Generation efficiency of +3 uranium. Data taken with cell shown in Fig. 1 with maximum magnetic stirring. (1) 44 m*M* U^{4+}, 0.1 *M* HCl; (2) 44 m*M* U^{4+}, 1.0 *M* HCl; (3) 11 m*M* U^{4+}, 0.1 *M* HCl.

increases as the concentration of hydrogen ion increases and as the operating potential becomes more negative (cathodic). Since that portion of the total generating current resulting from reduction of hydrogen ion decreases the current efficiency of generation of +3 uranium, it must be minimized. The governing factors are the concentrations of hydrogen ion and +4 uranium, the current density, and the stirring efficiency.

From current–potential curves obtained in hydrochloric acid media with and without +4 uranium present, the current efficiencies for the generation of +3 uranium at the mercury pool cathode as a function of current density have been evaluated and some typical results are shown in Fig. 3. The rationale of this method of determining current efficiency has been discussed in detail elsewhere[7].

The potential adopted by the mercury cathode becomes more negative (cathodic) with increasing current density. Because, as the potential becomes more negative, the current resulting from reduction of +4 uranium increases relatively more rapidly than that due to reduction of hydrogen ion, the current efficiency increases with increasing current density. As expected, at a given current density and a given concentration of +4 uranium, the current efficiency decreases as hydrogen ion concentration is increased (curves 1 and 2 in Fig. 3). When other requirements of a particular titration permit, the hydrogen ion concentration should not be much above 0.1 *M*.

Figure 3 demonstrates that 99.9% generation efficiency is attained with 44 m*M* +4 uranium in 0.1 *M* hydrochloric acid solutions. This is still not the highest current efficiency which is possible. By increasing the concentration of +4 uranium to 360 m*M*, the current resulting from its reduction at a given generation potential increases nearly ten-fold while the background current remains fairly constant. Thus, at this level of +4 uranium concentration with a current density of 18 mA cm^{-2}, the generation efficiency approaches 99.99%. With the large (16 cm^2) mercury electrode used in this work, this current density corresponds to a generating current of about 295 mA which was used in this study to titrate the 200-mg samples of uranium.

Another factor which governs the accuracy of titrations with +3 uranium is the rate of its oxidation by hydrogen ion. The rate of this reaction was measured in 0.1 *M* hydrochloric acid by generating a small excess of +3 uranium in the titration cell and potentiometrically following the decrease in its concentration with time. The observed rate of oxidation was approximately an order of magnitude faster if the solution was unstirred than if it was stirred. If the potential was noted in a quiescent solution after a period of oxidation and then noted again after the solution had been thoroughly stirred, the potential before stirring was consistently more anodic than after stirring. Since the potential of the indicator electrode is determined by the concentrations of the potential-determining species *at its surface*, it appears that the oxidation of +3 uranium by hydrogen ion is catalyzed at the electrode surface. Since the vicinity of the generating electrode is the only region in which a relatively large concentration of +3 uranium exists during a titration, the titration error arising from oxidation of +3 uranium by hydrogen ion is greater than would be expected from the rate of the homogeneous reaction.

The overall titration error increases with increasing hydrochloric acid concentration as shown by the following results for the titration of 21 mg of uranium in 44 m*M* +4 uranium with a 30-mA generating current:

Acidity (*M* HCl):	3.0	1.0	0.50	0.11	0.02
Titration error (%):	+1.43	+0.78	+0.42	+0.35	+0.35

As the acidity increases from 0.11 *M* to 1.0 *M*, the titration error increases by 0.43%. The decrease in generating efficiency of +3 uranium accounts for only +0.19% of this increase and the additional +0.24% can be attributed to an increased reaction rate of +3 uranium with hydrogen ion at the electrode surface.

Table I summarizes data on the titration error as a function of sample size.

Another source of error arises from oxygen leaking into the titration cell. A copper heater in series with the nitrogen line insured that the amount of oxygen in the nitrogen purge was negligible. The agar plug, however, trapped a significant concentration of oxygen which diffused into the test solution. By deaerating both compartments of the cell for 24 h before titrating, it was demonstrated that oxygen leaking

TABLE I

TYPICAL TITRATION RESULTS

(In all titrations the hydrochloric acid concentration was 0.11 *M* at the end-point. Total solution volume was 90 cm^3 and each titration required about 600 sec)

Uranium taken (mg)	*+4 Uranium (mM)*	*Generating current (mA)*	*Error (mg)*	*Error (%)*
2.113	44	2.9	+0.068	+3.2
2.113	44	2.9	+0.087	+4.2
21.13	44	30	+0.072	+0.34
21.13	44	30	+0.074	+0.35
21.13	44	30	+0.078	+0.37
63.46	120	110	+0.044	+0.07
211.42	360	294	+0.190	+0.09

from the agar plug constituted a major source of error, corresponding in an average 600-sec titration to about 0.04 mg or 0.20% of a 21-mg sample.

The balance of the error not accounted for by direct reduction of hydrogen ion and oxygen is attributable to the oxidation of +3 uranium by hydrogen ion. If it is assumed that the instantaneous concentration of +3 uranium at the electrode surface and /or the length of time that that concentration exists is proportional to the size of the uranium sample, then the titration error caused by this reaction should be approximately proportional to sample size.

Typical magnitudes of the various errors are illustrated by the titrations of 211 mg and 21 mg of uranium. For each sample an appropriate generating current and +4 uranium concentration were chosen so that the total titration time was *ca.* 600 sec. The titration solutions were each 0.11 *M* in hydrochloric acid at the end-points. For the 21- and 211-mg samples, respectively, direct reduction of hydrogen ion produced errors of +0.06 and 0.00%, oxidation of +3 uranium by hydrogen ion contributed +0.10 and +0.07%, and the errors from oxygen diffusing from the agar plug were +0.20 and +0.02%.

In the course of this study, it was noted that considerable uncertainty exists in the literature concerning the standard potential of the UO_2^{2+}/U^{4+} couple,

$$UO_2^{2+} + 4\,H^+ + 2\,e = U^{4+} + 2\,H_2O \qquad (1)$$

In 1908, Luther and Michie[8] measured +0.42 *vs.* N.H.E. as the standard potential of this couple. In 1910, Titlestadt[9] published a value of +0.404 V *vs.* N.H.E., while Khoplin and Gurevitch[10] in 1944 reported a potential of +0.407 V *vs.* N.H.E. All three groups obtained their results in the presence of sulfate which complexes +4 uranium more than +6. The effect of sulfate in shifting the observed potentials to more oxidizing values was illustrated by a study by Taylor and Smith[11] of the potential in chloride medium. They measured a standard potential of +0.334 V *vs.* N.H.E., considerably more reducing than any previous values. In 1949, Kraus and Nelson[12] measured the potential in 0.1 *M* hydrochloric acid at a mercury electrode, observing a formal potential of +0.334 V *vs.* N.H.E., and concluded that this value was within 20–30 mV of the standard potential. This potential was generally accepted and served as the basis for the calculation of the free energies of the +4 and +3 uranium ions by Rossini *et al.*[13].

We have calculated the standard potential of the UO_2^+/U^{4+} and UO_2^{2+}/U^{4+} couples from data reported by Nelson and Kraus[6] on the UO_2^+ disproportionation equilibrium

$$2\,UO_2^+ + 4\,H^+ = UO_2^{2+} + U^{4+} + 2\,H_2O \qquad (2)$$

and the well-characterized standard potential of the UO_2^{2+}/UO_2^+ couple.

$$UO_2^{2+} + e = UO_2^+\,;\; E_0 = +0.063\text{ V } \textit{vs.}\text{ N.H.E.} \qquad (3)$$

Nelson and Kraus reported a comprehensive study of the +6/+5/+4 uranium equilibrium in 1951. They found that the equilibrium constant of reaction 2 was greatly dependent on ionic strength, being $(1.7 \pm 0.3) \cdot 10^{+6}$ at infinite dilution at 25° but increasing to $(1.4 \pm 0.3) \cdot 10^{+9}$ in a perchlorate solution of ionic strength 1.97 *M*. Both spectrophotometric and potentiometric techniques were used in that study and both methods were in agreement.

The standard potential of the UO_2^{2+}/UO_2^+ couple has been measured at 25° with excellent agreement by several authors[14,15], who also found it to have a very small dependence on ionic strength. On the basis of these investigations, +0.063 V *vs.* N.H.E. is probably not in error by more than ± 3 mV.

The UO_2^+/U^{4+} standard potential, calculated from the equilibrium constant at infinite dilution of Nelson and Kraus and the standard potential of the UO_2^{2+}/UO_2^+ couple, is +0.429 V *vs.* N.H.E. It follows that the standard potential of the UO_2^{2+}/U^{4+} couple is +0.246 V *vs.* N.H.E. The considerable discrepancy between these values and the presently accepted potentials[16] of +0.62 V and +0.334 V *vs.* N.H.E., respectively, can be better understood in the light of the large effect of ionic strength on the +6/+5/+4 uranium equilibrium. When the effect of ionic strength is taken into consideration, the potential of +0.334 V *vs.* N.H.E. measured for the UO_2^{2+}/U^{4+} couple at an ionic strength of 0.1 *M* by Kraus and Nelson is quite plausible. The standard free energies consistent with the new standard potentials are −134.4 kcal mole^{-1} and −120.4 kcal mole^{-1} for U^{4+} and U^{3+}, respectively. All of these new potentials and free energies are probably much closer to the true values than those heretofore accepted.

SUMMARY

The most powerful reductimetric titrant used to date, +3 uranium, has been generated in acidic solution with nearly 100% current efficiency, and applied to the constant-current coulometric titration of +6 uranium. The titration error is +0.09% with a 211-mg uranium sample. The potentiometric titration curve for the titration of +6 uranium with +3 uranium has shown that the UO_2^{2+}/UO_2^+ couple is potential-determining in mixtures of +6, +5, and +4 uranium.

A brief review of the literature dealing with the standard potential of the UO_2^{2+}/U^{4+} and the UO_2^+/U^{4+} couples at 25° is presented; it is concluded that the values are +0.246 V and +0.429 V *vs.* N.H.E., respectively, instead of +0.334 V and +0.62 V *vs.* N.H.E. as previously accepted. The standard free energies of U^{3+} and U^{4+} are −120.4 kcal mole^{-1} and −134.4 kcal mole^{-1}, respectively, at 25°.

RÉSUMÉ

La coulométrie à l'aide d'uranium +3 (produit en milieu acide, avec un rendement près de 100%) est appliquée au titrage de l'uranium +6 par coulométrie à courant constant. L'erreur de titrage est de +0.09% pour un échantillon d'uranium de 211 mg. On examine les potentiels de l'uranium à divers états de valence, ainsi que les énergies libres standards de U^{3+} et U^{4+}

ZUSAMMENFASSUNG

Das stärkste bisher verwendete reduktimetrische Titrationsmittel, +3 Uran, wurde in saurer Lösung bei nahezu 100% Stromausbeute erzeugt und auf die coulometrische Titration von +6 Uran bei konstantem Strom angewendet. Der Titrationsfehler ist +0.09% bei einer Probe von 211 mg Uran. Die potentiometrische Titrationskurve für die Titration von Uran(VI) mit Uran(III) ergab, dass das UO_2^{2+}/UO_2^+-

Redoxpaar in Gemischen von +6, +5 und +4 Uran potentialbestimmend ist.

Es wird eine kurze Übersicht über die Literatur gegeben, in der die Standardpotentiale von UO_2^{2+}/U^{4+} und UO_2^{+}/U^{4+} bei 25° angeführt sind; es wird festgestellt, dass die Werte gegen Normalwasserstoffelektrode +0.246 V bzw. +0.429 V sind, statt wie bisher angenommen +0.334 V bzw. +0.62 V. Die freien Standardenergien von U^{3+} und U^{4+} sind -120.4 kcal mol^{-1} bzw. -134.4 kcal mol^{-1} bei 25°.

REFERENCES

1 A. SATO, *Bull. Chem. Soc. Jap.*, 40 (1967) 2107.
2 C. H. PRESCOTT, JR., *Abstr. Pap. Amer. Chem. Soc., 113th Meeting, 1948*, p. 29–0.
3 W. BILTZ AND C. FENDIUS, *Z. Anorg. Chem.*, 172 (1928) 386.
4 J. J. LINGANE, *Anal. Chim. Acta*, 50 (1970) 1.
5 V. F. PERETRUKHIN, N. N. KROT AND A. D. GEL'MAN, *Radiokhim.*, 12 (1970) 96.
6 F. NELSON AND K. A. KRAUS, *J. Amer. Chem. Soc.*, 73 (1951) 2157.
7 J. J. LINGANE, *Electroanalytical Chemistry*, 2nd Ed., Interscience, New York, 1958, p. 488 ff.
8 R. LUTHER AND A. C. MICHIE, *Z. Phys. Chem.*, 14 (1908) 826.
9 N. TITLESTADT, *Z. Phys. Chem.*, 72 (1910) 257.
10 W. G. KHOPLIN AND A. M. GUREVITCH, *Bull. Acad. Sci. USSR, Cl. Sci. Chim.*, 271 (1943); *Chem. Abstr.*, 38 (1944) 5451.
11 J. K. TAYLOR AND E. R. SMITH, *Report A*, 1972, August 29, 1944.
12 K. A. KRAUS AND F. NELSON, *J. Amer. Chem. Soc.*, 71 (1949) 2517.
13 F. D. ROSSINI, D. D. WAGMAN, W. H. EVANS, S. LEVINE AND I. JAFFE (Editors), *Selected Values of Chemical Thermodynamic Properties*, Parts I and II, National Bureau of Standards Circular 500, Washington, 1961.
14 E. S. KRITCHEVSKY AND J. C. HINDMAN, *J. Amer. Chem. Soc.*, 71 (1949) 2096.
15 D. M. H. KERN AND E. F. ORLEMANN, *J. Amer. Chem. Soc.*, 71 (1949) 2102.
16 J. J. LINGANE, *Electroanalytical Chemistry*, 2nd Ed., Interscience, New York, 1958, p. 650.

Analytica Chimica Acta
Elsevier Publishing Company, Amsterdam
Printed in The Netherlands

MICROCOULOMETRIC MEASUREMENT OF WATER IN MINERALS*

MARCELYN CREMER and H. NEIL ELSHEIMER
U.S. Geological Survey, Menlo Park, Calif. 94025 (*U.S.A.*)
and E. E. ESCHER
E. I. du Pont Instrument Products Division, Monrovia, Calif. 91016 (*U.S.A.*)
(Received 10th November 1971)

The determination of small amounts of water in rocks and minerals has long been and still is a troublesome analytical problem. Until recently, the most suitable methods for routine use have been gravimetric. Water is released and expelled from the sample by heat and collected either by condensation, in the case of the Penfield method[1] with modifications[2,3], or by absorption as described by Riley[4]. The separated water is then weighed. Other volatiles are often expelled with the water, hence various precautions must be taken to prevent their interference.

A more complex method involves fusion of the sample in an evacuated system by means of an induction furnace[5]. The released water is passed over hot uranium metal, and the volume of hydrogen is measured. Titration with Karl Fischer reagent[6] or physical measurements[7-9], such as conductivity or dielectric constant, may be used to a limited extent once the water has been separated and collected. A d.c.-arc spectrographic method has recently been described[10]. The sample is mixed with a quartz buffer and burned in a special electrode, and then the 306.36-nm head of the hydroxyl band is measured. Infrared absorption techniques have been reported for the determination of water in rocks[11] and granites[12].

Both gravimetric methods have been adapted to small samples. Sandell's microdetermination of water by the Penfield method requires 20–30 mg of sample[13]. Riley's absorption tube method requires only 10 mg of sample[14]. A microcoulometric titration method has also been reported[15]. Water is converted stoichiometrically into ammonia with sodamide heated to 80°. Coulometrically generated hypobromite is used to titrate the ammonia.

The experimental results described here have been obtained by microcoulometric measurement. For purposes of comparison, total water has been determined, in most cases, on the same samples by a modified Penfield method[3]. The electrolytic method is that of Keidel[16]. The sensing element of the instrument used consists of a pair of parallel platinum wires helically wound inside a glass capillary that is coated with phosphorus pentoxide. A voltage is impressed across the platinum wires that serve as electrodes. The gaseous water passing through the cell is continuously absorbed by the phosphorus pentoxide and electrolyzed by the impressed voltage into molecular hydrogen and oxygen.

---

* Publication authorized by the Director, U.S. Geological Survey.

The chemical and electrochemical reactions occurring are:

$$H_2O\,(g) + P_2O_5 \xrightarrow{(1)} P_2O_5 \cdot H_2O \xrightarrow{(2)} P_2O_5 + H_2\,(g) + \tfrac{1}{2}\,O_2\,(g)$$

Step one is a simple chemical absorption of gaseous water by P_2O_5 that renders the film electrically conductive. Step two is electrolysis of the water into its component elements of hydrogen and oxygen, accompanied by a transfer of charge from one cell electrode to the other. The electrolysis current can be integrated to give a measurement proportional to the total quantity of moisture electrolyzed over a period of time, in accordance with Faraday's first law.

EXPERIMENTAL

Apparatus

A Du Pont Type 26-321A-MA Moisture Analyzer with certain modifications was used. Dry cylinder nitrogen (99.995% purity, dew point $-90°$F) was passed continuously through a solid acrylic purge meter (flowmeter), Matheson Series 201, at a rate of 26 ml min^{-1} (0.055 SCFH Air) and through two magnesium perchlorate dryers. A Vycor microcombustion tube with bent capillary side arm (Corning no. 18680) was used as a sample chamber and was inserted with Teflon tubing between the second dryer and the moisture analyzer oven. A plug of silica wool–calcium carbonate–silica wool in the combustion tube and a plug of silica wool–Körbl combustion catalyst[17]–silica wool–calcium carbonate–silica wool in the moisture analyzer oven (Fig. 1) protected the tubing, flow control system, and electrolytic cell from corrosive acid gases expelled from the sample and insured the oxidation of any organic compounds or hydrogen in the gas stream. Heating the sample outside the instrument per-

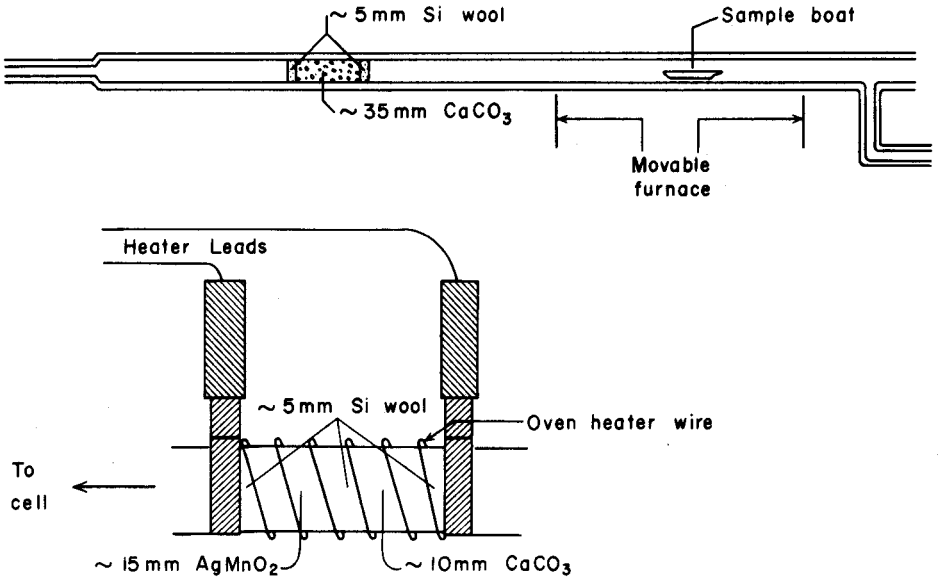

Fig. 1. Combustion tube (11.25 × 525 mm) and moisture analyzer oven fillings.

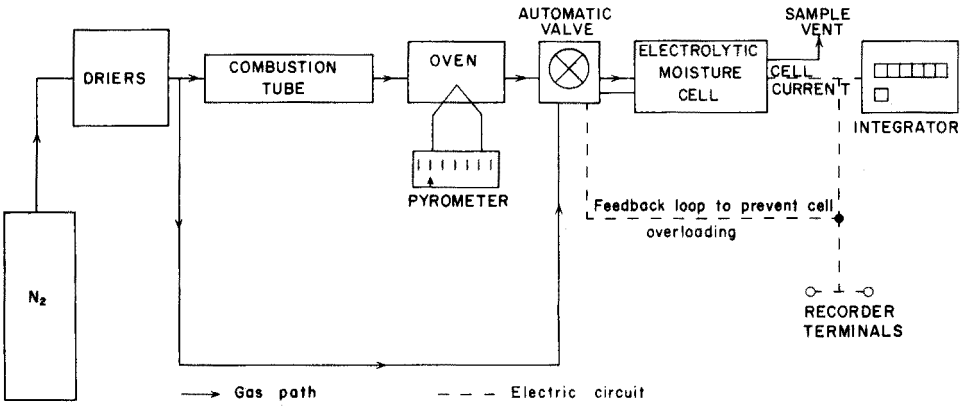

Fig. 2. Schematic of apparatus.

mitted the use of higher decomposition temperatures and provided space for the plugs. An Arthur Thomas microcombustion furnace (catalogue no. 5679-A) controlled by a variable transformer was positioned around the combustion tube. A second flowmeter was attached to the gas exit of the cell.

A block diagram of the instrument is shown in Fig. 2. The arrows indicate the path of the dry nitrogen gas as it carries the gaseous water from the sample in the combustion tube to the sensing elements. An internal variable transformer provided power for a heating element on the outside of the moisture analyzer oven. Temperature was indicated on a panel thermocouple meter. At the close of a heating cycle, an adjustable timer shut off the integrator and turned on a blower that rapidly cooled the moisture analyzer oven preparatory to running another sample.

The cell current integrating system consisted of a precision solid-state voltage-to-frequency converter and an electromechanical digital counter. The system was calibrated so that the counter read directly in micrograms. The smallest digit was 0.1 μg; full count was 100 mg.

The rate at which water enters the electrolysis cell must be limited. A too rapid rate overranges the integrating system and causes some of the water to pass through the cell without being absorbed. To prevent this problem, a servo valve was provided that throttled flow through the cell before the electrolysis current could exceed the acceptable limit. A small bypass flow was provided so that the valve would not shut off flow completely to produce a static condition.

Since the dried gas still contained a small amount of moisture, the integration circuit contained an adjustable bias voltage. This voltage was adjusted so that the integrator count rate was essentially zero with only the inert gas flowing through the cell. Thus, only the moisture from the sample contributed to the count.

Reagents

Calcium carbonate powder (A.R.-grade).

Körbl combustion catalyst (silver permanganate decomposition product), prepared[18] from A.R.-grade potassium permanganate and A.R.-grade silver nitrate.

Lead oxide yellow (low silver) powder, lead chromate powder, and copper oxide powder, all of A.R.-grade.

Pretreatment

Ignite Coors No. 00 porcelain boats for 1 h at 1000°. Store in a desiccator.

Prepare a 10+1+1 $PbO:PbCrO_4:CuO$ flux by intimate mixing and ignition for 30 min at 400°. Store in a desiccator.

Grind the sample to −100 mesh. Grind pyroxenes and amphiboles to −200 mesh. Dry the moisture analyzer system in the following manner. On the instrument panel, set the temperature to 450° and the adjustable timer for 1 h. Move the micro furnace to the right side of the combustion tube. Heat the furnace for 30 min with the transformer at *ca.* 130 V. Move the furnace over the calcium carbonate plug and lower the transformer setting to 50 V. When the integrator count rate decreases to 0.1 μg/6 sec, turn off the transformer and the timer. When the white light appears on the panel, the instrument is ready for loading. Dry the system after each period of non-continuous use.

Procedures

Moisture analyzer method. Determine a blank by weighing 0.5 g of flux in a preignited boat. Insert the boat into the combustion tube, set the instrument counter to zero, and proceed as in the drying process. When the count rate again decreases to 0.1 μg/6 sec, turn off the transformer and timer, and reload the instrument with a sample. Weigh a 10–50 mg portion (amount governed by expected percent of water) in a preignited boat. Cover with a tenfold weight of flux and proceed as in the blank determining process. Compute the percent of water by subtracting from the reading, the count due to blank and background. Use this procedure to check instrument performance periodically with a $CuSO_4 \cdot 5H_2O$ crystal without flux. Clean used boats by soaking them in concentrated hydrochloric acid for *ca.* three weeks.

Penfield method. Determine moisture using the Cruft[3] procedure with the following modifications. After aspirating the Penfield tube and without weighing it, add 0.500, 0.700 or 1.000 g (depending upon the expected total water content) of −100 or −200 mesh sample. Add sufficient flux to fill the long-stem funnel to two-thirds its height. In the case of phosphates, also add 1 g of ignited powdered silica or silicic acid. After adding the calcium carbonate and when the tube is sufficiently chilled, commence heating with a Meker-type blast burner and immediately increase the heat to a maximum to hasten the fusion and to decrease the heating time. After about 15 min, tap the bulk of the calcium carbonate into the molten fusion mixture. When a quiescent molten pool appears, heat for 5 min more (usually a total of 25 min from first heat application). Bring the tube to final dryness using the initial aspiration process.

RESULTS AND DISCUSSION

The minerals analyst is handicapped by the lack of adequate standards, when embarking on a new water-determining method. Precision is often lacking among analyses of the same samples done at varying times and in different laboratories. It is extremely difficult, therefore, to make meaningful interlaboratory comparisons of total water determinations. For this reason, the samples run by the moisture analyzer method have also been run by the modified Penfield method, the results of which are considered to be accurate within experimental error.

TABLE I

TOTAL WATER CONTENT (%) DETERMINED WITH THE MOISTURE ANALYZER AND THE PENFIELD METHOD

61-1332 *Fluorophlogopite* −100 *mesh*		4-178 *Amphibolite* −200 *mesh*		*M*109678[a] *Biotite* −100 *mesh*		3055-*Bio R* *Biotite* −200 *mesh*		*M*110920 *Piemontite* −270 *mesh*		*M*110921 *Piemontite* −270 *mesh*		*Soudan mine chlorite*[a]		$CuSO_4 \cdot 5H_2O$ *crystal*	
mg	%	*mg*	%	*mg*	%	*mg*	%	*mg*	%	*mg*	%	*mg*	%	*mg*	%
Moisture analyzer															
44.1	0.46	59.8	1.25	47.7	4.51	42.8	3.70	35.2	1.86	76.5	1.83	19.7	10.68	15.2	36.53
39.8	0.34	42.5	1.28	44.9	4.39	51.4	3.64	43.0	1.91	64.0	1.83	26.1	10.66	12.2	36.45
49.0	0.40	50.6	1.30	38.2	4.48	39.1	3.55	57.0	1.93	39.9	1.85	21.1	10.03	14.2	36.52
42.3	0.35	45.4	1.18	35.3	4.48	55.2	3.55	40.6	1.87	40.5	1.79	26.1	10.18	14.1	36.53
51.7	0.41	62.0	1.17	47.0	4.55	51.6	3.56	51.6	1.89	53.4	1.88			14.4	36.61
45.3	0.43	52.0	1.25	41.8	4.49	56.0	3.45	42.8	1.96	49.6	1.75			11.5	36.36
46.8	0.41	57.1	1.21	28.3	4.49	45.5	3.50	38.3	1.99	62.0	1.79				
42.6	0.46	56.0	1.21	30.3	4.51	65.1	3.44	51.0	1.87	64.6	1.78				
31.5	0.38	52.1	1.17	31.1	4.49	42.5	3.56	68.4	1.86	64.0	1.71				
36.7	0.46	49.1	1.27	21.3	4.47	38.0	3.62	51.9	1.89	53.7	1.85				
43.4	0.44	52.8	1.20	24.7	4.51	96.3	3.53								
		83.2	1.18	24.9	4.43	51.0	3.50								
	$\bar{X}_{11}=0.41$[c] $s=0.043$ R.D.$=0.49\%$		$\bar{X}_{12}=1.22$ $s=0.046$ R.D.$=3.77\%$		$\bar{X}_{12}=4.48$ $s=0.041$ R.D.$=0.92$		$\bar{X}_{12}=3.55$ $s=0.076$ R.D.$=2.14$		$\bar{X}_{10}=1.90$ $s=0.044$ R.D.$=2.35$		$\bar{X}_{10}=1.81$ $s=0.051$ R.D.$=2.82$		$\bar{X}_4=10.39$ $s=0.33$ R.D.$=3.18$		$\bar{X}_6=36.50$ $s=0.085$ R.D.$=0.23$ Theoretical $\%\ H_2O=36.08$
Penfield method															
0.41		(1.03)[b]		4.37		3.44		1.70		1.63		10.22			
		1.09		(4.28)[b]		3.46		1.73		1.67		10.60			
		1.10										10.10			
												10.58			
		$\bar{X}_2=1.10$		$\bar{X}_1=4.37$		$\bar{X}_2=3.45$		$\bar{X}_2=1.72$		$\bar{X}_2=1.65$		$\bar{X}_4=10.38$ $s=0.25$ R.D.$=2.41$			

[a] Furnace turned off over first $CaCO_3$ plug.

[b] Omitted from average.

[c] s = estimated standard deviation. R.D. = relative deviation = $\frac{s}{\bar{X}} \cdot 100\%$. $\bar{X}$ = average.

Precision

Table I illustrates the precision obtained with the moisture analyzer and compares the average results with those of the Penfield method. More than half the standard deviations of the moisture analyzer determinations lie between 0.04 and 0.05%, while the majority of the relative deviations fall within the 2–4% range.

In general, lack of better precision might be due in part to sampling variation more prevalent in small samples. Kleeman[19] has stated that, according to statistical theory, deviations may become significant if $< 10^6$ grains of rock sample are taken for analysis, for example, at -200 mesh, *ca.* 100 mg should be taken. With Kleeman's treatment and notation, Engels and Ingamells[20] have quantified the effects of sampling errors. By applying their method to total water in a hypothetical hornblende with 1% H_2O containing a 10% biotite contaminant with 4% H_2O, an overall relative sampling error can be calculated. If a 50-mg, -200 mesh sample is used, the overall relative sampling error is 0.32%. A 0.7-g portion of the same sample analyzed by the Penfield method suffers only a 0.09% sampling error. It can also be shown that the sampling error in the same hypothetical hornblende is far more sensitive to sample size than to degree of purity.

Figure 3, based on the data set forth in Table II, shows that the positive bias of the moisture analyzer results *versus* the Penfield results is a function of sample size in the case of the mixed minerals serpentine ($Mg_6(OH)_6Si_4O_{11}\cdot H_2O$ or $Mg_6(OH)_8Si_4O_{10}$) and brucite ($Mg(OH)_2$) at -200 mesh.

If the water determinations of Table I are uncorrected for the blank, the estimated standard deviation increases. Although the blank ranges from 0.01%

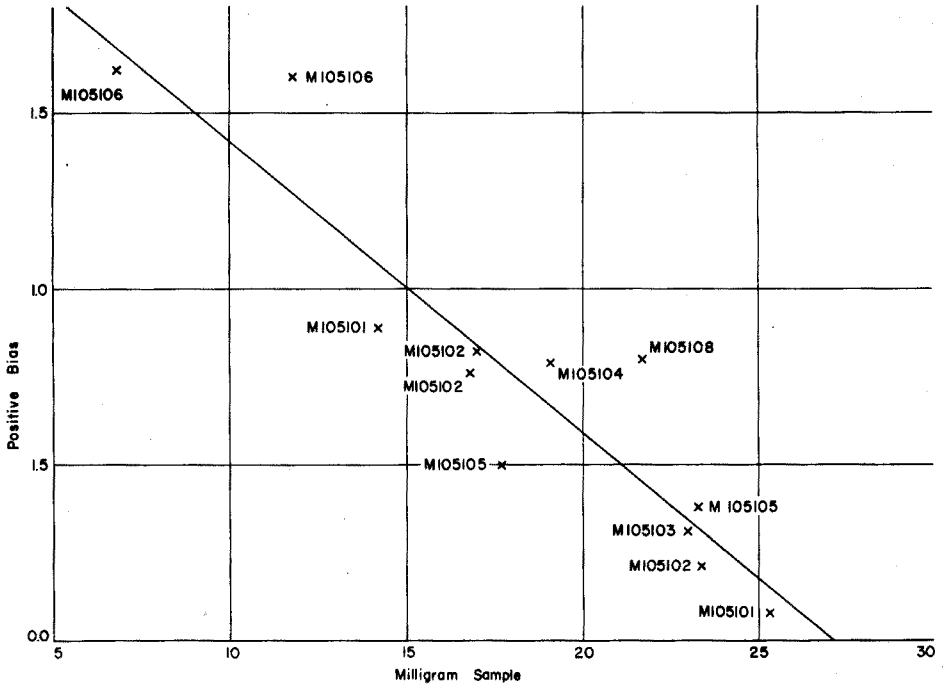

Fig. 3. Relationship of sample size to bias of moisture analyzer determinations (line fitted by least squares).

TABLE II

EFFECT OF SAMPLE SIZE ON MOISTURE ANALYZER DETERMINATIONS FOR A MINERAL WITH A HIGH WATER CONTENT

(Serpentine–brucite mixture, −200 mesh)

Sample	*Moisture analyzer*		*Penfield*	*Positive*
	% H_2O	*mg*	*% H_2O*	*bias*
M105101	16.2_9	14.2	15.40	0.89
M105101	15.4_8	25.3		0.08
M105102	17.2_8	16.8	16.52	0.76
M105102	17.3_4	17.0		0.82
M105102	16.7_3	23.4		0.21
M105103	17.1_1	23.0	16.80	0.31
M105104	16.2_9	19.1	15.50	0.79
M105105	16.0_8	17.7	15.58	0.50
M105105	15.9_6	23.3		0.38
M105106	18.3_9	6.8	16.76	1.62
M105106	18.3_7	11.8	16.78	1.60
M105108	16.6_0	21.7	15.80	0.80

(when a newly prepared bottle of flux is first opened) to 0.08 % (when the flux should be redried overnight at 110°), it does not seem to contribute to the data scatter. The increase in the blank values seems to stem chiefly from repeated exposure of a given bottle of flux to the laboratory atmosphere rather than from daily changes in humidity. Precision might also be improved in the moisture analyzer method if it were possible to mix flux and sample in the small porcelain boats as is done in the Penfield tubes. Also dependable material is needed for instrument calibration. Drummond "Microcaps" have recently been suggested for calibrating, but this laboratory has not yet completed its evaluation of the procedure.

Bias of moisture analyzer method

Table III, which also includes the average results of Table I, illustrates that there is no apparent correlation between bias and water magnitude when results obtained from the moisture analyzer method are compared to those from the modified Penfield method. With the exception of 7 samples, the moisture analyzer results demonstrate a positive bias—the largest group of samples falling within the 0.1–0.2 % bias range. A close similarity of bias exists within the group of biotites, between the 2 diopsides, the 2 piemontites, and in 2 of the 3 apatites.

The positive trend may be due, in part, to dust and moisture pick-up during weighing and loading, which involves a period of *ca.* 6 min, during 4 of which the sample of the serpentine–brucite mixture (M105108) lost 0.2 mg on standing in an to conduct an independent study of moisture pick-up in this laboratory. A 0.6-g sample of the serpentine–bruce mixture (M105108) lost 0.2 mg on standing in an open platinum crucible for a 24-hour period. The substance is not, therefore, particularly hygroscopic. Yet, 10-mg portions in either a platinum crucible or a porcelain boat may gain as much as 0.1 mg in a 10-min period.

TABLE III

COMPARATIVE SUMMARY OF WATER CONTENT (%) OF VARIOUS MINERALS

(Single determinations unless otherwise noted)

Sample	*Moisture analyzer*	*Penfield*	*Bias*
Almandine (M100975)	0.04	0.04	0.00
Amphibolite (4-178)	1.22 (12)	1.10 (2)	+0.12
Apatite (64M257)	0.69 (2)	0.59 (4)	+0.10
Apatite (64M259)	4.26 (2)	4.38 (2)	−0.12
Apatite (M105731)	0.18	0.04 (2)	+0.14
BioR (3055)	3.55 (12)	3.45 (2)	+0.10
Biotite (M109678)	4.48 (12)	4.37	+0.11
Biotite (M109679)	3.78 (2)	3.67	+0.11
Biotite (M109680)	4.69 (2)	4.59	+0.10
Biotite (M109681)	4.24 (5)	4.13	+0.11
Biotite (M103556)	4.20	4.08	+0.12
Chlorite (M104332)	12.23 (2)	11.47 (2)	+0.76
Chlorite (M104336)	11.42 (2)	11.12	+0.30
Chlorite (Soudan Mine)	10.39 (4)	10.38 (4)	+0.01
Chlorophaeite (M106503)	17.52 (2)	17.50	+0.01
Clinoptilolite (M103189)	15.28 (10)	15.64	−0.36
Clinopyroxene (M106532)	0.05 (3)	0.04	+0.01
Diopside (M105539)	0.00	0.08	−0.08
Diopside (M103550)	0.00	0.08	−0.08
Fluorophlogopite (61-1332)	0.42 (12)	0.41	+0.01
Hornblende (M103557)	2.17	1.91	+0.26
Hornblende (M106360)	1.01	1.03	−0.02
Hypersthene (M103549)	0.00	0.37	−0.37
Microcline (M103190)	0.60 (2)	0.34	+0.26
Piemontite (M110920)	1.90 (10)	1.72 (2)	+0.18
Piemontite (M110921)	1.81 (10)	1.65 (2)	+0.16

CONCLUSIONS

Approximately the same number of samples can be analyzed per day by either the moisture analyzer or the Penfield method. The latter has the advantage of a consistent blank for a given batch of flux when temperature and humidity remain relatively constant. In the former method, the blank drifts upward until the flux must be redried. The Penfield operation requires continual attention, whereas the moisture analyzer requires only intermittent attention. Other activities may be engaged in concurrently.

The moisture analyzer is most useful when a complete chemical analysis is required on a sample of < 1.5 g, that is, when a major portion of the sample cannot be spared for a macro Penfield determination. Compared to other micro methods, the moisture analyzer method is simple and convenient and requires no specific skills. If a careful study were made of the pertinent parameters, correction factors could probably be developed for the various mineral types in order to bring results in agreement with those obtainable by the macro Penfield method.

The authors thank C. O. Ingamells and credit him with the suggestions that permitted the successful adaptation of the method to minerals.

SUMMARY

A DuPont Moisture Analyzer is used in a microcoulometric method for determining water in minerals. Certain modifications, which include the heating of the sample outside the instrument, protect the system from acid gases and insure the conversion of all hydrogen to water vapor. Moisture analyzer data are compared to concurrent data obtained by a modified Penfield method. In general, there is a positive bias of from 0.1 to 0.2% in the moisture analyzer results and a similarity of bias in minerals of the same kind. Inhomogeneity, sample size, and moisture pick-up are invoked to explain deviations. The method is particularly applicable to small samples.

RÉSUMÉ

On propose une méthode microcoulométrique pour le dosage de l'eau dans les minerais. Les résultats obtenus par cette méthode (utilisant un contrôleur d'humidité DuPont) sont comparés avec ceux de la méthode de Penfield modifiée. Le procédé décrit convient particulièrement pour des petits échantillons.

ZUSAMMENFASSUNG

Ein DuPont-Feuchtigkeitsanalysator wird bei einer mikrocoulometrischen Methode zur Bestimmung von Wasser in Mineralen angewendet. Gewisse Abänderungen, u. a. die Erhitzung der Probe ausserhalb des Gerätes, schützen das System vor sauren Gasen und stellen die Umwandlung des gesamten Wasserstoffs zu Wasserdampf sicher. Die Ergebnisse des Feuchtigkeitsanalysators werden mit jenen verglichen, die nach einer modifizierten Penfield-Methode erhalten worden sind. Im allgemeinen liegen die Ergebnisse des Feuchtigkeitsanalysators um 0.1–0.2% höher, und es wird eine Gleichartigkeit der Abweichungen bei Mineralen derselben Art beobachtet. Die Abweichungen werden auf Inhomogenität, Probengrösse und Feuchtigkeitsaufnahme zurückgeführt. Die Methode eignet sich besonders für kleine Proben.

REFERENCES

1 S. L. Penfield, *Amer. J. Sci.*, 48 (1894) 30.
2 L. C. Peck, *Geol. Surv. Bull.* 1170, 1964.
3 E. F. Cruft, C. O. Ingamells and J. Muysson, *Geochim. Cosmochim. Acta*, 29 (1965) 581.
4 J. P. Riley, *Analyst*, 83 (1958) 42.
5 I. Friedman and R. L. Smith, *Geochim. Cosmochim. Acta*, 15 (1959) 218.
6 K. Fischer, *Z. Angew. Chem.*, 48 (1935) 394.
7 J. Mitchell, Jr. and D. M. Smith, *Aquametry*, Interscience, New York, 1948, p. 9ff.
8 D. J. Geary, *Determination of Moisture in Solids*, British Science Instrument Research Assoc., Chislehurt, Kent, 1956.
9 M. H. Aronson (Editor), *Moisture and Humidity Handbook*, Instruments Publishing Co., Pittsburgh, 1965.
10 A. Quesada and W. H. Dennen, *Geos (Caracas)*, 18 (1968) 41.
11 I. A. Breger and J. C. Chandler, *Anal. Chem.*, 41 (1969) 506.
12 J. W. Ancott and M. Marshall, *Mineral. Mag.*, 37 (1969) 256.

13 E. B. Sandell, *Mikrochim. Acta*, (1951) 487.
14 J. P. Riley and H. P. Williams, *Mikrochim. Acta*, (1959) 526.
15 T. Yoshimori and S. Ishiwari, *Bull. Chem. Soc. Jap.*, 42 (1969) 1282.
16 F. A. Keidel, *Anal. Chem.*, 31 (1959) 2043.
17 J. Horácek and J. Körbl, *Chem. Ind. (London)*, (1958) 101.
18 J. Körbl, *Chem. Listy*, 49 (1955) 858; 51 (1957) 27.
19 A. W. Kleeman, *J. Geol. Soc. Aust.*, 14 (1967) 43.
20 J. C. Engels and C. O. Ingamells, *Geochim. Cosmochim. Acta*, 34 (1970) 1007.

Analytica Chimica Acta
Elsevier Publishing Company, Amsterdam
Printed in The Netherlands

FURTHER INVESTIGATIONS OF ION-SELECTIVE ELECTRODES IN NON-AQUEOUS SOLVENTS

N. A. KAZARJAN* and E. PUNGOR
Institute for General and Analytical Chemistry, Technical University, Budapest (Hungary)
(Received 10th January 1972)

Recently the results obtained in a study of ion-selective membrane electrodes used in some non-aqueous solvents were summarized[1]. It was pointed out that the equations derived for aqueous media are also valid in non-aqueous media, if the solvents applied are alcohols.

There are many similarities between water and alcohols, and therefore this finding about the applicability of this theory of the membrane electrodes in aqueous and non-aqueous solvents did not seem surprising. However, the question then arose if the theoretical interpretation of the electrode behaviour would remain valid when other types of organic solvents were used.

To investigate this question, acetone was selected as a ketonic solvent and dimethylformamide as a basic solvent.

EXPERIMENTAL

Solvents and chemicals

Acetone and dimethylformamide (DMF) of REANAL quality were used. The experiments were carried out in mixtures of distilled water and the appropriate non-aqueous solvents. The mixtures were freshly prepared before use.

The amounts of the two solvents were generally changed in 10 or 20% steps.

All chemicals were of pro analysi grade. Before measurements, the chemicals were dissolved in the appropriate solvent mixture in the concentration desired.

Examination of the dissolution of the membrane layer

For this study silver iodide-based silicone rubber membrane disks were used. The membrane disks were weighed and immersed in the appropriate solvent mixture for a certain period of time. After soaking, the membrane disks were dried between filter paper and weighed on an analytical balance. Parallel to this, the colour change of the solvent mixture was observed.

Potential measurement

A precision pH meter (Model OP 205, Radelkis, Budapest) with an expanded scale was employed. The input resistance of the pH meter is greater than 10^{12} ohm.

The potential measurements were carried out in the following measuring cell: Ag/AgCl electrode–aqueous chloride solution–silicone rubber membrane– the appropriate halide dissolved in a solvent mixture–KNO_3 salt bridge–S.C.E.

---

* Permanent address: Mendeleev Institute of Chemical Technology, Moscow, U.S.S.R.

Determination of the solubility product of silver halide salts in aqueous acetone and dimethylformamide solution

The solubility products were determined on the basis of the potentiometric titration curves. For titration a solution containing the appropriate solvent mixture was prepared and titrated with an aqueous silver nitrate solution. The concentration of the titrant was two orders of magnitude higher than that of the solution to be titrated. As an indicator electrode, the appropriate halide-selective electrode was used. The solubility products were calculated from the titration curves by neglecting the dilution of the solution caused by the addition of the silver nitrate titrant.

Determination of the selectivity constants of iodide- and bromide-selective electrodes in aqueous acetone and dimethylformamide solutions

The selectivity constants were determined by two different methods in both solvent mixtures[2,3]. In the direct method, direct potential measurements were carried out in the appropriate non-aqueous solution containing a constant amount of potassium iodide or potassium bromide and various amounts of the ion for which the selectivity constant of the electrode was being examined. In the indirect method, a non-aqueous solution containing potassium iodide or bromide and another salt in the same concentration, was titrated with an aqueous silver nitrate solution; the concentration of the titrant was two orders of magnitude higher than that of the solution to be measured. In the former case, the concentrations measured at the break-point of the potential *vs.* $-\log c_1$ curve, and in the latter case the concentrations obtained when coprecipitation started in the solution, were used for experimental determination of the selectivity constants. The concentration of the iodide or bromide at the coprecipitation point was calculated with the help of the Nernst equation by considering the initial concentration of iodide or bromide and the potential decrease.

The selectivity constants were calculated as given in the literature[2,3], with the solubility products determined experimentally.

RESULTS AND DISCUSSION

The determination of the swelling of the silicone rubber-based silver iodide electrode in water–acetone and in water–DMF mixtures clearly showed that acetone can only be used in concentrations lower than 60%, because with higher concentrations a colour change of the solvent mixture was observed. When DMF was used, no similar effect was found in the whole concentration range.

TABLE I

SOLUBILITY PRODUCTS OF SILVER HALIDE SALTS IN AQUEOUS DIMETHYLFORMAMIDE MIXTURES

DMF:H_2O (*v/v*, %)	*Mole fraction of DMF*	*Solubility products*		
		AgI	*AgBr*	*AgCl*
0:100	—	15.96	12.36	9.82
10:90	0.0252	15.96	12.22	10.04
40:60	0.133	15.76	12.50	10.32
60:40	0.259	15.34	12.70	10.66

TABLE II

SOLUBILITY PRODUCTS OF SILVER HALIDE SALTS IN AQUEOUS ACETONE MIXTURES

Acetone: H_2O (*v/v*, %)	*Mole fraction of acetone*	*Solubility products*		
		AgI	*AgBr*	*AgCl*
0:100		15.96	12.36	9.82
10:90	0.0269	16.2	12.4	9.8
20:80	0.0583	16.2	12.6	10.0
30:70	0.0983	16.2	12.6	10.2
40:60	0.142	16.2	12.6	10.5

The results of measurements of solubility products of the silver halide precipitates are summarized in Table I for DMF and in Table II for acetone. Both Tables contain for comparison the values measured in distilled water. From these results it can be concluded that the behaviour of silver iodide electrodes does not alter too much when acetone–water mixtures are used as solvent. The situation with this solvent is similar to that observed in mixtures of distilled water and an alcohol. In contrast to this, DMF causes significant changes in the character of the precipitates. It is of interest that the silver iodide and chloride precipitates show significant alterations in the solubility product, whereas silver bromide does not. In connection with this finding, it should be stressed that the solubility product depends here in a different way on the composition of the solvent than has been found in the case of other solvents.

TABLE III

SELECTIVITY CONSTANTS OF AN IODIDE-SELECTIVE ELECTRODE TO BROMIDE IN MIXTURES OF DISTILLED WATER AND ACETONE

Acetone: H_2O (*v/v*, %)	*pK*	
	Theoretical	*Experimental*
10:90	3.82	3.75
20:80	3.68	3.60
30:70	3.62	3.56
40:60	3.56	3.55

TABLE IV

SELECTIVITY CONSTANTS OF AN IODIDE-SELECTIVE ELECTRODE TO BROMIDE IN MIXTURES OF DISTILLED WATER AND DIMETHYLFORMAMIDE

DMF: H_2O (*v/v*, %)	*pK*	
	Theoretical	*Experimental*
10:90	3.74	3.75
40:60	3.26	3.20
60:40	2.64	2.60

Since the electrodes did not respond properly to changes in halide concentration in concentrated DMF solutions, it was impossible to use them in mixtures with DMF contents above 60%.

A further interesting study was the measurement of the selectivity constants. The results obtained are summarized in Tables III and IV. The agreement between the values measured and calculated is very good.

The two solvents can be used for investigations of ion-selective electrodes only in mixtures of high water content. In both cases the electrodes would be damaged in more concentrated non-aqueous mixtures.

It was of interest to investigate how other solvents affect the behaviour of the electrodes. It was found, for example, that acetonitrile and methanol–benzene mixtures cannot be used as solvents in these investigations. In the former case, the electrode gave a constant potential which did not depend on the activity of the iodide ions, and in the latter case, the electrode became fragile on contact with the solvent.

SUMMARY

The applicability of silicone rubber-based ion-selective electrodes was studied in mixtures of distilled water with acetone and dimethylformamide. It was found that the two non-aqueous solvents can be used in investigations of ion-selective electrodes only in mixtures of high water content.

RÉSUMÉ

Les possibilités d'application des électrodes sélectives ioniques sont examinées en milieu eau distillée–acétone et diméthylformamide. On arrive à la conclusion que ces deux solvants non aqueux ne peuvent être utilisés que mélangés à beaucoup d'eau.

ZUSAMMENFASSUNG

Die Verwendbarkeit von ionenselektiven Elektroden auf Silikonkautschukbasis in Gemischen von destilliertem Wasser mit Aceton und Dimethylformamid wurde untersucht. Es wurde festgestellt, dass die beiden nichtwässrigen Lösungsmittel bei Untersuchungen ionenselektiver Elektroden nur in Gemischen mit hohem Wassergehalt verwendet werden können.

REFERENCES

1 N. A. Kazarjan and E. Pungor, *Anal. Chim. Acta*, 51 (1970) 213.
2 K. Tóth, *Candidate's Thesis*, Veszprém, 1969.
3 E. Pungor and K. Tóth, *Anal. Chim. Acta*, 47 (1969) 291.

Analytica Chimica Acta
Elsevier Publishing Company, Amsterdam
Printed in The Netherlands

UTILISATION DES CORRELATIONS DE HAMMETT A L'ETUDE DES EQUILIBRES TAUTOMERES

JEAN-CLAUDE HALLE ET ROBERT SCHAAL
avec la collaboration de ANTONIO DI NALLO
Laboratoire de Physicochimie des Solutions, E.N.S.C.P. (L.A. C.N.R.S. 146), 11 rue Pierre et Marie Curie, Paris V° (France)

(Reçu le 21 décembre 1971)

La relation classique de Hammett[1] :

$$\log K_X - \log K_H = \rho \cdot \sigma_X \qquad (1)$$

qui avait initialement pour but de rendre compte des effets électroniques du substituant X sur la réactivité d'une fonction chimique, a très vite perdu sa généralité en raison de la nécessité d'adapter la constante de substituant σ_X à la fonction chimique considérée[2-4]. L'abondance des échelles σ qui en a résulté n'a cependant pas détruit l'intérêt de l'équation de Hammett qui a ainsi contribué à une meilleure connaissance des effets de substituant en chimie organique. Le but de ce travail est de montrer l'efficacité de la relation de Hammett en ce qui concerne l'étude de l'influence du solvant sur l'ionisation protonique d'acides AH de même famille chimique et la possibilité de classer ces indicateurs en familles homogènes.

Nous désignerons respectivement par K_H^S et K_X^S les constantes d'acidité, déterminées dans le solvant S, de l'acide non substitué et de l'acide X-substitué. D'autre part, nous supposerons que la constante de substitutant σ_X est indépendante du milieu, ce qui revient à inclure l'effet de solvant dans la constante de réaction ρ qui dépend également de la fonction acide et de la température. Nous réunirons dans une même famille homogène les acides dont la substitution X s'accompagne, dans les solvants S_1 et S_2, d'une variation d'acidité vérifiant l'équation de Hammett, soit :

$$pK_H^{S_1} - pK_X^{S_1} = \rho^{S_1} \cdot \sigma_X$$
$$pK_H^{S_2} - pK_X^{S_2} = \rho^{S_2} \cdot \sigma_X$$

L'élimination de σ_X entre ces deux relations conduit à :

$$pK_X^{S_2} = \frac{\rho^{S_2}}{\rho^{S_1}} \cdot pK_X^{S_1} + pK_H^{S_2} - \frac{\rho^{S_2}}{\rho^{S_1}} \cdot pK_H^{S_1} \qquad (2)$$

Il ressort de cette expression que la linéarité du graphe $pK_X^{S_2} = f(pK_X^{S_1})$, de pente ρ^{S_2}/ρ^{S_1}, et dont l'ordonnée à l'origine ne dépend que des solvants, est un critère d'appartenance des indicateurs à la même famille de Hammett sans que nous ayons pour cela à effectuer un choix parmi tous les facteurs σ.

L'efficacité de ce procédé d'investigation est encore accrue si l'on travaille en milieu mixte. Le contrôle du classement des acides en familles homogènes, effectué à partir des paramètres relatifs aux solvants purs, dont la nature est parfois très

différente, est en effet rendu possible pour chaque mélange et l'effet du changement de solvant peut être ainsi analysé progressivement. C'est notamment le cas des mélanges avec l'eau du diméthylsulfoxyde dont l'étude thermodynamique[5,6] nous a déjà conduit à examiner sous cet aspect, le comportement des acides acétiques, des phénols et des indoles[7,8]. Nous présentons dans ce travail les résultats relatifs à quelques acides benzoïques et anilines (acidités φ-NH_3^+/φ-NH_2).

DÉTERMINATION DES CONSTANTES D'ACIDITÉ

Les constantes d'acidité K^S ont été déterminées potentiométriquement à 20° au moyen d'une électrode de verre (type Radiometer G.202 B) dont le fonctionnement réversible a été contrôlé dans chaque milieu S, à partir de solutions tamponnées, calibrées à l'électrode d'hydrogène[6]. Les solutions de mesure ont été réalisées à force ionique 10^{-2} M, en salifiant respectivement au demi les acides benzoïques et les anilines ($c = 2 \cdot 10^{-2}$ M), par de la soude ($b = 10^{-2}$ M) ou par de l'acide chlorhydrique ($a = 10^{-2}$ M). Dans ces conditions le pK_a^S relatif aux équilibres d'ionisation suivants :

$$AH + S \rightleftarrows A^- + S^+ \qquad BH^+ + S \rightleftarrows B + S^+$$

TABLEAU I

CONSTANTES D'ACIDITÉ DES ACIDES BENZOÏQUES X-SUBSTITUÉS ET DES CATIONS ANILINIUMS Y-SUBSTITUÉS DANS LES MÉLANGES EAU–DMSO ($t = 20°$)
(i = insoluble)

No.	*% DMSO en masse*	0	10.8	21.3	31.7	41.4	51.2	61.2	70.5	80.4	86.4	91.0	95.5	100
	X-													
1	*p*-OH	4.59[b]	4.65	4.78	5.06	5.34	5.70	6.21	6.97	7.95	8.80	9.49	10.22	11.8[f]
2	*m*-OH	4.08[b]	4.28	4.33	4.62	4.86	5.24	5.74	6.47	7.41	8.20	8.89	9.72	11.1[f]
3	*p*-OCH_3	4.47[b]	i	i	4.96	5.24	5.58	6.06	6.77	7.70	8.51	9.17	9.97	
4	*o*-OCH_3	4.09[b]	4.25	4.43	4.74	5.04	5.44	5.93	6.67	7.59	8.39	9.01	9.72	
5	H[a]	4.21[b]	4.33	4.48	4.70	4.92	5.25	5.74	6.40	7.30	8.08	8.69	9.45	10.9[e]
6	*p*-Cl	3.99[b]	i	i	i	i	i	5.21	5.87	6.65	7.42	8.06	8.67	10.1[f]
7	*m*-Cl	3.83[b]	i	4.00	4.19	4.40	4.66	5.06	5.67	6.50	7.16	7.78	8.32	
8	*o*-Cl	2.94[b]	3.08	3.30	3.57	3.81	4.26	4.80	5.42	6.23	6.99	7.61	8.25	9.29[h]
9	*p*-NO_2	3.42[b]	i	i	3.77	3.91	4.18	4.52	5.09	5.77	6.56	7.11	7.70	9.04[h]
10	*m*-NO_2	3.49[b]	3.55	3.60	3.79	3.95	4.22	4.54	5.13	5.81	6.54	7.16	7.80	9.17[h]
11	*o*-NO_2	2.17[b]	2.39	2.59	2.90	3.18	3.59	4.03	4.67	5.42	6.06	6.61	7.18	8.18[h]
12	diNO_2-3,5	2.82[b]	2.93	2.90	3.04	3.14	3.38	3.66	4.12	4.69	5.31	5.73	6.33	7.4[g]
	Y-													
13	*p*-OH	5.65[d]	5.53	5.37	5.34	5.21	5.08	4.99	4.93	4.93	5.04	5.27	5.40	
14	*p*-OCH_3	5.44[c]	5.29	5.24	5.04	4.90	4.72	4.58	4.46	4.40	4.48	4.65	4.75	
15	*o*-OCH_3	4.61[c]	4.47	4.27	4.16	4.03	3.81	3.57	3.38	3.18	3.24	3.48	3.47	
16	H	4.69[c]	4.55	4.35	4.26	4.06	3.87	3.64	3.42	3.31	3.32	3.46	3.61	3.7[e]
17	*p*-F	4.73[c]	4.54	4.33	4.20	4.01	3.77	3.52	3.25	3.02	3.10	3.24	3.36	
18	*p*-Cl	4.07[c]	3.88	3.65	3.50	3.28	2.99	2.78	2.47	2.27	2.31	2.36	2.52	
19	*p*-Br	3.95[c]	3.67	3.44	3.32	3.07	2.82	2.53	2.27	1.91	1.93	2.15	2.45	
20	*m*-Cl	3.60[c]	3.33	3.16	3.01	2.74	2.44	2.16	1.90	1.5	1.7	1.7	1.87	
21	*p*-COOH	2.41[b]	2.33	2.07	1.87	1.6	—	—	—	—	—	—	—	

[a] Réf. 6. [b] Réf. 9. [c] Réf. 11. [d] Réf. 12. [e] Réf. 13. [f] Réf. 14. [g] Réf. 15. [h] Réf. 16.

est relié à l'activité du proton solvaté dans S, que nous mesurons à l'électrode de verre, par les expressions:

$$pK_a^S = pS^+ - \log \frac{b+x}{c-b-x} + B(b+x)^{\frac{1}{2}}$$

avec $\log x = -pS^+ + B(b+x)^{\frac{1}{2}} \simeq -pS^+ + Bb^{\frac{1}{2}}$

et (3)

$$pK_a^S = pS^+ - \log \frac{c-a+x}{a-x} - Ba^{\frac{1}{2}}$$

avec $\log x = -pS^+ + Ba^{\frac{1}{2}}$

où B désigne le coefficient de Debye–Hückel estimé à partir des pentes des graphes qui conduisent aux produits ioniques[5].

Lorsque le pS^+ mesuré dépasse 4 unités, le calcul des constantes K_a^S se trouve simplifié car le terme x, qui rend compte de la dissociation propre de l'acide, devient négligeable*. On a alors:

$pK_a^S = pS^+ + 0.1\ B$ pour les acides benzoïques et

$pK_a^S = pS^+ - 0.1\ B$ pour les anilines.

Nos résultats qui sont rassemblés dans le Tableau I, sont en excellent accord

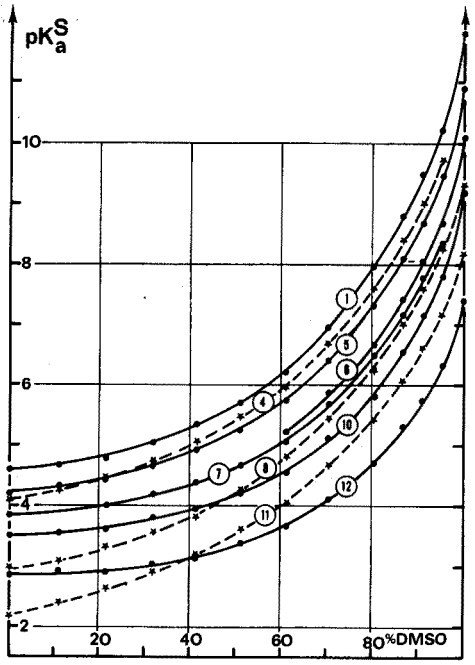

Fig. 1. Variation des constantes d'acidité des acides benzoïques avec le pourcentage en masse de DMSO. La numérotation est celle du Tableau I.

* L'erreur relative introduite est alors inférieure à 1%.

avec les déterminations faites dans l'eau à 20°*. Le Tableau I rapporte également les constantes d'acidité déterminées potentiométriquement dans le diméthylsulfoxyde anhydre au moyen d'une électrode de verre[14-16] ou d'une électrode d'hydrogène[13]: leurs valeurs permettent de prolonger de façon continue les courbes de pK_a^S établies dans les solvants mixtes** (Fig. 1).

INFLUENCE DU DIMÉTHYLSULFOXYDE SUR LES CONSTANTES D'ACIDITÉ

Alors que l'augmentation de la teneur en DMSO accroît le pK_a des acides moléculaires: acides benzoïques et acétiques, phénols et indoles[7], un effet contraire caractérise les cations aniliniums. Il convient cependant de noter qu'après une exaltation importante de l'acidité (au-delà de 50% de DMSO l'acidité du cation *p*-carboxyanilinium devient trop forte pour être déterminée par potentiométrie), les courbes $pK_a^S = f(\%\ \text{DMSO})$ présentent un minimum situé vers 80% de DMSO en masse ce qui identifie la situation à celle déjà observée dans un grand nombre de solvants hydroorganiques et notamment dans les mélanges eau–alcool[19,20]. Ce minimum est attribué à la compétition entre l'augmentation de la solubilité de la molécule B, lors-

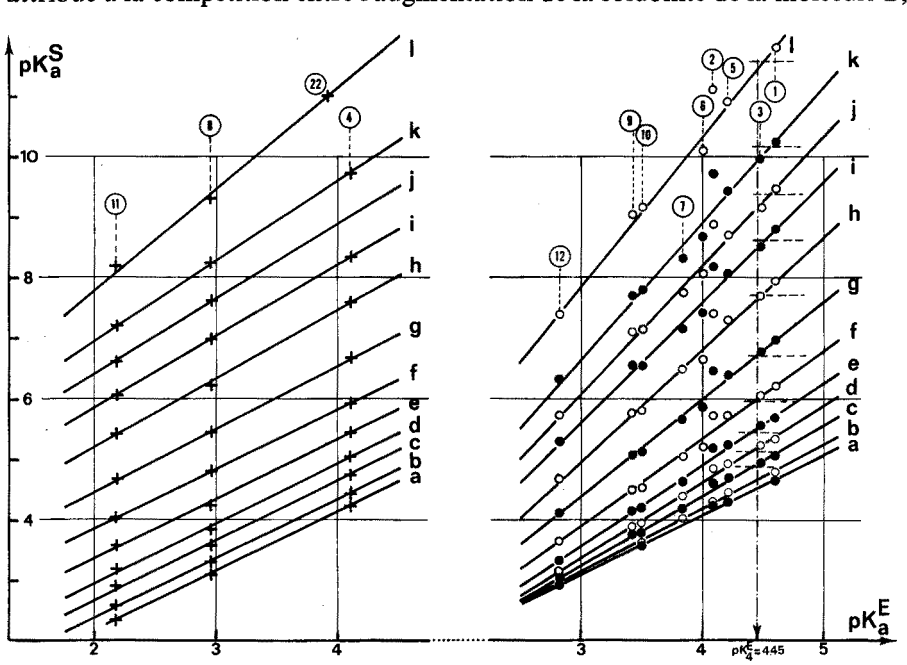

Fig. 2. Corrélations $pK_a^S = f(pK_a^E)$ relatives aux acides benzoïques substitués dans les mélanges contenant: 10.8, 21.3, 31.7, 41.4, 51.2, 61.2, 70.5, 80.4, 86.4, 91.0, 95.5 et 100% de DMSO en masse (droites de a à l). La numérotation est celle du Tableau I. Le composé 22 est l'acide méthyl-2 benzoïque: réf. 13.

* Entre 20 et 25°, l'effet de température sur le pK aqueux des acides benzoïques est pratiquement négligeable[10], ce qui justifie le report dans le Tableau I de quelques pK_a^E mesurés à 25°[9].

** Nous n'avons pas retenu les résultats d'une étude rapportant l'acidité dans ces mélanges, de quelques acides benzoïques[17]. Les pK_a obtenus sont, en effet, très supérieurs aux nôtres alors que nos valeurs coïncident, en ce qui concerne l'acide benzoïque, avec les mesures de Morel[18] et sont, de plus, cohérentes avec les déterminations réalisées dans le DMSO anhydre[13-16].

que la teneur en solvant organique augmente, ce qui exalte l'acidité du cation correspondant BH^+ et la diminution de l'activité de l'eau qui engendre un effet contraire[19].

Les graphes $pK^S = f(pK^E)$ qui rapportent à l'eau (E) les résultats obtenus dans les milieux mixtes S de teneur en DMSO variable, sont réunis dans les Figs. 2 et 3.

Alors que les acides benzoïques et les anilines *méta* et *para* substitués s'intègrent respectivement dans une même famille homogène, la substitution en *ortho* de la fonction carboxylique écarte l'indicateur de la corrélation. De plus, la linéarité des graphes $pK^S = f(pK^E)$ correspondants aux acides benzoïques *ortho* substitués justifie la réunion de ces composés en une autre famille. Nous avons d'ailleurs pu vérifier, à partir des constantes d'acidité mesurées par Thuaire[21] que le comportement des acides benzoïques dans les milieux hydro-éthanoliques, nécessite également une telle distinction. Cette situation s'oppose donc à celle des phénols pour lesquels nous avons montré l'existence d'une famille unique regroupant la plupart des phénols substitués en *méta*, *para* et *ortho*[7,8].

TABLEAU II

VARIATION DE ρ^S/ρ^E AVEC LA TENEUR DU MILIEU EN DMSO

%DMSO en masse		10.8	21.3	31.7	41.4	51.2	61.2	70.5	80.4	86.4	91.0	95.5	100
Ac. benzoïques	*m-, p-,*	1.0_0	1.0_5	1.1_6	1.2_5	1.3_5	1.4_4	1.6_0	1.8_5	2.0_0	2.1_3	2.2_7	2.5_1
substitués en	*o-*	1.0_0	1.0_0	1.0_0	1.0_0	1.0_0	1.0_0	1.0_4	1.1_3	1.1_8	1.2_4	1.3_3	1.7_4
Cations aniliniums		1.0_6	1.1_3	1.1_5	1.2_1	1.2_9	1.3_8	1.4_7	1.6_7	1.6_7	1.6_7	1.6_7	
Acides acétiques		1.0_2	1.0_4	1.0_4	1.0_7	1.0_7	1.1_0	1.1_5	1.2_5	1.3_4	1.4_2	1.5_2	1.9_3
Phénols		1.0_1	1.0_5	1.1_2	1.1_6	1.2_3	1.3_1	1.4_2	1.5_8	1.6_9	1.8_0	1.8_6	1.9_3

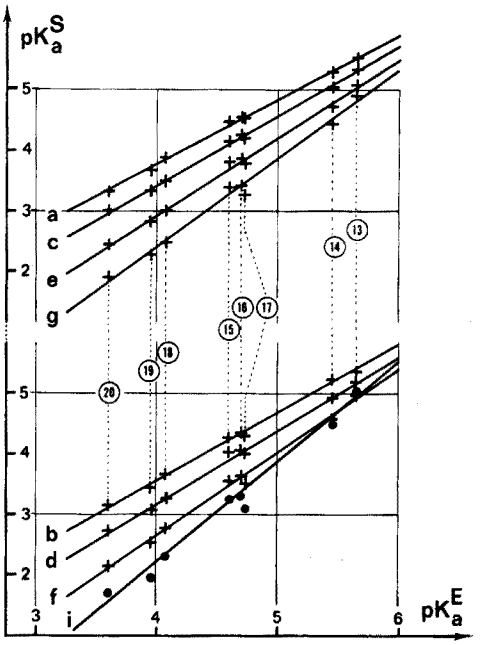

Fig. 3. Corrélations $pK^S_a = f(pK^E_a)$ relatives aux cations aniliniums substitués. Les milieux S sont identiques à ceux de la Fig. 2 et la numérotation est celle du Tableau I.

Dans le but d'examiner l'influence du diméthylsulfoxyde sur les constantes de réactions ρ^S, nous avons rassemblé dans le Tableau II les pentes des droites $pK^S = f(pK^E)$ des Fig. 2 et 3 et, afin d'effectuer la comparaison avec d'autres fonctions chimiques, nous avons également consigné dans ce Tableau, les résultats relatifs aux acides acétiques et aux phénols[8]. Quelle que soit la fonction chimique considérée, on observe une augmentation régulière de la constante de réaction ρ^S avec la teneur du milieu en DMSO. Ce fait traduit l'effet croissant des substituants et explique, au sein d'une même famille homogène la divergence des graphes $pK^S = f(\%$ DMSO) vers les mélanges riches en diméthylsulfoxyde (Fig. 1). L'évolution des constantes de réaction avec la composition du mélange solvant remet donc en cause la validité même des fonctions d'acidité construites en milieu ternaire à partir du classique procédé de recoupement de Hammett et Deyrup[22], puisque cette technique nécessite un parallélisme rigoureux entre indicateurs successifs sur toute l'étendue des compositions.

L'exaltation de ρ^S avec la teneur du milieu en solvant dipolaire aprotique est maximum pour les acides benzoïques *méta* et *para* substitués*. En revanche, on constate que la plus faible variation correspond aux acides benzoïques *ortho* substitués. L'évolution très voisine des valeurs du rapport ρ^S/ρ^E, relatif aux acides benzoïques *ortho* substitués d'une part et acétiques d'autre part, met d'ailleurs en évidence le rôle prépondérant de l'effet inducteur du substituant sur l'ionisation de la fonction carboxylique adjacente.

APPLICATION: ÉTUDE DE L'ACIDE *m*-AMINOBENZOÏQUE DANS LES MILIEUX MIXTES EAU–DMSO

Nous avons vu que, si l'élévation de la teneur en DMSO diminue l'acidité de l'acide benzoïque, elle exalte par contre la mobilité protonique du cation anilinium

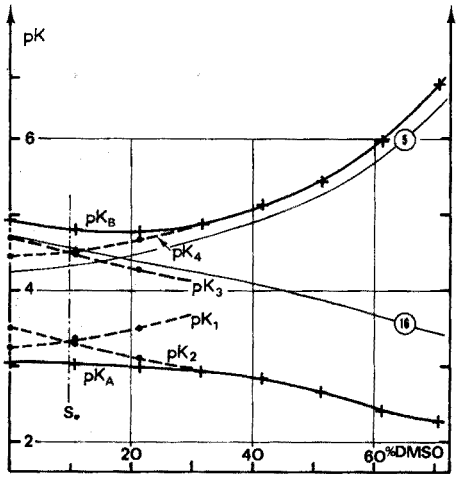

Fig. 4. Constantes d'acidité relatives à l'acide *m*-aminobenzoïque ($t = 20°$). La numérotation est celle du Tableau I.

* La valeur obtenue dans le DMSO pur (2.5_1) est identique à celle proposée par Kolthoff et Chantooni: 2.4_8[16] et très voisine du résultat de Ritchie et Uschold: 2.6[14a].

de sorte que l'écart qui sépare ces deux acidités décroît pour s'annuler dans le milieu contenant 18% de DMSO en masse où l'on assiste à l'inversion de l'ordre des acidités (Fig. 4). Ce résultat n'est pas sans incidence sur le comportement de l'acide *m*-aminobenzoïque. Il est en effet prévisible que si, dans les mélanges riches en eau, quatre espèces coexistent en équilibre selon le schéma suivant:

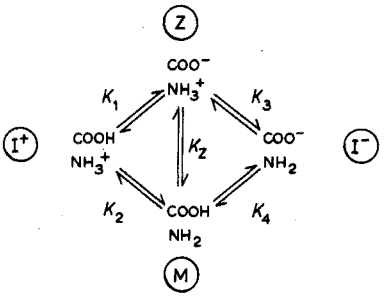

l'existence de la forme zwittérionique Z est peu probable dans les milieux riches en DMSO. Pour résoudre un tel système nous avons mesuré potentiométriquement les constantes apparentes K_A et K_B relatives aux équilibres suivants:

$$I^+ \overset{K_A}{\rightleftharpoons} X \overset{K_B}{\rightleftharpoons} I^-$$

où X représente le mélange des formes zwittérionique et moléculaire, dont le rapport K_Z ne dépend que du mélange solvant, en reprenant la méthode que nous avons précédemment décrite. En effet, dans la mesure où le coefficient d'activité du zwittérion est voisin de l'unité[24], les expressions (3) restent valables et conduisent respectivement aux pK_B^S et pK_A^S dont les valeurs sont rassemblées dans le Tableau III.

Lorsque les quatre espèces coexistent en solution, les constantes vraies K_1, K_2, K_3 et K_4 sont reliées aux constantes apparentes K_A et K_B par les trois relations indépendantes suivantes:

$$K_1 + K_2 = K_A$$
$$\frac{1}{K_3} + \frac{1}{K_4} = \frac{1}{K_B} \qquad (4)$$
$$\frac{K_1}{K_2} = \frac{K_4}{K_3} = K_Z$$

qui sont malheureusement insuffisantes pour déterminer les quatre constantes vraies. La résolution complète du problème nécessite donc une donnée supplémentaire et à cet regard diverses hypothèses extrathermodynamiques ont été envisagées[23,24,26]. Nous avons d'ailleurs utilisé l'une d'entre elles avec succès lors de l'étude, dans ces milieux mixtes, de l'inversion des deux acidités protoniques des acides trinitro-2,4,6 diphénylamine carboxyliques-4′ et -3′[8,25]. Nous proposons maintenant un nouveau procédé d'investigation qui est basé sur l'utilisation des corrélations précédemment décrites.

Si nous interpolons sur les droites $pK^S = f(pK^E)$ relatives aux acides benzoïques

TABLEAU III

CONSTANTES THERMODYNAMIQUES DE L'ACIDE *m*-AMINOBENZOÏQUE, DÉTERMINÉES À 20° DANS LES MILIEUX MIXTES EAU–DMSO

% DMSO en masse	0	10.8	21.3	31.7	41.4	51.2	61.2	70.5	80.4	86.4	91	95.5	100
pK_A	3.05	3.04	2.97	2.93	2.83	2.65	2.41	2.27	2.22	2.24	2.30	2.40	
pK_B	4.89	4.79	4.77	4.88	5.13	5.44	5.97	6.72	7.74	8.63	9.40	10.20	11.6[a]
pK_4	4.45	4.52	4.65				Identique à pK_B						
pK_3	4.69	4.46	4.27										
pK_Z	−0.24	0.06	0.38										
pK_2	3.49	3.31	3.12				Identique à pK_A						
pK_1	3.25	3.37	3.50										
t%	64	47	30										

[a] Référence 14a.

méta et *para* substitués (Fig. 2) les valeurs de pK_B^S correspondant à l'acide *m*-aminobenzoïque, nous obtenons, dans les mélanges contenant plus de 30% de DMSO, une excellente cohérence entre les diverses valeurs de pK_4^E ainsi interpolées ($pK_4^E = 4.45$). Ce résultat indique donc l'appartenance de l'acide *m*-aminobenzoïque à la famille homogène des acides benzoïques *méta* et *para* substitués et implique, qu'au-delà de 30% de DMSO en masse la molécule M est la seule espèce intermédiaire présente en solution. Dans ces mélanges, les constantes apparentes K_A et K_B s'identifient donc respectivement aux constantes vraies K_2 et K_4. D'autre part, les intersections des droites $pK^S = f(pK^E)$ relatives aux milieux titrant 10.8 et 21.3% de DMSO en masse avec la verticale $pK^E = 4.45$ permettent l'estimation très correcte des constantes vraies K_4 correspondant à ces milieux. Le système (4) est alors parfaitement défini et le calcul des constantes vraies K_3, K_2 et K_1 est aisé. Les valeurs obtenues, réunies dans le Tableau III, permettent de prolonger jusqu'à l'eau et de façon continue, les courbes déterminées potentiométriquement (Fig. 4). Les courbes pK_1 et pK_2 d'une part, pK_3 et pK_4 d'autre part se croisent dans le même milieu S_0 pour lequel $K_Z = 1$; nous pouvons également vérifier que dans ce mélange, contenant 10% de DMSO en masse, on a bien :

$$pK_B - pK_4 = pK_2 - pK_A = \log 2$$

Les taux de zwittérion

$$t = \frac{[Z]}{[M]+[Z]}$$

calculés dans le Tableau III, témoignent de l'effet considérable exercé par le diméthylsulfoxyde sur l'équilibre tautomère $M \rightleftharpoons Z$: 30% de solvant dipolaire aprotique suffit à déplacer totalement vers la gauche cet équilibre alors qu'en présence de méthanol il faut atteindre 60% de solvant organique pour obtenir un résultat identique[24]. En solution aqueuse, le taux de zwittérion obtenu : 64%, est comparable aux valeurs déjà avancées, compte tenu de l'imprécision notable qui accompagne de telles déterminations[24,26–31].

Nous avons tenté la vérification des résultats obtenus en transposant aux cations aniliniums la méthode des corrélations. L'interpolation sur les droites $pK^S =$

$f(pK^E)$ (Fig. 3) des pK_A mesurés potentiométriquement ne conduit pas à une valeur aqueuse unique de pK_2 ($3.6 < pK_2^E < 4.1$)*; l'exclusion du cation anilinium substitué en *méta* par la fonction carboxylique de la famille homogène constituée par la plupart des ions aniliniums est donc nécessaire, ce qui rend, dans ce cas, la méthode des corrélations inapplicable.

La comparaison des constantes vraies avec les pK_a des acides de référence permet d'autre part de préciser l'influence des substituants. Alors que la fonction carboxylique voit son acidité aqueuse diminuer d'environ 0.2 unité par la présence en *méta* du substituant $-NH_2$, l'introduction du groupe ammonio ($-NH_3^+$) sur ce même site provoque un effet contraire: l'exaltation d'acidité égale à 0.96 unité pK, comparable à celle du groupement *m*-triméthylammonium ($\sigma_{m(N(CH_3)_3^+} = 0.88$[3]), confirme le résultat de Serjeant[31]: $\sigma_{mNH_3^+} = 0.98$. En ce qui concerne l'ionisation du cation anilinium, l'augmentation d'acidité qui accompagne la substitution *m*-COOH est considérable ($\Delta pK^E = -1.20$). En revanche, le groupement *m*-COO^- laisse pratiquement invariable la mobilité protonique de la fonction $-NH_3^+$.

RÉSUMÉ

Les constantes d'acidité relatives à des acides benzoïques et cations aniliniums diversement substitués ont été mesurées par potentiométrie à 20° dans les mélanges eau–DMSO (S) et sont comparées aux pK aqueux (E) correspondants. La linéarité des graphes $pK_X^S = f(pK_X^E)$ permet de rassembler dans la même famille homogène les indicateurs dont la substitution X engendre une variation d'acidité vérifiant la classique relation de Hammett. Ce type de corrélation est mis à profit pour étudier l'équilibre tautomère zwittérionique de l'acide *m*-aminobenzoïque.

SUMMARY

The acidity constants for various substituted benzoic acids and anilinium cations have been measured potentiometrically in aqueous dimethylsulphoxide media at 20°. The values obtained (pK_X^S) are compared with the corresponding values for aqueous media (pK_X^E). The linearity of the $pK_X^S = f(pK_X^E)$ plots makes it possible to arrange in the same homogeneous series those compounds for which the substituent X causes a change in acidity verifying the classic Hammett relationship. This type of correlation is utilized to study the tautomeric zwitterion equilibrium of *m*-aminobenzoic acid.

ZUSAMMENFASSUNG

Die Aciditätskonstanten für verschiedene substituierte Benzoesäuren und Aniliniumkationen wurden potentiometrisch in wässrigen Dimethylsulfoxid-Medien bei 20° gemessen. Die erhaltenen Werte (pK_X^S) werden mit den korrespondierenden Werten für wässrige Medien (pK_X^E) verglichen. Die Linearität der Auftragung $pK_X^S = f(pK_X^E)$ ermöglicht es, in derselben homogenen Reihe jene Verbindungen

* Pour les plus fortes acidités, les pK_A obtenus potentiométriquement ont été contrôlés au moyen de mesures spectrophotométriques plus précises.

anzuordnen, bei denen der Substituent X eine Änderung der Acidität in Bestätigung der klassischen Hammett-Beziehung bewirkt. Diese Art der Wechselbeziehung wird für die Untersuchung des tautomeren Zwitterionen-Gleichgewichts von *m*-Aminobenzoesäure angewendet.

BIBLIOGRAPHIE

1 L. P. HAMMETT, *Chem. Rev.*, 17 (1935) 125; *J. Amer. Chem. Soc.*, 59 (1937) 96; *Trans. Faraday Soc.*, 34 (1938) 156; *Physical Organic Chemistry*, McGraw-Hill, New-York, 1940, chap. VII.
2 H. H. JAFFE, *Chem. Rev.*, 53 (1953) 191.
3 D. H. MCDANIEL ET H. C. BROWN, *J. Org. Chem.*, 23 (1958) 420.
4 C. LAURENCE ET B. WOJTKOWIAK, *Ann. Chim.*, 5 (1970) 163.
5 J. C. HALLE, R. GABORIAUD ET R. SCHAAL, *Bull. Soc. Chim. Fr.*, (1969) 1851.
6 J. C. HALLE, R. GABORIAUD ET R. SCHAAL, *Bull. Soc. Chim. Fr.*, (1970) 2047.
7 J. C. HALLE, *C.R. Acad. Sci.*, 271C (1970) 1109.
8 J. C. HALLE, *Thèse*, Paris, 1971, A.O. 5780.
9 R. A. ROBINSON ET R. H. STOKES, *Electrolyte Solutions*, Butterworths, 1959, p. 529 et 530.
10 R. A. ROBINSON ET R. H. STOKES, *Electrolyte Solutions*, Butterworths, 1959, p. 526.
11 A. I. BIGGS, *J. Chem. Soc.*, (1961) 2572.
12 J. M. VANDENBELT, C. HENRICH ET S. G. VANDEN BERG, *Anal. Chem.*, 25 (1954) 726.
13 J. COURTOT-COUPEZ ET M. LE DEMEZET, *Bull. Soc. Chim. Fr.*, (1969) 1033.
14 (a) C. D. RITCHIE ET R. E. USCHOLD, *J. Amer. Chem. Soc.*, 90 (1968) 2821;
(b) C. D. RITCHIE, *J. Amer. Chem. Soc.*, 91 (1969) 6749.
15 I. M. KOLTHOFF, M. K. CHANTOONI, JR. ET S. BHOWMIK, *J. Amer. Chem. Soc.*, 90 (1968) 23.
16 I. M. KOLTHOFF ET M. K. CHANTOONI, JR., *J. Amer. Chem. Soc.*, 93 (1971) 3843.
17 M. HOJO, M. UTAKA ET Z. YOSHIDA, *Kogyo Kagaku Zasshi*, 69 (1966) 885; *Chem. Abstr.*, 66 (1967) 2121 v; *Tetrahedron*, 27 (1971) 2713.
18 J. P. MOREL, *J. Chim. Phys.*, 67 (1970) 895.
19 R. GABORIAUD, *Ann. Chim.*, 2 (1967) 201.
20 R. GABORIAUD ET R. SCHAAL, *J. Chim. Phys.*, 66 (1969) 730.
21 R. THUAIRE, *J. Chim. Phys.*, 67 (1970) 1076.
22 L. P. HAMMETT ET A. J. DEYRUP, *J. Amer. Chem. Soc.*, 54 (1932) 2721.
23 R. GABORIAUD, I. MENTRE ET R. SCHAAL, *C.R. Acad. Sci.*, 268C (1969) 1093.
24 I. MENTRE, *Thèse*, Paris, 1970, A.O. 4954.
25 J. C. HALLE, F. TERRIER ET R. SCHAAL, *C.R. Acad. Sci.*, 270C (1970) 1684.
26 J. J. CHRISTENSEN, D. P. WRATHALL, R. M. IZATT ET D. O. TOLMAN, *J. Phys. Chem.*, 71 (1967) 3001.
27 E. J. COHN ET J. T. EDSALL, *Proteins, Amino Acids and Peptides*, Reinhold, New York, 1943.
28 A. BRYSON ET R. W. MATTHEWS, *Aust. J. Chem.*, 14 (1961) 237.
29 A. V. WILLI ET W. MEIER, *Helv. Chim. Acta*, 33 (1956) 318.
30 G. DEVOTO, *Gazz. Chim. Ital.*, 63 (1933) 247; 64 (1934) 371.
31 E. P. SERJEANT, *Aust. J. Chem.*, 22 (1969) 1189.

Analytica Chimica Acta
Elsevier Publishing Company, Amsterdam
Printed in The Netherlands

THE EVALUATION OF ERRORS CAUSED BY FLUX INHOMOGENEITIES IN THERMAL NEUTRON ACTIVATION ANALYSIS

E. BRUNINX
Philips Research Laboratories, Eindhoven (The Netherlands)

(Received 30th December 1971)

In thermal neutron activation analysis the concentration of a given element is usually determined by comparing the induced radioactivity of the element (of unknown concentration) with the radioactivity of a standard irradiated simultaneously.

$$\frac{A_x}{N_x} = \sigma\phi_x \tag{1}$$

$$\frac{A_s}{N_s} = \sigma\phi_s \tag{2}$$

Dividing eqn. (1) by eqn. (2) and rearranging gives

$$N_x = N_s \frac{A_x \sigma\phi_s}{A_s \sigma\phi_x} \tag{3}$$

where $N_x(N_s)$ = number of atoms of the required element in the sample (standard),
$A_x(A_s)$ = measured radioactivity of sample (standard) after irradiation (in dis sec^{-1}),
σ = cross-section for the (n,γ) reaction (in cm^2),
$\phi_x(\phi_s)$ = thermal neutron flux (n cm^{-2} sec^{-1}) received by sample (standard), and
A/N = specific disintegration rate (or disintegration rate per atom).

For many determinations, inaccuracies* (caused by systematic errors) up to 5–10% from the true value can be tolerated. For such cases, two assumptions are made in using eqn. (3):

(*a*) the sample and the standard receive the same flux during their simultaneous irradiation; and

(*b*) the energy distribution of the neutrons and thus also σ remains unchanged for sample and standard.

Because $\sigma\phi_x = \sigma\phi_s$, eqn. (3) simplifies to

$$N_x = N_s \frac{A_x}{A_s} \tag{4}$$

When the overall inaccuracy (caused by systematic errors) must be reduced to, *e.g.*, 1% or less of the true value of N_x, then the relative variations in $\sigma\phi$ must be known accurately.

* A complete discussion of the terms used here has been given by Eisenhart[1,2].

The aims of the investigations described here were: (1) to study the variation of $\sigma\phi$ along the whole length of the irradiation capsule in pneumatic irradiation channels with different irradiation characteristics; (2) to study in the same irradiation channels the variation of $\sigma\phi$ in a direction perpendicular to the length of the irradiation capsule (*i.e.* in the "equatorial plane"); (3) to choose on the basis of these data an irradiation channel where the variation of $\sigma\phi$ both in the length and in the "equatorial plane" is a minimum; this choice will also be governed by the ratio of fast/thermal neutron flux; (4) to estimate the systematic inaccuracy in activation analysis caused by inhomogeneities in the value of $\sigma\phi$ for a given set of standards and unknowns.

Since standards and samples are most easily handled as solutions, much effort was devoted to the design and use of containers for solutions.

All experiments were done with milligram quantities of the elements in question. The role of impurities was thus minimized and the results obtained can equally well be applied to smaller quantities.

EXPERIMENTAL

Reactor irradiation

All irradiations were done in the graphite-moderated reactor BR-1 (S.C.K.-C.E.N., Mol, Belgium). There are three pairs of pneumatic tubes (rabbits) in the BR-1 reactor; each pair has a nearly identical value for the thermal neutron flux and the cadmium ratio. The pneumatic tubes are labelled X28, X29; X27, X30; X26, X29 (see Fig. 1).

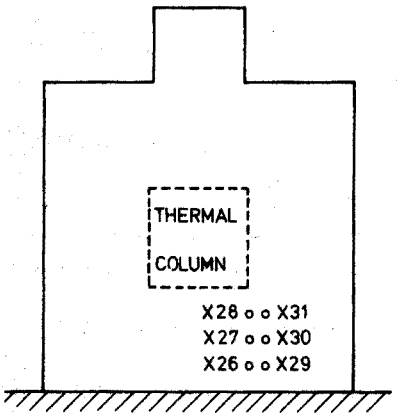

Fig. 1. Position of the six rabbits with respect to the thermal column inside the BR-1 reactor.

The irradiation containers used in these experiments had on overall length of 76 mm and a diameter of 25 mm. Irradiations lasted usually between 10 and 120 sec. The thermal neutron flux varied in the range 10^{10}–$3 \cdot 10^{11}$ n cm^{-2} sec^{-1}.

Flux measurement

Two classes of detectors were used.

(*a*) Solids—gold wire: 99.99% purity; diameter 0.254 mm; copper wire:

99.00% purity; diameter 0.12 mm; gold–aluminium alloy*: 1%:99%; discs of 8 mm diameter, thickness 0.1 mm.

(*b*) Solutions—gold solutions: concentration 1–10 mg ml^{-1}; gallium solutions: concentration 10 mg ml^{-1}. Gold wires of 0.254 mm diameter create a certain amount of neutron flux depression inside the wire (neutron self-shielding). The fractional reduction, f, of the neutron flux inside the sample is calculated by means of the formula proposed by Gilat and Gurfinkel[3]:

$$f = \frac{r\left[1 - \frac{n\sigma r}{2}\left(0.9228 + \ln\frac{1}{n\sigma r}\right)\right] + l[1 - \frac{4}{3}n\sigma r]}{r + l} \quad (5)$$

where r = radius of gold wire (or the inner radius of the polythene vials containing the solution) (cm),

n = atom density (atoms cm^{-3}),

σ = average thermal neutron cross-section (cm^2), and

l = length of wire (or depth of solution in vial).

For identical gold wires ($l = 18$ mm, $r = 0.127$ mm), $f = 0.90$. Absolute values of ϕ cannot be obtained without corrections. This self-absorption is not important for the present measurements, because the relative variation of $\sigma\phi$ along the length of the irradiation container is the subject of interest.

For gold solutions of 10 mg ml^{-1}, $f = 0.998$. The effect is thus much smaller and can be reduced, if necessary, simply by diluting the solutions. Copper and gallium have much lower cross-sections and f is practically = 1.0.

The various models of wire holders are shown in Fig. 2a–c: they all fit inside the standard irradiation can of the BR-1 reactor. All wire holders were made of perspex. The solution vials (Fig. 2d) were made of polythene. The only weak radioactivity observed after irradiation of sample containers was due to ^{24}Na; it never amounted to more than 0.1% of the total activity from ^{198}Au, ^{72}Ga or ^{64}Cu.

The ladder holders were always shot into the reactor so that the point marked 0 mm (see Fig. 2a and 5) went in first. The orientation of the solution holder was not important because the location of the six solution vials was symmetrical with respect to both ends. In order to avoid errors from pipetting, the solutions were always weighed on a microbalance and almost completely filled the small vial (volume *ca.* 0.7 ml). For the ladder and solution detectors, 8 and 6 values of $\sigma\phi$, respectively, were therefore obtained. All six rabbits were examined by means of the ladder and the solution detectors. Rabbits X28 and X31 were tested more intensively by means of a holder for one gold wire (W1, Fig. 2b) and a holder for six gold wires (W6, Fig. 2c). Rabbit X28 was also tested with a holder containing two aluminium–gold alloy discs at both ends (P1, Fig. 2e).

Counting

After irradiation the wire detectors were counted in the following way.

(*a*) A preliminary check was made by γ-ray spectrometry in order to make sure that no unexpected activities were present in the gold, gallium or copper samples. A NaI(Tl) detector (76 × 76 mm) coupled to a 400-channel analyser, or a Ge(Li)

* Kindly put at our disposal by M. Cops, S.C.K.-C.E.N., Mol, Belgium.

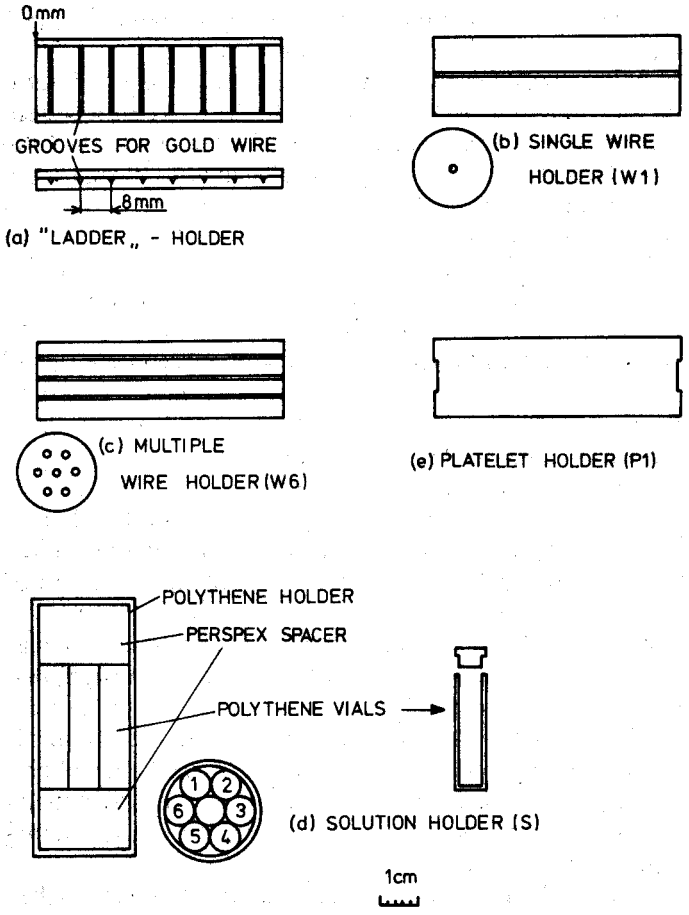

Fig. 2. Various holders for wires and solutions.

detector (67 cm^3) coupled to a 2048-channel analyser, were used.

(*b*) After this check all other measurements were done with a NaI(Tl) well-type detector (44.4 × 50.8 mm) and all pulses above 60 keV were counted integrally.

Solution samples were centrifuged for a few seconds in order to collect all the solution at the bottom of the polythene vial; this was necessary to remove drops of solution splattered on the walls and lid of the vial. Supports for solution and wire during counting are shown in Fig. 3.

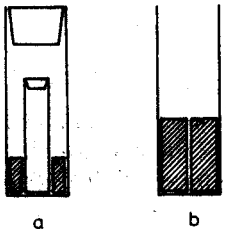

Fig. 3. Counting arrangement for (a) solution and (b) wires.

Earlier measurements were done with a Philips PW 4280 amplifier, and later measurements with an ORTEC 486 amplifier; both instruments were used in the integral counting mode. Dead time for both systems was determined with a set of calibrated ^{144}Ce, ^{137}Cs and ^{60}Co sources[4]. The standard deviation of the dead time varied between 2 and 3%. Count rates were $< 10^4$ c sec^{-1}. A total number of counts between $5 \cdot 10^5$ and 10^6 was collected. Collection of a larger number of counts was useless because instrumental variations then became more important than the gain in precision from counting statistics. In the earlier irradiations the radioactivity measurements were spread out over a period of several days. In later experiments the samples were counted continuously one after the other, each sample being counted five times.

The half lives of the nuclides counted were $^{198}Au = 2.698$ d[5,6]; $^{72}Ga = 14.1$ h[7]; $^{64}Cu = 12.8$ h[8].

Treatment of data

The raw counting data were first analysed by means of the program N decay, yielding the activity of a sample at a given time and the standard deviation of this measurement[9]. Next, all activities were corrected for possible small variations in the weight of the wires or solutions and expressed as specific counting rates (c sec^{-1} mg^{-1}). All activities are expressed in c sec^{-1} and were used as such. Consequently, absolute values of $\sigma\phi$ were not obtained since this would require the introduction of the counting efficiency. The variation in the specific counting rate (c sec^{-1} per atom) remains, nevertheless, proportional to the variation of $\sigma\phi$; in the following paragraphs $\sigma\phi$ only is used.

Solution detectors. The test used to decide whether $\sigma\phi$ varies from one vial to another is as follows[10]:

$(\sigma\phi)_1$, $(\sigma\phi)_2$ = measured specific activity of arbitrary samples 1 and 2, obtained by least squares analysis of n_1, n_2 measuring points.

S_1, S_2 = standard deviations of $(\sigma\phi)_1$, $(\sigma\phi)_2$ (obtained from the same analysis). We do not suppose that in this analysis S is uniquely due to counting statistics; other sources of error also contribute to the value of S. These extra error sources are not considered here.

$(\sigma\phi)_1$ is considered to be different from $(\sigma\phi)_2$ if

$$|(\sigma\phi)_1 - (\sigma\phi)_2| > t_{(1-\alpha/2)}\,(V_1 + V_2)^{\frac{1}{2}} \qquad (6)$$

where $t_{(1-\alpha/2)} = t_{0.975} = 95\%$ confidence limit for F degrees of freedom*.

$$F = \frac{(V_1+V_2)^2}{V_1^2/(n_1+1) + V_2^2/(n_2+1)} - 2$$

$$V_1, V_2 = \frac{(S_1)^2}{n_1}, \frac{(S_2)^2}{n_1}$$

Therefore $\sigma\phi$ for one arbitrary vial is compared with $\sigma\phi$ of the remaining vials. It is immediately clear from eqn. (6) that the smaller the standard deviation of a measurement, the smaller the neutron flux variation that can be detected. In this test it is entirely irrelevant which vial is chosen for comparison (or reference): all that it is

* The definitions and values of t, F can be found in any elementary statistics textbook.

necessary to know is whether the value of $\sigma\phi$ differs from one vial to another. Another parameter used to characterize the variation of $\sigma\phi$ between the six vials is the standard deviation defined by

$$S(\sigma\phi) = \left[\frac{\sum_{1}^{n}((\sigma\phi)_i - (\sigma\phi)_{Av})^2}{n-1}\right]^{\frac{1}{2}} \tag{7}$$

where $(\sigma\phi)_{Av} = \frac{\sum_{1}^{n}(\sigma\phi)_i}{n}$ and $n=6$ (number of vials).

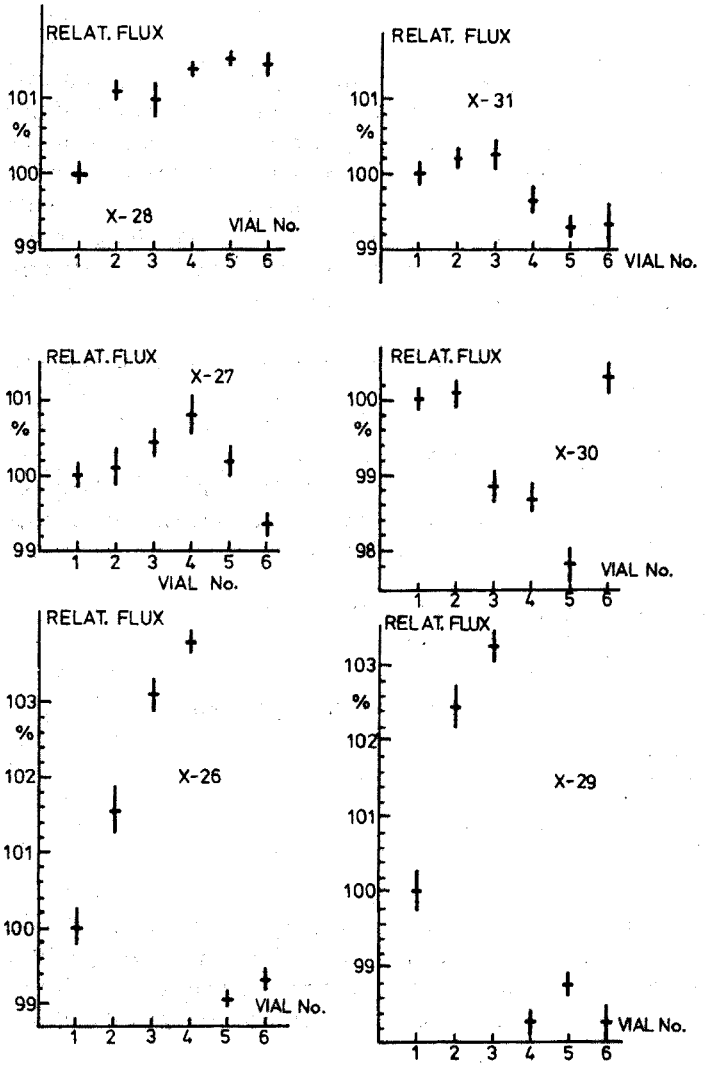

Fig. 4. Relative flux distribution for solutions in all six pneumatic tubes.

This value of $S(\sigma\phi)$ expressed in percent $S(\sigma\phi)/(\sigma\phi)_{Av} \cdot 100$ gives a direct idea about the spread of $\sigma\phi$ in the "equatorial plane" of the irradiation container.

For easy comparison, one of the $\sigma\phi$ values in Fig. 4 was arbitrarily set equal to 100% and all others were referred to it. The variation of $\sigma\phi$ in the "equatorial plane" of the irradiation container was measured in all six rabbits.

Ladder detectors. In these measurements the variation of $\sigma\phi$ along the length of the irradiation container was rather large so that any differences were clear on visual inspection. For an easy comparison the flux value at 36 mm distance was put equal to 100%. All six rabbits were examined with this detector.

RESULTS OF THE FLUX MEASUREMENTS

All rabbits

Figures 4 and 5 summarize the neutron flux data as measured with the solution and ladder detectors, respectively. The error bars represent standard deviations. Since the location of the rabbits X28, X27 and X26 is symmetrical with respect to X31, X30 and X29, the close resemblance of the pattern measured by the ladder detectors (Fig. 5) can be easily understood. The largest variations in $\sigma\phi$ along the length of the irradiation container were found in X26 and X29; the difference was 5% from one end to the other (which is still small compared with the difference found in many other nuclear reactors). The inhomogeneity of $\sigma\phi$ in these two rabbits was also reflected in the solution measurements where standard deviations of 2.0% and 2.2% were observed (see Table I).

TABLE I

$S(\sigma\phi)$ VALUES AND FLUX DATA FOR ALL CHANNELS

Rabbit	$S(\sigma\phi)$ (%)	*Approximate neutron flux* ($n\ cm^{-2}\ sec^{-1}$)	
		$\phi(thermal)$	$\phi(fast)$[a]
X28	0.6	$3.3 \cdot 10^{11}$	$1.6 \cdot 10^{9}$
X31	0.4	$3.3 \cdot 10^{11}$	$1.6 \cdot 10^{9}$
X27	0.5	$2.3 \cdot 10^{11}$	$2.1 \cdot 10^{10}$
X30	1.0	$2.3 \cdot 10^{11}$	$2.1 \cdot 10^{10}$
X26	2.0	$9.7 \cdot 10^{10}$	$0.7 \cdot 10^{10}$
X29	2.2	$9.7 \cdot 10^{10}$	$0.7 \cdot 10^{10}$

[a] All neutrons with energies higher than thermal neutrons.

The fast neutron flux in the two rabbits X26 and X29 was fairly high, and would be partly moderated in the polythene and the solution, giving rise to an increased neutron flux in about three of the six vials (see Fig. 4). Inspection of Fig. 4 shows that a high value of $\sigma\phi$ in one of the vials was nearly always accompanied by a low $\sigma\phi$ value in a vial 2–3 positions further away. This effect decreased with decreasing fast neutron flux.

The ladder measurements in rabbits X28, X31, X27 and X30 showed a nearly identical variation of $\sigma\phi$ along the length of the irradiation container (Fig. 5). The

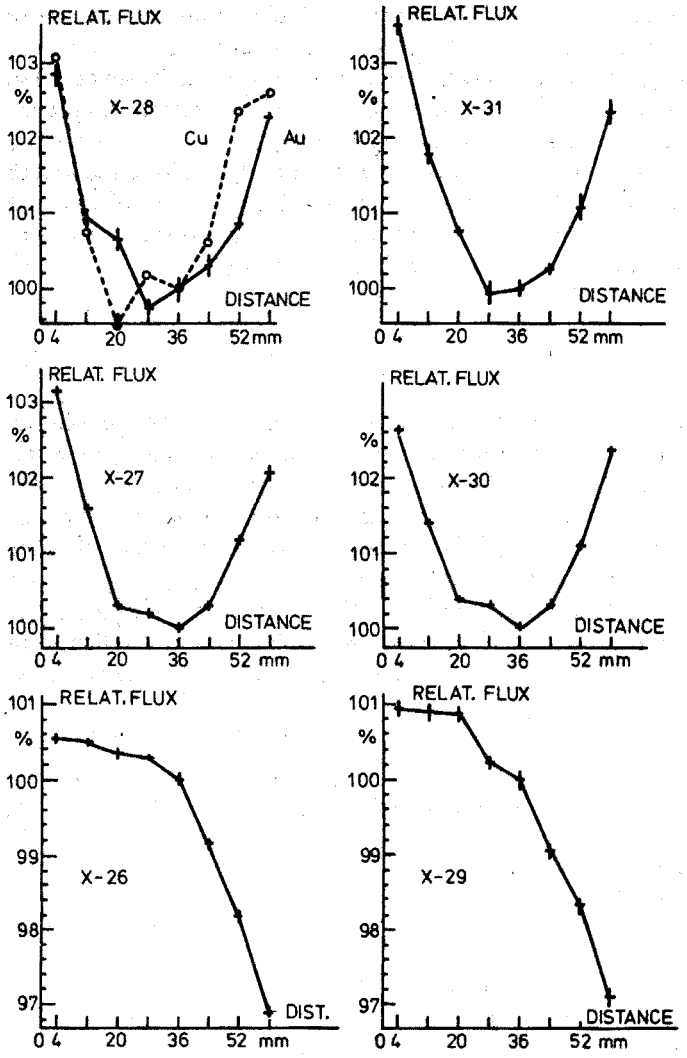

Fig. 5. Relative flux distribution for gold in all six pneumatic tubes.

solution detectors all indicated lower values of $S(\sigma\phi)$. Rabbits X28 and X31 had slightly better characteristics than X27 and X30.

Rabbits X28 and X31

Further tests were made in rabbit X28 by means of the holders W1 (with one gold wire) and W6 (with six gold wires) (Fig. 2b, c). X31 was tested with three gold wires. The general trend of the $\sigma\phi$ data confirmed the results found with the ladder and the solution detectors that in the central part of these rabbits (between 16–49 mm) $\sigma\phi$ was nearly constant. In one of the ladder experiments (X28) the gold wire was replaced by a copper wire (having a much lower cross-section). The variation of $\sigma\phi$ obtained with this material (see Fig. 5) had the same shape as that obtained from the gold

wire measurements: the gold wires do not therefore influence (or perturb) the neutron flux of the neighbouring wires. Similarly the use of the gold–aluminium alloy discs in X28 and located at both ends of the holder P1 (Fig. 2) yielded a difference of 2% between the $\sigma\phi$ values measured at both ends of the holder. This also compared favourably with pure gold wire measurements, where the difference between both ends was about 1% (Fig. 5).

Gallium solutions and gold solutions of varying concentration were irradiated in the rabbits X28 and X31 and the standard deviation $S(\sigma\phi)$ was determined in the usual way. Table II summarizes the results.

TABLE II

INFLUENCE OF THE SOLUTION CONCENTRATION ON $S(\sigma\phi)$

Rabbit	*Composition of solution*	$S(\sigma\phi)$ (%)
X28	Au, 10 mg ml^{-1}	0.6
X28	Au, 10 mg ml^{-1}	0.7
X28	Au, 1 mg ml^{-1}	0.3
X28	Ga, 10 mg ml^{-1}	0.4
X28	Ga, 10 mg ml^{-1}	0.3
X31	Ga, 10 mg ml^{-1}	0.3

The reduction in $S(\sigma\phi)$ for, *e.g.*, gold solutions of 1 mg ml^{-1}, is a direct result of the decrease of the neutron absorption in solutions of lower concentrations.

Choice of the irradiation channel and evaluation of errors due to the variation of $\sigma\phi$

Examination of the $\sigma\phi$ values of X26 and X29 shows large variations both for the ladder and solution detectors. It is therefore not advisable to use these rabbits for activation analysis requiring a high accuracy.

Comparing the results for rabbits X28, X31, X27 and X30, one may be tempted to choose for activation analysis X27 or X30 on the basis of the ladder data since these rabbits show the smallest variation of $\sigma\phi$ between 16 and 49 mm. However, it must be remembered that the epithermal flux is considerably larger in these two rabbits. This increased fast neutron flux (see Table I) may be responsible for the somewhat larger spread in $S(\sigma\phi)$ for X27 and X30. Therefore, X28 and X31 present the best compromise for activation analysis.

The arrangement of Fig. 2d is suitable for an evaluation of the errors in the determination of N_x (see eqn. 3) when a certain combination of standards and unknowns is used. As an example, six identical gallium solutions (10 mg ml^{-1}) were irradiated in rabbit X28 and the value of $S(\sigma\phi)$ was found to be 0.3%. The individual measured values of $\sigma\phi$ are given in Table III. We shall consider four samples as standards and two samples as unknowns; the standards and the unknowns can be arranged in a number of ways *e.g.* standards in vial 1, 2, 4 and 5, and samples in vials 3 and 6. Three possible arrangements are shown in Table III. The standard deviation of the $\sigma\phi$ values varied between 0.04 and 0.06%. The averages were calculated with equal weights for all $\sigma\phi$ values.

TABLE III

FLUCTUATION OF SYSTEMATIC ERRORS FOR DIFFERENT SAMPLE ORIENTATIONS

Sample no.	1	2	3	4	5	6	*Average*	*Error*
ϕ	100.0	99.4	99.6	99.8	99.8	100.2		
Arrang. 1	X	S	S	X	S	S	99.8	−0.2, −0.0
Arrang. 2	S	X	S	S	X	S	99.9	+0.5, −0.1
Arrang. 3	S	S	X	S	S	X	99.8	+0.2, −0.4

Consider arrangement 1. The standards are in 2, 3, 5 and 6. The average of $\sigma\phi$ is 99.8. The value of $\sigma\phi$ for sample 1 is, however, 100.0 introducing therefore a systematic error of -0.2%. In position 4, the error is $99.8-99.8=0.0\%$. In arrangement 3 the errors are respectively $+0.2$ and -0.4%. The reason for these varying errors is simple. The neutron density inside the reactor is invariable under given operating conditions at a given point. The cylindrical irradiation container can however rotate (during transport) and therefore occupy a variety of orientations with respect to the inner core of the reactor. The exact orientation of the vials 1, 2,..... is thus unknown This lack of orientation induces a systematic error whose magnitude varies at random. The only way to suppress this type of error is to use either a pneumatic transport system so that the orientation of the rabbit is fixed, or to rotate the cylindrical irradiation container around the axis, during the irradiation.

CONCLUSIONS

The overall accuracy which can be obtained for thermal neutron activation analysis in a nuclear reactor depends partly on random errors (such as counting statistics) and partly on systematic errors. An important source of systematic errors of fluctuating magnitude originates not only in the varying values of the thermal neutron flux at the irradiation position of the capsule containing standards and unknowns, but also in the uncontrollable position of the rabbit inside the reactor.

A good knowledge of the variation of the thermal neutron flux along the length and in the "equatorial" plane of the irradiation capsule, together with data on the thermal and the fast neutron flux, will permit the choice of an irradiation position where the systematic errors are kept to a minimum.

An entirely fixed position, or even better, rotation of the capsule inside the reactor can eliminate this type of systematic error.

SUMMARY

Relative flux variations have been measured in six pneumatic channels of a graphite-moderated reactor. Wires as well as solution detectors were used. The influence of these variations on the accuracy of activation analysis has been estimated in one irradiation channel for a given combination of standards and samples.

RÉSUMÉ

Une étude est effectuée sur l'évaluation des erreurs, causées par un flux

irrégulier lors de l'analyse par activation aux neutrons thermiques. Les variations de flux relatives ont été mesurées dans six canaux pneumatiques d'un réacteur au graphite. L'influence de ces variations sur l'exactitude de l'analyse par activation a été estimée dans un canal d'irradiation pour une combinaison donnée de standards et d'échantillons.

ZUSAMMENFASSUNG

Relative Flussänderungen wurden in sechs pneumatischen Kanälen eines graphitmoderierten Reaktors unter Verwendung von sowohl Draht- als auch Lösungsdetektoren gemessen. Der Einfluss dieser Änderungen auf die Genauigkeit der Aktivierungsanalyse wurde in einem Bestrahlungskanal für eine vorgegebene Kombination von Standards und Proben ermittelt.

REFERENCES

1 C. Eisenhart, *J. Res. Natl. Bur. Stand.*, 67 C (1963) 161.
2 C. Eisenhart, *Science*, 160 (1968) 1201.
3 J. Gilat and Y. Gurfinkel, *Nucleon.*, 21, No. 8 (1963) 143.
4 G. Rudstam, *Nucleon.*, 19, No. 12 (1961) 62.
5 E. Lockett and R. Thomas, *Nucleon.*, 11, No. 3 (1953) 14.
6 R. Bell and L. Yaffe, *Can. J. Phys.*, 32 (1954) 416.
7 *Nuclear Data Sheets*, Vol. 1–6, National Academy of Sciences–National Research Council.
8 J. Tobailem, *J. Phys. Radiat.*, 16 (1955) 48.
9 W. Roos, *Nat. Lab. Tech. Note* 139/70, unpublished.
10 M. G. Natrella, *Natl. Bur. Stand. Handbook*, 91, 3-2b, 1966.

Analytica Chimica Acta
Elsevier Publishing Company, Amsterdam
Printed in The Netherlands

SHORT COMMUNICATION

The occurrence of multiple peaks in the determination of various elements by the "Delves sampling cup" method

D. CLARK, R. M. DAGNALL and T. S. WEST
Department of Chemistry, Imperial College of Science and Technology, London, S.W.7 2AY (England)
(Received 15th December 1971)

The use of the "Delves sampling cup" technique in atomic absorption spectrophotometry[1] has been investigated in this department for the determination of mercury[2]. It was noted during this work that a range of determinations was possible although in many instances multiple absorption peaks were recorded. A recent report[3] also outlined the determination of elements other than lead, but no mention of multiple absorption peaks was made. In view of the influence such phenomena are likely to have on the analytical precision and sensitivity, the occurrence of multiple peaks is described in this communication; the range of application of this technique is also indicated.

Apparatus

The cup and tube apparatus have been previously described[1,2]. Both air–acetylene and nitrogen–hydrogen flames were used on a 5-cm triple-row capillary burner. All measurements were carried out with the Perkin-Elmer 290 Atomic Absorption Spectrophotometer (equipped with u.v. lenses, mirrors and windows and an EMI 6256B photomultiplier) in conjunction with a Hitachi 159 recorder. The transient absorption signals were recorded as peaks in the absorbance mode of operation; however, large absorbance signals were measured on a 0–100% transmittance scale with the emission accessory. Hollow-cathode lamps were used for the majority of the elements examined and these were operated *via* the spectrometer internal supply at currents giving optimal signal:noise ratio. When hollow-cathode lamps were not available or were unsuitable with respect to intensity, then electrodeless discharge lamps were used in $\frac{1}{4}$- or $\frac{3}{4}$-wave cavities.

Microwave energy was supplied by a "Microtron 200" generator (Electro-Medical Supplies, London, U.K.). The radiation from the discharge lamps was mechanically chopped before entry into the flame by a synchronous chopper operated from the 117-V, 50-Hz supply of the spectrometer auxiliary discharge lamp socket.

Reagents

Analar-grade chemicals were used and all solutions were prepared with deionized distilled water. Stock solutions were stored in plastic reagent bottles and all concentrations below 100 p.p.m. were prepared daily.

Anal. Chim. Acta, 60 (1972)

TABLE I

EXPERIMENTAL PARAMETERS

Element	*Wavelength (nm)*	*Coarse select element setting*	*Monochromator bandpass (nm)*	*Working range (ng)*	*Sensitivity (ng/1 % absorption)*	*Detection limit (ng)*	*Radiation source*	*Number of absorption peaks*	*Flame type*[a]
Hg	253.65	153	0.2	20–200	1.8	0.5	EDL	3	N_2/H_2
Pb	283.3	206	0.7	1–20	0.1	—	HCL	1	Air/C_2H_2
As	193.7	48	2.0	50–400	3.9	40	EDL	4	N_2/H_2
	197.2	53	0.7	100–900	5.6	5	EDL	4	N_2/H_2
	189.0	37	0.7	100–2,000	5.0	10	EDL	4	N_2/H_2
	189.0	37	0.7	50–400	3.5	10	EDL	4	$N_2/H_2/O_2$ enriched[b]
Zn	213.8	83	2.0	0.05–0.5	0.1	$5 \cdot 10^{-3}$	HCL	2	Air/C_2H_2
	307.5	250	2.0	500–10,000	100	300	HCL	2	Air/C_2H_2
Sb	231.2	112	0.7	50–500	10	2	HCL	3	Air/C_2H_2
	217.6	90	0.7	50–1,000	25	40	HCL	3	Air/C_2H_2
	206.8	69	2.0	60–1,000	20	30	HCL	3	Air/C_2H_2
Cu	324.7	280	0.7	50–500	3.6	1.5	HCL	2	Air/C_2H_2
Ag	328.1	286	2.0	10–60	0.37	0.05	HCL	1	Air/C_2H_2
	338.3	306	2.0	5–100	0.62	0.4	HCL	1	Air/C_2H_2
Cd	326.1	283	2.0	50–2,000	24	5	HCL	2	N_2/H_2
	228.8	109	2.0	1–20	0.12	0.2	HCL	2	N_2/H_2
Tl	276.8	194	2.0	10–100	0.7	0.5	EDL	2	Air/C_2H_2
	276.8	194	2.0	50–500	4.2	10	EDL	2	$N_2/H_2/O_2$ enriched[b]
	377.6	377	0.7	50–200	1.5	15	EDL	2	Air/C_2H_2
Sn	224.6	101	2.0	50–1500	7	1	EDL	2	Air/C_2H_2
Se	206.3	52	2.0	50–2300	12	22	EDL	1	N_2/H_2
Bi	223.1	99	2.0	50–1500	16	15.5	HCL	1	N_2/H_2
	223.1	99	2.0	50–500	5	5	HCL	1	Air/C_2H_2
Ga	287.4	213	0.7	Analytically useless	833	330	EDL	1	Air/C_2H_2
Co	240.7	130	0.2	100–1,000	35	20	HCL	2	Air/C_2H_2

[a] Flow rates varied to give maximal sensitivity for each element.

[b] Nitrogen 4.6 l min^{-1} (30 psig), hydrogen 6.4 l min^{-1} (12 psig), oxygen 1.9 l min^{-1} (10 psig).

Results and discussion

The results for several elements are shown in Table I. Sample volumes of 5 μl were used, and the working range assumes no scale expansion and a maximum absorbance value of 0.6. The sensitivity is defined as the average slope of the calibration curve over the working range, measured in ng for a 1% absorption. This definition was adopted because linear working curves were not obtained in all instances, even under minimum damping conditions. The detection limit quoted is for a signal (peak height): background noise ratio of 1.

The results in Table I suggest that only elements which are relatively easily volatilized and atomized can be determined by this technique. Attempts to atomize elements such as Al, Ba, Ca, Ge, Mg, V and W with air–acetylene and nitrous oxide–acetylene flames (in conjunction with a fused alumina absorption tube and a carbon boat situated within the "red feather" zone of the latter flame) were unsuccessful. The elements Co, Cu, Ga, Sn and Sb do not appear to have been investigated previously by this technique. The flame condition recorded in the last column of Table I indicates the optimal flame type required to give maximum sensitivity with the instrumentation used. The number of absorption peaks recorded for each element is shown also in Table I and, as can be seen, only Pb, Ag, Se, Bi and Ga gave rise to a single absorption peak. For all other cases the rate of volatilization, sample volume, sample concentration and the matrix are likely to affect the analytical precision and sensitivity, because these factors directly affect the degree of peak separation.

The reason for multiple absorption peaks is not fully understood, but certainly in some cases it is related to the production of different valency states of the analyte element. Similar observations have been made in emission studies[4]. The number of absorption peaks was not related to the concentration of the analyte element. In each case, absorption was checked at various wavelengths to confirm that atomic absorption and not molecular absorption was observed.

The use of integration instead of peak-height measurement has been suggested[5] for transient absorption and emission signals. The presence of multiple absorption peaks in this work further emphasizes the need for signal integration even if the time constant of the system is small compared with the signal duration.

We would like to thank the Science Research Council for the award of a C.A.P.S. grant to one of us (D.C.) and Perkin-Elmer Limited, Beaconsfield, U.K., for the loan of some of the instrumentation used in this study.

REFERENCES

1 H. T. DELVES, *Analyst*, 95 (1970) 431.
2 D. CLARK, R. M. DAGNALL AND T. S. WEST, *Anal. Chim. Acta*, 58 (1972) 339.
3 J. D. KERBER AND F. J. FERNANDEZ, *At. Absorpt. Newsl.*, 10 (3) (1971) 78.
4 K. M. ALDOUS, R. M. DAGNALL, B. L. SHARP AND T. S. WEST, *Anal. Chim. Acta*, 54 (1971) 233.
5 R. M. DAGNALL, B. L. SHARP AND T. S. WEST, *Nature*, 234 (1971) 69.

Analytica Chimica Acta
Elsevier Publishing Company, Amsterdam
Printed in The Netherlands

SHORT COMMUNICATION

Solvent extraction separations with bathophenanthroline

Applications to the microanalysis of elements in uranium by atomic absorption spectrophotometry*

R. W. SPARKS, O. A. VITA and C. R. WALKER

Chemical Analysis Department, Technical Division, Goodyear Atomic Corp., P.O. Box 628, Piketon, Ohio 45661 (U.S.A.)

(Received 11th November 1971)

Uranium compounds used as feed sources for the gaseous diffusion process and various other nuclear applications must meet rigid purity specifications set by the U.S. Atomic Energy Commission. To measure conformance to these specifications, uranium compounds must be analyzed for many trace elements such as copper, iron, and nickel.

The concentrations of these elements in uranium are often determined colorimetrically or by emission spectroscopy; however, there are disadvantages associated with both methods. Colorimetric procedures are subject to elemental interferences and are time-consuming, because separate determinations must be made for each element. Emission spectrographic procedures lack accuracy. To eliminate these disadvantages, the determination of these elements by atomic absorption spectroscopy was investigated. The direct determination of these elements in uranium by atomic absorption gave poor sensitivity and spread radioactive contamination from the aspiration of uranium solutions; thus, the direct method was undesirable. However, development of a solvent extraction method for copper, iron and nickel from uranium, based on the bathophenanthroline–hexone extraction system[1,2], before direct analysis of the hexone extract by atomic absorption has eliminated these difficulties.

With this separation procedure, the detection of these elements was significantly improved, both by the concentration of the elements and the increased sensitivity of atomic absorption for these elements in an organic solvent[3]. The use of this method also eliminated the problem of radioactive contamination.

Recommended standard procedure

Dissolve uranium oxide, metals, or compounds in 8 *M* nitric acid (20 ml per 5 g U) and fume the solution to dryness. Dissolve the residue in 10 ml of 0.1 *M* nitric

* Presented in part at the Twelfth Conference on Analytical Chemistry in Nuclear Technology, Gatlinburg, Tenn., October 8–10, 1968.

acid and dilute to 100 ml with water. Pipette an aliquot of the solution (containing up to 100 μg of Cu, Fe, and Ni) into a beaker. Add 10 ml of 10% (w/v) sodium acetate, and 4 ml of 10% (w/v) hydroxylamine hydrochloride to the solution. Adjust the solution to a pH of 3 with ammonium hydroxide or nitric acid. Add 5 ml of 0.25% (w/v) bathophenanthroline (4,7-diphenyl-1,10-phenanthroline) dissolved in ethanol to the solution. Transfer the solution to a 125-ml separatory funnel and adjust the volume to about 75 ml with distilled water. Heat the sample solution in a water bath at 80–90° for 30 min and cool. Add 10 ml of hexone to the separatory funnel, mix thoroughly, stopper, and shake for 3 min. Discard the raffinate. Add 5 ml of wash solution (4 ml 10% (w/v) hydroxylamine hydrochloride, and 0.5 ml of 0.25% (w/v) bathophenanthroline–ethanol diluted with 100 ml of 0.01 *M* hydrochloric acid) to the separatory funnel. Stopper and shake for 30 sec. Discard the raffinate and analyze the extract for the desired elements by atomic absorption spectroscopy.

Prepare four uranyl nitrate standards (about 3 g U) spiked with 0, 20, 50, and 100 μg each of copper, iron, and nickel. Dissolve and extract the standards using the recommended procedure.

The instrumental conditions, which apply to the Perkin-Elmer 303 atomic absorption spectrophotometer equipped with a Boling burner, are presented in Table I.

TABLE I

INSTRUMENTAL CONDITIONS

Burner height	12 mm
Aspiration rate	3 ml min^{-1}
Slit setting	3
Air flow	30 lb gauge, 9.0 manifold setting
Acetylene flow	10 lb gauge, 5.0 manifold setting
Wavelength (nm)	copper, 324.75; iron, 248.33; nickel, 232.00

Effect of pH on extraction

The extraction of each of the elements with the bathophenanthroline–hexone system is dependent on the hydrochloric acid concentration as shown in Fig. 1. Extraction of copper, iron, and nickel is essentially complete (97%) from hydrochloric acid at pH 3. With nickel the extraction efficiency is 99.8% at pH 1, but drops off slightly at pH 3. Iron is extracted efficiently at pH 1–3, but extraction efficiency decreases beyond this range and then starts to increase again at pH 5. In the extraction of copper, the pH does not significantly affect the extraction efficiency in the pH range 1–6. However, since sodium acetate does not act as a sufficient buffer solution at low pH levels, a pH of 3 was determined to be the best hydrochloric acid concentration for extracting all three elements simultaneously.

Evaluation of instrumental conditions

The effects of burner height and acetylene flow rate on absorbance of copper, nickel and iron were also evaluated. The effect of the Boling burner height is shown in Fig. 2. Copper absorbance is best at 5.5 mm, and nickel absorbance is best at about 12 mm. Although there is some difference in the sensitivity of copper between

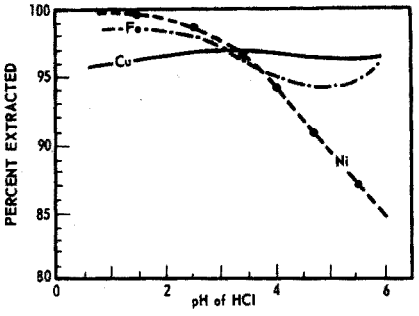

Fig. 1. Effect of acid concentration on extraction.

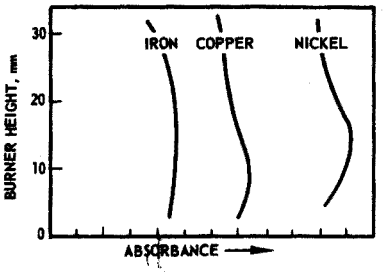

Fig. 2. Effect of burner height on absorbance.

5.5 and 12 mm, it was not significant; therefore, a burner height of 12 mm is recommended.

The effects of fuel-to-air ratio on absorption were studied by maintaining the air flow at a constant manifold setting and varying the acetylene flow rate. The effects of acetylene flow on absorption are shown in Fig. 3. Acetylene flow rate was somewhat critical in the case of iron; the higher the flow rate setting, the less absorption. Nickel started to drop off at about 5.5 and copper was not affected substantially by the flow rate. To ensure maximum absorption for each element and stable operation, the flowmeter setting should be 4.5 for iron and nickel, and 5.0–5.5 for copper.

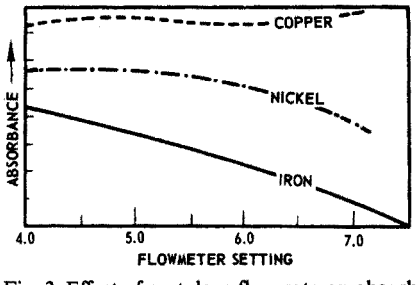

Fig. 3. Effect of acetylene flow rate on absorbance. Acetylene, 10 lb gauge; solvent, hexone.

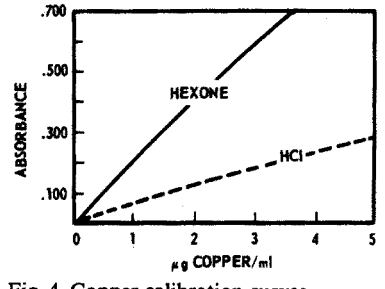

Fig. 4. Copper calibration curves.

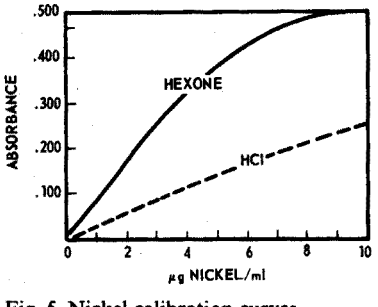

Fig. 5. Nickel calibration curves.

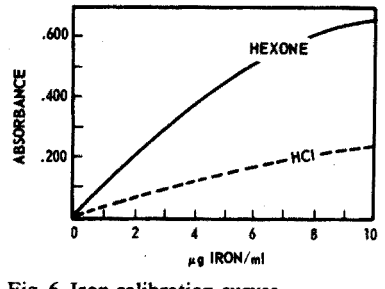

Fig. 6. Iron calibration curves.

Calibration curves

Figures 4, 5, and 6 are the calibration curves for copper, nickel and iron, respectively. These curves show the absorbance for each element and a comparison of sensitivities in hexone and hydrochloric acid. For nickel the sensitivity ratio for hexone to HCl is 3.0 at 232.0 nm. For copper the sensitivity ratio for hexone to HCl is 3.3 at 324.75 nm, and for iron the sensitivity ratio for hexone to HCl is 3.4 at 248.33 nm. In every case, the presence of hexone increases the sensitivities of all three elements significantly.

Analyses of prepared standards

Several prepared uranium standards were spiked with copper, nickel and iron and analyzed by the recommended procedure. The results are shown in Table II.

TABLE II

ANALYSES OF PREPARED STANDARDS
(20 standards were analyzed in each case)

	Copper	*Iron*	*Nickel*
Concentration (μg/g U)	1.5	1.5	1.7
Relative standard deviation (%)	± 3.2	± 4.2	± 1.9
Percent bias	−2.3 ± 1.5	2.2 ± 2.0	1.0 ± 0.9

REFERENCES

1 G. F. Smith, W. H. McCurdy, Jr. and H. Diehl, *Analyst*, 77 (1952) 418.
2 R. J. Guest and F. P. Rolsen, *Canadian Department of Mines and Technical Surveys, Mine Branch, Report NP*-8834, 1956.
3 J. W. Robinson, *Atomic Absorption Spectroscopy*, Marcel Dekker, New York, 1966, pp. 82–86.

Analytica Chimica Acta
Elsevier Publishing Company, Amsterdam
Printed in The Netherlands

SHORT COMMUNICATION

Dosage de traces de nickel dans l'eau de mer par spectrophotométrie d'absorption atomique

H. RAMPON et R. CUVELIER
Production/Laboratoires, Centre de la Hague, C.E.A., Herqueville (France)
(Reçu le 21 juin 1971)

Divers essais effectués au Centre de la Hague ont conduit les laboratoires à doser plusieurs éléments dans l'eau de mer, généralement par spectrophotométrie d'absorption atomique. Calcium, magnésium, sodium et même cuivre et fer peuvent être dosés directement, sans préconcentration[1] ; mais d'autres éléments, en particulier le nickel, doivent être concentrés avant le dosage.

La matrice eau de mer est très gênante : par sa concentration en sels dissous (de l'ordre de 40 g l^{-1}), par la nature de ses sels (en particulier le chlorure de sodium), et par le nombre d'anions et de cations pouvant s'y trouver.

Une concentration par la chaleur et obtention de cendres, est difficile et longue. Une étude a donc été effectuée pour concentrer et séparer le nickel par extraction sélective.

Le dosage du nickel dans les eaux a été traité par de nombreux auteurs : Burrell[1] utilise une préconcentration au moyen de résines, extraction au dithiocarbamate de sodium et co-précipitation ; et West *et al.*[2] proposent une méthode d'absorption atomique, insuffisamment sensible pour l'eau de mer. Riley et Taylor[3] emploient des résines échangeuses d'ions et procèdent à des élutions au moyen d'acides minéraux.

Enfin, récemment Zeitlin *et al.*[4] préconisent une méthode colorimétrique rapide, pouvant être adaptée à l'absorption atomique. 750 ml d'eau de mer sont filtrés sur millipore (0.45 μm) ; on procède (en présence de citrate de sodium à un pH 9–10) à quatre extractions successives du complexe nickel–diméthylglyoxime, en milieu chloroforme, et à trois réextractions du nickel en milieu acide chlorhydrique. On forme le complexe Ni^{4+}/diméthylglyoxime par oxydation à l'eau de brome, et on effectue la colorimétrie à 442 nm.

Pour l'absorption atomique, la méthode est considérablement simplifiée.

Partie expérimentale

Appareillage. Spectrophotomètre type "303" Perkin-Elmer. Longueur d'onde 232.0 nm. Fente 3. Flamme air–acétylène (débit en unités arbitraires : air = 8.8 et $C_2H_2 = 9$). Lampe à cathode creuse "nickel", courant de source 20 mA.

Solutions étalons de nickel à 0.25 μg ml^{-1}, 0.5 μg ml^{-1} et 1 μg ml^{-1} dans l'acide nitrique environ 0.1 *M*.

Extraction. Introduire 500 ml d'eau à analyser, préalablement filtrée sur millipore 0.45 μm, dans un bécher d'un litre. Ajouter 25 ml de solution de citrate de sodium à 20% (p/v) et 5 ml de solution de diméthylglyoxime à 1% (p/v) dans l'ethanol. Ajuster à un pH compris entre 9 et 10 par l'ammoniaque concentré et ajouter 10 ml de chloroforme. Extraire dans un erlenmeyer d'1 l, avec forte agitation magnétique, pendant 5 min. Séparer avec ampoule à décanter et recueillir la phase solvant sans entraîner l'interphase. Répéter trois fois l'opération avec 5 ml de chloroforme et terminer par un lavage de la phase aqueuse épuisée avec 10 ml de tétrachlorure de carbone. Réunir toutes les phases solvant recueillies dans un bécher de 50 ml.

Concentration. Evaporer lentement le solvant sur plaque chauffante sous hotte ventilée, à siccité sans calciner. Reprendre par 1 ml d'acide chlorhydrique fumant. Ajouter 5 ml d'eau distillée et évaporer à siccité sans calciner. Reprendre enfin par de l'acide nitrique 0.1 *M* et ajuster à 5 ml (en fiole jaugée) par l'acide nitrique 0.1 *M*. L'échantillon est alors prêt pour l'analyse par absorption atomique.

Mesurer les absorptions atomiques des solutions de nickel contenant 0.25, 0.5 et 1 μg Ni ml^{-1} (en milieu nitrique environ 0.1 *M*) et celle de la solution concentrée.

$$\textit{Calcul. } X = C \cdot \frac{V}{v}$$

où X = concentration (μg ml^{-1} Ni) de l'eau à analyser,
C = concentration (μg ml^{-1} Ni) de la solution concentrée,
V = volume (ml) de la prise d'essai,
v = volume final de la solution concentrée.

Résultats et discussion

Ce mode opératoire présente un certain nombre de modifications par rapport à celui indiqué par Zeitlin *et al.*[4], modifications inspirées par les résultats obtenus au cours de plusieurs essais, avec eau distillée et eau de mer. Il est nécessaire d'utiliser des solutions de nickel extraites dans les mêmes conditions; sinon les résultats obtenus sont trop faibles (10% en moyenne).

Cette perte en nickel dans la phase aqueuse, serait due à la solubilité du chloroforme dans l'eau. C'est pourquoi les extractions en phase chloroforme, sont complétées par un lavage de la phase aqueuse au tétrachlorure de carbone. Cette nouvelle phase (récupération du solvant dissous en phase aqueuse) est jointe aux précédentes phases chloroforme; ce qui permet d'arriver à un rendement d'extraction, final, voisin de 100%.

On peut doser ainsi, après concentration, des teneurs en nickel de 0.5 μg ml^{-1} à 1 μg ml^{-1}, avec des reproductibilités inférieures à 5%.

Les limites de concentration dosable, théoriquement, sont environ 1 μg l^{-1} pour une prise de 500 ml ramenée à 5 ml et 0.5 μg l^{-1} pour une prise de 1000 ml ramenée à 5 ml, à condition que l'extraction soit à 100%, ce que nous n'avons pas vérifié.

Les résultats obtenus en employant le mode opératoire préconisé sont donnés dans le Tableau I.

Conclusion

La comparaison de la méthode de dosage par absorption atomique avec la

TABLEAU I

CONTRÔLE PAR ADDITION DE NICKEL

(Prise d'essai: 500 ml d'eau de mer)

Ni ajouté ($\mu g\ ml^{-1}$)	*Ni trouvé* ($\mu g\ ml^{-1}$)		*Ni retrouvé* ($\mu g\ ml^{-1}$)
	Méthode directe (droite d'étalonnage)	*Méthode par addition de nickel étalon*	
0	3.6	3.5	—
5	8.5		4.9
10	13.6		10.0
20	23.4		19.8

méthode colorimétrique fait apparaître un gain de temps appréciable dû à la suppression d'un certain nombre d'opérations plus ou moins délicates nécessaires en colorimétrie, en particulier pour supprimer des interférences ou amener des éléments à un certain état de valence. D'autre part, les opérations sont simples et assez rapides; il est possible que le domaine d'application puisse être étendu à d'autres types de solutions que l'eau de mer.

BIBLIOGRAPHIE

1 D. C. Burrell, *Anal. Chim. Acta*, 38 (1967) 447.
2 S. L. Sachdev, J. W. Robinson et P. W. West, *Anal. Chim. Acta*, 38 (1967) 499.
3 J. P. Riley et D. Taylor, *Anal. Chim. Acta*, 40 (1968) 479.
4 E. Kentner, D. B. Armitage et H. Zeitlin, *Anal. Chim. Acta*, 45 (1969) 343.

Analytica Chimica Acta
Elsevier Publishing Company, Amsterdam
Printed in The Netherlands

SHORT COMMUNICATION

An improved separation and determination of uranium in seawater*

GREGORY LEUNG, YOUNG S. KIM and HARRY ZEITLIN

Department of Chemistry and Hawaii Institute of Geophysics, University of Hawaii, Honolulu, Hawaii 96822 (U.S.A.)

(Received 18th December 1971)

Recently the application of a novel adsorbing colloid flotation technique was described[1,2] for the separation of trace amounts of molybdenum and uranium from seawater considered to be present as MoO_4^{2-} and $UO_2(CO_3)_3^{4-}$ respectively. The separation of the two anionic species was achieved in 2–3 min by a surfactant–collector–gas system comprised of negatively charged sodium dodecyl sulfate, positively charged iron(III) hydroxide, and air. In the case of uranium, the recovery was 82% as determined by the measurement of the absorbance of the uranium–rhodamine B complex at 555 nm. A previous report[1] that thorium hydroxide is a more efficient collector of molybdenum from seawater than iron(III) hydroxide prompted an investigation to ascertain whether the use of thorium hydroxide coupled with the measurement of fluorescence intensity of the uranium–rhodamine B complex would lead to improvement in the recovery and increase in the sensitivity of the determination.

Experimental

Apparatus and equipment. A Beckman DU spectrophotometer with a fluorescence attachment was used to measure fluorescence intensity. The fluorescence accessory was calibrated with quinine sulfate solution. Other equipment including the flotation unit was similar to that described previously[1].

Reagents. All chemicals were of analytical grade. The standard solution of uranium and all other reagents were as in the previous paper[2].

Separation of uranium from seawater. The previously described flotation procedure was used to separate the uranium[1]. To 500-ml samples of filtered seawater containing 0.0, 2.0, 4.0, and 6.0 μg of uranium, were added 2 ml of 0.1 *M* thorium nitrate solution. The pH was adjusted to 5.7 ± 0.1 with 1 *M* hydrochloric acid and the sample was transferred to the flotation cell. The flow of gas was adjusted to 10 ± 2 ml min^{-1} and 3 ml of 0.05% (w/v) sodium dodecanoate solution in 95% ethanol were injected into the cell. After 2–3 min the froth was removed and collected into a small Erlenmeyer flask with the aid of a suction tip attached to an aspirator.

* Hawaii Institute of Geophysics Contribution No. 468.

Analysis. The froth was treated exactly as described previously[2], except that the volume of salting agent was changed to 15 ml. The pink complex solution was transferred to a Vycor test tube and the fluorescence intensity measured at the previously determined maximum of 575 nm.

The working curve was constructed by plotting the fluorescence intensity *versus* concentration of uranium in spiked seawater samples. Typical data obtained are given in Table I.

TABLE I

CALIBRATION DATA AND RECOVERY

Sample	*Fluorescence intensity*[a]			*Recovery*[e] (%)
	B[b]	*A*[c]	*C*[d]	
Seawater (500 ml) +0.0 μg U	8.5	0.0	0.0	
Seawater (500 ml) +2.0 μg U	17.5	9.0	10.0	90.0
Seawater (500 ml) +4.0 μg U	27.2	18.7	20.0	93.5
Seawater (500 ml) +6.0 μg U	35.3	26.8	30.1	89.2
				Ave. 90.0

[a] Fluorescence intensity measured in per cent scale on the Beckman DU spectrophotometer.
[b] Reagents solution used as blank.
[c] B−8.5=A.
[d] Standard calibration data without flotation process.
[e] The recovery calculated from the fluorescence reading of sample and standard.

Results and discussion

A pH of 5.7±0.1 was adopted for the separation of uranium from seawater since maximal recovery was obtained at this pH in a comparable study with iron(III) hydroxide[2]. The sodium dodecyl sulfate surfactant failed to float the colloidal thorium hydroxide to the surface. A clean separation and stable froth were achieved by substitution of sodium dodecanoate as the surfactant. Both sodium dodecyl sulfate and sodium dodecanoate are anionic surfactants and should be capable of collecting the positively charged thorium hydroxide; the reason for failure of the former to do so is not clear.

By use of sodium dodecanoate and thorium hydroxide the recovery of uranium from seawater based on that added was improved from 82[2] to *ca.* 91% (Table I). The results may be explained on the basis of the Paneth–Fajans–Hahn rule according to which the effectiveness of the collector depends on the ability of the uranium tricarbonate anion to form with Th^{4+} on the surface of the thorium hydroxide, a compound which is of lower solubility than that formed on the iron(III) hydroxide. It appears that the solubility of the compound so formed is an important factor in the process of coprecipitation of trace elements[3]. The fluorescence intensity of 8.5% represented the uranium originally present in the seawater and amounted to 3.1 μg l^{-1}, in general agreement with other workers[4,5].

The absorption and the fluorescence intensity methods were compared for the measurement of the uranium–rhodamine B complex for the determination of

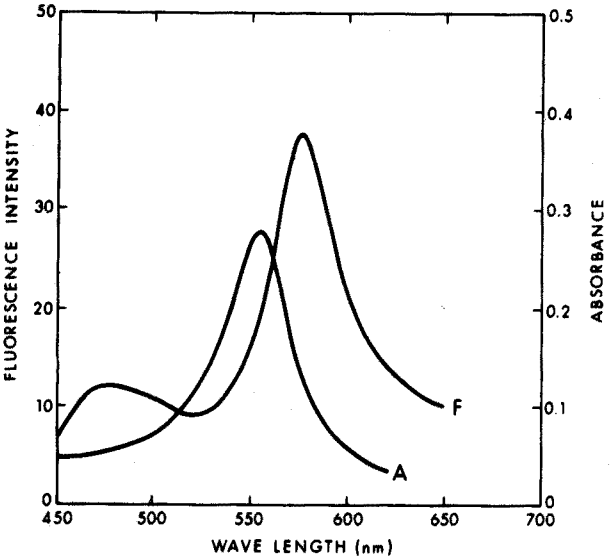

Fig. 1. Fluorescence and absorption spectra of uranium–rhodamine B complex. The fluorescence intensity was measured on the per cent transmittance scale.

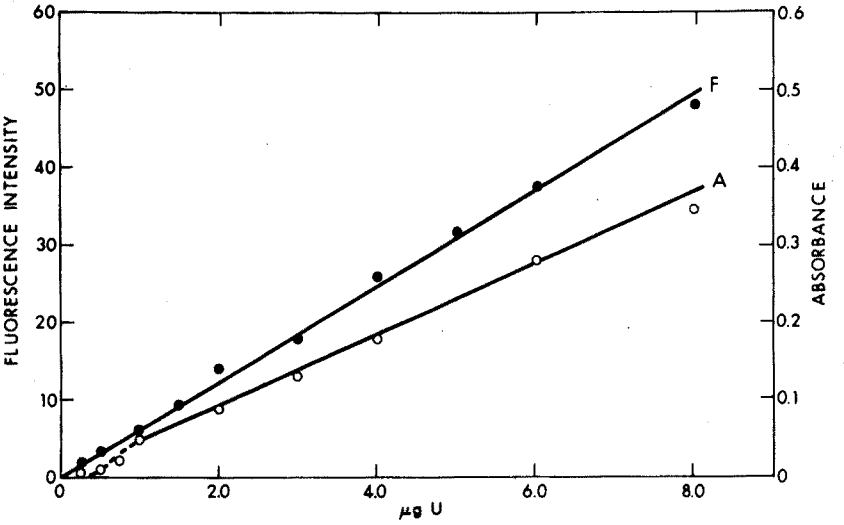

Fig. 2. A comparison of the sensitivity of fluorescence intensity and absorption measurement.

uranium following separation from seawater by the adsorbing colloid flotation technique. The use of absorption methods has been described by other workers[2,6,7] but fluorescence apparently has not been applied for quantitative purposes to uranium although it has been used qualitatively in a spot test[8]. The absorption and fluorescence spectra are shown in Fig. 1. The fluorescence spectrum of the uranium–rhodamine B complex showed a maximum of 575 nm and this wavelength was adopted in the determination.

The sensitivity of the two methods was compared. The results (Fig. 2) indicate that fluorescence intensity gives better sensitivity. It is not possible to compare the slopes of the two curves directly plotted on the same graph since intensity of fluorescence is plotted in % transmittance whereas the other utilizes absorbance units. It is evident, however, that the linear relationship between concentration of uranium and intensity of fluorescence can be extended below 1 μg per 5.0 ml of reagent solution. On the other hand it was difficult to obtain consistent results in this concentration range by absorbance measurements. Reproducibility tests carried out on four replicate seawater samples to which 2.0 μg of uranium was added showed a relative standard deviation for the fluorescence intensity readings of 2.8%.

The results of this study confirm a previous communication[9] to the effect that adsorbing colloid flotation may be of general applicability for the separation from seawater of a variety of trace metallic ions through selection of the proper surfactant–collector system.

G. L. wishes to acknowledge the financial support of the National Science Foundation.

REFERENCES

1 Y. S. Kim and H. Zeitlin, *Sep. Sci.*, 6 (1971) 505.
2 Y. S. Kim and H. Zeitlin, *Anal. Chem.*, 43 (1971) 1390.
3 Y. S. Kim and H. Zeitlin, *Anal. Chim. Acta*, 51 (1970) 516.
4 J. P. Riley and G. Skirrow, *Chemical Oceanography*, Vol. 2, Academic Press, London–New York, 1965, pp. 391–392.
5 Y. Sugimura, *Nature*, 204 (1964) 464.
6 F. de Silva and L. de Moura, *Int. Conf. Peaceful Uses At. Energy*, 23 (1958) 537.
7 H. H. Ph. Moeken and L. A. H. van Neste, *Anal. Chim. Acta*, 37 (1967) 480.
8 F. Feigl, *Spot Tests in Inorganic Analysis*, Elsevier, Amsterdam–New York, 1958, p. 208.
9 Y. S. Kim and H. Zeitlin, *Chem. Commun.*, 13 (1971) 672.

Analytica Chimica Acta
Elsevier Publishing Company, Amsterdam
Printed in The Netherlands

SHORT COMMUNICATION

Microdosage direct de bore dans le sang par la méthode fluorimétrique à l'HMCB

D. MONNIER, C. A. MENZINGER et M. MARCANTONATOS
Département de Chimie Minérale et de Chimie Analytique de l'Université, 1211-*Genève*-4 (*Suisse*)
(Reçu le 26 novembre 1971)

Le microdosage du bore dans les milieux biologiques présente un intérêt considérable dans le domaine médical. La mise en évidence du bore dans différents tissus : foie, coeur, rein, cerveau, rate, etc., et dans les milieux biologiques : sang, urine, lait, démontre l'importance qu'il joue dans la matière vivante[1]. Parmi les méthodes permettant le dosage de traces de cet élément dans les milieux biologiques figurent la colorimétrie[2-6] et l'absorption atomique[7].

Le but du présent travail est d'appliquer la méthode fluorimétrique à l'hydroxy-2-méthoxy-4-chloro-4'-benzophénone (HMCB)[8], au dosage direct de traces de bore dans le sang. En effet, grâce à la sensibilité, à la fidélité et à la sélectivité de ce réactif, il est possible d'effectuer un dosage de bore précis, rapide et sans séparation. La quantité de bore dans le sang, donnée dans la littérature, varie dans de très larges limites selon la méthode mise en oeuvre. Le travail effectué par Bader et Brandenberger[7] a montré que la quantité du bore dans le sang complet varie entre 0.25 à 0.80 p.p.m. Ce sont aussi les valeurs que nous avons obtenues.

Partie expérimentale

Réactifs et solutions. Hydroxy-2-méthoxy-4-chloro-4'-benzophénone (HMCB) recristallisé trois fois dans un mélange eau–éthanol[8].

Solution aqueuse à 100 μg B ml^{-1} (acide borique p.a. Merck), conservée dans un flacon en quartz ou polyéthylène.

Solution sulfurique à 10 μg B ml^{-1}, conservée dans un flacon en quartz.

Solution saturée de $Ca(OH)_2$ p.a. Merck, 2 g par 100 ml d'eau tridistillée, filtrée.

Matériel et appareillage. Tubes à essais en quartz transparent, diamètre 14 mm, longueur 130 mm (Société Electrothermique de la Tour-de-Trême).

Spectrofluorimètre Zeiss (modèle ZFM 4 C), lampe à mercure comme source d'excitation, étalon fluorescent Zeiss et cuves de quartz de 1 cm d'épaisseur.

Micropipette Eppendorf de 10, 20, 50 et 100 μl.

Destruction des matières organiques du sang

La destruction totale des matières organiques dans les milieux biologiques est difficile et elle est nécessaire sinon les fluorescences parasites sont trop élevées. Nous avons donc proposé une technique spéciale permettant un dosage direct et sans

séparation du dosage de traces de bore dans ces milieux et en particulier dans le sang.

Lors de la calcination, il est nécessaire de fixer le bore, sous une forme stable et non-volatile. Pour cela, nous avons entrepris l'étude de différents agents alcalins (Tableau I). D'autre part, nous trouvons dans la littérature un choix de méthodes[2,3,5-7,10] utilisant différents supports minéraux.

TABLEAU I

ÉTUDE DE DIFFÉRENTS AGENTS ALCALINS

Agent alcalin	*Remarques*	*Erreur*
Acétate de magnésium	Difficile à mettre en solution dans l'acide sulfurique concentré après calcination	10 à 50%
Acétate de calcium	Très mauvais	Non déterminée
Acétate de magnésium + hydroxyde de calcium	Mêmes remarques que pour acétate de magnésium	10 à 50%
Hydroxyde de calcium	Très bon	±5%

Nous avons choisi l'hydroxyde de calcium en solution saturée, étant données la bonne reproductibilité des résultats et sa solubilité dans l'acide sulfurique concentré.

La calcination est faite directement avec des tubes à essais en quartz, pour obtenir une meilleure reproductibilité, plutôt que d'employer des creusets en quartz, qui impliquent forcément un transvasement, source d'erreur par perte éventuelle de bore, ou contamination. Pour travailler dans les meilleures conditions possibles, il a fallu procéder à une étude sur les températures et le temps convenant le mieux à la calcination. Des essais effectués entre 400 et 700° ont montré que la température de 550° est suffisante pour une calcination complète et évite la volatilisation partielle du bore observée aux températures supérieures. Quant aux essais de durée de la calcination, effectués entre 60 et 100 min, ils nous ont montré que celle de 100 min est suffisante.

Cependant la calcination ne permet pas d'éliminer totalement les fluorescences résiduelles ; il a donc été nécessaire de procéder à une minéralisation par voie humide avec un mélange acide sulfurique/eau oxygénée à 30% en trois étapes. L'intensité de la fluorescence diminue après chaque étape de minéralisation, dès la troisième, elle est pratiquement négligeable dans le domaine du spectre du complexe HMCB–B. Une étude systématique sur la minéralisation par l'eau oxygénée à 30% et les interférences sur le réactif (HMCB) ont été effectuées par Liebich[11].

Courbe d'étalonnage. Nous avons établi une courbe d'étalonnage pour des quantités de bore comprises entre 5 et 30 ng/4 ml sur des solutions étalon de bore, après avoir préalablement procédé aux opérations d'évaporation, de calcination et de minéralisation. Elle a été comparée aux valeurs d'une autre courbe d'étalonnage établie directement, c'est-à-dire sans effectuer les diverses opérations citées. Il y a parfaite concordance entre elles (Fig. 1), donc les opérations analytiques ne provoquent

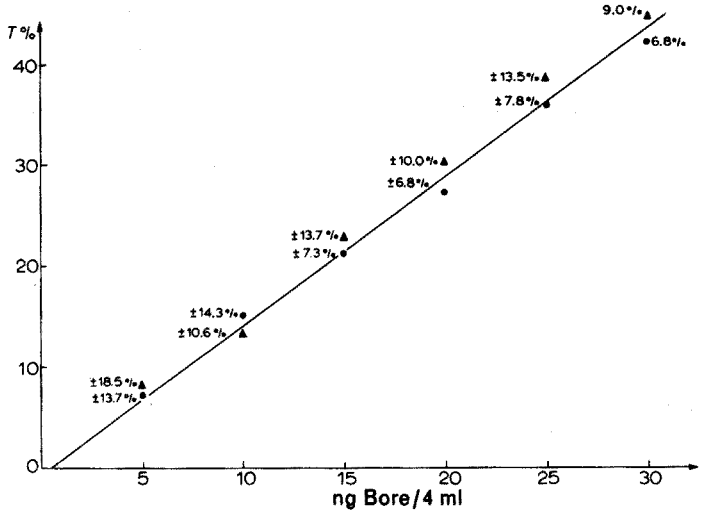

Fig. 1. Courbe d'étalonnage directe et après opération analytique. (——) Courbe d'étalonnage sur solution étalon de borate. (●) Résultats sur solution étalon de borate après les diverses opérations de minéralisation ($n=10$). (▲) idem, autre opération ($n=6$). Coefficient de corrélation $r=0.997$.

ni pertes par volatilisation, ni contamination. Les points de ces courbes ont été obtenus par diverses personnes. Les résultats en sont d'autant remarquables.

Application de la méthode à l'HMCB au dosage direct de submicrotraces de bore dans le sang

Mode opératoire. Des prises de 0.05 à 0.15 ml de sang complet (contenant comme anticoagulant du citrate de sodium, 20% en volume) sont introduites dans des tubes à essais en quartz, ainsi que 0.2 ml d'une solution d'hydroxyde de calcium saturée; on dilue avec de l'eau tridistillée pour obtenir un volume final constant qui est de 0.35 ml dans nos conditions de travail.

Le blanc est constitué de 0.2 ml d'hydroxyde de calcium saturé, à compléter avec de l'eau tridistillée à 0.35 ml.

Ces échantillons sont évaporés à sec, sous un épiradiateur, et calcinés dans un four à moufle (la température du four est portée de 20° à 550° en 60 min) à 550° pendant 100 min.

Les tubes à essais de quartz renfermant les échantillons sont fermés par un couvercle de quartz.

Les résidus calcinés sont repris avec 3.7 ml d'acide sulfurique concentré. Trois minéralisations successives sont effectuées avec 0.1 ml d'eau oxygénée à 30% à la température de 200° pendant 30 min[9]. Il est important qu'H_2O_2 soit complètement éliminé. Après refroidissement on ajoute 0.2 ml d'une solution sulfurique d'HMCB, fraîchement préparée à la concentration de 1.05 mg/10 ml.

Le développement de la fluorescence se fait dans une étuve à 70° pendant 40 min. Après refroidissement à température ambiante, on effectue la lecture fluorimétrique à 490 nm (excitation 365 nm). L'appareil est étalonné à l'aide de l'étalon fluorescent Zeiss.

Il est possible de faire ces dosages en série de 10 ou 20 et même davantage.

Résultats. Le Tableau II donne les résultats de deux séries d'analyses effectuées sur deux pools de sang. La quantité de bore trouvée pour le premier (S_1) est égale à 0.61 ± 0.06 p.p.m., pour le deuxième (S_2), elle est égale à 0.86 ± 0.06 p.p.m. (Tableau II).

Une publication future fera l'objet d'études plus approfondies, concernant le sang, le sérum et l'urine.

TABLEAU II

RÉSULTATS DU DOSAGE DE BORE DANS LE SANG[a,b]

m (g)	V_e (ml)	S_1 Premier pool				S_2 Second pool			
		T_x T_{x+e}	q (ng)	E_N (p.p.m.)	E_M (p.p.m.)	T_x T_{x+e}	q (ng)	E_N (p.p.m.)	E_M (p.p.m.)
0.0422	—	36.1	24.9		0.590	46.0	38.0		0.90
0.0422	0.1	48.7	33.6	0.559		57.5	47.5	0.890	
0.0633	—	56.4	38.9		0.61	69.0	57.0		0.901
0.0633	0.1	69.6	48.0	0.600		83.0	68.6	0.926	
0.0844	—	77.4	53.4		0.632	89.0	73.6		0.872
0.0844	0.1	91.8	63.3	0.632		99.5	82.2	0.856	
0.1055	—	97.9	67.5		0.640	108.0	89.3		0.846
0.1055	0.1	111.3	76.8	0.632		121.0	100.0	0.853	
0.1266	—	114.9	76.9		0.626	123.0	101.6		0.803
0.1266	0.1	127.5	87.9	0.616		135.5	112.0	0.8056	
		$T_e = 14.5$		$E_N = 0.61 \pm 0.06$	$E_M = 0.62 \pm 0.04$	$T_e = 12.1$		$E_N = 0.865 \pm 0.06$	$E_M = 0.865 \pm 0.06$

[a]
m = Masse d'échantillon.
V_e = Volume de solution étalon de conc. égale à 100 ng bore/ml H_2SO_4 ajouté, n_e = quantité en ng = 10.
T_x, T_{x+e}, T_e = Transmission par rapport au blanc renfermant respectivement x ng, $(x+10)$ ng et 10 ng de bore.
q = Quantité de bore dosée (ng).
E_N = Résultat obtenu par la méthode étalon mixte.
E_M = Résultat obtenu par la méthode étalon externe.

[b] *Méthode de l'étalon mixte* E_N

$$\text{p.p.m. de bore} = \frac{T_{x+e} - T_e}{T_e} \cdot \frac{n_e \cdot V_e}{m_x} \cdot 10^{-2} \text{ ou}$$

$$\text{p.p.m. de bore} = \frac{T_{x+e} - T_e}{T_e} \cdot \frac{V_e \cdot 10^{-1}}{m_x}$$

Méthode de l'étalon externe E_M

$$\text{p.p.m. de bore} = \frac{T_x}{T_e} \cdot \frac{n_e \cdot V_e}{m_x} \cdot 10^{-2}$$

Nous remercions le Fonds National Suisse pour la Recherche Scientifique grâce auquel nous avons pu entreprendre ce travail, de même que les personnes qui ont mis aimablement des échantillons à notre disposition.

REFERENCES

1 H. Momsen, *Vitalst. Zivilisationskr.*, XX, 65 (1968) 113.
2 A. Kaczmarczyk, *Anal. Chem.*, 43 (1971) 271.
3 A. Soloway et J. R. Messer, *Anal. Chem.*, 36 (1964) 433.
4 T. Konikowski et L. E. Farr, *Clin. Chem.*, 11 (1965) 378.
5 W. C. Smith, A. J. Goudie et J. N. Sivertson, *Anal. Chem.*, 27 (1955) 295.
6 R. Truhaut, C. Boudène et N. Phu Lich, *Bull. Soc. Chim. Fr.*, 8 (1966) 2551.
7 H. Bader et H. Branderberger, *At. Absorpt. Newsl.*, 7,1 (1968) 1.
8 M. Marcantonatos, A. Marcantonatos et D. Monnier, *Helv. Chim. Acta*, 48 (1965) 194.
9 D. Monnier, B. Liebich et M. Marcantonatos, *Z. Anal. Chem.*, 247 (1969) 188.
10 B. Liebich, D. Monnier et M. Marcantonatos, *Anal. Chim. Acta*, 52 (1970) 305.
11 B. Liebich, *Thèse*, Genève, 1971.
12 M. Marcantonatos, D. Monnier et J. Daniel, *Anal. Chim. Acta*, 35 (1966) 309.

Analytica Chimica Acta
Elsevier Publishing Company, Amsterdam
Printed in The Netherlands

SHORT COMMUNICATION

Dissolution of high-fired plutonium oxide for the determination of plutonium

L. M. ANGELETTI and W. J. BARTSCHER
European Institute for Transuranium Elements, Euratom, P.O. Box 2266, 75-Karlsruhe (Germany)
(Received 31st December 1971)

The dissolution of sintered plutonium oxide constitutes a major problem in routine analysis: depending on the sintering conditions, the material becomes more or less inert to commonly applied acid solvents, such as nitric or sulfuric acid. Even in the presence of 0.1 *M* hydrofluoric acid[1] or with concentrated hydrobromic acid[2,3], dissolution proceeds rather slowly. Other special procedures have been proposed which are either too complicated for routine work—*e.g.* heating with hydrochloric acid in sealed tubes[4], or chlorination with geaseous chlorine in alkali chloride melts in presence of carbon[5]—or which result in high concentrations of certain anions, *e.g.* phosphate[6] or fluoride[7,8], which interfere in subsequent operations. Similar difficulties arise in the case of mixed uranium–plutonium or thorium–plutonium oxides prepared from mechanical mixtures of the components and in which the plutonium is not completely in solid solution.

In a search for a rapid and simple procedure for dissolving large numbers of samples in routine analysis which would yield solutions compatible with subsequent electroanalytical measurements (*e.g.* constant current potentiometry), the use of sulfate fluxes as proposed by Cunningham[3] and Feldman[9] and in more detail by Milner *et al.*[10], appeared quite promising. The melting point of these fluxes is rather low so that the fusion can be carried out in glass vessels. Sulfate ions, even if present in high concentrations, do not interfere in the subsequent analytical operations.

The application of different acid sulfate fluxes to the above-mentioned problem was therefore investigated, in order to establish a standard dissolution procedure for either pure plutonium oxide or oxide mixtures containing high-fired plutonium oxide.

Experimental

Fusion with sodium–potassium pyrosulfate. Weigh up to 150 mg of powdered plutonium oxide or an equivalent quantity of mixed oxides and transfer to a 100-ml silica round-bottom flask. Add 5 g of a mixture of sodium pyrosulfate and potassium pyrosulfate (4 + 1) and mix thoroughly. Cover the flask with a watch glass and heat carefully to about 400° until a clear melt is obtained. Cool, dissolve in 15 ml of 5 *M* nitric acid and dilute with water. In this solution plutonium can be determined by titration with cerium(IV) solution[10].

Dissolution in ammonium sulfate–sulfuric acid. Weigh out 150 mg of plutonium oxide or an equivalent quantity of uranium–plutonium or thorium–plutonium oxides

and transfer to a 100-ml round-bottom flask. Add 5 ml of 9 *M* sulfuric acid, 2.5 g of ammonium sulfate, and 1 ml of 14 *M* nitric acid (the latter only if uranium is present). Put a refrigerating column on the flask and heat to boiling under reflux for 30 min. Insert a collector between the flask and the condenser and heat to fumes of sulfur trioxide for 2 h. Cool and dilute with water. In the case of thorium–plutonium oxides the fuming period must be prolonged to 4 h; at least 70 ml of water must be added and the solution should be left overnight, in order to ensure complete dissolution of thorium sulfate. In the final solution thus obtained plutonium and other constituents can be analysed by methods in which nitrate interferes.

Results and discussion

All experiments were carried out with oxide samples calcined or sintered at 1600°. Before dissolution they were milled to obtain a fine powder.

Fusion with sodium–potassium pyrosulfate. Heating plutonium oxide with potassium pyrosulfate alone gave a clear melt, but 24 h after dissolving the melt in 5 *M* nitric acid, a brown crystalline precipitate was observed when the plutonium concentration was too high. With sodium pyrosulfate alone no clear melt could be obtained. A mixture of sodium pyrosulfate and potassium pyrosulfate (4+1), however, gave clear melts and stable solutions in 5 *M* nitric acid. The time necessary for fusion of 150 mg of plutonium oxide with 5 g of this mixture and dissolution of the melt in 15 ml of 5 *M* nitric acid was about 30 min.

This method proved to be applicable also to high-fired uranium–plutonium oxides, even if they did not entirely consist of a solid solution. In this case up to 500 mg of sample could be dissolved in 5 g of the sulfate flux. The method could not be applied, however, to the dissolution of thorium–plutonium oxides. A clear melt was obtained, but this could not be dissolved completely in either sulfuric or nitric acid, the latter being the medium in which the titration of plutonium with cerium(IV) solution to a constant-current potentiometric end-point is usually carried out[11].

Results for samples of plutonium oxide and uranium–plutonium oxide, which show the completeness of dissolution, are listed in Table I.

TABLE I

FUSION WITH SODIUM–POTASSIUM PYROSULFATE (4+1)

Sample	*Results of analysis* (%)				
	PuO_2	UO_2	*Sum*	*Mean*	*Stand. dev.*
Plutonium oxide calcined at 1600°	99.92				
	100.15			99.98	0.17
	99.87				
	99.81				
	100.17				
Uranium–plutonium oxides	20.21	79.77	99.98		
	20.15	79.83	99.98	100.07	0.13
	20.14	80.05	100.19		
	20.00	79.96	99.96		
	20.11	80.11	100.22		

Dissolution in ammonium sulfate–sulfuric acid. In experiments with ammonium hydrogensulfate it was found that dissolution could be accelerated by addition of sulfuric acid. Heating a mixture of 150 mg of plutonium oxide, 2.5 g of ammonium sulfate and 5 ml of 9 *M* sulfuric acid to fumes for 1 h gave a clear stable solution on subsequent dilution with water. In this way, plutonium solutions can be prepared for analytical methods in which nitrate interferes.

The same method can be applied to the dissolution of high-fired thorium–plutonium oxides, but a longer dissolution time is needed, *viz.* 4 h. Since the solubility of thorium sulfate is low, this salt can precipitate on dilution with water, and only slowly dissolves after further dilution.

Mixed uranium–plutonium oxides are easily dissolved in the same way, if some nitric acid is added to the sulfate mixture, in order to ensure oxidation of uranium to the hexavalent state. If a nitrate-free solution is needed, the nitric acid can be evaporated quantitatively from the flux before dilution with water.

Results of this method are shown in Table II.

TABLE II

DISSOLUTION WITH AMMONIUM SULFATE–SULFURIC ACID

Sample	*Results of analysis (%)*				
	PuO_2	UO_2	*Sum*	*Mean*	*Stand. dev.*
Plutonium oxide calcined at 1600°	99.98				
	99.97			100.02	0.05
	100.06				
	100.08				
	100.03				
Uranium–plutonium oxides	5.31	94.79	100.10		
	10.00	30.28	100.28	100.06	0.14
	14.76	85.17	99.93		
	19.39	80.62	100.01		
	39.52	60.45	99.97		
Thorium–plutonium oxide, containing 2.60% PuO_2	2.60				
	2.57			2.59	0.017
	2.58				
	2.61				
	2.60				

Conclusions

For the rapid dissolution of either pure plutonium oxide or uranium–plutonium mixed oxide samples, fusion with a mixture of sodium pyrosulfate and potassium pyrosulfate is preferable to a treatment with one of these salts alone. The time needed for a single dissolution is about 30 min.

Dissolution in ammonium sulfate–sulfuric acid is more time-consuming, but it needs less manual work than the fusion method, and can be executed in several dissolvers simultaneously. This method is therefore of particular use in the dissolution of large series of samples. Furthermore, it allows the dissolution of thorium–plutonium mixed oxides. In this case the time demand is about 5 h.

The authors wish to thank Mr. B. Giovannone for his valuable assistance in the execution of the experiments.

REFERENCES

1 C. H. H. Chong, T. W. Crochett and J. W. Doty, *J. Inorg. Nucl. Chem.*, 31 (1969) 81.
2 R. J. Jones, *Report TID*-17029.
3 B. B. Cunningham, in G. T. Seaborg and J. J. Katz, *The Actinide Elements*, National Nuclear Energy Series IV-14 A, McGraw Hill, New York, 1954.
4 D. Crossley and G. W. C. Milner, *Report AERE-R* 6127.
5 G. E. Benedict and W. L. Lyon, *USP* 3011865, 1961.
6 R. M. Black and J. L. Drummond, *Report TRG* 1072 (*D*).
7 L. Maly, *Radiokhim.*, 3 (1961) 195.
8 H. W. Crocker, *Report HW* 68655.
9 C. Feldman, *Anal. Chem.*, 32 (1960) 1727.
10 G. W. Milner, A. J. Wood, G. Weldrick and G. Phillips, *Analyst*, 92 (1967) 239.
11 J. Corpel and F. Regnaud, *Anal. Chim. Acta*, 35 (1966) 508.

Analytica Chimica Acta
Elsevier Publishing Company, Amsterdam
Printed in The Netherlands

SHORT COMMUNICATION

A general purpose vapor-phase extractor, filtration, and decantation apparatus for air- and water-sensitive non-volatile solids

SIDNEY G. GIBBINS
Department of Chemistry, University of Victoria. Victoria, British Columbia (Canada)
(Received 18th October 1971)

A general purpose vapor-phase extractor[1], filtration, and decantation apparatus for the concentration and purification of extremely water- and air-sensitive compounds is described. The all glass, stopcock-free apparatus permits manipulation of sensitive compounds with organic solvents for unlimited periods. In the use of the apparatus to determine optimal conditions for separation based on solubility and vapor-phase extraction, an experimental point of no return is never reached. The techniques discussed, originally developed for air- and water-sensitive compounds, have general application.

The apparatus

The basic units of the apparatus are three 500-ml round-bottom flasks whose necks have been bent and sealed to glass tubing as shown in Fig. 1 (side view and top view). A major advantage is that one bulb may be used for storage of a material while

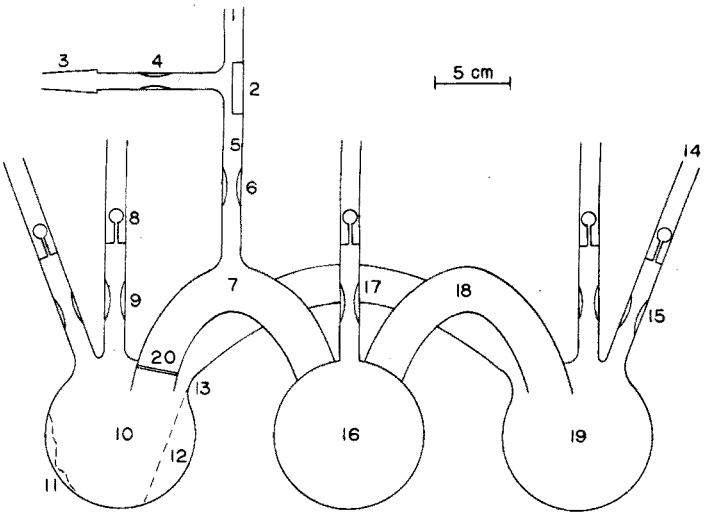

Fig. 1. Vapor-phase extractor, filtration and decantation apparatus, front view.

the other two are used to separate a fraction of the mixture. The coarse sintered disk (20), 25 mm o.d., is positioned as close to bulb (10) as possible. The length of most glass tubing, 12–14 mm o.d., is a convenient minimum. The abundance of fragile bulb break seals permits addition of solvents and removal of sample components.

Samples and solvents are transferred to and from the apparatus as described for the single-stage extractor[1]. One important modification is required when clamping the apparatus to the vertical support rod (21) of Fig. 2. Clamping in a horizontal

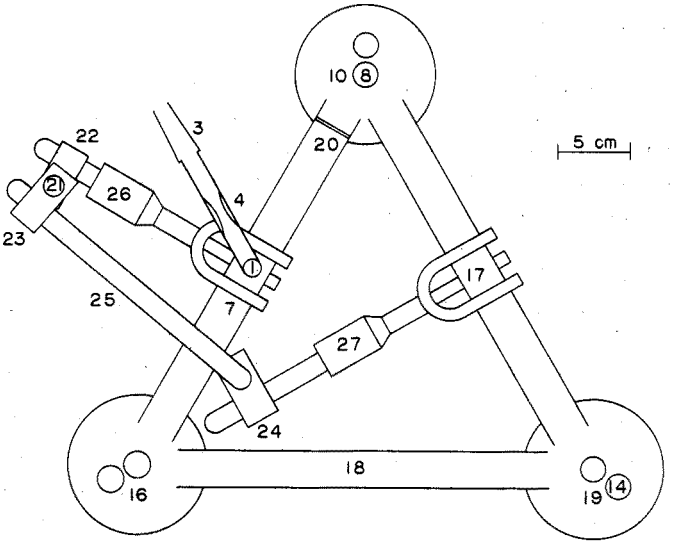

Fig. 2. Clamping of vapor-phase extractor, filtration, and decantation apparatus, top view.

position by one three-finger clamp at (7) to a vertical principal support rod results in a torque which tends to produce a twisting of the major apparatus plane (defined by the centers of the three bulbs) toward the vertical position. The horizontal position is stabilized by use of a second three-finger clamp at (17) (Fig. 2). This clamp is fastened to the vertical section of a bar (25) which is bent in the shape of the letter U and rotated 90° so that the two parallel arms are horizontal. The extremities of the two horizontal arms are secured to the major support rod by standard 90° clamp holders (23). The vertical section of this auxiliary rod lies within the apparatus perimeter. The introduction sample bulb[1] is clamped over tube (1) in the inverted position by a third three-finger clamp which is connected to the principal support rod (21). In Fig. 2 the rectangular sections (22), (23), and (24) are intended only to symbolize clamp holders.

Method of use

The operations of vapor-phase extraction, filtration, and decantation involve pouring of solutions from one bulb to another. This is accomplished by rotating the apparatus about an axis perpendicular to the plane defined by the center of the connecting tube, *e.g.* (7), and the centers of the two bulbs involved in the transfer. If convenient, liquid should not be in the third bulb because of the possibility of accidental transfer to the lower receiver bulb. When the apparatus is not connected to

either a sample receiver or the vacuum line *via* the inner standard taper joint (3), it is readily hand-manipulated.

The two purification techniques, filtration[2] and vapor-phase extraction[1], complement each other. Filtration is preferred if the product can be freed of more soluble contaminates by washing and if the degree of loss of solution is tolerable. The degree of loss depends on solubility and quantity of both the sought compound and the impurities, and also on the quantity of the solvent. As the solubility of the sought compound approaches that of the impurities, filtration becomes less suitable. Filtration is also unsuitable if the impurity is an adhering oil which cannot be washed from the precipitate without excessive dissolution.

Vapor-phase extraction is useful in the purification of slightly (0.02–0.05 *M*) to moderately soluble compounds both in the presence and absence of an adhering contaminating oil. It is also useful when the apparent solubility of the sought compound is enhanced by the contaminants. For separation of compounds of similar solubility, neither filtration nor extraction is useful.

The apparatus is used to purify compounds by a two-stage process involving extraction and/or filtration–decantation. Any order of steps is suitable. In the description that follows, the raw mixture is placed in a bulb which is determined by the operation sequence. As a result of the first-stage separation, some dissolved components are transferred to an intermediate bulb. After the second-stage separation, the more soluble impurities which are concentrated in solution are ultimately transferred to the final bulb and the solid residue which remains in the intermediate bulb is redissolved and returned to the initial bulb for further purification. Products extracted or dissolved away from other components in the first stage can be examined in the intermediate bulb for evaluation and determination of the second-stage operation. Not only may the least soluble component be separated from more soluble ones but the converse is also possible when suitable conditions prevail. In the purification techniques outlined below, products may be removed from the closed system by the sample withdrawal technique[1] at any stage. Subsequently, either the same solvent can be used for further purification of the remaining mixture or a different solvent can be added and its solution–extraction properties determined.

When the objective is the purification of the least but still moderately soluble component of a mixture, a double vapor-phase extraction process is used. Initially, the starting mixture, which may contain substantial amounts (>50%) of the more soluble impurities, is deposited on the walls (11) of bulb (10)[1]. By vapor-phase extraction, the more soluble impurities are concentrated at the "bottom" of bulb (10) in pool (12) which is then decanted to the intermediate bulb (19). After evaporation of the solvent from the solute in bulb (19), the residue is examined for the least soluble component if its properties, *e.g.* color, so permit. This residue is subjected to a second vapor-phase extraction. The extract solution is transferred to the final bulb (16) and the solid residue is re-dissolved and returned to the initial bulb (10). During the second extraction, there may also be spontaneous extraction of the products in bulb (10). By careful decantation, this extract solution is retained in bulb (10) when the extract solution in bulb (19) is poured into the final bulb (16). Repetition of the double extraction process leads to the least soluble component in bulb (10) being progressively purified. Compromise between degree of purification and product loss into the extract solution is inherent in the process. Loss of the least soluble component into

the extract solution is related to duration of the operation when there is moderate solubility. The two-stage vapor-phase extraction process is more suitable for purification of moderately soluble compounds whereas the single-stage extraction[1] is satisfactory for less soluble compounds. Each extraction stage takes several days or longer.

The apparatus can be utilized for the removal of a less soluble contaminant from a more soluble compound. Loss of the latter corresponds to its solubility in about 120% of the solvent required to produce a saturated solution of the contaminant. The purification process comprises of two types of operation: in the primary stage A, all the products in bulb (10) are dissolved. The solvent is then evaporated until the solution is almost saturated in the contaminant, while the bulk of the more soluble component precipitates. After filtration of this solution into bulb (16), a fraction of the liquor containing the contaminant will continue to wet the purified precipitate in bulb (10). The secondary stage B comprises two solution operations. Solvent is condensed in bulb (10), the products are dissolved, and the solvent is evaporated to the same extent as in stage A. This solution is decanted to bulb (19) and further concentrated by solvent evaporation to 20% of the volume initially in (19); 80% of the more soluble compound precipitates and the remaining solution is decanted to bulb (16). The solid in bulb (19) is re-dissolved and returned to bulb (10). The first part of stage B is intended to achieve maximal removal of the contaminant from bulb (10) by a relatively large solvent volume. In the second part, maximal recovery of the more soluble component is the primary objective. The operations are based on the assumption that the amount of wetting liquor retained on the solid in bulbs (10) and (19) after filtration–decantation is proportional to the quantity of solid. Each stage of the purification process results in contaminant reduction by about an order of magnitude. If further purification is required, stage B is repeated. Stage A is omitted if the contaminant produces such a small amount of saturated solution that a relatively large fraction continues to wet the solid after filtration.

Utilization of the apparatus for vapor-phase extraction of large quantities (>50 g) of initial material containing a large fraction of more soluble impurities is accomplished by a first-stage filtration to concentrate the impurities in solution. A second-stage vapor-phase extraction on the solid products remaining in the initial bulb further concentrates the least soluble compound.

Another successful procedure is a cold-temperature vapor-phase extraction which is carried out by depositing the raw solid products on the upper portions of the vessel and placing a piece of dry ice next to the material to be extracted. The solvent condenses, forms a saturated solution and then drains to a pool at the vessel bottom.

These examples should indicate the variety of manipulations possible. Since each experiment has its own unique problems, no attempt is made to be more specific in the application of the apparatus.

Applications

The techniques were employed in the separation of non-volatile, solid products formed in the reaction of iron(III) chloride with phenyl magnesium bromide under an atmosphere of hydrogen[3]. A yellow crystalline solid $Mg_4Br_{3.5}Cl_{0.5}FeH_6(THF)_8$, only slightly soluble in tetrahydrofuran, was successfully purified by both the single

and double stage vapor-phase extraction process. The former is simpler to operate but the latter diminishes and in some cases eliminates loss into the extract solution. A moderately soluble white crystalline solid produced by the reaction was separated from the yellow hydride and the very soluble black components by a combination of the filtration–decantation process and vapor-phase extraction with both diethyl ether and tetrahydrofuran.

The examples indicate the versatility and the usefulness of the apparatus to determine the optimal separation conditions for a wide range of experimental problems. Extensive preliminary experimentation is possible without product loss from the closed system or loss by reactivity with air or water. At no time is any physical separation carried beyond a point of no return.

REFERENCES

1 S. G. Gibbins, *Anal. Chem.*, 43 (1971) 1349.
2 S. G. Gibbins, *Anal. Chim. Acta*, 56 (1971) 486.
3 S. G. Gibbins, *Vth Intern. Conf. on Organometallic Chemistry, Moscow, U.S.S.R., August* 1971.

Analytica Chimica Acta
Elsevier Publishing Company, Amsterdam
Printed in The Netherlands

SHORT COMMUNICATION

A study of the titration of nitric acid with 1,3-diphenylguanidine in pyridine medium

L. M. MUKHERJEE, DAVID W. SUWALA and RONALD S. SCHULTZ
Chemistry Department, Illinois State University, Normal, Ill. 61761 (*U.S.A.*)
(Received 13th October 1971)

In the titration of an acid (HX) with an uncharged base (B), in pyridine as the solvent, the following equilibria must be considered:

$$HX\,(H^+X^-) \overset{K_{HX}}{\rightleftharpoons} H^+ + X^- \tag{1}$$

$$B + H^+ \overset{K_B}{\rightleftharpoons} BH^+ \tag{2}$$

$$BH^+ + X^- \overset{K'}{\rightleftharpoons} BH^+X^-\ (BHX) \tag{3}$$

An attempt has been made to examine these equilibria by considering a conductometric titration of nitric acid with 1,3-diphenylguanidine as the base.

Theory

Assuming that the ionic activity coefficients are equal, at any point in the titration when the total base concentration attains a value C_B, application of the principle of material balance and charge neutrality yields

$$K' K_B^2 [H^+]^2 f_i^2 [B]^2 + (1 + K_B[H^+] + K' K_B [H^+]^2 f_i^2)[B] - C_B = 0 \tag{4}$$

where f_i denotes the ionic activity coefficient and $[H^+]$ and $[B]$ represent the equilibrium concentration of the species indicated. Provided that K', K_B, $[H^+]$ and f_i are correctly ascertained, eqn. (4) can be solved for $[B]$ to yield $[BH^+]$ and $[X^-]$ from the relations

$$[BH^+] = K_B[H^+][B] \tag{5}$$

and

$$[X^-] = [H^+] + [BH^+] \tag{6}$$

Accordingly, the conductance $(1/R)$ of the solution can be expressed as

$$\frac{1}{R} = \frac{\lambda_{H^+}[H^+] + \lambda_{BH^+}[BH^+] + \lambda_{X^-}[X^-]}{1000\,\theta} \tag{7}$$

where θ denotes the cell constant $(1/A\ cm^{-1})$ and λ represents the ion mobility.

In the present case, the equilibrium concentration of hydrogen ion, $[H^+]$, at any stage of the titration was evaluated from an estimated value of f_i and the

hydrogen ion activity measured directly with the cell $Hg|HgCl_{2(s)}, LiCl_{(s)}$ ref. $||HX+B|$ glass at 25°. Since, however, a_{H^+} is related to the e.m.f. E of the cell in the manner

$$a_{H^+} = 10^{(E - E^{0*}_g - E_{ref})/0.05916} \quad (8)$$

where E^{0*}_g and E_{ref} are constants pertaining to the glass electrode and the reference electrode, respectively, the electrode assembly had to be calibrated. For this purpose, solutions of known concentrations of nitric and hydrobromic acid ($pK_{HNO_3} = 4.06$, $pK_{HBr} = 4.36$)[1] were used in the cell without any base added; a value of 0.273 V was calculated for the sum $E^{0*}_g + E_{ref}$ from the relation

$$E^{0*}_g + E_{ref} = E - 0.02958 \log C + 0.02958\ pK \quad (9)$$

which is derived[1] by substituting the square root of the product of molarity (C) and the over-all dissociation constant (K) of the particular acid for a_{H^+} in eqn. (8). The hydrogen ion activities of the titrated solutions obtained on the basis of this initial calibration were then transformed into equilibrium concentrations by using three trial values, *viz.*, 0.771, 0.775, and 0.800 for the activity coefficient, f_i; it was assumed that the latter remains more or less constant during the course of the titration. (The first value of f_i was obtained from the ratio $a_{H^+}/[H^+]$ for the pure acid solution, the $[H^+]$ being assumed to be given as the product of Λ_c/Λ_o (degree of dissociation) and the total concentration of the acid used.)

For each trial, a series of values of K_B were assumed in the range $1.2 \cdot 10^5$ to $2.2 \cdot 10^5$ at ten equal intervals and the simulated plots of $1/R$ (eqn. 7) *vs.* fraction titrated were compared with the observed one.

Experimental

Pyridine was purified as described previously[1]. Both nitric acid and hydrobromic acid were used as their pyridinium salts; 1,3-diphenylguanidine was a high-purity Eastman product. All other chemicals were of reagent quality.

In both potentiometric and conductance measurements the working solutions were prepared by adding different amounts of 1,3-diphenylguanidine to a constant volume of the nitric acid solution placed in separate containers.

A Beckman GS pH meter was used for the e.m.f. measurements. The $Hg|HgCl_{2(s)}, LiCl_{(s)}$ reference electrode was prepared as described earlier[2]. The Beckman model 39303 glass electrode was never allowed to come in contact with water. It required prolonged pre-soaking with pyridine before use; the electrode was usually kept immersed in the solvent when not in use.

Details of conductance measurements have been given elsewhere[3].

All measurements refer to a temperature of $25 \pm 0.5°$.

Results and discussion

The present calculations are based on the limiting ion conductances: $\lambda^0_{H^+} = 49.6$[4]; $\lambda^0_{NO_3^-} = 52.6$[4] and $\lambda^0_{BH^+} = 18.6$. The value of $\lambda^0_{BH^+}$ represents the average of results obtained from Kraus and Bray's treatment[5] of conductance of four 1,3-diphenylguanidinium salts, *viz.*, the nitrate, bromide, iodide and the picrate[6]; a value of $1.011 \cdot 10^4$ for K' was obtained from the results for the nitrate salt.

Figure 1 shows the results of this treatment based on the postulated reactions (eqns. 1–3) together with the plots of data on the observed conductance and the e.m.f.

values of the cell that were used in determining a_{H^+}. The theoretical conductance plot shown is based on $K_B = 2.2 \cdot 10^5$ and $f_i = 0.800$. As is evident, the agreement with the experimental results is excellent.

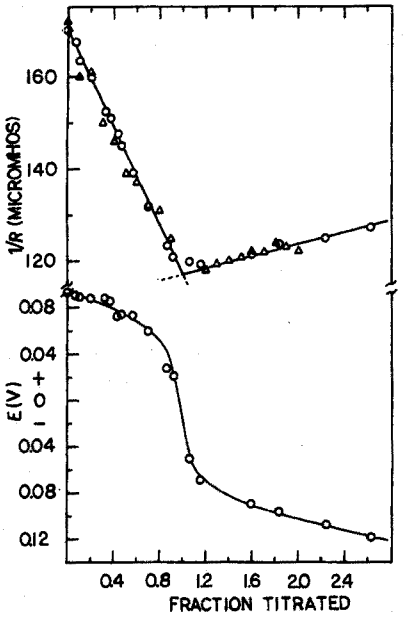

Fig. 1. Plots of e.m.f. of the cell and the observed and calculated conductance as a function of fraction titrated. (○) Observed; (△) calculated. $C_{HNO_3} = 0.0104\ M$; $\theta = 0.6992\ cm^{-1}$.

REFERENCES

1 L. M. Mukherjee, J. J. Kelly, W. Baranetzky and J. Sica, *J. Phys. Chem.*, 72 (1968) 3410.
2 S. Bruckenstein and L. M. Mukherjee, *J. Phys. Chem.*, 64 (1960) 1601.
3 L. M. Mukherjee and J. M. Lukacs, Jr., *J. Phys. Chem.*, 73 (1969) 3115.
4 D. A. Burgess and C. A. Kraus, *J. Amer. Chem. Soc.*, 70 (1948) 706.
5 C. A. Kraus and W. C. Bray, *J. Amer. Chem. Soc.*, 35 (1913) 1315.
6 David W. Suwala, *M.S. Thesis*, Polytechnic Institute of Brooklyn, Brooklyn, N.Y., 1970.

Analytica Chimica Acta
Elsevier Publishing Company, Amsterdam
Printed in The Netherlands

SHORT COMMUNICATION

Redox indicator titrations in N,N-dimethylformamide

ROBERT D. BRAUN and JOHN T. STOCK
Department of Chemistry, University of Connecticut, Storrs, Conn. 06268 (*U.S.A.*)
(Received 29th October 1971)

Although the behavior of chemical indicators in non-aqueous titrimetry has been extensively studied, the applications are nearly all to acid–base titrations[1-3]. The study by Rao and Murthy[4] of the titration of hydroquinone in acetonitrile with cerium(IV) solution is an example of the use of redox indicators. These workers found that ferroin, diphenylamine, methyl red, and Janus green all gave satisfactory results. It has recently been shown that a number of potentiometric redox titrations in N,N-dimethylformamide (DMF) can be acceptably precise, even at millimolar titrand concentrations[5,6]. Some possibilities of chemical indication in the more promising systems of these earlier studies have now been examined.

Experimental

Alizarin red S (C.I. 58005), Buffalo black (C.I. 20470), Janus green B (C.I. 11050) and methylene blue (C.I. 922) were used as 0.1% solutions in DMF. The potassium thiocyanate in DMF solution was saturated. Other reagents were as in previous work[6].

Titrations were carried out in 50-ml Erlenmeyer flasks with magnetic stirring. In the titration of air-sensitive solutions such as of titanium(III), ascorbic acid, and thiolactic acid, the flasks were capped so that the process could be carried out under a stream of nitrogen. Except where otherwise indicated, 15-ml aliquots of *ca.* 0.01 *M* titrand and 2 drops of indicator solution were used. In nearly all cases the concentration of the titrant was also *ca.* 0.01 *M*.

In preliminary titrations that were carried out without added indicator, color changes near the expected end-point were often noted. However, end-points obtained by this method were rarely reliable to better than $\pm 10\%$. Except where otherwise stated, titrations with the aid of indicators required from 5 to 10 min for performance. The results of all acceptable or partially acceptable titrations are summarized in Table I. All systems were examined by the use of methylene blue, Janus green, alizarin red, and Buffalo black as indicators. Indication by potassium thiocyanate was attempted only with systems that involved copper(II) or iron(III).

Copper(II) as oxidant

In the titration of titanium(III) with copper(II), methylene blue gave a color-

TABLE I

REDOX INDICATOR TITRATIONS IN DMF

Titrant	*Titrand*	*Indicator*	*No. of runs*	*Standard dev.* (%)
Copper(II)	Titanium(III)[a]	Methylene blue	10	0.7
Titanium(III)	Copper(II)	Methylene blue	10	0.5
Titanium(III)	Copper(II)	Janus green	10	0.4
Titanium(III)	Copper(II)	Buffalo black	10	0.4
Copper(II)	Cysteine	KSCN	9	2.5
Chromium(VI)	Titanium(III)[b]	Methylene blue	10	1.0
Titanium(III)	Chromium(VI)	Janus green	15	0.7
Chromium(VI)	Ascorbic acid[c]	Methylene blue	10	1.0
Ascorbic acid	Chromium(VI)	Methylene blue	10	2.6
Iron(III)	Titanium(III)	KSCN	10	1.7
Titanium(III)	Iron(III)	KSCN	10	2.3
Iron(III)	Ascorbic acid[a]	Methylene blue[d]	10	1.3
Mercury(II)	Ascorbic acid	Methylene blue[d]	10	2.3
Mercury(II)	Thiolactic acid	Alizarin red	10	2.8
Thiolactic acid	Mercury(II)	Alizarin red	10	1.5

[a] Titrand volume, 10 ml.
[b] Concentration, 0.05 *M*.
[c] Titrand volume, 50 ml.
[d] Plus 3 drops of 25% Bu_4NOH.

less to blue end-point signal. This and the blue to colorless signal obtained in the reverse titration gave reproducible results. The purple to red-purple change given by Janus green in the titration of titanium(III) was not sufficiently sharp to be useful. However, the blue to red-purple change observed in the titration of copper(II) with titanium(III) provided very satisfactory end-point indication. In fact, a sharp copper end-point was obtained when the copper was accompanied by a two-fold excess of iron(III), so that the process may have uses in the analysis of technical copper-containing materials. Buffalo black was of no use in the titration of titanium(III) with copper(II), but gave a useful blue to gray change in the reverse titration. Alizarin red gave no response in either the forward or the reverse titration. Potassium thiocyanate (5 ml of saturated solution) was found to act as a rather poor colorless to red indicator in these titrations. The titration of titanium(III) with copper(II) had to be done slowly (total time, *ca.* 20 min), while the reproducibility of the reverse titration was poor (standard deviation, s.d., 4.4% for 10 runs).

When methylene blue was used in the titration of ascorbic acid with copper(II), the colorless to blue change occurred when only about 15% of the expected amount of titrant had been added. This indicator also failed in the reverse titration. Attempts to use Janus green, alizarin red, Buffalo black, or potassium thiocyanate as indicator in either the forward or the reverse titration were all unsuccessful.

The colorless to red transition given by potassium thiocyanate permitted the rather imprecise titration of cysteine with copper(II). Results for the reverse titration were poor (s.d., 5.4% for 10 runs). None of the other indicators responded in either the forward or the reverse titration.

In the attempted titration of thiolactic acid with copper(II) in the presence of

either methylene blue or potassium thiocyanate, color change occurred quite early in the process. The other indicators failed to respond in either the forward or the reverse titration.

Ammonium dichromate (chromium (VI)) as oxidant

Although methylene blue gave a reproducible colorless to blue end-point signal in the titration of titanium(III) with chromium(VI), no response was obtained in the reverse titration. Janus green did not respond in the forward titration, but gave a reproducible blue to red-purple transition in the titration of chromium(VI) with titanium(III). Alizarin red and Buffalo black appeared to be unaffected in both forward and reverse titrations.

In the titration of ascorbic acid with chromium(VI), the yellow to blue-green transition afforded by methylene blue gave good end-points. This indicator was less satisfactory in the reverse titration, when the dark green to orange-green change had to be approached slowly. Even when the end-point was arbitrarily chosen as an orange-green tint that did not revert to green in 30 sec, the precision was mediocre. None of the other indicators responded in either the forward or the reverse titration.

None of the indicators responded in the titration of cysteine with chromium(VI) or in the reverse titration.

Iron(III) as oxidant

In the titration of titanium(III) with iron(III), end-points obtained as the colorless to orange transition afforded by potassium thiocyanate exhibited mediocre precision. Similar remarks apply to the reverse titration. In the titration of titanium(III) with iron(III) in the presence of methylene blue, no response attributable to this indicator was seen. In the reverse titration, a green to yellow transition occurred when only about one third of the titrant had been added. No response was obtained with any of the other indicators.

The first addition of iron(III) to ascorbic acid in the presence of methylene blue caused a blue coloration. The run was repeated after adding both methylene blue and 3 drops of 25% tetrabutylammonium hydroxide in methanol. The red color that appeared near the beginning of the titration then changed quite sharply to colorless or blue. Results taken as the point of disappearance of the red color were reasonably precise. It was later found that similar results could be obtained when the methylene blue was omitted. The red color may be due to the formation of an iron(II)–ascorbic acid complex. Methylene blue gave no response in the reverse titration.

Mercury(II) as oxidant

When titanium(III) solution that contained methylene blue was titrated with mercury(II), a blue color developed at or beyond the equivalence point. This development took about 3 min, so that the titration was impracticably slow. Color change in the reverse titration occurred when only about one third of the expected volume of titrant had been added. Although color changes in the forward and reverse titrations were observed when the other indicators were used in turn, these changes were premature, unsharp, or both.

A blue color developed very early in the titration of ascorbic acid with mercu-

ry(II) in the presence of methylene blue. The use of methylene blue with 3 drops of 25% tetrabutylammonium hydroxide gave a colorless through gray to blue-gray transition. End-points taken as the first appearance of blue-gray were largely masked by the gray background and exhibited mediocre precision. The other indicators did not respond. When Alizarin red S was used in the titration of mercury(II) with ascorbic acid, a cloudy red to white change occurred near the end-point. The precision was very poor (s.d., ±8.0% for 10 runs). None of the other indicators responded.

Alizarin red caused a yellow to orange color change in the titration of thiolactic acid with mercury(II), and a change from red to colorless or faint yellow in the reverse titration. Although these titrations were practicable, the precision was not very good. No response was shown by any of the other indicators in either the forward or the reverse titration.

The blue color of cobalt(II) and the red color that developed on addition of mercury(II) masked any color changes that may have been caused by the various indicators.

Conclusions

The present studies and those reported earlier[6] demonstrate that, in general, potentiometry is preferable to chemical indication for redox titrations that are to be performed in DMF. The potentiometric method is not only more sensitive, but also is more widely applicable. For example, millimolar concentrations of cobalt(II) can be precisely titrated with mercury(II) to a potentiometric end-point, but the high color of cobalt-containing solutions prevents any chemical indicator response from being seen. "Indicator" titrations possess the supreme advantage of simplicity and can be of value in favorable cases. However, at titrand concentrations of 0.01 *M*, only the titrations of titanium(III) with copper(II) or chromium(VI), of copper(II) with titanium(III), and of ascorbic acid with chromium(VI) exhibited a precision better than 1%. Several other titrations showed a precision of about 2%.

This work was carried out with the partial support of the University of Connecticut Research Foundation.

REFERENCES

1 J. T. Stock and W. C. Purdy, *Chemist-Analyst*, 48 (1959) 22, 50, 55.
2 W. C. Purdy and J. T. Stock, *Chemist-Analyst*, 50 (1961) 88, 92.
3 W. Huber, *Titrations in Nonaqueous Solvents*, Academic Press, New York, 1967, pp. 36, 86, 225.
4 G. P. Rao and A. R. V. Murthy, *Z. Anal. Chem.*, 180 (1961) 169.
5 J. T. Stock and R. D. Braun, *Microchem. J.*, 15 (1970) 519.
6 R. D. Braun and J. T. Stock, *Anal. Chim. Acta*, 60 (1972) 167.

Analytica Chimica Acta
Elsevier Publishing Company, Amsterdam
Printed in The Netherlands

SHORT COMMUNICATION

Enzyme electrode for glucose

GEORGE G. GUILBAULT and GLENN J. LUBRANO
Department of Chemistry, Louisiana State University in New Orleans, New Orleans, La. 70122 (*U.S.A.*)

(Received 18th December 1971)

Enzyme electrodes have been developed for urea[1,2] and for amino acids[3] by immobilizing an enzyme layer around a cation-selective glass electrode. More recently a potentiometric electrode for amygdalin has been developed[4] by coupling β-glucosidase to a cyanide-responsive membrane electrode and a membrane polarographic electrode system has been developed[5] that can be used for several biological systems. In this communication, an amperometric enzyme electrode selective for glucose is described.

The electrode consists of a catalytic platinum electrode with the platinum covered by a thin layer of glucose chemically bound to polyacrylamide[6]. The enzyme is held over the disk by means of cellophane and an O-ring. The electrode is placed in a solution of glucose and a potential of 0.6 V (*vs.* S.C.E.) is impressed across the electrode. Glucose diffuses into the enzyme layer where it undergoes hydrolysis according to the reaction.

$$\text{glucose} + O_2 + H_2O \xrightarrow{\text{glucose oxidase}} \text{gluconic acid} + H_2O_2$$

The hydrogen peroxide formed diffuses both out of the layer and toward the platinum sensor where it is oxidized. A current is produced that is proportional to the concentration of hydrogen peroxide and thus to the initial concentration of glucose.

Experimental

Apparatus. A Heath Polarograph System (Model EUA-19-2) was used as a two-electrode polarograph with constant potential.

Reagents. Glucose. A stock solution of 1.0 *M* glucose was prepared with β-D (+)-glucose (Sigma Chemical Company) in 0.1 *M* phosphate buffer pH 6.0 and allowed to equilibrate overnight.

Glucose oxidase. Chemically bound glucose oxidase was prepared with glucose oxidase type II (Sigma Chemical Company) and acrylamide (Eastman Kodak Co.) as described[6].

Procedure. The electrode was pretreated daily by applying a negative potential (−0.2 V *vs.* S.C.E.) until the cathodic current decayed to a low value, then a slightly anodic potential (0.05 V *vs.* S.C.E.) until the current decayed close to zero, and finally a potential of 0.6 V until the anodic current decayed to a low value. The electrode was then placed in a 50-ml stirred glucose solution and the resulting current recorded with time. After each measurement the electrode was washed by placing it in a stirring buffer solution.

Results and discussion

Since the glucose concentration was low (0.05–20 m*M*) calibration curves could be obtained from either the initial rate of reaction or from the steady-state current. Figure 1 shows a calibration curve for the glucose electrode based on the initial rate occurring within the first 12 sec. A calibration curve based on the steady-state current at 1-min reaction time is also shown. Each point is an average of three measurements. The reproducibility of the measurements was less than 2% for rate measurements and less than 1% for steady-state current measurements. The error obtained by fitting the points to a linear least squares was *ca.* 3% for the rate calibration curve and *ca.* 5% for the steady-state curve. The error for the steady-state curve was large for a linear least-squares fit, because the current started to taper off at concentrations above 15 m*M* glucose. If the 20-m*M* point were omitted from the fit the error would only be 2%.

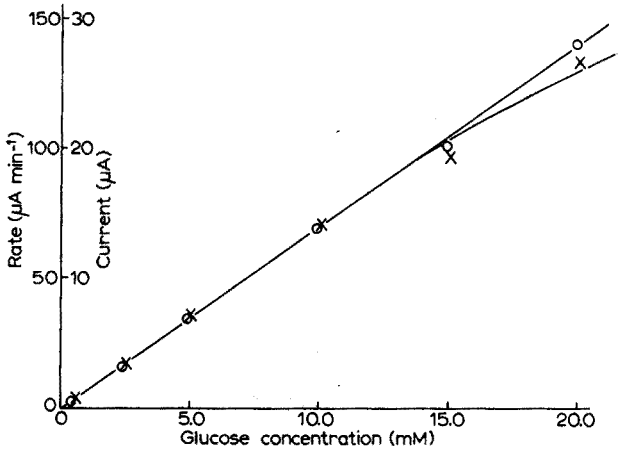

Fig. 1. Calibration curve for glucose. (×) Steady-state current (current axis, μA); (⊙) reaction rate method (rate axis, μA min^{-1}).

At present, we are optimizing conditions for the glucose electrode and preparing to develop uric acid, xanthine and other enzyme electrodes using the same principle of hydrogen peroxide detection. There are several biochemically important reactions that involve an enzyme in the production of hydrogen peroxide from a specific substrate. The electrodes described here used chemically bound enzymes. It is also possible to use enzyme layers consisting of only enzyme in buffer trapped by a cellophane membrane and enzyme trapped in a polyacrylamide matrix. Long-term stability depends on the type of enzyme layer but a stability of several weeks has been observed.

The authors thank S. S. Kuan for preparing the chemically bound glucose oxidase.

REFERENCES

1 G. G. Guilbault and J. Montalvo, Jr., *J. Amer. Chem. Soc.*, 91 (1969) 264.
2 G. G. Guilbault and J. G. Montalvo, *J. Amer. Chem. Soc.*, 92 (1970) 2533.
3 G. G. Guilbault and E. Havankova, *Anal. Chem.*, 42 (1970) 1779.
4 R. A. Llenado and G. A. Rechnitz, *Anal. Chem.*, 43 (1971) 1457.
5 L. C. Clark, Jr., *U.S.Pat.* 3,539,455, Nov. 10, 1970.
6 J. K. Inman and H. M. Dintzis, *Biochem.*, 8 (1969) 4074.

ANNOUNCEMENT

VIIth International Symposium on Chromatography and Electrophoresis

Brussels, September 13–15, 1972

The Belgian Society of Pharmaceutical Sciences has the honour to announce that they will organize their VIIth Symposium on the theoretical aspects and the various practical applications of Chromatography and Electrophoresis, from September 13 to 15, 1972. This Symposium will have two main subjects: 1. Liquid Instrumental Chromatography. 2. Electrofocusing. All specialists in these techniques are cordially welcome. Lectures outside the two themes will be accepted in a restricted number.

All persons interested in chromatography are cordially invited to attend this Symposium. Registration will be accepted until August 1st 1972. Those of the participants who wish to present a paper should register before May 1st 1972. The official languages of the Symposium are French, Dutch, German and English.

During the Symposium, a scientific exhibition will be organized.

Any other information concerning this Symposium can be obtained from the Secretariat of the Belgian Society of Pharmaceutical Sciences, 11, rue Archimède, 1040 Brussels.

Analytica Chimica Acta
Elsevier Publishing Company, Amsterdam
Printed in The Netherlands

BOOK REVIEWS

F. T. Weiss, *Determination of Organic Compounds: Methods and Procedures*, Chemical Analysis, Vol. 32, Wiley–Interscience, 1971, x + 475 pp., price £8.25.

There have been many texts in recent years on specialized aspects of organic analysis, and particularly on mass spectrometry, nuclear magnetic resonance, and gas chromatography. Practical analysts have been rather overwhelmed by the volume of information and may have wondered if any place remained in an up-to-date laboratory for any type of classical procedure. This eminently sensible book by Dr. Weiss of the Emeryville Shell Development Company, based on many years of experience of organic analysis, provides a most useful guide to the proper place for the various techniques in quantitative organic analysis.

The book is divided into three parts. The first major part deals with the determination of the various functional groups. In the second part, analysis of polymers, surface-active agents and petroleums, and trace analysis are discussed. Finally, various very useful laboratory techniques and procedures are described in detail. In all parts of the book, tested procedures are given and these are compared for their practicability in routine analytical situations. The coverage ranges from classical functional group determinations through spectroscopic methods to gas chromatography and radiochemical analysis; elemental analysis and physical measurements are not included owing to lack of space.

This is an excellent book. It is wholeheartedly recommended to the novice for whom it will provide valuable guidance to the selection of the optimal technique for a particular analysis. It is also recommended to the experienced as a fine exposition of how old and new techniques can play their complementary roles in solving the problems of organic analysis.

A. M. G. Macdonald (Birmingham)

B. Meyer, *Low Temperature Spectroscopy*, American Elsevier Publishing Company, New York, 1971, xii + 653 pp., price £15.70.

There is a sub-title to this book, namely *Optical properties of molecules in matrices, mixed crystals and frozen solutions*, which indicates its coverage. It is restricted to visible and near ultraviolet transitions observed in absorption, fluorescence or phosphorescence; infrared and electron resonance studies are excluded.

The major part of the book consists of brief comments on individual systems with associated tabular matter and a bibliography which includes the full title of papers cited in addition to the usual reference. This organized version of what must be the author's card index file is complete to July, 1969 and appears to be an effective reference work. There are also two chapters on equipment for obtaining low temperature matrices and optical spectra therefrom. The first 100 pages are devoted to more theoretical introductory matters.

The trouble with this style of book is that while everything is mentioned, nothing is really discussed. And some of the statements are so bald as to be misleading. Thus, the reader seeking instruction and understanding might be misled on p. 61 into believing that spin–orbit coupling was not noticeable in Russell–Saunders coupling and that its magnitude was connected with nuclear mass rather than nuclear charge. Crucial to understanding the field are the singlet–triplet radiationless processes and on p. 73 these are introduced thus—"Intersystem crossing is defined as a radiationless transition between spin forbidden states. ISC induces phosphorescence by stealing energy from higher excited states, and it weakens phosphorescence through draining of the triplet to S_0." This is a typical muddled half-truth. It is, of course, the transitions not the states which are spin-forbidden. The phosphorescence is not exactly induced by ISC which merely populates the upper level and the stealing analogy implies that the higher excited state remains intact throughout. Another sentence, p. 114, states dogmatically "Mixed crystals are solid at room temperature".

Analytical applications are not specifically discussed. On balance, I find this worthwhile as a reference work, but unhelpful as a text book or monograph.

D. H. Whiffen (Newcastle upon Tyne)

M. R. F. Ashworth, *Analytical Methods for Organic Cyano Groups*, Monographs in Organic Functional Group Analysis, Vol. 6, Pergamon Press, Oxford, 1971, xiii + 142 pp., price £3.75.

The monograph contains both qualitative and quantitative analytical data concerning organic cyano compounds, which are described under the subject headings of chemical methods and physical methods of analysis.

From an analytical method point of view, much space seems to be devoted to the consideration of reactions of negative value, leaving a somewhat limited quantity of practical applications to be sifted out. Nevertheless the text is reasonably easy to read and the summary tables of specific analyses are of particular value, in that they are clearly presented and of useful content, coupled with a simple reference crosscheck.

The physical methods section, embracing techniques such as spectroscopy, mass spectrometry, chromatography, ion exchange and polarography, gives, on first reading, the impression of being unnecessarily compact. On further digestion, however, it has to be admitted that the relevant information is available, often contained in the "method at a glance type" tables which somewhat dominate this section.

Overall, the book provides a useful reference point, which will cater to a greater or lesser extent for all types of specialist work in any way concerned with cyano groups.

J. F. Wheeler (Welwyn Garden City)

Treatise on Analytical Chemistry, Edité par I. M. Kolthoff et P. J. Elving, Part II, Vol. 14, Wiley–Interscience, xvii + 444 pp., prix £11.75.

Ce 14ème volume est le 3ème consacré à l'analyse organique et débute par les halogènes, les données analytiques des autres éléments ayant été traitées dans les vol. 12 et 13.

L'auteur ne s'appesantit pas sur les diverses méthodes de dosage ni sur la minéralisation. Le tout est traité de façon très succincte. La bibliographie n'est pas très développée non plus et s'arrête, semble-t-il, en 1966. C'est un peu tôt pour un ouvrage qui paraît en 1971.

Signalons aussi le fait que les méthodes de décomposition (minéralisation) sont citées sans renvoi à celles décrites dans ce même ouvrage, dans le vol. 12, par ex. à propos du fluor.

Le chapitre intitulé insaturation, dont les principaux sujets sont: Propriétés physique, chimique, physico-chimique et spectrales, Séparations, Détection et Détermination des non saturés, est plus détaillé. Il est complété par une imposante bibliographie (380) qui s'étend jusqu'en 1968. On trouve une foule de renseignements concernant les méthodes de dosage les plus modernes.

Outre les méthodes chimiques (nitration, absorption dans l'acide sulfurique, gravimétrie, les titrations aussi bien volumétriques qu'électrochimiques), il est aussi mention de la coulométrie, des dosages cinétiques, infra-rouges, u.v., Raman, de même que de la spectrométrie de masse et de la récente titration coulographique cumulative.

La partie suivante est consacrée à la détermination des groupes alcyls, puis O-alkyle, N-alkyle et S-alkyle. Trente pages sont réservées à la détermination des éthers et époxy. Les méthodes physiques entre autres jouent un rôle fondamental dans le dosage des peroxydes organiques (u.v., n.m.r., e.p.r., analyse thermique).

A la fin de chaque chapitre, un paragraphe est réservé aux méthodes recommandées. Le choix est de valeur car il est fait par des spécialistes reconnus et rendra de ce fait de grands services aux chimistes analystes.

D. Monnier (Genève)

T. R. Crompton, *Chemical Analysis of Additives in Plastics*, International Series of Monographs in Analytical Chemistry, Vol. 46, Pergamon Press, Oxford, 1971, xii + 162 pp., price £7.00.

The subject matter of this book is not as comprehensive as the author would have us believe from his title. Such additives as lead stabilisers, fire retardants, fillers, pigments and organo-tin stabilisers are not mentioned but constituents such as residual monomers, catalyst residues and polymer volatiles are. The chemical analysis of these materials is almost all carried out by ultraviolet and infrared spectrophotometry after separation of the components by thin-layer or gas–liquid chromatography.

The major part of the book concerns the analysis of plastics for the nature and amount of antioxidant and/or u.v. absorber present. The first chapter deals with

the determination of known compounds in polyolefines, *in situ*, by spectroscopic methods and in extracts by both chemical and spectroscopic procedures. Methods of extraction are discussed in this chapter and plasticisers in poly(vinylchloride) are introduced at this stage. Other additives determined are organic peroxides and monomer residues, both by polarographic methods.

The second and third chapters describe the chromatographic separation and spectroscopic identification and determination of the extracted additives, again mostly antioxidants and u.v. absorbers with some mention of plasticisers. The last chapter deals with the applications of gas–liquid chromatography to the analysis of antioxidants and to the examination of volatiles from polyolefines and polystyrene. Only two errors of proof reading were detected but the reproduction of the photographs is poor in a book as expensive as this one. This text can be recommended as an excellent practical guide for the determination, separation and identification of antioxidants in hydrocarbon polymers.

L. H. Ruddle (Welwyn Garden City)

Methods of Biochemical Analysis, Edited by David Glick, Vol. 19, Interscience Publishers–J. Wiley & Sons, Inc., New York, 1971, vii + 632 pp., price £9.85.

This is an appreciably larger volume than earlier ones and the five topics considered are dealt with at some length. H. Haglund gives an account of practical applications of isoelectric focusing on pH gradients in which the use of natural gradients and density gradients, with particular consideration of sucrose gradients, is described, together with gel and zone convection electro-focusing. S. Hannesian deals with mass spectrometry in the determination of the structure of simple carbohydrates and their methyl glucosides, acetyl derivatives, methyl ethers, trimethylsilyl ethers, acetals, dithioacetals, ketals and dithioketals and of antibiotics and other natural products containing sugars.

In a well documented article, J. H. Clamp, T. Bratti and R. E. Chambers deal with the determination of carbohydrates in biological materials by gas–liquid chromatography. G. W. Leddicotte, in a review supported by more than 1,000 references, deals with the application of activation analysis of the biological trace elements in medicine, dentistry, pharmacology, zoology, botany and agriculture.

Finally, J. Homolka gives an account of the principles and applications of the polarography of proteins in biological and clinical chemistry, a field which is less well-developed than other branches of chemistry.

H. G. Bray (Birmingham)

CONTENTS

(continued on page 4 of cover)

Continued from inside page of cover